Cyprus University of Technology

Faculty of Engineering and Technology
Department of Civil Engineering and Geomatics

Doctoral Dissertation

Agent-based modelling and simulation of human mobility in the context of infectious disease spread: Development and application for the case of COVID-19 spread in Larnaca, Cyprus

Philippos Fayad

Limassol, May 2026

CYPRUS UNIVERSITY OF TECHNOLOGY

FACULTY OF ENGINEERING AND TECHNOLOGY

DEPARTMENT OF CIVIL ENGINEERING AND GEOMATICS

Doctoral Dissertation

AGENT-BASED MODELLING AND SIMULATION OF HUMAN MOBILITY IN THE CONTEXT OF INFECTIOUS DISEASE SPREAD: DEVELOPMENT AND APPLICATION FOR THE CASE OF COVID-19 SPREAD IN LARNACA, CYPRUS

Philippos Fayad

Supervisor

Professor Phaedon Kyriakidis

Limassol, May 2026

Examination Committee

Approval Form

Doctoral Dissertation

AGENT-BASED MODELLING AND SIMULATION OF HUMAN MOBILITY IN THE CONTEXT OF INFECTIOUS DISEASE SPREAD: DEVELOPMENT AND APPLICATION FOR THE CASE OF COVID-19 SPREAD IN LARNACA, CYPRUS

Presented by

Philippos Fayad

Supervisor (Member of the Examination Committee): Professor Phaedon Kyriakidis
Department of Civil Engineering and Geomatics, Cyprus University of Technology

Signature ______________________________

Chairman of the Examination committee: Professor Diofantos Hadjimitsis
Department of Civil Engineering and Geomatics, Cyprus University of Technology

Signature ______________________________

Member of the Examination Committee: Professor Andreas Tsatsaris
Department of Surveying and Geoinformatics Engineering, University of West Attica

Signature ______________________________

Cyprus University of Technology

Limassol, May 2026

Advisory Committee

Approval Form

Doctoral Dissertation

AGENT-BASED MODELLING AND SIMULATION OF HUMAN MOBILITY IN THE CONTEXT OF INFECTIOUS DISEASE SPREAD: DEVELOPMENT AND APPLICATION FOR THE CASE OF COVID-19 SPREAD IN LARNACA, CYPRUS

Presented by
Philippos Fayad

Supervisor: Professor Phaedon Kyriakidis
Department of Civil Engineering and Geomatics, Cyprus University of Technology

Member of the Advisory Committee: Associate Professor Constantinos Tsioutis
Department of Medicine, European University Cyprus

Member of the Advisory Committee: Associate Professor Dimitris Kavroudakis
Department of Geography, University of the Aegean

Cyprus University of Technology

Limassol, May 2026

Copyrights

ACKNOWLEDGEMENTS

I would like to express my deepest gratitude to all those who stood by me throughout this demanding and transformative journey.

First and foremost, I am sincerely grateful to my supervisor, Professor Phaedon Kyriakidis, for giving me the opportunity to pursue this research and for his continuous guidance, patience, and unwavering support throughout the entire duration of my PhD. His trust, encouragement, and academic insight played a crucial role in shaping both this work and my development as a researcher.

I would also like to warmly thank the members of my advisory committee, Associate Professor Constantinos Tsioutis (Department of Medicine, European University Cyprus) and Associate Professor Dimitris Kavroudakis (Department of Geography, University of the Aegean), for their valuable knowledge, thoughtful feedback, and meaningful guidance. Their contribution has been essential in strengthening the quality and direction of this research.

My gratitude also goes to the academic staff and administrative personnel of the department, who were always willing to assist and support me whenever needed. Their professionalism and readiness to help contributed significantly to a positive research environment.

I am equally thankful to my fellow PhD candidates and colleagues for the shared experiences, discussions, and mutual support throughout this journey.

Finally, and most importantly, I would like to thank my family, for being my constant source of strength and motivation.

To my wife and my child,
whose love, patience, and support gave me the strength to complete this journey.

Relevant Publications

Journal Papers

- **Fayad, P**., Kyriakidis, P., Tsioutis, C. . and Kavroudakis , D. . (2024) "A Survey to Capture the Mobility Behavior of Residents in the Republic of Cyprus", European Journal of Geography, 15(4), pp. 305–318. doi: 10.48088/ejg.p.fay.15.4.305.318.

Conference Papers

- **Fayad, P**.; Hadjipetrou, S.; Leventis, G.; Kavroudakis, D. and Kyriakidis, P. (2023): Designing an Agent-Based Model for a City-Level Simulation of COVID-19 Spread in Cyprus. In Proceedings of the 13th International Conference on Simulation and Modeling Methodologies, Technologies and Applications, ISBN 978-989-758-668-2, ISSN 2184-2841, pages 218-224. DOI: 10.5220/0012054000003546.

- Kyriakidis, P., Kavroudakis, D., **Fayad, P**., Hadjipetrou, S., Leventis, G., and Papakonstantinou, A. (2021): Promoting the adoption of agent-based modelling for synergistic interventions and decision-making during pandemic outbreaks, AGILE GIScience Series: OpenAccess Proceedings of the Association of Geographic Information Science in Europe, 2, 44, Copernicus Publications. https://doi.org/10.5194/agile-giss-2-44-2021, 2021.

Abstract / Conference presentations

- Kyriakidis, P., Kavroudakis, D., Papakonstantinou, A.,Hadjipetrou, S., Leventis, G., and **Fayad, P**. (2020): The role of geospatial modeling and simulation in synergistic decision making during pandemics (in Greek), in: Book of Abstracts of the 11th Panhellenic Conference of the Hellenic Association for Geographical Information Systems (HellasGIs), Athens, Greece, November 18-20, 2020; ISSN: 2529-1564.

- **Fayad, P**. (2024): Agent-based modelling and simulation of human mobility in the context of infectious disease spread (in Greek), in: the 3rd Doctoral Colloquium of the Cyprus Rectors' Conference, Nicosia, Cyprus, April 13, 2024.

- **Fayad, P**. and Kyriakidis, P. (2022): The geography of Covid-19 spread in Cyprus: A spatiotemporal analysis of the outbreak and the vaccination strategy followed, in: Book of Abstracts of the 16th Conference of European Association of Geographers (EUROGEO), Mytilene, Greece, May 5–6, 2022.

ABSTRACT

This dissertation investigates the role of geoinformatics in enhancing the understanding and management of epidemiological crises, using the COVID19 pandemic in Cyprus as a case study. The research integrates spatial analysis, cartographic visualization, and agent-based modelling to examine how human mobility and behavioral patterns influence disease transmission.

A comprehensive geoinformatics framework was developed, including static and dynamic maps as well as an interactive Web-GIS platform, enabling the monitoring and visualization of the spatial and temporal evolution of COVID19. In parallel, empirical mobility data were collected through a large-scale questionnaire survey, providing detailed insights into the spatiotemporal behavior of Cypriot residents.

Building on these data, a novel agent-based model (EPIMO-LCA) was designed to simulate the spread of the virus at the local level, incorporating realistic mobility patterns and demographic characteristics. The model was validated against real epidemiological data during the Delta and Omicron phases, demonstrating its ability to reproduce observed trends and assess the effectiveness of non-pharmaceutical interventions.

The findings highlight the critical role of human behavior in shaping epidemic dynamics and demonstrate the value of localized, data-driven modelling approaches for supporting evidence-based public health decision-making.

Keywords: Geoinformatics; Human Mobility; Agent-Based Modelling; COVID19; Spatial Epidemiology

ΠΕΡΙΛΗΨΗ

Η παρούσα διδακτορική διατριβή διερευνά τον ρόλο της Γεωπληροφορικής στην ενίσχυση της κατανόησης και διαχείρισης επιδημιολογικών κρίσεων, χρησιμοποιώντας ως μελέτη περίπτωσης την πανδημία COVID19 στην Κύπρο. Η έρευνα ενσωματώνει χωρική ανάλυση, χαρτογραφική οπτικοποίηση και προσομοίωση βασισμένη σε πράκτορες (Agent-Based Modelling – ABM), προκειμένου να εξετάσει τον τρόπο με τον οποίο η ανθρώπινη κινητικότητα και τα πρότυπα συμπεριφοράς επηρεάζουν τη μετάδοση της νόσου.

Αναπτύχθηκε ένα ολοκληρωμένο πλαίσιο γεωπληροφορικής, το οποίο περιλαμβάνει στατικούς και δυναμικούς χάρτες, καθώς και μια διαδραστική πλατφόρμα Web-GIS, επιτρέποντας την παρακολούθηση και οπτικοποίηση της χωροχρονικής εξέλιξης της COVID19. Παράλληλα, συλλέχθηκαν εμπειρικά δεδομένα κινητικότητας μέσω εξειδικευμένου ερωτηματολογίου, παρέχοντας λεπτομερείς πληροφορίες σχετικά με τη χωροχρονική συμπεριφορά των κατοίκων της Κύπρου.

Με βάση τα δεδομένα αυτά, αναπτύχθηκε ένα καινοτόμο μοντέλο προσομοίωσης βασισμένο σε πράκτορες, το EPIMO-LCA, με στόχο την προσομοίωση της εξάπλωσης του ιού σε τοπικό επίπεδο, ενσωματώνοντας ρεαλιστικά πρότυπα κινητικότητας και δημογραφικά χαρακτηριστικά. Το μοντέλο επικυρώθηκε με πραγματικά επιδημιολογικά δεδομένα κατά τις περιόδους επικράτησης των παραλλαγών Delta και Omicron, αποδεικνύοντας την ικανότητά του να αναπαράγει τις παρατηρούμενες επιδημιολογικές τάσεις και να αξιολογεί την αποτελεσματικότητα μη φαρμακευτικών παρεμβάσεων.

Τα ευρήματα αναδεικνύουν τον καθοριστικό ρόλο της ανθρώπινης συμπεριφοράς στη διαμόρφωση της επιδημιολογικής δυναμικής και επιβεβαιώνουν την αξία των τοπικά προσαρμοσμένων, βασισμένων σε δεδομένα προσεγγίσεων μοντελοποίησης για την υποστήριξη τεκμηριωμένης λήψης αποφάσεων στη δημόσια υγεία.

Λέξεις-κλειδιά: Γεωπληροφορική; Ανθρώπινη Κινητικότητα; Agent-based modelling; COVID19; Χωρική Επιδημιολογία

TABLE OF CONTENTS

LIST OF TABLES

LIST OF FIGURES

LIST OF ABBREVIATIONS

ABM	Agent-Based Model
COVID19	Coronavirus Disease 2019
ECDC	European Centre for Disease Prevention and Control
EPIMO-LCA	Epidemiological Mobility Model for Larnaka
GIS	Geographic Information System
GPS	Global Positioning System
HMS	Human Mobility Schedule
IDR	Infection–Detection Rate
IHME	Institute for Health Metrics and Evaluation
MoH	Ministry of Health
NPI	Non-Pharmaceutical Intervention
SEIR	Susceptible–Exposed–Infectious–Recovered
Web-GIS	Web-based Geographic Information System
WHO	World Health Organization

1 Introduction

Human and physical Geography, Spatial Analysis and Modeling, and the emerging field of Geoinformatics are crucial research areas within the discipline of Geography. These fields have made substantial contributions to understanding the spread of infectious diseases over time. By integrating geography, geoinformatics, and epidemiological modeling, strategic measures and decisions can be formulated and implemented in specific regions or entire countries. This interdisciplinary approach allows for the design and evaluation of various case scenarios, such as enforcing quarantine and curfew, mandating mask usage, or gradually lifting restrictive measures. The combination of these disciplines has the potential to greatly influence spatial decision-making and significantly contribute to the global efforts in combating deadly pandemics. Healthcare professionals have recognized the significance of traditional maps and, more recently, Geographic Information Systems (GIS) in monitoring and combating the spread of diseases. The earliest known instance of mapping the connection between location and health dates back to 1694 when it was employed in efforts to contain a plague outbreak in Italy (Dent, 2006). Since then, maps kept evolving and became crucial tools for comprehending and tracking infectious diseases like yellow fever, cholera, and the 1918 influenza pandemic. The advent of computerized GIS in the 1960s further expanded the possibilities for analyzing, visualizing, and identifying disease patterns.

The field of geoinformatics has proven invaluable in epidemiological research, decision-making, planning, management, and information dissemination. It has found applications in health, such as the surveillance and monitoring of vector-borne and waterborne diseases (Glass et al., 1995; Malone et al., 2001; Roberts et al., 1994), environmental health (Kistemann et al., 2002), assessing environmental hazards and their impact on public health (Astorri et al., 2002), predicting traffic accidents and estimating traffic accident risks (Mills & Neuhauser, 1999), as well as for policy and planning purposes (Scholten & de Lepper, 1991). GIS holds health and disease data specific to particular areas, alongside diverse environmental data. This enables researchers to establish more informed and comprehensive links between a population's geographical location and their health status, surpassing what can be achieved with conventional tabular data. Consequently, the utilization of GIS in health studies has the potential to enhance both the quantity and quality of epidemiological research, as well as the delivery and accessibility of healthcare services. It allows for assessments of a region's healthcare, services, and overall health. Additionally, GIS finds applications in public health informatics, aiding in the efficient planning of healthcare services, enhancing access, streamlining logistics, and identifying areas with health-related challenges.

Nowadays, mobility research spans various domains and serves as a foundational framework for numerous applications. In transportation planning, these studies are indispensable for optimizing routes, improving public transit networks, and mitigating traffic congestion. Urban studies utilize mobility research to inform decisions on city design, land use, and resource allocation, fostering the creation of sustainable urban environments. The impact of mobility on social behavior and community dynamics is explored in social sciences, while environmental assessments leverage mobility data for designing eco-friendly transportation systems. Businesses draw on mobility insights for market research, strategic decision-making, and marketing strategies. Mobility studies also play a crucial role in disaster response, smart city development, tourism management, and security and law enforcement, addressing complex challenges and advancing interdisciplinary solutions.

Epidemiology benefits from insights into human mobility patterns (Lessani et al., 2023) to model and predict the spread of diseases, contributing to effective public health strategies (Kyriakidis et al., 2021). Understanding how diseases spread globally and locally has become increasingly crucial, especially with recent advancements in information technologies and computing resources which have allowed for more realistic and accurate modeling of disease spreading patterns (Pillai et al., 2024). Recent advances in our understanding of human mobility have significantly shaped the latest generation of epidemiological models. This newfound knowledge has led to more realistic and accurate representations of the global spread of diseases (Fabbri et al., 2024). As a result, researchers can now incorporate the complexities of human mobility to better predict, analyze, and develop strategies for controlling the transmission of infectious agents (Fayad et al., 2023).

The recent COVID19 pandemic has highlighted the significant impact of human mobility on the transmission of the virus within and between urban areas. With its global spread, the COVID19 disease has had a profound effect on both the global economy and public health. The Republic of Cyprus has also been affected, with over 1,500 deaths and

600,000 infections, accounting for more than 50% of its total population (World Health Organization, 2023). During periods of epidemiological crises, government decisions and policies aimed at containing the spread of infectious diseases may involve implementing non-pharmaceutical interventions (NPIs). These interventions can include measures such as self-restriction, lockdowns, business closures, and the mandatory use of surgical masks in both indoor and outdoor settings. While NPIs have demonstrated their effectiveness in reducing the rate of infection transmission (Buhat et al., 2020) and relieving the burden on healthcare systems (such as hospital overcrowding), they also have significant socio-economic implications in the short and long term (Novakovic & Marshall, 2022). This highlights the significance of enforcing effective policies/measures and making informed and timely decisions to prevent, control, and mitigate the consequences (Cui et al., 2006).

The modeling of human-environment interactions allows us to comprehend the spatial dynamics of these relationships, leading to more informed decision-making. Mathematical models have played a significant role in addressing infectious diseases by providing simplified approaches to understanding mobility and interactions among individuals (Bachar et al., 2021; Hethcote, 1989, 2000; Kifle & Obsu, 2022; Vytla et al., 2021). These models have been instrumental in enhancing our understanding of transmission mechanisms (Crooks & Hailegiorgis, 2014; Merler et al., 2015; Willem, 2015) and simulating future scenarios (Gomez et al., 2021; Kerr et al., 2021; Kyriakidis et al., 2021; Shastry et al., 2022; Silva et al., 2020).

As a relatively new approach, Agent-based models (ABMs) utilize individual, autonomous agents that interact to simulate complex systems where actions and behaviors are described using simple rules. In a typical agent-based model, three primary elements are essential: a) Agents, which define their attributes and behaviors, b) Agents' relationships and interaction methods, specifying how and with whom they interact and c) Agents' environment, detailing their surroundings and operating conditions. ABM have gained significant popularity as one of the most widely used computational models. They are especially renowned for their ability to simulate the mobility of autonomous entities, known as agents, within complex systems (Mehdizadeh et al., 2022). These models operate based on predefined rules of behavior that guide the interactions among agents, whether in a spatial environment or a social network. ABMs offer a powerful and adaptable approach for capturing the dynamics of individual decision-making and interactions. They provide a more detailed and realistic representation of complex phenomena by simulating the behaviors and interactions of individual agents. This flexibility allows ABMs to effectively study a wide range of topics, including the spread of infectious diseases, social dynamics, transportation systems, and many others.

By using ABMs, researchers can gain insights into the emergent properties and collective behaviors that arise from the interactions of individual agents within a system (Bonabeau, 2002). This makes ABMs a valuable tool for understanding the complexities of real-world systems and informing decision-making processes. An ABM is a specialized computational model characterized by its object-oriented, stochastic nature, capable of conducting dynamic simulations to analyze interactions among entities in both spatial and temporal dimensions, thus uncovering important patterns within the studied phenomenon (Tracy et al., 2018). This particular modeling framework comprises three core elements, namely agents, environment, and interaction, and finds extensive application in fields where simplifying complex systems is of paramount importance, including economics (Heckbert et al., 2010), mobility (Loraamm, 2020), and supply chain management (X. Chen et al., 2013).

1.1 Research Contributions

The overarching objective of this doctoral research is to demonstrate the potential of geoinformatics as an integrated framework for understanding, monitoring, and managing epidemiological crises, using the COVID19 pandemic in Cyprus as a case study. The research focuses on the role of human mobility, spatial connectivity, and behavioral patterns in shaping the transmission dynamics of infectious diseases. To address this objective, the study adopts a multidisciplinary approach that combines spatial analysis, cartographic visualization, and ABM. Through this integration, the research investigates how spatiotemporal human behavior influences the spread of the SARS-CoV-2 virus and how public health interventions interact with these dynamics. The contribution of the thesis is structured around two complementary components.

The first component involves the development of geoinformatics-based visualization tools, including static maps, dynamic cartographic representations, and an interactive Web-GIS platform. These products provide a comprehensive depiction of the spatial and temporal evolution of COVID19 in Cyprus and support the exploration of epidemiological patterns at multiple scales. Despite the availability of global datasets, such integrated and locally focused cartographic products were previously lacking in the Cypriot context, thus addressing a significant research gap.

The second component focuses on the development of a data-driven agent-based model (EPIMO-LCA), designed to simulate the spread of COVID19 based on realistic human mobility behavior. A key innovation of this research is the incorporation of empirical mobility data, collected through a large-scale questionnaire survey approved by the Cyprus Bioethics Committee (n=787). The survey captures detailed information on daily movement patterns, activity schedules, and behavioral responses to pandemic measures, enabling the model to reflect the real-world dynamics of the population. By analyzing the collected data (responses) from the questionnaire, the primary mobility profiles of Cypriot residents were established and incorporated into the ABM epidemiological model to adapt it as closely as possible to the reality of Cyprus.

The EPIMO-LCA model, developed using the NetLogo software, integrates these behavioral inputs with epidemiological processes to simulate disease transmission at the local level, with a focus on the city of Larnaka. The model further enables the evaluation of NPIs, such as mask use and social distancing, providing insights into their effectiveness under varying behavioral conditions.

Overall, this research contributes to the field by:

1. Developing the first comprehensive Web-GIS platform and cartographic framework for COVID19 in Cyprus,
2. Introducing the first mobility-driven ABM tailored to the Cypriot context, and
3. Establishing an integrated geoinformatics–epidemiology framework that combines spatial data, human behavior, and simulation modelling.

Through these contributions, the thesis highlights the critical role of geoinformatics in supporting evidence-based decision-making and preparedness planning for future public health crises.

This doctoral-level research (https://epimo-geo.ct.ws) has received scholarship grants from the State Scholarships Institution of Cyprus (cyscholarships.gov.cy) and the Sylvia Ioannou Foundation (sylviaioannoufoundation.org).

1.2 Thesis Outline

This dissertation is organized into seven chapters that collectively develop its theoretical foundations, methodological framework, and applied contributions. The structure ensures a progressive transition from conceptual understanding to empirical application and interpretation.

Chapter 2 establishes the theoretical background of human mobility modelling, introducing key concepts such as time, distance, and population flow, and reviewing the main theories that explain mobility patterns across spatial scales. It also examines human mobility behavior and discusses relevant data sources and processing techniques, providing the conceptual basis for linking mobility to disease transmission.

Chapter 3 explores the role of geoinformatics in epidemiology, focusing on the monitoring, mapping, and simulation of disease spread. It includes a historical overview of health geomatics, reviews disease mapping and simulation techniques, and introduces agent-based modelling as a key methodological approach for representing complex epidemiological processes.

Chapter 4 presents the COVID19 pandemic in Cyprus as the central case study. It examines containment measures, vaccination strategies, and epidemiological surveillance practices, while also presenting the cartographic outputs of the thesis, including static and dynamic maps and a Web-GIS dashboard. These outputs demonstrate the practical application of geoinformatics in supporting public health decision-making.

Chapter 5 investigates the human mobility behavior of Cypriot residents through a dedicated questionnaire survey. It describes the survey design, demographic characteristics, and representativeness of the sample, and presents findings related to mobility patterns, activity schedules, and behavioral responses to pandemic measures. These results form the empirical foundation for the modelling framework.

Chapter 6 introduces the EPIMO-LCA agent-based model, detailing its data inputs, methodological structure, and implementation. The chapter also presents the validation of the model against real-world data for both the Delta and Omicron phases, highlighting its ability to reproduce observed epidemiological trends and to assess the impact of behavioral and policy-related factors.

Chapter 7 concludes the dissertation by synthesizing the findings, discussing the scientific contributions, evaluating model limitations, and outlining future research directions. It emphasizes the broader implications of integrating geoinformatics, human mobility, and simulation modelling for understanding and managing epidemiological crises.

2 Human Mobility Models

Understanding movement streams of individuals from one location to another provides valuable insights for modeling human mobility behavior and characteristics in various applications, including the estimation of migratory flows, traffic forecasting, urban planning, and epidemic modeling. The importance of knowing Individual movement statistics and mobility flows is also essential for business applications like geo-marketing, where determining the effectiveness of placing advertisements in specific locations relies on understanding the number of people passing through those areas. Quantitative descriptions of human mobility assist the understanding of the processes associated with human movement and their impact on communities and the environment.

Unlike migratory flows with broader temporal and spatial scales, daily individuals' movements are routine excursions that exhibit shorter durations and distances and are characterized by patterns. The routine movement of a progressively increasing population significantly affects both individual lives and environmental conditions. Socio-economic factors such as wage inequalities, variations in living conditions, and the impacts of globalization are now key influences on movement patterns, replacing earlier drivers like inhospitable areas, conflicts, climate change and food shortage. Studies in Europe and the United States have revealed that transportation constitutes the second-largest expenditure category after housing. Additionally, transportation is identified as the second-largest source of greenhouse gas emissions into the atmosphere. Meanwhile, mobile phones have become central to our lives over the past years, serving as crucial sources of information and communication. With their sensing capabilities, smartphones are extensively used in various activities such as health monitoring (Torous et al., 2014) and monitoring crowds in both ordinary and disaster scenarios (Wu & Solmaz, 2018; Sadiq et al., 2015). Furthermore, researchers propose unconventional applications enabled by smartphones, including crowdsourcing (Chatzimilioudis et al., 2012) and opportunistic communication (Karamshuk et al., 2011). Human mobility plays a pivotal role in the performance of such applications.

In the work of Asgari et al. (2013), the three distinct baselines found in Human Mobility studies (fig.1) are discussed extensively.

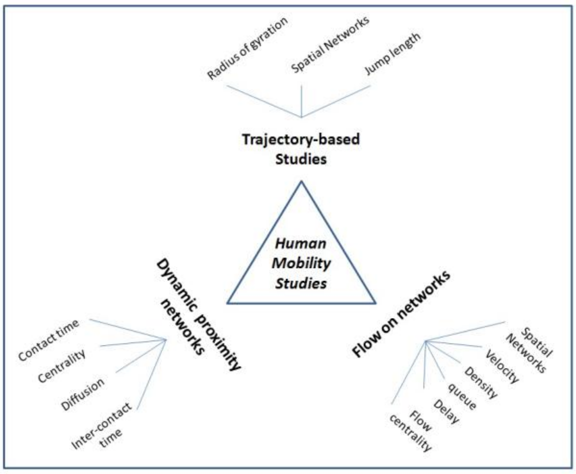

Figure 1. The three main baselines in Human Mobility studies according to Asgari et al. (2013).

Trajectory-based studies, primarily focused on analyzing individual trajectories involve the examination of statistical measures (eg. jump length and radius of gyration) to identify patterns and models in individuals' movements. Dynamic proximity networks focused on people within mobile ad hoc networks, involves uncovering habits in human movements and patterns in connectivity (meeting frequencies, average contact duration, etc.) to predict future encounters. The third and last category concerns flow on various networks and includes infrastructure systems like road and transportation networks.

Figure 2 illustrates the procedure for developing a human mobility model. These steps involve collecting real-life mobility data, filtering the acquired data, modeling the environment, and understanding people's behavioral decisions. The developed mobility model, which generates synthetic mobility traces, is subject to verification and calibration through comprehensive analyses utilizing diverse metrics from real-life mobility traces.

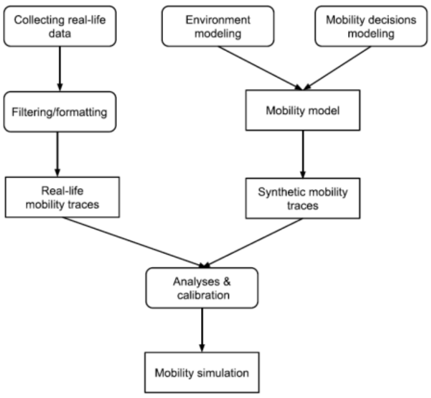

Figure 2. The procedure of creating a human mobility model. Processes (rounded box) and associated products (sharp box). (Solmaz & Turgut, 2019).

The implementation of a human mobility simulation is essential for realistically assessing and developing new strategies in various fields, including urban transportation planning, crowd management, disaster management, epidemics, social networks and many more.

2.1 Concepts and elements

According to Solmaz & Turgut (2015), Human mobility metrics are broadly grouped into three categories, Movement-based metrics, Link-based metrics, and Network-based metrics. In the movement-based metrics category, individual mobility traces contribute to metrics such as flight length, speed, pause time, number of places visited, visit frequency, and mean-squared distance (***MSD***). Link-based metrics center on the effects of mobility on spatiotemporal relations or similarities among individuals, including intercontact time (***ICT***), recontact rate/count, contact duration, node density, temporal variance of node density, pairwise distance, and relative velocity. Network-based metrics focus on the impact of human mobility on network performance, with metrics like message delay, data loss ratio, transmission count, and energy consumption used for model comparisons.

Furthermore, metrics can be also categorized as Spatial metrics, Temporal metrics and Social metrics. Spatial metrics encompass parameters like flight length, speed, number of places visited, and mean-squared distance (***MSD***). Temporal metrics include visit frequency and pause time. Social metrics, on the other hand, are linked to interpersonal contacts and involve metrics such as intercontact time (***ICT***), recontact rate, contact duration, and node density.

Figure 3 below contains the characteristics of the most significant metrics in terms of the two types of classifications mentioned previously.

Metric	Mov.-based	Link-based	Netw.-based	Spatial	Temporal	Social
Flight length	✓			✓		
Pause time	✓				✓	
Speed	✓			✓	✓	
Number of visits	✓			✓		
Visit frequency	✓				✓	
Mean-squared distance	✓			✓		
Intercontact time		✓			✓	✓
Recontact rate		✓			✓	✓
Contact duration		✓			✓	✓
Node density		✓		✓		
Node density variance		✓		✓	✓	
Pairwise distance		✓		✓		
Relative velocity		✓		✓	✓	
Message delay			✓		✓	
Data loss ratio			✓			
Transmission count			✓	✓		
Energy consumption			✓			

Figure 3. Human mobility metrics classification. Source: Solmaz & Turgut (2019).

2.1.1 Time

The "Intercontact Time" (***ICT***) social metric measures the time gap between two consecutive contacts of a pair. This metric holds significance for applications like opportunistic communication, influencing factors such as transmission scheduling and routing. Additionally, contact duration, representing the time spent in contact between pairs, plays a crucial role in routing decisions. Both ***ICT*** and contact duration contribute to understanding and optimizing communication patterns in human mobility scenarios.

The "Pause time" metric, also known as waiting time or visiting time, differs from contact duration as it represents the time individuals spend independently, regardless of other people. This metric provides insights into individual behavior during pauses or visits, contributing to a comprehensive understanding of human mobility patterns.

2.1.2 Distance

The "Flight length" metric, also known as jump size or jump length, is a widely utilized mobility metric in literature. It is computed by averaging the distances between two consecutive visiting places. Statistical characteristics such as mean, variance, and standard deviations of flight lengths are crucial to analyze diffusion patterns and assess the reliability of mobility models.

The "Mean-Squared Distance" (***MSD***) is another widely used metric that reflects diffusion patterns. It is calculated by determining the total travel distances covered by individuals from the beginning of the simulations. ***MSD*** provides valuable insights into the overall movement and dispersion of individuals in a simulated environment and representing the average squared distance from the origin after a time t (equation 1) and it has the unit of an area.

$$\mathrm{MSD}(t) = \langle (\mathbf{r}(t) - \mathbf{r}_0)^2 \rangle \equiv \langle \Delta\mathbf{r}(t)^2 \rangle. \qquad \text{(eq. 1)}$$

In this context, ***r0*** is a vector denoting the origin of an individual concerning the reference point or start location of the trajectory. On the other hand, ***r(t)*** signifies the successive position of the same individual at time ***t***. The average is computed across various independent trajectories or individuals.

The “radius of gyration” metric describes the typical distance of an individual from the center of mass of their trajectory. The observation of sub-diffusive behavior in humans at specific scales indicates that they tend to move a characteristic distance away from their initial locations. This characteristic distance is quantified by the radius of gyration, denoted as ***rg***, which is defined as the root mean square distance of a set of points from a given axis. The general formulation of ***rg*** is expressed with the following mathematical equation (equation 2).

$$r_g = \sqrt{\frac{1}{N}\sum_{i=1}^{N}(\mathbf{r}_i - \mathbf{r}_0)^2}$$ (eq. 2)

Here, ***ri*** represents the coordinates of the ***N*** individual points or ***N*** measurements of location, and ***r0*** is the position vector of the center of mass of the set of points, calculated as ***rcm = ΣN i=1ri/N***.

It’s important to note that the radius of gyration is not equivalent to the square root of the Mean Squared Displacement, although the two quantities are related. This relationship arises because the former is a central second moment, while the latter is a second moment of the origin. The radius of gyration, influenced by both the spatial distribution of visited locations and the time spent (or total number of visits) in each location, is a metric that is used to characterize the typical distance covered by an individual and it does not measure the significance of each location. If an individual is spending a majority of their time in the most visited locations, such as home and work, might have a large radius of gyration if these two locations are far apart. Conversely, even if the most visited locations are close, large values of the radius of gyration may be observed if the individual frequently visits distant locations.

To address these considerations, the “k-radius of gyration” ***r(k)g*** metric is used (equation 3), which is computed over an individual’s k most frequently visited locations (***L1, …, Lk***) (Pappalardo et al., 2015). In this way the influence of location visit frequency is considered.

$$r_g^{(k)} = \sqrt{\frac{1}{N_k}\sum_{j=1}^{k} n_j(\mathbf{r}_j - \mathbf{r}_{cm}^{(k)})^2},$$ (eq. 3)

Here, ***Nk*** represents the sum of visits to the ***k*** most frequented locations, ***r(k)cm*** is the center of mass computed based on those locations, and nj is the number of visits to the jth most visited location. If $r_{(2)g} \approx r_g$ then the characteristic traveled distance is mainly influenced by the two most frequented locations. On $r_{(2)g} \ll r_g$ the other hand, if , the two most frequented locations do not accurately characterize the individual's travel pattern, necessitating the consideration of more locations.

Studying and analyzing Global Positioning System (GPS) data has identified two distinct classes of individuals, "returners" and "explorers". For k-returners, the characteristic distance traveled is primarily influenced by their recurrent movement between a few favored locations. Consequently, their radius of gyration is effectively approximated by their k-radius of gyration for ***k ≥ 2***. On the other hand, k-explorers exhibit a tendency to wander among a variable number of diverse locations, resulting in a k-radius of gyration significantly smaller than their overall ***rg*** (fig. 4 below).

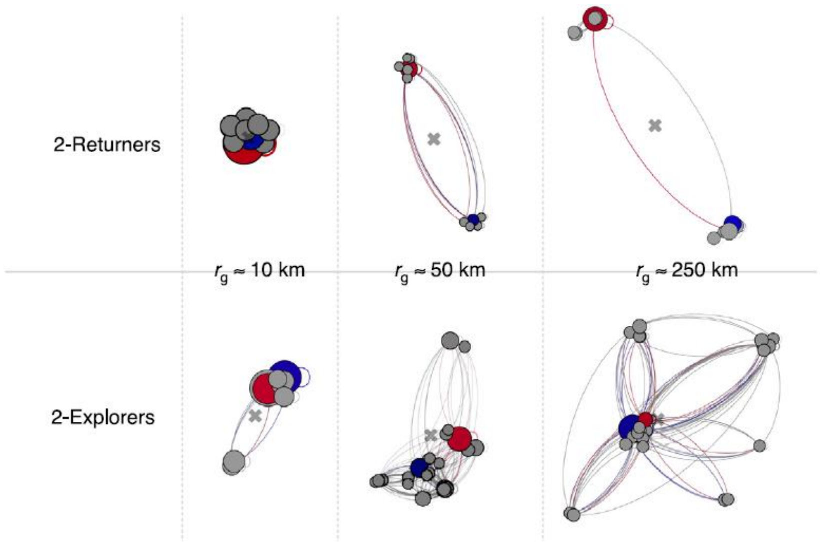

Figure 4. The mobility networks of "returners" and "explorers" for k = 2. Nodes (represented by circles) signify the geographic locations visited by individuals, while links indicate observed travel between two locations. Source: Pappalardo et al. (2015).

As the total radius ***rg*** remains small, the two most significant locations (red and blue) are in close proximity for both two-explorers and two-returners. However, as the total radius increases, a distinction in behavior emerges. For returners, the two critical locations move apart, while for explorers, they remain close, and additional clusters of locations appear far from the center of mass (the gray cross).

2.1.3 Population Flow

The “number of places visited” metric, also known as the number of waiting points, becomes particularly valuable when evaluating if a mobility model accurately captures the daily routines of individuals residing in urban areas. An excessively high number of places visited, for instance exceeding 22, may indicate a lack of realism in the model. This is because individuals typically spend their time at essential locations such as work, home, and perhaps a few additional places in a day, with the majority falling within the range of 5 to 17 (Schneider et al., 2013).

The “frequency of visits” metric provides insights into the likelihood and anticipated timing of a person revisiting the same location. In a typical daily-life scenario, an individual might visit their workplace twice a day—once in the morning and once after lunch. In contrast, another mobility model designed to simulate the person’s movements within the office environment might depict multiple visits to their desk while a meeting room could be visited only once by the same individual. This metric helps characterize the recurring patterns and preferences in an individual’s movement within specific spaces.

As individuals tend to return home with daily and weekly trajectories beginning and ending at the same location, it’s crucial to differentiate locations based on their significance. Ranking is one approach, where rank 1 is assigned to the most visited location (most expected home or work), while other places like schools or local shops have higher ranks. An example of such an approach is found in the work of (González et al., 2008), where location ranks were determined based on the frequency of a user’s position recorded near the corresponding cell tower. The research concluded with the observation that visitation frequency follows a Zipf law, suggesting that the likelihood of finding a user at a location with rank L is approximately $P(L) \sim 1/L$. An alternative approach involves representing an individual’s mobility pattern as a network.

A straightforward approach to represent the movement of Individuals between locations Is to partition the area of interest into distinct zones, denoted as $I = 1, \dots, n$, and quantify the count of individuals traveling from zone I to zone j for all i. These counts, represented as Tij, constitute the elements of the Origin–Destination (***OD***) matrix (equation 4). The matrix is structured as n x m, with n being the number of distinct ‘Origin’ zones, m being the number of ‘Destination’ zones. In most cases, an area under examination is divided into an equal number of origin and destination points, $\boldsymbol{n = m}$. The size n of the Origin-Destination (***OD***) matrix is dependent on the spatial scale or resolution at which the data has been collected.

$$OD(t) = \begin{bmatrix} T_{11} & T_{12} & \dots & T_{1m} \\ T_{21} & T_{22} & \dots & T_{2m} \\ \vdots & \vdots & \ddots & \vdots \\ T_{n1} & T_{n2} & \dots & T_{nm} \end{bmatrix} \quad \text{(eq. 4)}$$

Traditionally, zones in ***OD*** matrices represent administrative units, ranging from census units to entire municipalities or regions. The number of zones, denoted as n, is contingent on the spatial scale and resolution of the collected data. Until the 2000s, the conventional methods for estimating ***OD*** matrices primarily relied on travel surveys or traffic counting. Nowdays, due to advancements in technology and data availability, individual digital footprints are being used to construct ***OD*** matrices. Alternatively, they can result from models, such as the classic 4-step transport model used in urban planning. ***OD*** matrices hold particular significance in models of human mobility at the population level, rather than at the individual level. ***OD*** matrices illustrate the traffic status between crucial nodes in traffic networks, showcasing values that signify either the count of individuals traveling or the average travel time.

A primary objective of examining human mobility is to analyze the flow of the population between various locations (Holme, 2003; Hunter et al., 2011). In contrast to microscopic level where each individual is observed individually, the macroscopic level is more relevant to the dynamic description of traffic as it considers individuals as non-separate entities. The macroscopic variables presented below transform the discrete nature of traffic into continuous variables.

Density (k) represents the number of observed objects per kilometer of road and can be calculated, at specific point in time (***S1***), as:

$$k = \frac{n}{\Delta X} \quad \text{(eq. 5)}$$

Where ***ΔX*** is the length of the road section and n indicates the number of vehicles at ***t1*** on the location interval ***ΔX***. If the total space occupied by the n vehicles is equal to ***ΔX***, then:

$$k = \frac{n}{\sum_i S_i} = \frac{1}{S} \quad \text{(eq. 6)}$$

Flow rate (q) represents the number of vehicles that pass a certain cross-section per time unit and can be calculated, at any location (***x2***) and measurement interval (***S2***), as:

$$q(x_2, t_2, S_2) = \frac{m}{\Delta T} \quad \text{(eq. 7)}$$

Where m represents the number of vehicles that pass location ***x2*** during the time interval ***ΔT***. The time interval ***ΔT*** is the sum of the m headways. By introducing the mean headway ***h***, the expression for the traffic flow rate differentiates:

$$q = \frac{m}{\sum_i h_i} = \frac{1}{h} \quad \text{(eq. 8)}$$

Mean speed (***u***) is calculated as the ratio of the flow rate to the density. The mean speed is dependent on factors such as location, time, and the measurement interval.

$$q = k \cdot u \quad \text{(eq. 9)}$$

The definition of the mean speed is also called the fundamental relation of traffic flow theory (equation 9 above) and it connects flow rate, density, and mean speed, allowing for the straightforward determination of the third variable when two are known.

2.2 Main Theories

Geography, arguably the first discipline to systematically analyze mobility data and develop relevant theoretical frameworks, has played a pivotal role in the study of human mobility. Throughout the twentieth century, theoretical contributions to the understanding of human movement largely originated from geography, sociology, and economics, with a predominant emphasis on population-level dynamics. When distance is considered a key determinant of movement and spatial interaction, Ravenstein's seminal work (1885) on the "laws of migration" is widely regarded as the foundational point of departure.

Taking into account factors such as migrant type (e.g., male or female, young or old) and the role of distance, Ernst Georg Ravenstein, a geographer known also for his contributions to cartography, was among the first scholars to propose systematic explanations and predictions of migration patterns both within and across national borders. Initially formulating seven laws, Ravenstein subsequently expanded them to nine in his 1889 work (Ravenstein, 1889):

a. Most migrants tend to travel short distances, with the “currents of migration” directed primarily toward major commercial and industrial centers capable of absorbing them.
b. The absorption process unfolds as inhabitants of areas surrounding a rapidly growing town migrate to it, leaving gaps in rural regions filled by migrants from more remote districts. This creates migration flows reaching to '‘the most remote corner of the kingdom.’’
c. The process of dispersion operates inversely to absorption, exhibiting similar features.
d. Every major current of migration generates a compensating counter-current.
e. Migrants traveling long distances generally prefer migrating toward large commercial or industrial centers.
f. Urban residents are less prone to migration than those in rural areas.
g. Females demonstrate greater migratory tendencies than males.
h. Towns experience more growth through immigration than natural increase.
i. The volume of migration increases with improvements in transport and the expansion of industry.

Although based on non-quantitative and observational evidence, Ravenstein’s laws successfully identified socio-economic determinants and spatial constraints as central to migration behavior, thereby laying the groundwork for a vast body of subsequent research. Over time, while these laws have been refined and reinterpreted, their core principles remain influential and continue to inform contemporary scholarship on population movement.

A few years later, American sociologist Samuel Stouffer (1940) introduced the Law of Intervening Opportunities in the 1940s, a significant refinement to Ravenstein's laws, particularly addressing Ravenstein's observations about migrants favoring shorter distances and commercial centers. He proposed that the number of people traveling a particular distance is directly proportional to the number of opportunities available at that distance and inversely proportional to the number of intervening opportunities. Essentially, trips between two locations are influenced primarily by the relative accessibility of socio-economic opportunities between those locations. Here, "opportunity" refers to a potential destination for the end of a traveler's journey, while an “intervening opportunity” is one that the traveler rejects in favor of continuing on. Stouffer's original formulation is expressed as follows (equation 10).

$$\frac{dy(r)}{dr} \propto \frac{1}{x}\frac{dx(r)}{dr}, \quad \text{(eq. 10)}$$

The cumulative number of migrants moving a distance r from their original location, denoted as $y(r)$, and the cumulative number of intervening opportunities, $x(r)$, can be related through integration, assuming x is a continuous function $x(r)$ of distance. The integrated expression is given by:

$$y(r) = \log x(r) + C, \quad \text{(eq. 11)}$$

where C is a constant representing the number of opportunities at the origin location. This implies that the relationship between mobility and distance is indirect and established only through an auxiliary dependence via the intervening opportunities. In this context, the higher the number of intervening opportunities between two locations at distance r , the smaller the number of migrants likely to travel that distance. This insight helps explain why rural migrants might move to urban centers over large distances, while those already situated in commercial centers tend to be comparatively more stationary.

During the same period as Stouffer, George Kingsley Zipf, a Harvard philologist, was developing on his well-known observation of the rank-frequency dependence in linguistics, commonly referred to as Zipf’s law. Zipf's argument for this relation considered the tension between two competing factors. The first, termed the Force of Diversification, is linked to the likelihood of populations residing close to the source of raw materials (commodities) to minimize transportation costs to production centers. This leads to the formation of multiple urban centers with smaller populations, given that commodity sources are not localized. On the other hand, the second effect, known as the Force of Unification, involves the tendency of populations to gather in urban centers, decreasing the effort needed to transport finished products to consumers. In contrast to the former effect, this has the opposing consequence, resulting in fewer centers with larger populations. Combining these considerations under some unrealistic assumptions, such as an equitable share of national income and self-sufficiency of urban centers (i.e., production and consumption at equal levels), the share of any center i in the total flow of goods is proportional to its population Pi. Consequently, the flow of goods between two centers is proportional to the product of their populations. Finally, to minimize the cost and work associated with transportation, this flow must be inversely proportional to the distance between centers (equation 12).

$$w_{ij} \propto \frac{P_i P_j}{r_{ij}}, \qquad (12)$$

Where, between two population centers ***i*** and ***j***, ***wij*** represents the flow of goods and ***rij*** is the distance between the centers. The designation of Zipf's formulation as the Gravity law, likening it to Newtonian mechanics, stems from references to '"forces'' and its functional dependence on distance.

Despite the common theme of geographical distance shared by Ravenstein, Stouffer, and Zipf, the functional impact on movement differs notably in the Intervening Opportunities and Gravity Law models. Nonetheless, both models exerted a substantial influence on successive research, initiating two significant lines of parallel investigation and attempts at unification.

Part of the academic development in the 1950s, quantitative and theoretical geography has long been dedicated to the measurement, comprehension, and forecasting of individuals' movements in both space and time (Adams, 2001; Berry, 1993). In this period, Swedish geographer Torsten Hägerstrand laid the foundations of time geography and introduced several conceptual and graphical tools to formalize individuals' trajectories through space and time.

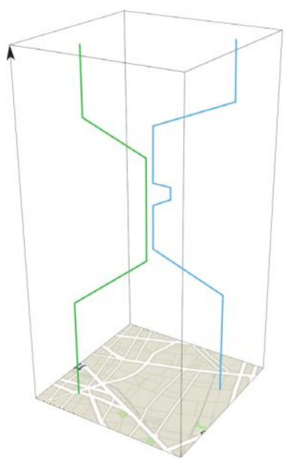

Figure 5. Utilizing cubes to represent the interaction of geographical space and time, this concept of time geography was initially introduced by Torsten Hägerstraand (1970). The 2D plan signifies geographical space, while the vertical axis represents time.

His influential work (Hägerstraand, 1970) is renowned for proposing the representation of individual trajectories in a cube, often referred to as the ‘‘space–time aquarium’’. In this representation (figure 5), the horizontal axis denotes the geographical space, while the vertical axis signifies time. Hägerstrand developed a ‘‘notation system’’, a set of graphical conventions, to illustrate the constraints imposed by social life on individual daily trajectories. Additionally, he provided methods to represent the co-presence and synchronization of multiple individuals in space, along with various graphical conventions useful for depicting the structure and behavior of individual human mobility.

In the 1990s, time geography experienced a natural revival, particularly when the modeling of human mobility transitioned towards individual-based simulation, often referred to as micro/multi-agent or agent-based simulation (Chardonnel, 2007). This shift is attributed to the increase in computing power as well as the development of more expressive programming frameworks, enabling the development of more sophisticated models of human dynamics. Despite the increasing complexity of these models, they remained artificial, as relevant data of comparable complexity and resolution for their calibration was not readily available.

2.3 Human Mobility Behavior

Understanding the behavioral dimension in Human Mobility is crucial for developing realistic models that accurately capture how individuals make decisions related to travel, commute, and interactions. It involves investigating the motivations, preferences, and constraints that shape human movement, leading to valuable insights. Various aspects of behavior must be explored, including the factors influencing route choices, the frequency and duration of interactions, response to external stimuli, and the overall dynamics of movement patterns. In this context, Marcel Hunecke (2009) delineated two distinct sets of factors influencing individual mobility behavior as personal factors and external factors (fig.6). The pertinent personal factors influencing individual mobility encompass socio-demographic characteristics and attitudinal factors. Socio-demographic aspects, determining individual options and needs for mobility activities, and attitudinal factors, encompassing values, norms, and attitudes play a pivotal role in shaping preferences and habits regarding specific activities, destinations, routes, and means of transport of individuals (Hunecke, 2009).

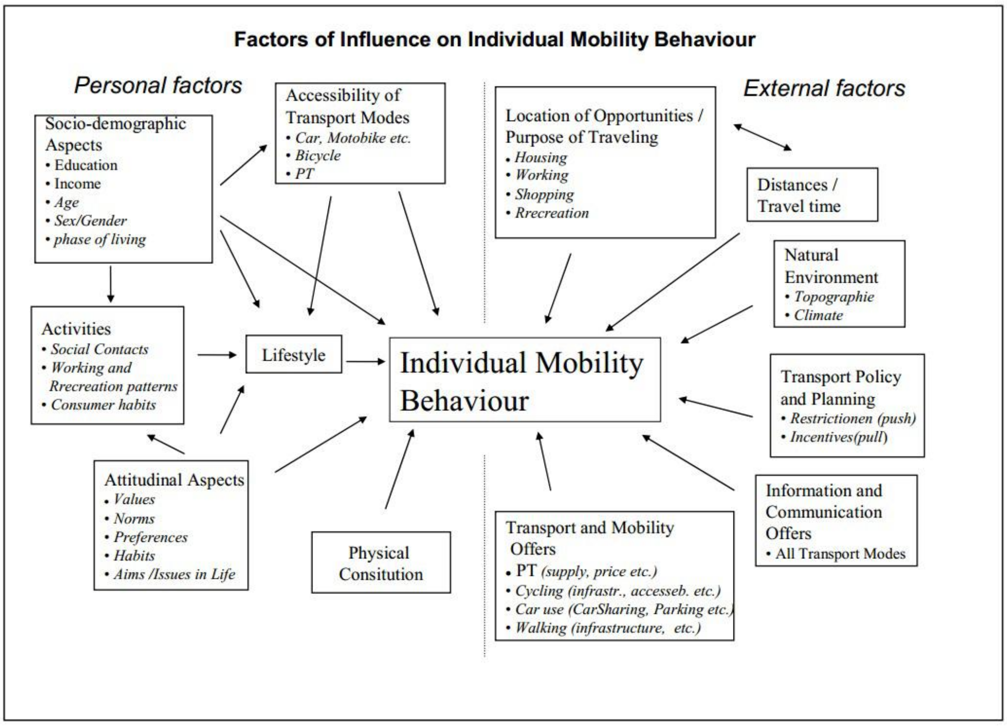

Figure 6. Factors influencing individual mobility behavior. Source: (Hunecke, 2009).

Additionally, Csáji et al. (2013) identified diverse spatial features in human mobility trajectory data, employing these features for clustering distinct types of mobility behavior. In a similar vein, Zignani et al. (2013) endeavored to construct a model for deducing the probability distributions of various human behavior features through the analysis of human mobility traces.

Geospatial data analysis techniques play a crucial role in capturing and interpreting spatial patterns and interactions, providing essential support for modelling complex systems such as human mobility and its implications in epidemiological processes (Pergantas et al., 2017). Mobility research, encompassing diverse domains, serve as a foundational framework for various applications. In the realm of transportation planning, these studies are pivotal for optimizing routes, enhancing public transit networks, and alleviating traffic congestion. Epidemiology benefits from the insights into human mobility patterns to model and predict the spread of diseases, contributing to effective public health strategies. Urban studies utilize mobility research to inform decisions on city design, land use, and resource allocation, fostering the creation of sustainable urban environments. The impact of mobility on social behavior and community dynamics is explored in social sciences, while environmental assessments leverage mobility data for designing eco-friendly transportation systems. Businesses draw on mobility insights for market research, strategic decision-making, and marketing strategies. Mobility studies also play a crucial role in disaster response, smart city development, tourism management, and security and law enforcement, addressing complex challenges and advancing interdisciplinary solutions. Furthermore, human mobility models are versatile and find applications across diverse domains such as traffic forecasting (Kitamura et al., 2000), activity-based modeling (Bhat & Koppelman, 1999), and transportation networks design (Ukkusuri et al., 2007). Additionally, these models are employed in scenarios requiring simplified representations, like the study of virus spreading and epidemic evolution (Kleinberg, 2007; Nicolaides et al., 2012), evaluating human exposure to air pollutants (Hanson, 2005), and simulating mobile networks of wireless devices (Rhee et al., 2008).

The exploration of human mobility encompasses various intriguing subjects. Firstly, there is a focus on modeling the probabilistic distributions of attributes linked to human movement, such as travel distance and duration. This involves fitting different models, including the Lévy walks model, to real-world data to elucidate the underlying reasons. Another subject delves into understanding individual activity-based mobility patterns, aiming to gain insights into people's activities and categorize them (e.g., at home, working, shopping) (Hasan et al., 2013). Additionally, predictive modeling is employed to anticipate the next places individuals are likely to visit (Noulas et al., 2012). Identifying individual transportation modes, such as walking, driving, or riding buses, constitutes another significant aspect. This involves continuous tracking of an individual's locations to accurately determine their mode of transportation. Lastly, the study of densities and flows within a building is centered on comprehending human density and movement within large structures. The objective is to analyze patterns of movement and concentration of individuals in the building environment, providing valuable insights into the dynamics of human mobility in confined spaces. Expanding on the concept of various dimensions of Human Mobility, Karamshuk et al. (2011) delineated the properties of Human Mobility across three primary dimensions (spatial, temporal, and social). In literature, each of these dimensions has been examined at a variety of scales, including a spatial network analysis conducted at global and country (Balcan et al., 2009; Csáji et al., 2013), regional (Garske et al., 2011) and city (Giannotti et al., 2011; T. Hunter et al.,

2011) scales. Higher scales, like campuses or building scales (Hossmann et al., 2011; Zhao et al., 2008), have also been examined.

Human mobility is manifested at various distances, from short-range (e.g. walking) to long-range (airplane, car, trains, etc.) travelling. In contrast to short-range mobility, which typically spans limited distances, long-range transportation covers thousands of kilometers utilizing land, air and sea transportation. Air transport holds crucial significance in facilitating global connectivity, serving as a linchpin in the world economy and fostering the exchange of people, ideas, and unfortunately, diseases. Sea transportation provides another example of long-range mobility. While historically sea transportation played a central role in long-range human mobility, nowadays it is utilized mainly for cargo movement. Studies of sea transportation networks often depict ports as nodes, connected by links representing routes traversed by major cargo liners (Fremont, 2007). The weight assigned to these links usually corresponds to the frequency of ships or trips along the route.

2.3.1 Local Scale Models

In pedestrian movement, managing large concentrations of people such as those encountered during festivals, music concerts, sporting events, or religious ceremonies, poses challenges in terms of service demand, transportation, and public safety. Incidents like avalanches in stadiums or congestions in crowded places emphasize the need for strategies to ensure efficient evacuation during emergencies. This underscores the importance of understanding empirical patterns in pedestrian movement and constructing relevant models.

Modeling frameworks for pedestrian movement can be categorized based on how individual pedestrians are considered. In scenarios focused on crowd control, metrics like crowd velocities or pressures are of interest and a large number of individuals are considered. Fields characterizing the system's state, such as pedestrian density, local velocity, or exit flow, can be defined at each point in space and time. In situations like crowd congestion near exits, shock waves, moving fronts, and intermittent exit flow patterns can emerge, leading to phenomena like avalanches and stop-and-go effects (Helbing et al., 2006). Alternatively, agent-based modeling provides a detailed simulation of the state of each individual (agent). This approach is well-suited for modeling heterogeneous populations where agents may exhibit distinct features.

In the context of micro-scale human mobility, the Social Force Model (SFM) is introduced by Helbing and Molnár (Helbing & Molnár, 1995). This model focuses on simulating crowd dynamics by considering social forces influenced by pedestrian densities and directions of pedestrian streams. Given the crucial importance of simulating pedestrian dynamics, especially in scenarios like building evacuations, pedestrian behavior is categorized into normal and panic situations. The dynamics of pedestrian crowds in these situations are detailed in (Helbing et al., 2002). In a related work, Helbing and Johansson delve into key concepts such as the social force concept, panic situations, freezing-by-heating, crowd turbulence, and emergence (Helbing & Johansson, 2009). They also present an evolutionary approach for parameter calibration in SFM using video tracking data.

2.3.2 Regional-Global Scale Models

The study of intra-urban mobility within cities is driven by several factors, including the availability of ample data due to rapid urbanization. Cities, being early adopters of technology with large populations, provide rich data sources such as mobile phone records and social networking applications. Additionally, the challenges posed by congestion and its associated energy costs, particularly in terms of CO_2 emissions from individual vehicles, underscore the need for accurate measurements of transportation flows. Intra-urban mobility research also addresses issues of socioeconomic inequality, residential segregation, and diverse transport modes within cities, including privately owned vehicles, buses, metros, etc. The exploration of phenomena like "familiar strangers" (Sun et al., 2013) and the properties of hidden temporal networks formed by individuals that temporarily co-locate in the same spaces, but do not know each other, adds depth to understanding urban mobility dynamics.

Undoubtedly, one of the most critical applications of research in human mobility and transportation systems is its impact on epidemic spreading. Understanding how diseases spread globally and locally has become increasingly crucial, especially with recent advancements in information technologies and computing resources which have allowed for more realistic and accurate modeling of global disease spreading patterns. Recent advances in our understanding of human mobility have significantly shaped the latest generation of epidemiological models. This newfound knowledge has led to more realistic and accurate representations of the global spread of diseases. As a result, researchers can now incorporate the complexities of human mobility to better predict, analyze, and develop strategies for controlling the transmission of infectious agents on a global scale.

While air transportation has long been recognized as a major factor in disease dissemination (A. Rvachev & Longini, 1985; Flahault & Valleron, 1992), incorporating air traffic data into epidemic models has become feasible in the past decade (Colizza et al., 2006; Hufnagel et al., 2004). Studies in this domain not only shed light on the patterns of diseases like influenza (Viboud et al., 2006), which is an example of a contact disease that annually spreads worldwide, but also provide insights into various other contact and vector-borne diseases such as SARS (Bauch et al., 2005), malaria (Huang & Tatem, 2013), yellow fever (Johansson et al., 2012), and emerging threats like Ebola (Jones et al., 2008). Although each disease comes with its unique characteristics, necessitating customized modeling that incorporates specific mechanisms related to its transmission, the world airport network (WAN) can assist as an important component for the arrival and propagation of diseases, with estimates of each airport's potential contribution to a pandemic within the network (Lawyer, 2015).

In the context of realistic models for epidemic spreading, the literature has predominantly employed two main frameworks, agent-based modeling and metapopulations. Agent-based modeling involves simulating the behavior and interactions of individual agents within a population while on the other hand, metapopulations refer to a collection of local populations interconnected by the movement of individuals between them. In the context of epidemics, metapopulation models consider the spatial structure of populations, with different localities representing subpopulations. Both agent-based modeling and metapopulation modeling offer valuable insights into the spread of epidemics, allowing researchers to explore realistic scenarios and understand how individual behavior or population structures influence the dynamics of infectious diseases. The choice between these frameworks often depends on the specific characteristics of the epidemic under study and the level of detail required for the analysis. As also previously noted, human mobility happens over a diverse range of distances. An acceptable grouping consists of intra-urban mobility (covering distances in the range of 1–10 kms), inter-urban mobility (covering a broader range, approximately 100 kms) and lastly, Inter-country and international traveling (extending over distances around 1000 kms). It is important to note that a trip can involve multiple connections and may be multimodal, incorporating various modes of transportation, each with its associated waiting-time distributions (Gallotti & Barthelemy, 2014). Thus, a deep understanding of mobility necessitates consideration of the multimodal nature of transport and the transitions between different modes.

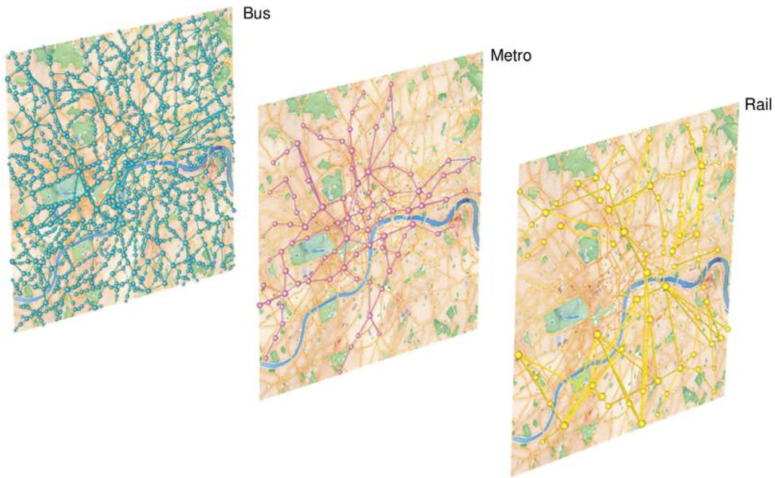

Figure 7. A multilayer network approach to mobility considering the public transport networks in the London metro area, including distinct layers representing the bus, subway, and rail networks. Source: Figure from (Gallotti & Barthelemy, 2015).

Recent advancements in the analysis of multiplex or multilayer networks have provided a robust framework for conducting such analyses (Boccaletti et al., 2014; Kivela et al., 2014). In these networks, nodes can exist in one or multiple layers, and each layer consists of a set of links or interactions between nodes. When a substantial portion of nodes is present in all discernible layers, the network is termed multiplex.

While the time spent on a given trip is roughly proportional to the distance traveled, the mode of transportation must also be considered, which, in turn, depends on the distance. Short-range travel (like walking, cycling or public transportation) involves slower transportation modes with frequent stops while long-range travel is executed by faster means (like trains or planes) with fewer stops. This relationship between distance, travel times, and speed is depicted in figure 8, illustrating the connection between apparent speed (geodesic distance divided by travel time) and travel distance (Varga et al., 2016). Additionally, observations indicate that the apparent speed (v) increases with travel distance, following a power-law functional form (Gallotti & Barthelemy, 2014).

Regarding travel time, Marchetti (1994) introduced the concept of a travel time budget in the context of intra-urban mobility. Building on ideas developed by Zehavi (1977), Marchetti suggested a travel time budget of around one hour per day, regardless of the specific location. This suggests that as transportation technology advances, resulting in increased speed, individuals cover more distance within the allotted time, contributing to urban sprawl. This assumption is captured by the rational locator hypothesis (Levinson & Wu, 2005), suggesting that individuals maintain a roughly constant journey-to-work travel time by adjusting their home and workplace. Additionally, researchers noted that the majority of individuals tend to travel relatively short distances, while a small fraction consistently covers distances exceeding a hundred kilometers. Subsequent investigations (González et al., 2008; Simini et al., 2012) revealed that individual travel patterns converge into a unified spatial probability distribution suggesting that humans exhibit simple and replicable patterns in their movements regardless of the varied nature of their travel experiences.

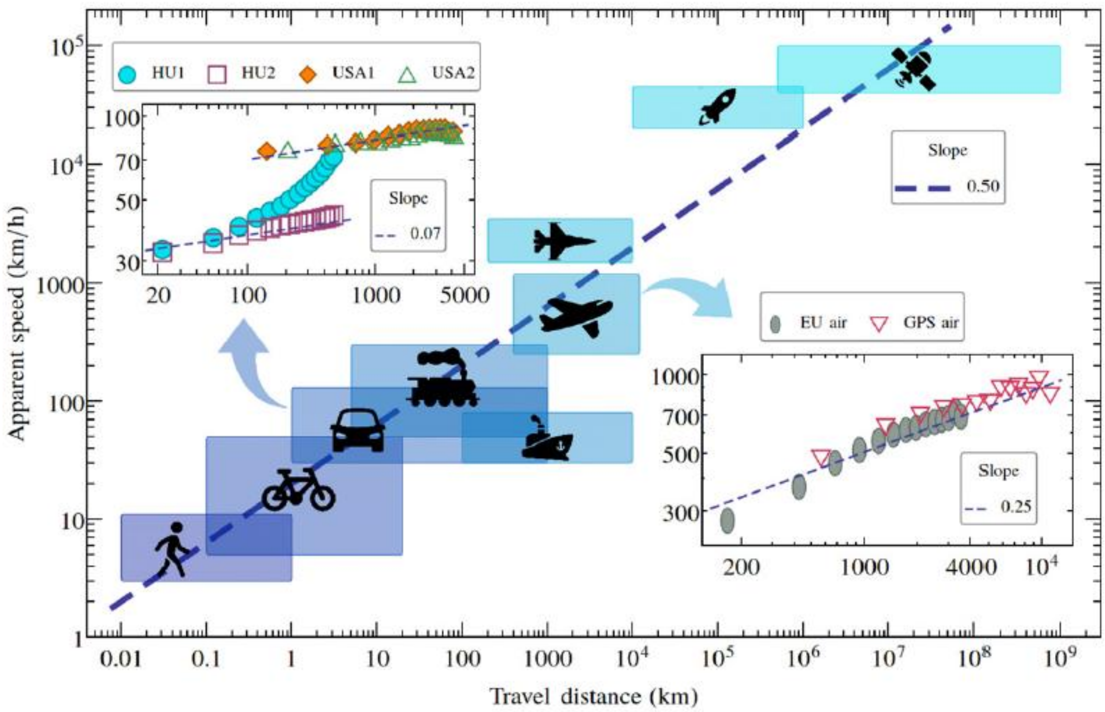

Figure 8. The relationship between apparent speed and travel distance (Varga et al., 2016). The intervals for different transportation modes are represented by boxes, and the insets display the average results for cars (top left) and plane travel (bottom right). The dashed lines in the figure correspond to power-law fits, highlighting the characteristic patterns observed in the data.

As the movement of an object with a certain mass at a specific speed necessitates a given amount of energy, mobility is fundamentally tied to energy. Therefore, employing energy concepts becomes crucial in comprehending human travel behavior (Kölbl & Helbing, 2003). Furthermore, observations suggest that the average travel times associated with various modes of transportation exhibit an inverse relationship with the energy consumption rates observed in the respective physical activities (Rowland, 1998).

Intra-urban mobility within cities stands out as one of the most extensively studied applications, due to various compelling factors. Major cities, characterized by early technology adoption, boast large populations, resulting in increased smartphone users and high densities of phone antennas. The abundance of data plays a central role, with rapid urbanization leading to a growing global population residing in urban areas. Consequently, the spatial resolution of data from Call Detail Records (CDR) and social networking applications collected in cities, is significantly higher compared to rural or non-urban areas.

2.4 Mobility Data and Processing

Traditionally, the development of human mobility models involves extracting information from mobility surveys (Hanson & Huff, 1988; Schlich & Axhausen, 2003). These surveys are designed to collect comprehensive data on travel choices in order to provide detailed travel behavior of individuals. Nowadays, various methods are employed for human mobility data collection, with GPS traces being a preferred choice due to their higher spatial and temporal accuracy compared to other techniques. The widespread adoption of mobile phones and use of the GPS marked a turning point, leading to an exponential increase in data generation related to human movement. Combined with continuous advancements in computing power and sophisticated data-mining methods, this transformation enabled the track of movement at finer spatial resolution, for both population and individual level. The increase of mobile phones, particularly the large volume of information gained from call detail records (CDRs) and Online Social Network (OSN) technologies allowed the analysis of human movement at a very fine temporal and spatial resolution. Additionally, the widespread adoption of cell phones globally facilitates multi-scale studies and analyses at various levels, from neighborhoods to entire countries, and even encompassing international travel and movement across borders.

However, privacy concerns must be carefully addressed during data collection. While some datasets claim to maintain user anonymity, it is crucial to acknowledge that those collecting the data may still have knowledge of the users. To enhance privacy, data collection should incorporate techniques ensuring user anonymity, like encrypting personal information before database storage or introducing noise to the dataset to prevent the differentiation of individuals' information.

As observed mobility data serve as a vital resource for parameter calibration and model validation, the main eleven types of such data found in literature consists of records from national censuses, tax revenue, currency transactions, local travel surveys, GPS traces, Wi-Fi access points, online social network, public transport smart cards, Bluetooth detection, video tracking and call detail records.

a) National Census

National surveys, known as censuses, serve as an important source of data collected at the national level. During these surveys, householders respond to inquiries about the sociodemographic and economic status of family members. Of particular relevance to mobility studies are questions related to workplace location, as well as the current and previous residences of individuals. This collective information becomes helpful in estimating country migration flows and traveling streams. National censuses are conducted at different times across various countries, and the type of information collected varies across regions and time periods. In most countries national censuses typically are conducted every ten years and offer limited details about where people spend their time or how they travel.

b) Tax Revenue

Using tax revenue data, aggregated migration flows can be estimated by identifying individuals who have changed their residence or workplace locations in the intervening fiscal year. This process involves matching coded returns for the current filing year with those filed during the previous year. The comparison focuses on the mailing addresses on the two returns. If the addresses are identical, the individual is categorized as a non-migrant. Conversely, any discrepancy in address information leads to the categorization of the individual as a migrant.

c) Currency Transactions

Currency transactions are another source of mobility data. While difficult to collect, the most accessible method for obtaining such data is through online bill-tracking websites that monitor the global dispersal of individual banknotes. When a banknote moves between geographical locations, it is indicative of being carried by an individual. As a result, the data collected from such movements can be employed to infer trajectories and patterns of human mobility. Despite being a convenient and extensive source of mobility data, using currency to detect human mobility patterns poses challenges like the lack of information on the number of individuals carrying a specific note. On-site currency transactions made with paper money or bank cards also represent human movements between geographical locations in the physical world.

d) Local Travel Surveys

Local surveys, unlike national censuses, offer more detailed information, such as the purpose of travel, frequency and mode of transport. However, the enhanced accuracy, resolution, and variety of meta-data come with a trade-off in spatial extent, as local surveys cover smaller areas (city or neighborhoods) and involve fewer respondents compared to national censuses, which encompass entire countries. Local surveys are often complemented with additional data sources, like GPS tracks. This integration allows for precise records of an individual's position, combined with annotated descriptions of the purposes of each trip (Liang et al., 2013; Schneider et al., 2013). As data from local surveys are constrained by scale and potential self-reporting errors, both local surveys and national censuses lack the capacity to offer a dynamic and comprehensive portrayal of human mobility (Palmer et al., 2013).

e) Call Detail Records

Given that mobile phones are typically personal devices primarily carried by a single person, mobile phone Call Detail Records (CDRs) are among the most game-changing data technologies of the last decade in the field of human mobility studies. As all major cell phone companies maintain records containing customer information related to calls and text messages, these records incorporate crucial details like the time of the call/message and the specific cell tower responsible for routing the communication. Thus, user's approximate location can be calculated from the geographic coordinates of the cell tower. Unlike currency tracking or traditional data sources such as the national census and local surveys, CDRs provide the capability to characterize individual mobility patterns, often at a relatively high spatio-temporal resolution allowing for a more detailed understanding of how individuals move over time and space. Several concerns related to the quality of this type of data include inconsistent temporal frequency and low accuracy of recorded locations as it describes the position of the cell tower rather that the precise location of the individual carrying the phone. As cell towers have different cover ranges, from dense urban areas (meters) to rural regions (kilometers), an individual in rural areas may transmit all communication via a single tower during their daily routine while an individual in urban areas may ping several towers even while moving the exact equal distance. This variability in tower coverage can result to a user being considered stationary despite actual significant movement. As such data are not publicly available, researchers must directly communicate with mobile phone operators to obtain this data. The sensitivity of CDRs raises confidentiality concerns, leading to restrictions on sharing the data among different research groups. Consequently, the reproducibility of studies utilizing CDRs becomes problematic (De Montjoye et al., 2013).

f) GPS traces

Requiring signals from at least four satellites to provide precise information on locations, GPS datasets offer the highest accuracy in tracking movement trajectories. GPS trackers compute device positions at regular intervals, enabling researchers to trace individuals' movements with accuracy and temporal frequency. Rhee et al. (Rhee et al., 2011) were the first to delve into the statistical properties of human mobility using GPS tracks. Unlike CDRs, GPS traces offer precise measurements of people's positions and velocities with greater precision and constant frequency, but their applicability is limited to outdoor locations due to signal strength constraints. This restriction makes GPS traces unsuitable for applications in small and large indoor environments, such as buildings, airports, or amusement parks. Additionally, large datasets of GPS traces are often not accessible to the scientific community and while cloud-based mobile applications like Google Maps can collect GPS traces from a global user base, these datasets are not publicly available. Nevertheless, initiatives like OpenStreetMap (Haklay & Weber, 2008), which enable users to voluntarily upload individual GPS traces, are a valuable source. Due to all difficulties mentioned before, such datasets typically involve fewer users, around several thousand, compared to mobile phone data, which can include millions of users.

g) Wi-Fi Access Points

Utilizing the dense coverage and distinct MAC addresses of WiFi access points, records are gathered through regular mobile devices by scanning nearby WiFi access points. Given the higher density of WiFi access points compared to cell stations, Aps offer more continuously available location data with increased accuracy, typically below 100 meters (Lin et al., 2010). These datasets provide details such as the device ID, start time, location and duration of access. However, the collection of Aps necessitates individuals to carry additional devices or install specialized smartphone applications, making it labor-intensive and less scalable.

h) Online Social Network

Attracting millions of daily users globally, Online Social Network (OSN) and social media platforms are, nowadays, significant sources of location information. With the integration of GPS and Wi-Fi chips in smartphones, social media platforms, like Instagram, Facebook and many other, gather geotagged data. This data includes geographic coordinates, timestamps, and additional details related to the location or user-generated content like texts, check-ins at certain places or photos. In comparison to CDRs, OSNs' advantages include easy accessibility, large volume and richer contextual information associated with geographical positions, allowing a more comprehensive study of mobility in various contexts (eg. Mood evolution, crisis management, etc.). However, similar to other data sources, there are several limitations like suspiciously high activity, rapid movement between consecutive check-ins, or incomplete data is crucial during data cleanup (Hawelka et al., 2014). Disadvantages also include temporal gaps and spatial discontinuities. Moreover, mobility and interaction data from online social networks require validation to ensure it accurately represents the general population.

i) Public Transport Smart Cards

As all means of public transport, like buses and trains, contain automated fare collection systems nowadays, Public Transport Smart Card (PTSC) records appear valuable resources for understanding the functioning of public transportation systems as well as the mobility patterns of individuals. However, such data exhibit geographical sparsity, incompleteness, and bias towards individuals commuting via public transportation.

j) Bluetooth Detection

Bluetooth Detection (BD) data uses a passive technique to collect data by detecting nearby Bluetooth-enabled devices without requiring active participation from collectors. The unique Bluetooth MAC identifier allows for tracking specific devices, making BD data suitable for studying human mobility within buildings, given the typical 10-meter range of Bluetooth in smartphones (Schauer et al., 2014). Challenges include the need for additional sensor installations in specific locations and the limited availability of Bluetooth-enabled smartphones.

k) Video Tracking

With the plethora of publicly available media from video-sharing platforms like YouTube or Dailymotion, video tracking has become a respected data collection technique for human mobility research. Furthermore, as most cities have deployed security cameras for constant monitoring of crowded environments, such as stadiums and main roads, these videos are particularly useful for understanding crowd dynamics and micro-mobility. While using computer vision techniques to extract specific behavior, ensuring anonymity in video tracking requires considerable effort. However, for videos publicly shared on web platforms like YouTube, individuals appearing in the videos don’t have anonymity. Therefore, utilizing computer vision with public videos is considered a valuable method for extracting certain statistical characteristics of micro-mobility decisions.

Data preprocessing is a crucial step comprising data transformation, which ensures the data is in an appropriate format for subsequent analysis, and noise handling, which is imperative for obtaining reliable results. Noise in mobility data is categorized into two main types. The first type, system noises, encompass biases and errors arising from imperfections in data collection systems and are addressed through interpolation and filtering techniques. On the other hand, human noises manifest as biases and errors introduced by human behavior, predominantly evident in geotagged social media OSN data. Especially in the context of OSN data, human noises have become a significant concern. Social media platforms are primarily used for communication, and geographic tags are user-generated, making the collected data susceptible to users' moods, thoughts, and external incentives (Rost et al., 2013). The handling of human noise in such datasets poses challenges due to the absence of relative information. Consequently, addressing this type of noise becomes a complex task, emphasizing the need for careful consideration when incorporating OSN data into human mobility studies.

Regarding data analysis, the following seven main methods appear in literature.

1. Heuristic Logic: Heuristic logic involves establishing data processing rules based on life experience or common logic. It is frequently utilized in tasks like detecting staying spots from raw location data or identifying places of interest. For instance, setting distance and time thresholds when extracting staying spots from call detail record data.
2. Statistics: Statistical analysis in human mobility research involves three primary types. This includes extracting conclusive statistics from complex mobility attributes or research results, fitting statistical models to describe mobility attributes and conducting statistical tests to evaluate research findings. Examples range from classification evaluation matrices (Ghorpade et al., 2015) to fitting truncated power laws (Hasan et al., 2013) and employing Monte Carlo simulations (Vazquez-Prokopec et al., 2013).
3. Visualization: Data visualization proves to be a potent tool in comprehending mobility data and displaying patterns. Notable visualization formats include scatter plots on maps for visualizing trajectories and significant locations (Ghorpade et al., 2015; Zhong et al., 2016), bar charts or histograms for studying mobility attribute values in consecutive time intervals (Demissie et al., 2016), and heatmaps for revealing spatial or temporal distributions of specific human activities (Jia et al., 2012; Mohamed K. et al., 2017).
4. Graph Theory: This method constructs a graph-based model to explore connections between people's staying or visited places. As a result, daily motifs can be extracted, and complex network models can be built to examine connections between places visited by the same individuals.
5. Optimization: When fitting statistical models or addressing context-fitting problems, optimization techniques are employed. This includes applying maximum likelihood methods to fit distributions to distance values or solving problems like mapping trips to origin-destination pairs.
6. Classification: Classification is applied in mobility research to identify place categories (Hasan et al., 2013), classify people into different profiles (Zhong et al., 2016), and determine individuals' transportation modes (Ghorpade et al., 2015). Various classifiers, such as tree-based models, support vector machines, and artificial neural networks, may be employed, often requiring a trial-and-error process to select the most suitable one.
7. Clustering: Clustering is predominantly used in mobility research to find staying spots and places of Interest (Jia et al., 2012), cluster people based on mobility patterns (Mohamed K. et al., 2017), and group sensing stations by utility patterns (Zhong et al., 2016). Common algorithms include density-based spatial clustering (DBSCAN) and k-means clustering.

3 Geoinformatics in Epidemiology

The integration of geoinformatics into epidemiology has profoundly transformed the way diseases are studied, monitored, and simulated. Traditional epidemiological methods, though valuable, often lacked the spatial and temporal resolution needed to capture the full dynamics of disease spread within heterogeneous populations and complex environments. Geoinformatics provides the tools to address this gap by combining spatial data, GIS, and advanced computational approaches, enabling more accurate analysis of how diseases emerge, spread, and persist across different scales.

This chapter explores the integration of geoinformatics within epidemiology, focusing on its contribution to monitoring, mapping, and modelling disease spread. It begins by examining how health geomatics has shaped the historical evolution of spatial epidemiology, tracing developments from early disease maps to contemporary GIS-based systems. Through this lens, the chapter reviews the advancement of disease mapping techniques—from descriptive cartographic representations to dynamic, data-driven visualizations that enhance the understanding of outbreak patterns and transmission dynamics. The discussion then turns to disease spread simulation methods, where geospatial data and computational modelling converge to represent infection pathways and identify potential hotspots, thereby improving epidemic forecasting and response planning.

Building on this foundation, the chapter introduces ABM as a computational approach increasingly employed in epidemiological research. ABMs simulate the behavior and interactions of individual agents—representing people, places, or institutions—within spatially explicit environments. By capturing heterogeneity, mobility behaviors, and social interactions, ABMs provide a more realistic representation of epidemic processes than traditional aggregate models. They allow complex dynamics such as superspreading events, local clustering, and behavioral adaptation to emerge from individual-level rules. The section also distinguishes between generic epidemiological ABMs and disease-specific applications, emphasizing their respective methodological characteristics and areas of use.

Finally, the chapter highlights the pivotal role of ABMs in the context of the COVID19 pandemic. These models enabled researchers to simulate disease dynamics under varying mobility restrictions and policy interventions, offering valuable insights into public health decision-making. By integrating geoinformatics with agent-based modelling, flexible frameworks were developed for scenario testing, policy evaluation, and real-time epidemic monitoring. This progression, from historical perspectives to modern, spatially explicit ABMs, illustrates how geoinformatics has evolved into an indispensable tool for understanding and managing infectious disease challenges in the 21st century.

3.1. Monitoring Disease Spread

For more than two millennia, scholars have examined the intricate relationship between health and geographical location. This enduring interest gradually shaped a research tradition that, over two centuries ago, led to the creation of the first disease maps (Pickle, 2002). These early efforts laid the groundwork for the formal establishment of epidemiology in the 19th century, where geographers played a decisive role (Krieger, 2003). The visualization of quantitative health data through cartography has a rich history, with numerous examples of pioneering mapping work (Tufte, 2013). Prior to the development of computer-assisted mapping, however, researchers faced significant challenges, particularly in handling large and complex datasets. The emergence of digital computing in the 1960s transformed the field, enabling the growth of quantitative thematic mapping and eventually leading to the development of GIS (Burrough et al., 2015).

A GIS is defined as a computer-based tool for collecting, editing, integrating, visualizing, and analyzing spatially referenced data (Gatrell & Elliott, 2015). In epidemiology, GIS has proven especially valuable for monitoring and managing infectious diseases, particularly vector-borne illnesses, by linking environmental factors to patterns of disease occurrence. In recent decades, GIS has been increasingly employed to manage outbreaks such as Ebola and measles. For example, during the 2014 Disneyland measles outbreak, GIS mapping was instrumental in illustrating the spatial distribution of affected individuals and predicting possible pathways of transmission (Brown, 2015). Similarly, GIS has contributed to monitoring and mitigating malaria, onchocerciasis, and Lyme disease (Gattrell & Loytonen, 1998).

Public health surveillance encompasses several essential functions, including epidemic monitoring, early detection of infections, and the design of health interventions (L. M.

Lee et al., 2010). According to the WHO (2025), surveillance systems serve to (1) track progress toward public health goals, (2) evaluate intervention effectiveness, (3) monitor epidemics and related challenges, (4) establish public health priorities and strategies, and (5) anticipate emergencies. Small states, including islands such as Cyprus, often benefit from their compact populations and lack of land borders, which can facilitate containment strategies (Cuschieri et al., 2022).

The integration of GIS with remote sensing has further enhanced epidemiological research. Risk maps generated through this combination allow researchers to identify environmentally favourable conditions for disease transmission and to develop more targeted intervention strategies (Kazmi & Usery, 2001; Dung et al., 2017). Nykiforuk and Flaman (2011) classified the use of GIS in health research into four main themes: (1) disease surveillance, (2) risk analysis, (3) healthcare access and planning, and (4) community health profiling. Disease surveillance encompasses mapping and modeling, which provide insight into the spatial distribution and dynamics of disease (Wall & Devine, 2000). Risk analysis is the process of evaluating, managing, communicating, and monitoring the impacts on health, while Healthcare accessibility refers to a population's ability to access healthcare services when they are required (Cromley, 2012). GIS allows us to analyze the connections between various factors related to healthcare needs and how these services are provided. Finally, community health profiling helps identify local health needs and environmental determinants, supporting better planning of healthcare resources (Jack & Holt, 2008). For instance, areas lacking access to green spaces might require strategies like prescribing exercise at local gyms since safe parks for walking may not be available. Community health profiling helps establish the connections between individuals and their environments, ensuring that the healthcare needs of diverse communities are adequately addressed (Plescia et al., 2001).

The advantages of GIS in health research are numerous. These include: enhanced availability of geospatial health data (Boelaert et al., 1998), more efficient data collection, the enrichment of datasets through spatial dimensions (Briggs, 2002), and reduced risk of human error via direct geolocation input from digital devices. Moreover, GIS supports environmental health studies (Doi et al., 2013), cost-effective healthcare planning, and improved understanding of the connections between community health and environmental factors such as water quality, air pollution, or access to green spaces (Choi et al., 2006). In summary, GIS plays a crucial role in improving the efficiency, accuracy, and depth of health informatics research. It empowers researchers to explore complex relationships between health and the environment, ultimately contributing to more effective healthcare planning and decision-making.

Nevertheless, several limitations must also be acknowledged. GIS analyses depend heavily on the quality and availability of spatial health data, which can be uneven across regions (Boelaert et al., 1998). Methodological variability between different GIS software can affect research outcomes, while ethical issues, particularly concerning confidentiality of geospatial health data, pose additional challenges (Ölvingson et al., 2002).

A comprehensive review of 132 studies published between 1978 and 2020 highlights two primary domains in which GIS has advanced health research: epidemic surveillance and modeling, and the evaluation of healthcare accessibility and spatial inequalities (Khashoggi & Murad, 2020). These findings confirm the central role of GIS in linking epidemiological data with spatial analysis, thereby enabling more effective disease surveillance, healthcare planning, and resource allocation.

3.1.1 A Brief History of Health Geomatics

The evolution of health geography has played a fundamental role in shaping modern spatial epidemiology, highlighting the importance of place, environment, and human activity in disease dynamics (Tsatsaris, 2026). These approaches emphasize the integration of spatial data and geographic analysis in understanding and managing public health challenges. The relationship between health and geography can be traced back to antiquity. Hippocrates, often regarded as the father of medicine, was among the first to systematically explore how environmental and locational factors affect human health. In his treatise On Airs, Waters, and Places, he noted that populations living in mountainous areas with variable climates and abundant clean water tended to be more resilient and vigorous, while those residing in low-lying, humid regions were more prone to illness. He further theorized that proximity to stagnant waters could increase susceptibility to diseases such as malaria, thereby linking geography, environment, and health centuries before the concept of epidemiology was formally established.

This spatial awareness of health continued through the work of other early scholars. Around the 9th century, the Persian physician Al-Razi demonstrated an applied form of spatial reasoning when selecting the site for a hospital in Baghdad. By placing pieces of meat across different city locations and monitoring the rate of decay, he chose the site where the meat remained fresh the longest, interpreting this as an indicator of clean air and healthy environmental conditions. This method, though rudimentary, reflects an early form of spatial health assessment based on environmental suitability.

The earliest known spatial health map dates back to 1694 in Bari, Italy, created by royal auditor Philip Arrieta (fig.9) to document and manage the spread of plague (Koch, 2005). His cartographic representation incorporated three essential spatial strategies of containment, such as coastal patrols, quarantine walls, and military cordons. The map employed visual symbols (churches, hospitals, and natural features) to illustrate disease distribution and containment measures, offering one of the first examples of mapping used directly for epidemic management.

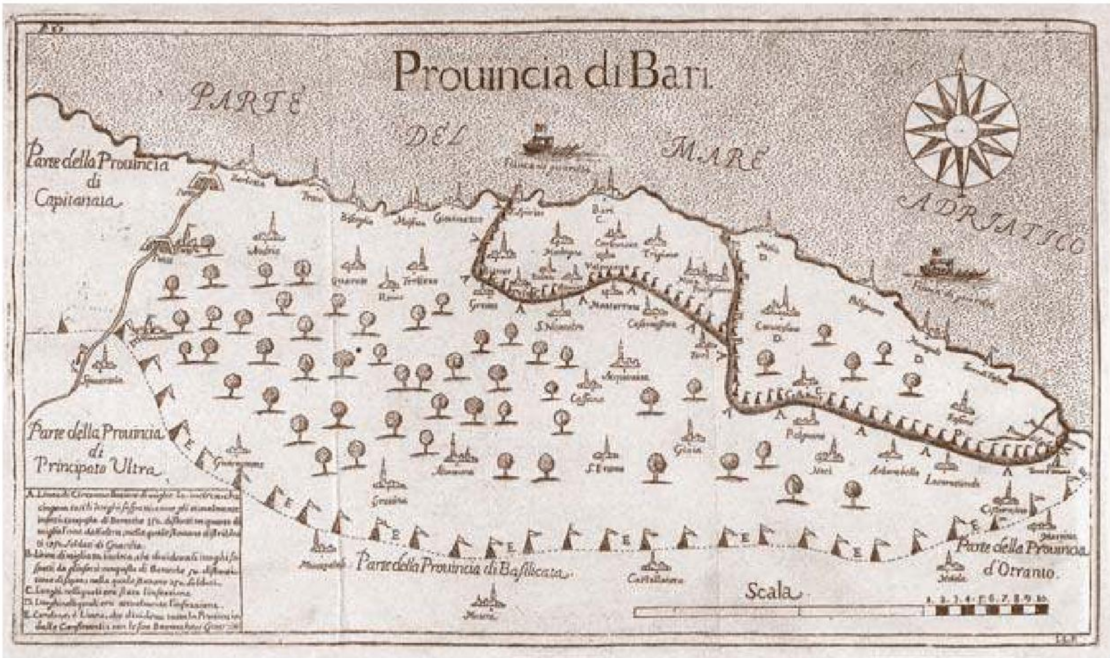

Figure 9. The first spatial health map of the plague disease in Bari, Italy, 1694. Cities were depicted using simple illustrations, either as churches (marked with a cross) or hospitals (lacking a cross), while trees symbolized uninhabited areas.

The field advanced significantly in 1854 during the London cholera epidemic. John Snow's (1855) now-iconic cholera map (fig. 10) marked the beginning of modern epidemiology and spatial health analysis. By plotting cholera cases in relation to streets, households, and water pumps, Snow demonstrated that the disease was transmitted through contaminated water rather than airborne “miasma”. Dr. Snow, now acknowledged as the father of modern epidemiology, adopted an innovative approach to combat the epidemic by creating spatial maps that incorporated various important elements related to the disease, such as outbreak sites, roadways, property boundaries, and water distribution lines. When these elements were added onto the map, a striking pattern emerged, revealing that cholera cases were concentrated along the water lines, notably around a specific water pump where a significant number of deaths (depicted in black on the map) occurred. Consequently, the spatial maps provided proven evidence that cholera was disseminated through water, countering the prevailing belief that the disease spread via airborne transmission. His innovative use of spatial mapping not only helped halt the outbreak but also laid the foundation for epidemiological cartography and the future development of GIS.

Figure 10. Spatial distribution of cholera cases in London, England, produced by Dr. Snow, 1854.

Another milestone came in 1875 with Alfred Haviland’s publication of an atlas mapping cancer mortality across England and Wales (fig.11). His color-coded maps revealed regional patterns of high cancer prevalence, thereby highlighting the role of environmental factors in disease risk and illustrating how spatial data could inform public health planning and intervention (Arnold-Forster, 2020).

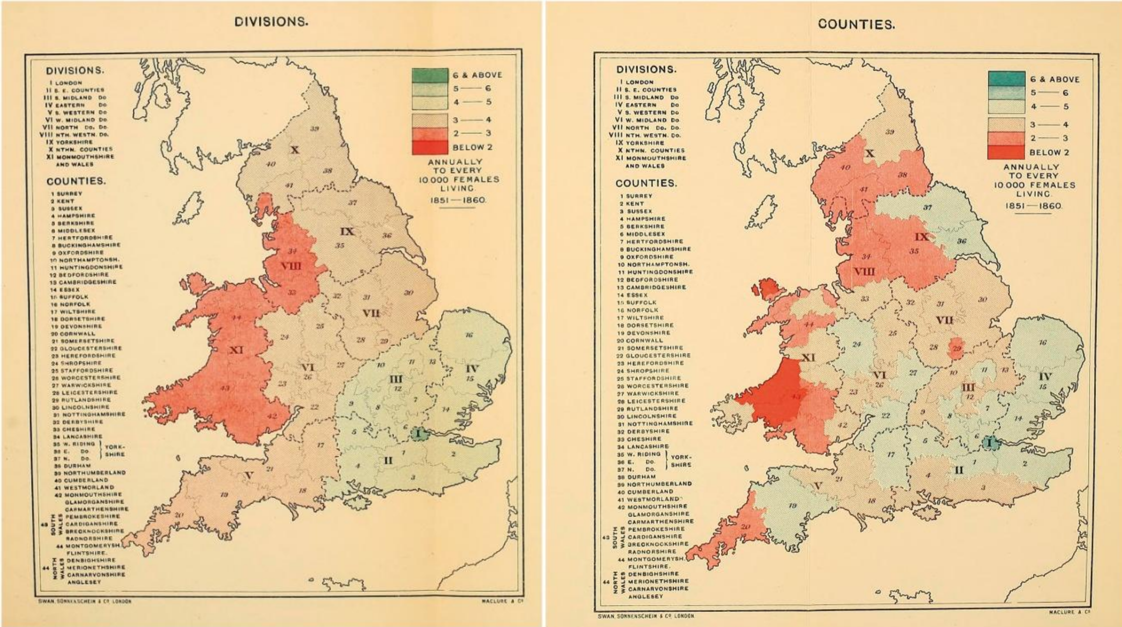

Figure 11. One of the atlas maps of geographical distribution of cancer disease in the Divisions and Counties of England and Wales, produced by Haviland, 1875.

The transition from traditional paper-based maps to digital tools began in the 1960s with the emergence of computer-assisted cartography. This technological shift provided the foundation for GIS, making it possible to store, manipulate, and analyze large spatial datasets with increasing accuracy and efficiency (Clarke, 1996). During the 1970s and 1980s, GIS applications expanded into multiple scientific fields, including public health, where they were used to optimize hospital placement, integrate urban and health planning, and support epidemiological research. By the 1990s, institutions such as the U.S. Centers for Disease Control and Prevention (CDC) had formally incorporated GIS into disease surveillance and healthcare resource allocation (Croner, 1998). Leveraging this technology, the CDC has been at the forefront of enhancing public health through various initiatives such as disease surveillance, resource allocation for healthcare, environmental risk assessment, and the management, analysis, and modeling of spatial data. The CDC's initial mission with GIS implementation was focused on preventing the spread of malaria within the United States.

The turn of the 21st century marked a period of rapid advancement in spatial health applications. In 2006, the U.S. Environmental Protection Agency used GIS to investigate an outbreak of West Nile virus in Pennsylvania, mapping vector ecology and transmission pathways to trace the virus’s spread Through a comprehensive analysis of various contributing factors like mosquitoes, blood transfusion, breastfeeding, and hospital infection, the agency successfully identified the virus's point of origin and mapped its transmission extent, particularly through healthcare centers, utilizing GIS technology.. Around the same time, the CDC and World Health Organization (WHO) jointly developed the Atlas of Heart Disease and Stroke using ArcGIS technology, a landmark project highlighting how geospatial analysis could be applied globally to major non-communicable diseases. According to the WHO (World Health Organization, 2004), heart disease and stroke claim the lives of nearly 17 million individuals each year, with smoking and an unhealthy diet being key contributors to these health issues.

Today, many countries deploy advanced GIS-enabled surveillance systems for infectious disease control. These systems allow real-time monitoring and spatial prediction of outbreaks, providing critical support for rapid response. However, significant challenges remain, particularly in low-resource settings, where limited infrastructure, inadequate training, and insufficient funding hinder effective system implementation (Mandyata et al., 2017). Despite these constraints, the integration of GIS into epidemiology represents one of the most significant methodological advances in modern public health, enabling researchers and policymakers to better understand and manage the complex interplay between geography, environment, and disease.

The historical trajectory of health geomatics illustrates how the integration of geography and health has gradually evolved from observational theories and rudimentary mapping practices into sophisticated, technology-driven systems. Each milestone, from Hippocrates' environmental observations to Snow's cholera map and the institutional adoption of GIS by organizations such as the CDC and WHO, demonstrates the growing recognition of spatial data as an indispensable tool in public health. Building on this historical foundation, the following section focuses on disease mapping as a distinct and practical application of geomatics in epidemiology. This approach not only enhances the understanding of disease distribution and transmission but also provides actionable insights for prevention, control, and health policy planning.

3.1.2 Disease Mapping and Simulation

Advancements in computing technology, statistics, and data accessibility have opened new opportunities for epidemiological research with a strong geographical dimension.

Disease mapping is one of the most fundamental applications of GIS, enabling researchers and policymakers to visualize spatial variations in health outcomes, identify unusual patterns, and investigate associations with environmental risk factors. While basic mapping remains central, modern GIS also supports advanced spatial analyses that allow for a deeper understanding of disease dynamics and the factors influencing their distribution. The usefulness and reliability of disease maps depend largely on the availability, accuracy, and quality of underlying data, as well as the analytical methods applied. Hence, although disease maps are powerful tools, they must be used with caution to avoid misinterpretation or biased conclusions.

According to Lawson (1999; 2000), the objectives of disease mapping can be grouped into three major categories. First, maps serve to describe spatial variation in disease incidence, allowing researchers to develop hypotheses on potential causal factors. Second, they help identify high-risk areas, which is critical for targeted prevention and intervention strategies. Third, disease mapping contributes to producing reliable risk maps, which can inform public health planning by guiding the allocation of healthcare resources and improving preparedness for future outbreaks. These functions highlight the dual role of disease mapping as both a scientific research tool and a practical decision-making instrument in public health.

Different cartographic techniques can be employed to represent disease incidence and risk patterns. Four common types of disease maps are outlined by Kistemann et al. (2002). Dot maps provide precise spatial references for individual health events using coordinate points. Choropleth maps rely on shading or colors to represent morbidity or mortality rates across defined geographical units, facilitating pattern recognition at a regional level. Flow maps illustrate temporal and spatial dynamics, capturing how diseases spread or recede over time. Finally, diagram maps integrate additional quantitative information into a spatial framework, enhancing interpretability. Beyond these traditional methods, advances in GIS have introduced the use of animated maps, which are particularly effective in visualizing the spread of communicable diseases over time and space.

The effectiveness of disease maps also depends on several methodological considerations. Two widely used approaches are maps of standardized rates and maps of statistical significance. While standardized rates help estimate disease frequency across regions, they can be unreliable in areas with small populations or limited case numbers, where random fluctuations may distort results.

Equally important are design choices such as colour schemes, the number of categories, and cutoff points, which can significantly influence interpretation. As Elliott et al. (1996) caution, maps can unintentionally, or even deliberately, create misleading impressions depending on how data is classified or visualized. For this reason, consistency in scale and presentation across multiple maps is crucial when comparing risks between different areas.

Despite these methodological strengths, the use of GIS in disease mapping does not fully resolve two persistent challenges: data availability and data quality. Errors in spatial data, whether from imprecise measurements, aggregation, or reporting biases, can undermine the validity of analyses. A key issue is the so-called scale effect, whereby patterns observed at one geographical level (e.g., provinces) may differ significantly when examined at a finer scale (e.g., neighbourhoods or grid cells). While finer spatial resolution often provides more epidemiologically relevant insights, it also raises concerns about misinterpretation, increased analytical costs, and potential breaches of individual privacy. Balancing specificity with confidentiality remains a critical consideration, especially when dealing with sensitive health data. Choosing the right analysis scale or level of data aggregation involves a trade-off between specificity and precision: smaller geographic areas provide more specific and locally relevant findings but also introduce more imprecision and potential bias.

Finally, the practical implementation of disease mapping often requires the integration of multiple software tools. Epidemiological data may need to be analysed statistically or modelled before being reintegrated into GIS platforms for visualization. This iterative process underscores the interdisciplinary nature of disease mapping, combining elements of epidemiology, statistics, computer science, and cartography. When effectively applied, disease maps become indispensable tools for monitoring health disparities, tracking outbreaks, informing interventions, and ultimately improving population health outcomes.

In summary, disease mapping provides a powerful foundation for understanding the spatial distribution of health outcomes, identifying high-risk areas, and informing targeted interventions. However, while maps are essential for visualizing past and present disease patterns, they offer limited predictive capacity. To address this gap, modern epidemiology increasingly relies on simulation models that integrate spatial data, demographics, and behavioural factors to anticipate how diseases might spread under different scenarios. The next section, therefore, shifts from descriptive mapping to the simulation of disease spread, highlighting how computational models complement GIS by enabling dynamic forecasting and supporting proactive public health decision-making.

The simulation of disease spread has emerged as a central pillar of modern epidemiology, offering a way to anticipate epidemic trajectories, evaluate intervention strategies, and improve preparedness for future outbreaks. While traditional mathematical models such as the SIR (Susceptible–Infected–Recovered) framework provided the foundation for epidemiological analysis, the increasing complexity of modern societies, coupled with advances in computational power and data availability, has paved the way for more sophisticated modelling approaches. While several modelling approaches exist, two main frameworks dominate the literature: ABM and metapopulation models. Although both have contributed valuable insights, ABM provides a more detailed, flexible, and realistic representation of epidemic processes, making it especially suitable for high-resolution studies such as the one undertaken in this dissertation.

Agent-based modelling is a bottom-up approach where each individual in a population is represented as a distinct "agent" with specific attributes, behaviours, and interaction patterns. This framework enables researchers to capture heterogeneity across the population, such as differences in age, occupation, mobility, or compliance with interventions, while also accounting for stochasticity in individual interactions. Unlike aggregate models, ABM can incorporate behavioural adaptations (e.g., mask use, social distancing, vaccine uptake) and simulate complex phenomena such as super-spreading events, clustered outbreaks, and the localized effects of interventions. During the COVID19 pandemic, ABM proved particularly powerful in assessing the impact of layered policies such as school closures, workplace restrictions, and targeted lockdowns, offering detailed insights into the micro-level mechanisms that drive macro-level epidemic dynamics. The main limitation of ABM, its need for granular and sometimes hard-to-obtain data, can increasingly be mitigated through the use of digital mobility traces, census data, and high-performance computing, thereby strengthening its role as the most realistic framework available for epidemic simulation.

In contrast, metapopulation models adopt a higher-level view, dividing the population into subgroups (e.g., cities, regions) and assuming homogeneous mixing within each subgroup. While Initially introduced in the context of ecology (Hanski, 1998), this approach has the advantage of analytic tractability and lower data requirements but it often fails to capture the heterogeneity of individual behavior or the fine-scale spatial and social structures that drive disease transmission. For example, metapopulation frameworks such as the Global Epidemic and Mobility model (GLEaM) (Balcan et al., 2009) have been useful for understanding the global spread of influenza-like illnesses or the role of international travel in the early stages of COVID19. However, their simplifying assumptions limit their capacity to model behavioural dynamics, local interventions, or heterogeneous compliance—all of which proved crucial in shaping epidemic outcomes.

Both agent-based modeling and metapopulation modeling offer valuable insights into the spread of epidemics, allowing researchers to explore realistic scenarios and understand how individual behaviors or population structures influence the dynamics of infectious diseases. The choice between these frameworks often depends on the specific characteristics of the epidemic under study and the level of detail required for the analysis. Future directions for these models may involve incorporating real-time information and communication technology (ICT) data on mobility, as suggested by many studies (Jia et al., 2012; Tizzoni et al., 2014). Additionally, there is potential for exploring hybrid frameworks that combine elements of both agent-based and metapopulation modeling, as proposed in (Ajelli et al., 2010). These advancements could enhance the accuracy and adaptability of epidemic spreading models in response to dynamic and evolving scenarios.

The strengths of ABM make it particularly well-suited for contexts where localized interactions and behavioral variability are decisive, as was the case during COVID19. Unlike metapopulation models, which prioritize scalability at the expense of granularity, ABM enables the exploration of what-if scenarios grounded in realistic individual and household-level dynamics. For public health planning, this translates into the ability to design more nuanced, adaptive, and context-sensitive interventions rather than one-size-fits-all strategies. Importantly, ABM's flexibility also allows for integration with real-time data streams, such as mobile phone mobility data, digital contact tracing outputs, or genomic sequencing, thus bridging the gap between static models and dynamic epidemic realities.

Looking ahead, the increasing availability of high-resolution data and advances in computational resources are expected to further enhance the applicability of ABM. Hybrid models that integrate ABM with metapopulation structures may provide a useful compromise for very large-scale simulations. However, the clear trend in epidemiological research points toward agent-based approaches as the gold standard for capturing the complex interplay of biology, behavior, and environment in epidemic spread.

This dissertation builds upon this paradigm, employing ABM as the primary framework for simulating disease transmission and evaluating intervention strategies in a way that is both empirically grounded and policy-relevant. The following section (3.2) delves deeper into the foundations and components of agent-based modeling. Specifically, it examines the representation of agents and their mobility behaviors, the role of social relationships and environments, the development of epidemiological ABMs, and their application to the study of COVID19.

3.1.3 Combating COVID19

A significant portion of COVID19 research has relied heavily on geographic data analyzed through GIS and spatial statistical tools. These approaches have proven critical in multiple dimensions of the pandemic response. They help clarify the dynamics of spatial transmission, improving communication with health officials, policymakers, and affected communities (Desjardins et al., 2020). They also enhance the accuracy of infection estimates, facilitate the early detection of emerging outbreaks, and contribute to more effective public health interventions (Coccia, 2020). Moreover, geospatial methods support the optimization of healthcare service locations, leading to faster response times, better allocation of resources, and improved patient outcomes (Kuupiel et al., 2020). Mapping human mobility patterns through geospatial analysis has further enabled the design of scientific, policy, and social measures adapted to the challenges of the pandemic (Chan et al., 2020; Mollalo et al., 2020). Finally, predictive spatial modeling has assisted in anticipating the potential geographic spread of the disease, offering essential insights for planning and preparedness (Giuliani et al., 2020). In sum, geoinformatics has empowered public health systems by enabling better-informed decision-making, strategic planning, and community-level mobilization against COVID19.

In a world where diseases can spread rapidly across borders, timely dissemination of information becomes critical. Modern GIS technologies have emphasized real-time data, web-based tools, and efficient data sharing to support rapid responses. Among these, interactive dashboards proved indispensable in conveying information about the spread of SARS-CoV-2 to both specialists and the wider public (Esri China, 2021). Dashboards not only enhanced transparency but also allowed individuals and communities to stay informed and take protective measures, while supporting authorities in managing communication and fostering trust.

The most prominent global examples were the dashboards developed by Johns Hopkins University – JHU (fig.12) and the WHO (fig.13).

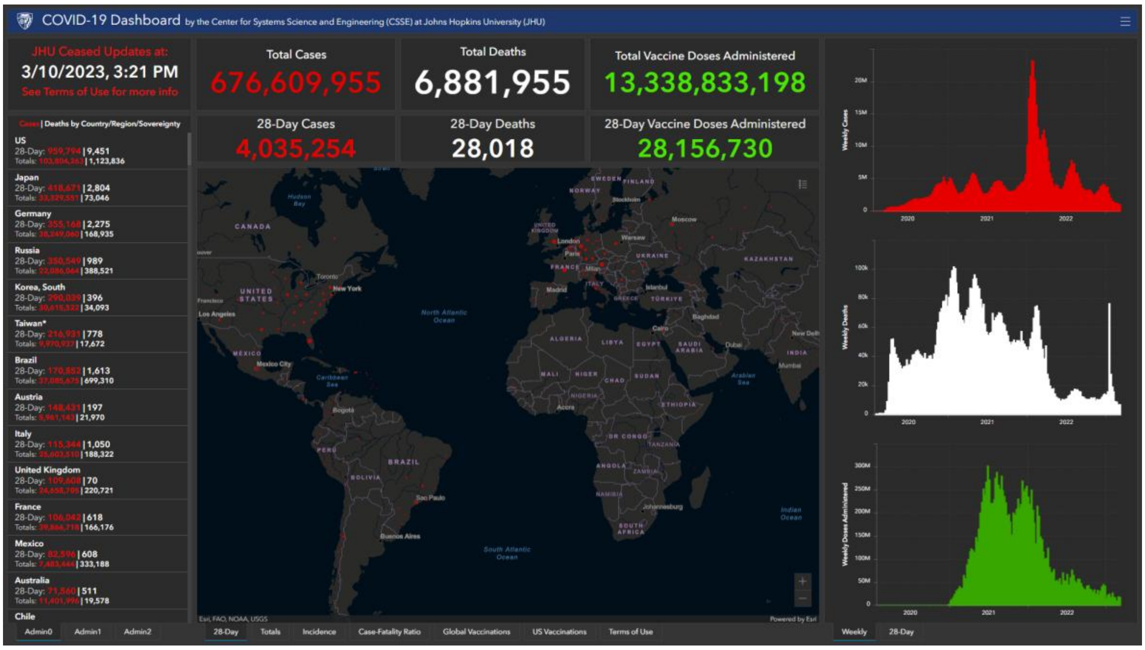

Figure 12. After three years of continuous operation, Johns Hopkins discontinued its COVID19 dashboard in March 2023. The two raw data repositories remain accessible for data collected between 1/22/20 and 3/10/23, including cases, deaths, vaccines, testing, and demographics: https://www.arcgis.com/apps/dashboards/bda7594740fd40299423467b48e9ecf6.

The JHU CSSE dashboard, launched on January 22, 2020, by Lauren Gardner and her team, rapidly became the most recognized platform for near real-time updates on confirmed cases, fatalities, and recoveries worldwide. Its interactive map and data visualizations were widely cited by the media and researchers, setting the standard for pandemic data communication (Johns Hopkins, n.d.). The JHU CSSE dashboard features an interactive map that pinpoints and tallies confirmed cases, fatalities, and recoveries while graphs provide insights into the virus's progression over time. Thus, users were gaining access to information on the most recent data update, including the date, time, and data sources. Similarly, the WHO dashboard provided global statistics and country-level updates on confirmed cases, deaths, and vaccination progress, serving as an authoritative reference for governments and international organizations.

The WHO introduced its own interactive online dashboard, delivering country-level reports on confirmed cases, daily death counts, and evolving trends (WHO COVID19 Weekly Epidemiological Updates and Monthly Operational Update Reports, n.d.).

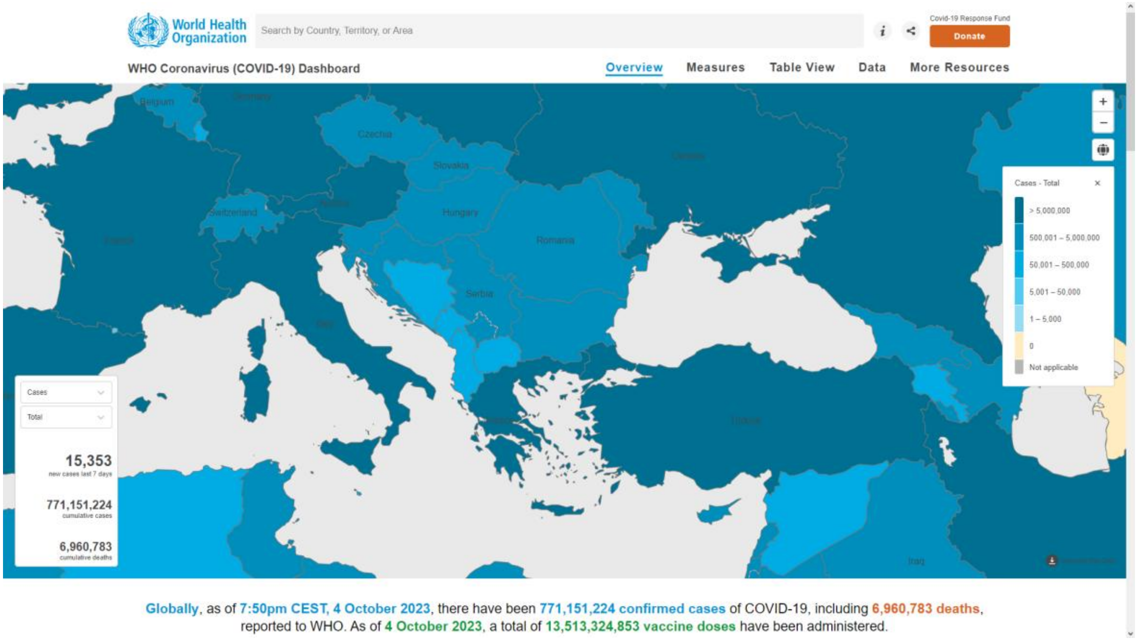

Figure 13. The WHO COVID dashboard (https://covid19.who.int). Source: The WHO COVID19 Dashboard, 2021

Beyond visualization, GIS and spatial statistics were widely applied to explore correlations between COVID19 patterns and environmental factors such as temperature, wind speed, solar radiation, and humidity (Paez et al., 2021). Hotspot analyses were used to identify clusters of confirmed cases, deaths, or vulnerable populations, guiding timely interventions and highlighting patterns of risk for healthcare workers and first responders. Proximity and network analyses assessed access to healthcare facilities, revealing disparities in resilience across urban areas (Jovanović et al., 2020). Spatial statistical methods such as Global and Local Moran's I, spatial autocorrelation, and Local Indicators of Spatial Association (LISA) were also employed to uncover clustering of cases and assess how different communities were disproportionately affected, including the relationship between socio-demographic variables (e.g., race, income) and COVID19 mortality rates.

Finally, the flexibility of GIS software and statistical platforms played an important role. Tools like ArcGIS and open-source alternatives (e.g., QGIS, RStudio) enabled both advanced analyses and web-based application development for contact tracing and surveillance. Platforms like RStudio and its ecosystem provide robust support for both statistical and spatial analyses (Bivand, 2021). The use of open data and open-source software further promoted reproducibility and accessibility, especially for underserved communities. A notable example is the work of Paez et al. (2021), who conducted open and reproducible spatial analyses by sharing both their data and code publicly, setting a valuable precedent for transparent scientific research.

3.2 Agent-based Modelling (ABM)

ABM represents a computational paradigm that conceptualizes complex systems as a collection of autonomous, self-governing entities, agents, whose behaviors and interactions give rise to emergent system-level patterns. Unlike traditional top-down approaches, ABM is rooted in the principles of complexity science, where macroscopic dynamics are not imposed but instead emerge organically from the micro-level rules governing individual actors (Grimm et al., 2010). The Overview, Design concepts and Details (ODD) protocol for describing Individual-and ABMs is now widely accepted and used to document such models in journal articles. As a standardized document for providing a consistent, logical and readable account of the structure and dynamics of ABMs, some research groups also find it useful as a workflow for model design. Even so, there are still limitations to ODD that obstruct its more widespread adoption. Such limitations are discussed and addressed in this paper: the limited availability of guidance on how to use ODD; the length of ODD documents; limitations of ODD for highly complex models; lack of sufficient details of many ODDs to enable reimplementation without access to the model code; and the lack of provision for sections in the document structure covering model design rationale, the model's underlying narrative, and the means by which the model's fitness for purpose is evaluated. We document the steps we have taken to provide better guidance on: structuring complex ODDs and an ODD summary for inclusion in a journal article (with full details in supplementary material; Table 1); using ODD to point readers to relevant sections of the model code; update the document structure to include sections on model rationale and evaluation. We also further advocate the need for standard descriptions of simulation experiments and argue that ODD can in principle be used for any type of simulation model. Thereby ODD would provide a lingua franca for simulation modelling (Bonabeau, 2002; Grimm et al., 2020). This bottom-up framework is particularly suited to epidemiology, where the spread of infectious diseases is inherently shaped by individual-level heterogeneity, stochasticity, and social structures.

At its core, ABM is built upon three fundamental components: (i) agents, (ii) relationships, and (iii) the environment. Agents are autonomous units that possess attributes, decision-making capacities, and behavioural rules. They interact with other agents and their environment in ways that may be cooperative, competitive, or adaptive. Relationships define the structures and mechanisms by which agents connect (social, spatial, or organizational) while the environment provides the spatial or contextual domain in which interactions unfold. Together, these components allow ABMs to replicate dynamic processes, capturing not only the outcomes of individual decisions but also the emergent properties of the system as a whole. In epidemiological contexts, agents often represent individuals, households, or groups, whose daily routines, social contacts, and mobility patterns collectively determine the trajectory of disease transmission.

The strength of ABM lies in its ability to represent heterogeneity, nonlinearity, and adaptation. In his study, (Axtell, 2000) explores various reasonings for employing agent-based modeling while (Bonabeau, 2002) identifies several conditions under which ABM is particularly effective: (a) when interactions are complex, nonlinear, or discrete, (b) when space plays a central role and agents occupy dynamic positions, (c) when the population is heterogeneous, (d) when the interaction topology is complex and (e) when agents exhibit adaptive or intricate behaviours.

Complementing this, Macal & North (2014) emphasize that ABM is most appropriate when:

- The system relies on the development of new dynamic mechanisms, not solely on historical data.
- The system naturally involves agents as a representation.
- There is a need to accurately represent individual behavior.
- Agents' decisions, choices, and behaviors can be precisely described.
- Individual agents exhibit a spatial component in their behaviors and interactions.
- The system comprises a large number of agents, states, and interactions.
- Individual agents form groups, modify their behaviors, engage in learning, and employ dynamic interactions.
- Individual agents maintain dynamic relationships with other agents.
- It is crucial to model agents' abilities to adapt, learn, network, and form groups.

Epidemiology naturally satisfies most of these conditions, underscoring the suitability of ABM as a methodological framework for studying infectious disease dynamics.

Nevertheless, several methodological considerations must be addressed when developing ABMs. First, it is essential to define the model's purpose and scope, since highly general frameworks often lack the explanatory power of models tailored to specific research questions. Second, the representation of agents is particularly challenging, as human behavior is frequently irrational, context-dependent, and shaped by unobservable or difficult-to-quantify factors. Agents operate based on objectives and goals, engaging in interactions guided by specific relationship rules that shape their behavior. Their social dynamics are captured through interaction and grouping protocols that incorporate specific mechanisms (fig.14). These complexities necessitate careful model calibration and validation. Third, computational requirements are non-trivial: as models grow more detailed and incorporate larger populations, they become increasingly demanding in terms of memory, runtime, and processing power. This trade-off between granularity and feasibility remains a recurring challenge for ABM practitioners.

Despite these challenges, ABM provides a distinctive flexibility that mathematical or equation-based models often lack. It can incorporate spatial heterogeneity, explicit social networks, and diverse behavioral patterns while preserving the ability to examine emergent outcomes across multiple scales. For infectious disease modeling, this means that ABM can represent fine-grained spatiotemporal processes, capture the effects of behavioral interventions, and simulate alternative scenarios that account for uncertainty and adaptation. Agents interact in each time step based on predefined attributes and decision rules, engaging with both their environment and other agents, allowing the unfolding of epidemic trajectories to be observed and analyzed.

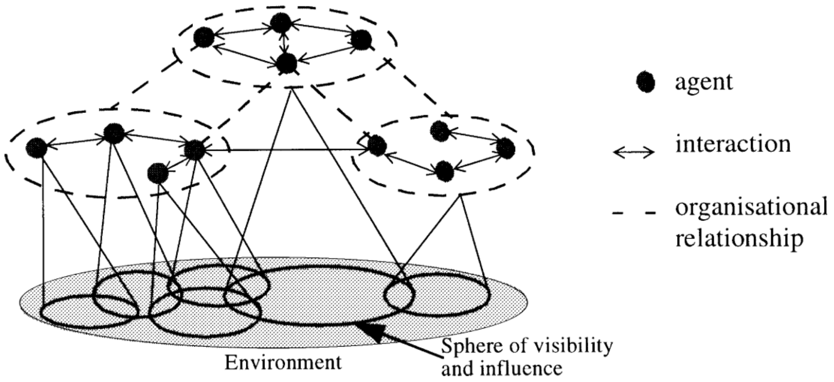

Figure 14. The essential concepts of agent-based computing (Jennings, 2000).

However, one significant drawback of the ABM approach is the need for multiple model executions to assess the robustness of results. A single execution may not provide sufficient information about the theory's solidity, whereas multiple executions with varying initial conditions and parameters can yield insights into the impact of these changes on the results.

Historically, early large-scale applications of ABM were pioneered within the TRANSIMS (Transportation Analysis Simulation System) project at Los Alamos National Laboratory during the 1990s. Originally designed to simulate daily activities in Portland, Oregon, incorporating census data on population, mobility, and socioeconomic characteristics, TRANSIMS was later adapted to study epidemic evolution (Simon et al., 1999). Building on this foundation, EPISIMS (Epidemic Disease Simulation System) applied ABM techniques to evaluate intervention strategies against smallpox outbreaks (Eubank et al., 2004). Similar frameworks were subsequently developed to examine the spread of avian influenza (H5N1) in Southeast Asia, assessing policy interventions and mobility restrictions. During the 2009 H1N1 influenza pandemic, ABMs gained further traction across Europe, where they were used to evaluate mobility-based interventions, vaccination strategies, and risks associated with laboratory-generated virus strains (Merler et al., 2013). These historical milestones highlight ABM's growing role in epidemiology, as it evolved from transportation modeling into one of the most powerful tools for simulating epidemic dynamics.

Beyond epidemiology, ABM has been widely adopted across diverse fields, including archaeology (Cegielski & Rogers, 2016), environmental planning (Zellner, 2008), air traffic control (Conway, 2006), social psychology (Smith & Conrey, 2007), disaster management (Bae et al., 2018), crime analysis (Malleson et al., 2013), ecology (Testa et al., 2012), economics (Bookstaber, 2012), energy systems (J. Chen et al., 2012), agriculture (Leyk et al., 2009), immunology (Folcik et al., 2007), healthcare and pharmaceutical R&D (Hunt et al., 2013), and marketing (Kuhn et al., 2010; North et al., 2010). A summary of selected applications across thematic areas is provided in Table 1.

Table 1. Examples of agent-based applications found in literature, per thematic area.

Thematic Area	ABM Focus
Archaeology	Trends in archaeological simulation including ABM (Cegielski & Rogers, 2016)
Environment	Overview of agent-based modeling for environmental planning and policy analysis Planning (Zellner, 2008)
Air Traffic Control	Air traffic control to analyze control policies and performance of an air traffic management facility (Conway, 2006)
Social Psychology	Using ABM for theory building in social psychology (Smith & Conrey, 2007)
Natural disasters	Evaluation of Disaster Response System Using With Geospatial and Medical Details (Bae et al., 2018)
Crime Analysis	A realistic virtual urban environment, populated with virtual burglar agents (Malleson et al., 2013)
Ecology	Predator-prey relationships between transient killer whales and other marine mammals (Testa et al., 2012)
Economics	Using ABMs for analyzing threats to financial stability (Bookstaber, 2012)
Energy Analysis	A building occupant network energy consumption decision-making model (J. Chen et al., 2012)
Agriculture	A spatial individual-based model prototype for assessing potential pesticide exposure of farmworkers conducting small-scale agricultural production (Leyk et al., 2009)
Biomedical	The Basic Immune Simulator, to study the interactions between innate and adaptive immunity (Folcik et al., 2007)
Healthcare	A systematic assessment of use cases and requirements for enhancing pharmaceutical research and development productivity through agent-based modeling (Hunt et al., 2013)
Market Analysis	Consumer marketing model developed with a Fortune 50 firm (North et al., 2010) Consumer airline market share (Kuhn et al., 2010)

In parallel, a number of ABM software platforms have emerged, significantly expanding accessibility and standardization of agent-based simulation. Some of the most prominent include RePast (*The Repast Suite*, 2025), AnyLogic (*AnyLogic Simulation Software*, 2025), GAMA (*GAMA Platform*, 2025) and NetLogo (*NetLogo Software*, 2025). These platforms provide integrated environments for model design, execution, visualization, and analysis, supporting applications across disciplines. Their continued development has facilitated the dissemination of ABM methods within epidemiology and beyond, enabling the exploration of complex systems through flexible, user-driven simulation approaches.

In contrast to mathematical modeling, where concepts can be precisely formulated and communicated using formal mathematical notation, early applications of ABM encountered substantial challenges in terms of clarity and reproducibility. One of the main limitations was the absence of a standardized workflow protocol, which often resulted in incomplete, ambiguous, or inconsistent model descriptions. This lack of methodological rigor severely hindered replication efforts and made it difficult to compare models across studies. The recognition of these shortcomings highlighted the need for a unified framework that could ensure transparency, reproducibility, and comparability of ABM studies, ultimately leading to the development of the ODD protocol.

The ODD framework (acronym for Overview, Design concepts, and Details) was introduced as a standardized language for documenting ABMs. Its primary objective is to improve the transparency and completeness of model descriptions, thereby addressing one of the central criticisms directed at ABMs, their perceived irreproducibility. As Grimm et al. (2010) emphasize, the goal of ODD is to provide model descriptions that are at once sufficiently detailed to allow replication, yet clear and concise enough to be easily understood by researchers across disciplines.

The ODD protocol structures ABM documentation into three main categories:

1. Overview, presenting the purpose, state variables, and scale of the model.
2. Design concepts, articulating the key design principles, including adaptation, emergence, interaction, stochasticity, and observation.
3. Details, describing the initialization process, input data, and submodels in sufficient technical detail to enable replication.

In practice, this structure corresponds to seven elements (fig.15), which together create a consistent blueprint for communicating model design, assumptions, and mechanisms. While not overly technical, the ODD format deliberately emphasizes accessibility, making ABM descriptions easier to write, read, and reproduce, irrespective of the hardware or software used for implementation.

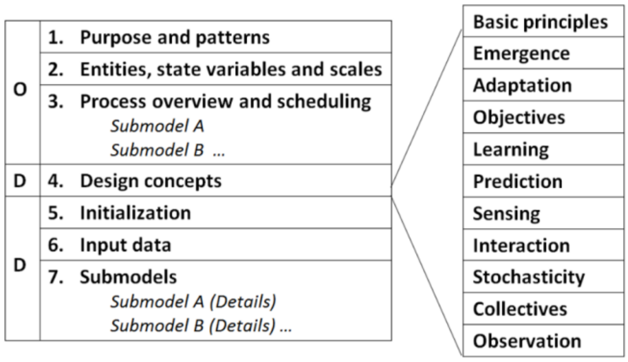

Figure 15. The structure of model descriptions - ODD protocol (Grimm et al., 2020).

The adoption of ODD has contributed significantly to the standardization and cumulative advancement of ABM research. It has facilitated model comparison, reuse, and extension, while also promoting transparency and accountability in the modeling process. Increasingly, new ABM frameworks and applications incorporate ODD as a core component of their documentation process. For example, the COMOKIT model (Gaudou et al., 2020), developed to simulate COVID19 transmission dynamics, explicitly adopts the ODD protocol (*O.D.D. Description of the COMOKIT Model*, 2020) to ensure clear, replicable reporting of its structure, assumptions, and mechanisms.

3.2.1 Agents, Mobility and Environments

Artificial individual entities known as agents lie at the core of ABM, representing autonomous units designed to execute predefined tasks and interact within a virtual environment. Agents can be conceptualized as digital individuals, endowed with attributes and behaviors that enable them to move, adapt, and interact with one another and with their surroundings. As described by (Jennings, 2000), agents are clearly identifiable entities with distinct boundaries and interfaces, situated in a particular spatial environment and engineered to serve a specific purpose. They possess autonomy, modularity, and the ability to engage in social interactions, while their states can change conditionally over time based on internal attributes and external influences. Importantly, complex behavioral patterns are not explicitly coded but rather emerge from the local interactions between agents, making ABMs a powerful framework for simulating collective dynamics.

A typical agent-based system endows its agents with several defining properties:

- Autonomy, the ability to act independently without centralized control. Agents act independently within the environment, free from external influences, and interact with other agents
- Modularity, whereby each agent is a self-contained functional unit with distinct attributes, behaviors, and decision-making capabilities.
- Sociality, the capacity to communicate, exchange information, and influence others. Agents collaborate with one another following interaction protocols, which include communication, influence, and information exchange mechanisms.
- Conditionality, the tendency to change states dynamically as a function of their interactions and experiences. Agents are assigned a state or condition that changes over time based on a combination of attribute and behavior variables.

Beyond these baseline characteristics, agents can have either static or dynamic attributes (fig. 16 below) and can also exhibit goal-oriented behavior, adaptive learning, or stochastic decision-making, depending on the design objectives. Their mobility patterns are particularly important in epidemiological ABMs, since they dictate how agents encounter each other and transmit infections. Movement can be represented through simple stochastic rules (e.g., random walk or constant-speed trajectories), or through realistic mobility schedules, incorporating daily or weekly routines across workplaces, schools, markets, religious centers, and other points of congregation. More sophisticated models can embed geographic data such as transportation networks, roads, or public transit to generate realistic patterns of human mobility.

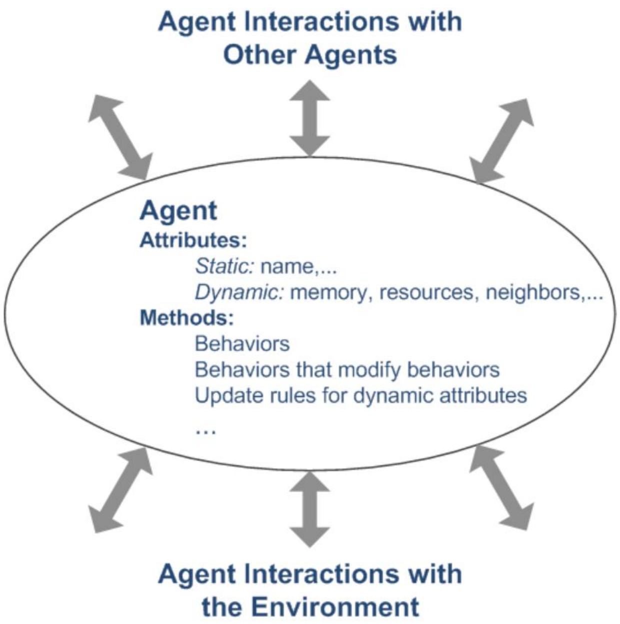

Figure 16. Agents' properties and attributes (Macal & North, 2014).

Tracy et al. (2018) provide an example of a hypothetical ABM model in public health (fig.17), illustrating how individual characteristics both influence and are influenced by community characteristics, social connections, aging, and human movement.

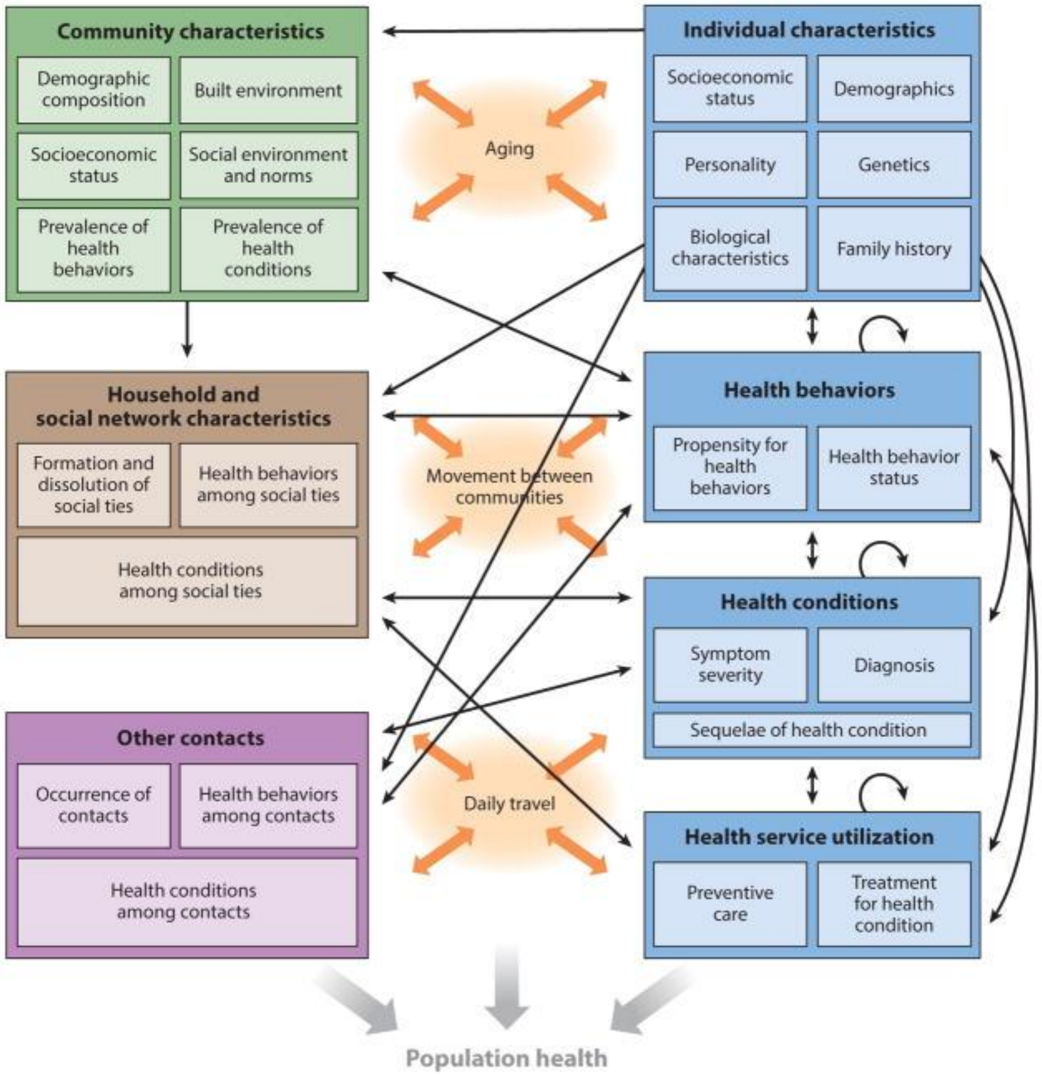

Figure 17. An illustration of a hypothetical ABM in Public Health showcasing how individual characteristics can affect other factors. "Together, these interactions and biologic, behavioral, and social processes make up the system from which population health emerges" (Tracy et al., 2018).

Equally critical is the environment within which agents are situated and interact. The environment defines the spatial and social structures that constrain or enable interactions, ranging from abstract grids and networks to high-fidelity representations of real-world geographies. For example, simple models may employ two-dimensional lattices (Duan et al., 2013), while more advanced implementations integrate GIS data, including elevation, land use, and urban infrastructure (fig.18) These features are particularly relevant when modeling diseases influenced by environmental factors such as temperature, humidity, or the presence of vectors (e.g., mosquitoes). Factors such as temperature, precipitation, and the presence of insects (e.g., mosquitoes) capture critical disease transmission dynamics that might otherwise be overlooked. However, as more factors are included, the ABM becomes increasingly complex, leading to a computationally intensive process that requires additional time and data.

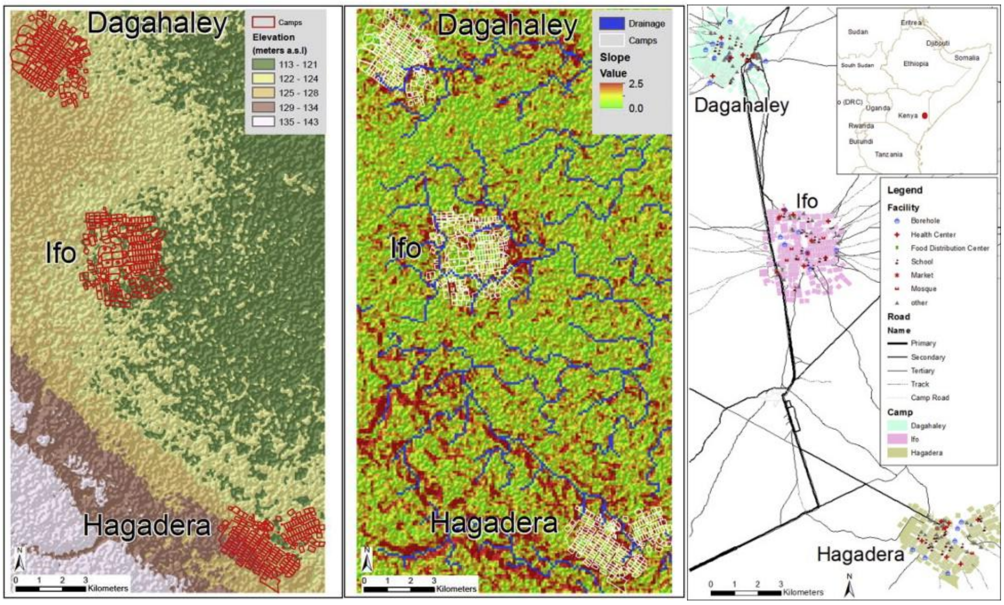

Figure 18. The example of the ABM proposed by Crooks & Hailegiorgis (2014) using geospatial data. Left: digital elevation data, Center: environmental data and Right: city infrastructure (roads, buildings, etc).

The design of the environment also dictates how relationships between agents are formed and sustained. In practice, agents interact not with all others, but within well-defined neighborhoods or networks that capture social, familial, or professional relationships. Five common topologies illustrate these structures (fig.19): (i) grid-based cellular automata, (ii) Euclidean spatial coordinates, (iii) static or dynamic network connections, (iv) GIS-based geospatial representations, and (v) “soup” models in which space is abstracted away and interactions are randomized. Each topology makes assumptions about “who meets whom, where, and why,” and thus strongly influences transmission dynamics in epidemiological simulations.

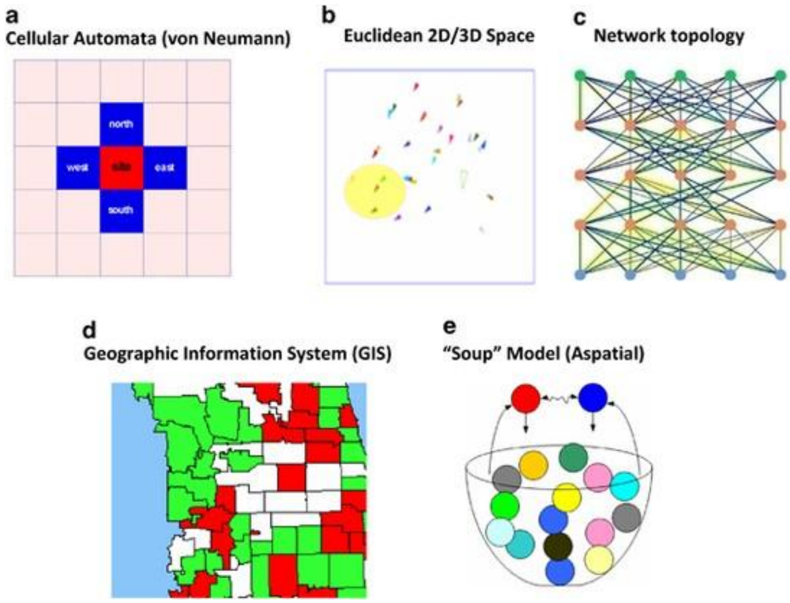

Figure 19. Topologies for agent relationships and social interaction (North et al., 2010).

In cellular automata space (fig.19a), the agents' environment is depicted using a grid or lattice comprising cells that define their locations via cell indices. In a Euclidean space (fig.19b), agents' positions are specified using spatial coordinates within a 2D or 3D environment. Network topology (fig.19c) represents agents' locations as relative nodes within a static network with predetermined links or within a dynamic network with active links determined by their relationships. In a GIS environment (fig.19d), agents' locations are described using geographical units or spatial coordinates within a 2D or 3D environment that includes realistic geospatial landscape components. Lastly, in a "Soup" non-spatial model (fig.19e), agents' locations are undefined.

Ultimately, the interplay between agent properties, mobility behaviours, and environmental structures forms the foundation of ABMs. By combining individual-level heterogeneity with realistic spatial and social contexts, ABMs can capture emergent system-level patterns such as epidemic waves, clusters, and superspreading events—phenomena that would otherwise be obscured in aggregate mathematical models. Building on this foundation, the next step is to explore how ABMs have been specifically employed in epidemiology, where their ability to simulate heterogeneous populations and complex contact structures has proven particularly valuable. This discussion naturally leads to their application regarding the recent COVID19 pandemic, which provided an unprecedented testing ground for epidemiological ABMs and highlighted both their potential and their challenges.

3.2.2 Epidemiological ABMs

For decades, the study of infectious disease dynamics relied primarily on mathematical, equation-based models. Mathematical modeling offers a range of techniques for investigating, analyzing, and forecasting the transmission dynamics of infectious diseases. Such approaches, including the classic SIR model by Bailey (1975), the SIS model of Kermack & McKendrick (1927), and their subsequent extensions such as SIQS (Zhang et al., 2014) and SIVS (Arino et al., 2003), have provided valuable insights into outbreak trajectories and the effectiveness of large-scale interventions. These models remain indispensable tools, particularly when the population is assumed to be homogeneous and interactions are aggregated at the population level. However, while these models have been effective in explaining the overall dynamics of epidemics on larger scales, they rely on general variables and, as a result, cannot offer accurate predictions on smaller scales at a finer resolution. Attempting to involve various populations and behaviors will lead to an overcomplicated mathematical model that requires a large number of complex equations and parameters. As behaviors in a system become more and more complicated, the complexity of the differential equations that will describe these behaviors increase exponentially leading to very complex and problematic mathematical equations.

This limitation underscores the added value of ABM. Unlike population-aggregated mathematical models, ABMs can explicitly represent individuals (agents), their behaviours, and their interactions with one another and with their environments. This individual-level perspective allows epidemiological ABMs to incorporate heterogeneous contact patterns, mobility behaviours, social networks, and environmental contexts, all of which play a central role in real-world disease transmission (Eubank et al., 2004). Importantly, ABMs capture emergent phenomena such as epidemic waves, clusters, or superspreading events that arise from local interactions and are often invisible to equation-based approaches. Even small variations in agent behaviour can generate non-linear and sometimes unexpected system-wide consequences, providing researchers with valuable mechanistic insights into the complexity of disease spread.

The strength of ABMs in epidemiology lies not only in their flexibility but also in their adaptability to different contexts and levels of granularity. Models can be built at the scale of households, communities, cities, or nations, and they can integrate transportation systems, urban environments, or specific ecological factors such as mosquito habitats in malaria simulations. This adaptability has made ABMs an attractive tool for public health, particularly when evaluating intervention strategies that act at the level of individuals, such as testing, vaccination, quarantine, isolation, or behavioural modifications. Unlike traditional models, ABMs make it possible to simulate "what-if" scenarios that test both the direct and indirect consequences of interventions under diverse conditions. Additionally, ABMs allow for virtual experimentation with interventions and policies, facilitating the testing of diverse scenarios and the identification of optimal intervention combinations to achieve specific goals and contributing to the development of effective strategies for epidemic prevention and control.

Nevertheless, the design of epidemiological ABMs involves a constant balance between realism and simplicity. While the richness of agent-based simulations allows detailed representation of disease, society, mobility, and environment, models must still adhere to the "KISS" principle ("Keep It Simple, Stupid") to remain interpretable and computationally feasible. Overly complex designs may hinder validation, calibration, and reproducibility. To address these challenges, the field has developed standardized protocols (such as the ODD framework) that ensure clarity, comparability, and replicability of ABMs across studies.

In the last two decades, the world has faced numerous infectious diseases, including SARS (2003), H1N1 (2009), Ebola (2014), and Zika (2016). Prior to COVID19, HIV/AIDS stood as one of the most pressing global health challenges, particularly in regions with limited access to healthcare, such as parts of Africa.. Some of these models are designed as flexible, general-purpose platforms capable of simulating different pathogens (M. S. Barrett et al., 2008), while others focus on highly specific disease dynamics in well-defined contexts. General models facilitate broad scenario testing but often lack fine-grained realism, whereas specific models can provide more accurate insights but demand extensive data and computational resources. Both approaches have contributed significantly to epidemic planning, preparedness, and retrospective outbreak analysis.

Given the impracticality of conducting real-world experiments to observe the impact of a disease on a population, agent-based simulation models offer a robust approach for studying the dynamics of infectious disease outbreaks. Through the application of various case scenarios and the simulation of interactions, these models capture the behaviors that illustrate how a population may be affected and how it should respond to an outbreak. In an epidemiological ABM, four essential elements must be clearly defined (fig.20).

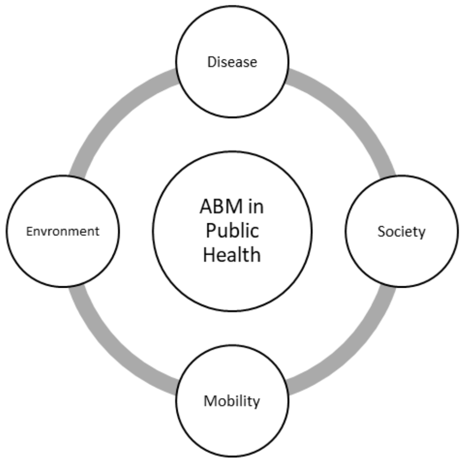

Figure 20. The four interconnected components of an epidemiological ABM.

Hunter et al. (2017) describe these interconnected components as follows: (a) disease, which specifies the nature of the infectious disease, including how it is transmitted between agents and its behavior in an infected agent; (b) society, which specifies the population being simulated; (c) transportation, which specifies how agents move through the environment; and (d) environment, which specifies the spatial extent in which the agents will move and interact.

The nature and dynamics of disease transmission are critical components of the simulation process. For instance, infectious diseases can be transmitted to humans through direct contact with other humans, other species (including animals and parasites), or even through the consumption of contaminated drinking water or food. Moreover, models can simulate the mechanisms of super-spreading events by identifying certain agents as super spreaders (Duan et al., 2013).

A broad range of epidemiological ABMs has been developed, with significant variability in scale, complexity, and methodological approach. Broadly, they can be divided into disease-specific models, which focus on capturing the unique dynamics of a particular pathogen, and generic ABMs, which provide reusable modeling frameworks applicable to a variety of infectious diseases. Table 2 below summarizes representative epidemiological ABMs reported in the literature, highlighting the diversity of applications across diseases, geographic contexts, and methodological approaches.

Table 2. Examples of infectious disease epidemiological ABMs in the literature

Disease / Pathogen	Study Area	Description / Technique	Reference
Ebola	Liberia	Transmission and intervention modeling	Merler et al. (2015)
H1N1	Mexico	Mobility-driven spread analysis	Frias-Martinez et al. (2011)
Influenza	Poland	Population-level SEIR-based ABM	Rakowski et al. (2010)
Influenza	Buffalo, NY (USA)	Incorporates urban mobility & environments	Mao (2014)
Malaria	Southern France	Incorporates mosquito ecology, temperature, vegetation, water	Linard et al. (2009)
Cholera	Dadaab refugee camp (Kenya)	Coupled with hydrological model	Crooks & Hailegiorgis (2014b)
HPV (Human Papillomavirus)	Denmark	Vaccination impact modeling	Olsen & Jepsen (2010)
Mumps	Portugal	Demographic-driven model	Simoes (2006)
Tuberculosis	Saskatchewan, Canada	Contact-network model without transport	Tian et al. (2013)
H5N1 (Avian Influenza)	USA	Spread dynamics and interventions	Dibble et al. (2007)
SARS	Global	Contact-network based modeling	Duan et al. (2013)
Generic ABM	USA	EpiSimdemics simulation tool	C. L. Barrett et al. (2008)
Generic ABM	Ontario, Canada	Population-scale epidemic modeling	Aleman et al. (2011)
Generic ABM	Allegheny County, Pennsylvania (USA)	High-resolution population simulation	B. Y. Lee et al. (2010)
Generic ABM	Italy	GIS-based epidemic spread	Ajelli et al. (2010)
Generic ABM	Global	Pandemic-scale scenarios	Bobashev et al. (2007)
Generic ABM	Global	Early conceptual epidemic ABM	Dunham (2005)
Generic ABM	Global	Network-driven epidemic dynamics	Epstein et al. (2008)
Generic ABM	Burnaby, Canada	GIS-enhanced epidemic model	Perez & Dragicevic (2009)
Generic ABM	Small Australian town	Simulation of influenza spread	Skvortsov et al. (2007)

Disease-specific ABMs have been used to explore outbreaks of viruses such as Ebola in Liberia (Merler et al., 2015), H1N1 in Mexico (Frias-Martinez et al., 2011), and influenza in Poland (Rakowski et al., 2010). Other studies emphasize the role of environmental factors, such as the malaria model for southern France, which incorporated mosquito ecology and climatic variables (Linard et al., 2009), or the cholera model of the Dadaab refugee camp in Kenya, which integrated hydrological processes (Crooks & Hailegiorgis, 2014). Similarly, Olsen & Jepsen (2010) modelled the spread of HPV in Denmark, focusing on vaccination impact, while Dibble et al. (2007) studied the spread of avian influenza (H5N1) in the United States. Mao (2014) developed a detailed influenza model in Buffalo, NY, incorporating buildings, roads, and residential areas to reflect mobility and household interactions, while Simoes (2006) modelled mumps in Portugal, and Tian et al. (2013) applied a network-based tuberculosis model in Saskatchewan, Canada.

On the other hand, generic ABMs provide flexible frameworks that can be applied across diseases and locations. For example, C. L. Barrett et al. (2008) introduced EpiSimdemics, a large-scale simulation platform for the United States, while Ajelli et al. (2010) developed a GIS-based epidemic model for Italy. Other notable works include Aleman et al. (2011) in Ontario, B. Y. Lee et al. (2010) in Allegheny County (USA), and Perez & Dragicevic (2009) in Burnaby, Canada, all of which integrate demographic and spatial data. Dunham (2005) and Epstein et al. (2008) presented global-scale ABMs, while Bobashev et al. (2007) developed a generic pandemic simulation framework. Models by Skvortsov et al. (2007) in small Australian towns further demonstrate the adaptability of ABMs to various spatial scales. Duan et al. (2013) extended this approach globally by modelling SARS spread through contact networks.

A key distinction among these studies lies in their representation of space and mobility. Several ABMs rely on GIS-based datasets to reconstruct realistic natural and social environments (Ajelli et al., 2010; C. L. Barrett et al., 2008; Crooks & Hailegiorgis, 2014; Simoes, 2006). Others adopt a fine-grained urban approach, such as Mao's (2014) influenza model in Buffalo, which captured the influence of school and workplace closures. By contrast, simpler frameworks, such as Dunham (2005) and Duan et al. (2013), place agents on grids or networks, prioritizing computational efficiency over environmental realism. Moreover, some models exclude transportation altogether, instead relying on contact networks to represent social interactions and transmission dynamics.

In these frameworks, infection spreads through probabilistic interactions within a predefined network, independent of geographic mobility. This approach was used in the tuberculosis model of Tian et al. (2013) and the HPV model of Olsen & Jepsen (2010). Such methods significantly improve computational efficiency and reduce simulation time, particularly in cases where disease spread is less sensitive to daily mobility patterns.

Taken together, the diversity of ABMs in the literature highlights their adaptability across diseases, regions, and modeling purposes. While generic models maximize flexibility and reusability, disease-specific ABMs enable more detailed representation of pathogen-specific dynamics. This trade-off between generality and realism remains central in epidemiological ABM development.

In their recent study, Hunter et al. (2017) conducted a comprehensive review and categorization of 20 ABMs specifically focused on human infectious diseases. Their objective was to examine the current landscape of epidemiological agent-based models, classify these existing simulations, and establish a taxonomy for such models. This taxonomy aims to facilitate a better understanding and comparison of different models. Based on their review of the models, they identify four primary applications of ABM in the field of epidemiology related to infectious diseases:

1. Disease Dynamics Research: This application involves using ABM to study and gain new insights into the dynamics of disease transmission, simulating how diseases spread in real-world outbreak scenarios.
2. Agent-Based Modeling Research: Here, the focus is on the development of novel approaches and methodologies for agent-based modeling itself, advancing the techniques used in ABM.
3. Epidemic Planning: ABM is employed to develop and analyze strategies and policies for managing potential outbreak scenarios. It helps in devising effective tactics and preparedness measures.
4. Lessons Learned: This application involves leveraging ABM to draw lessons from past examples, both successes and failures, to inform and improve future disease management and prevention efforts.

Taken together, epidemiological ABMs represent a critical methodological advance in infectious disease modeling, offering a bridge between theory and practice. Their ability to integrate detailed individual-level dynamics with broader social and environmental contexts has positioned them as indispensable tools in modern public health. The importance of these models became particularly evident during the COVID19 pandemic, which provided an unprecedented opportunity to apply and test epidemiological ABMs on a global scale. The following subsection (3.2.3) will therefore focus specifically on COVID19–related ABMs, highlighting their unique contributions and challenges during one of the most significant health crises of the 21st century.

3.2.3 ABMs for COVID19

The COVID19 pandemic, caused by the SARS-CoV-2 virus, marked a turning point in the global understanding and application of epidemiological modeling. The increasing interconnectedness of modern societies—driven by rapid urbanization, globalization, and climate-induced disruptions—had already highlighted the heightened risks of infectious disease emergence (Daszak et al., 2000). When COVID19 emerged in late 2019, its rapid spread across continents revealed not only the vulnerability of global health systems but also the limitations of traditional modeling approaches in capturing the complexity of transmission dynamics. With over 700 million confirmed cases and millions of deaths worldwide (WORLDOMETER, 2025), governments and scientists faced the dual challenge of forecasting epidemic trajectories and designing interventions that could effectively balance public health protection with socioeconomic sustainability. Healthcare systems and hospitals faced severe strain, often necessitating stringent control measures and mobility restrictions like isolating cases and implementing social distancing to contain further transmission. Additionally, the slow pace of vaccine development, combined with urbanization and globalization, posed challenges for outbreak control, even with extensive international collaboration.

Traditional compartmental models, most notably the Susceptible–Exposed–Infectious–Recovered (SEIR) framework, offered a natural starting point. SEIR models categorize individuals into epidemiological states (fig.21) and track transitions over time, providing valuable insights into the timing of epidemic peaks while considering external factors like the virus's airborne transmission potential (Liu et al., 2020). Meanwhile, different variations of the so called SEIR model, have been extensively used in an ABM context to assess planned interventions used to combat COVID19 (Altun et al., 2021; Kim & Cho, 2022; Taghizadeh & Mohammad-Djafari, 2022).

Over time, SEIR models showcased their advantages rendering them important tools for policy makers and governments when coupled with network-driven dynamics being capable of predicting with high accuracy any epidemic peaks taking into account external factors such as the virus transmission over air (Liu et al., 2020). Although SEIR models might be considered adequate for modelling and forecasting other diseases, as far as COVID19 is concerned, Moein et al. (2021) showed that a more complex approach that takes into account mortality rates and hospital capacity as well should also be considered when attempting to make a pandemic forecasting feasible.

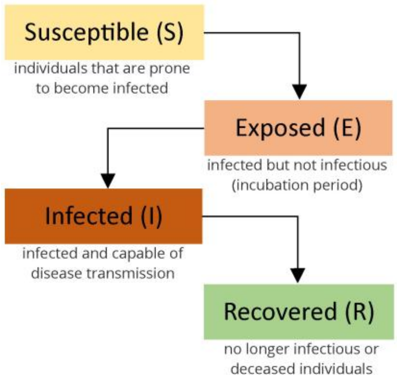

Figure 21. Diagram of a typical S.E.I.R Model.

COVID19 presented unique challenges that made purely equation-based models insufficient. These included asymptomatic transmission, heterogeneous social contact structures, superspreading events, and the nonlinear effects of NPIs such as lockdowns, mobility restrictions, and school closures. To address these complexities, researchers rapidly turned to ABMs, which were uniquely suited to represent individual heterogeneity, diverse mobility patterns, and the social dynamics of human interactions. Health experts and scientists should always regard any pandemic situation within a tight temporal context so as to accomplish its minimum possible spread, while achieving better forecasts (Yang et al., 2021) for the future.

Since the onset of the pandemic, an unprecedented number of ABMs have been developed to simulate COVID19 dynamics, test intervention strategies, and provide decision support for governments and health authorities. Many of these models still draw inspiration from SEIR-type compartmental structures, embedding them within an agent-based framework where transitions between compartments occur at the individual level. This allows for the incorporation of social networks, behavioral variability, and spatial heterogeneity, features that are essential to capture the complexity of COVID19 spread. While they share common structural elements, often grounded in SEIR-like compartmental dynamics, their implementation varies depending on geographic scale, policy objectives, and methodological design. Some models prioritize epidemiological accuracy and parameter calibration, while others emphasize policy experimentation or the integration of socioeconomic effects.

Table 3 provides a comparative overview of these major COVID19 ABMs, summarizing their geographic scope, methodological focus, strengths, and limitations. Collectively, these models illustrate both the versatility and the challenges of ABMs in supporting evidence-based decision-making during a global health crisis.

Table 3. Comparative overview of major COVID19 ABMs in the literature

Model	Scope / Study Area	Main Features	Strengths	Limitations
Covasim (Kerr et al., 2021)	Global, Adaptable to local/national levels	SEIR-based ABM simulates testing, contact tracing, vaccination and NPIs	High flexibility, strong calibration tools, widely adopted open source	High computational cost for large populations simplified behavioral dynamics
COVID-ABS (Silva et al., 2020)	Brazil (macro & regional)	Links health and economic outcomes, models NPIs and healthcare demand	Integrates epidemiological and economic effects, explores policy trade-offs	Coarse-grained representation of individuals limited mobility detail
CityCOVID (Ozik et al., 2021)	Chicago, USA (urban scale)	High-resolution urban ABM with realistic mobility and social networks	Captures heterogeneity in urban dynamics strong policy relevance	Data-intensive; limited transferability to non-urban contexts
COMOKIT (Gaudou et al., 2020)	Vietnam & generalizable	Modular ABM, integrates individual health, behavior, and policy modules	High modularity, supports "what-if" policy experiments	Calibration challenges, requires detailed local data
OpenABM-Covid19 (Hinch et al., 2021)	UK (national scale)	Models contact networks, testing, isolation, and app-based tracing	Explicit network representation, rapid scenario testing	Focused on specific intervention types, less emphasis on long-term dynamics

CoV-ABM (Jalayer et al., 2020)	Delaware, USA (≈1M population)	SEIHRD dynamics and virus environmental persistence, spatiotemporal viral density and household activity	Identifies infection hubs; local census-driven, decision support	Computational complexity, single-region validation
Telangana ABM (Narassima et al., 2020)	Telangana, India (>31 million agents)	Synthetic population, district-level NPIs, immunity scenarios	Large scale, local policy insights	District-level interactions and NPI assumptions
Kolkata City ABM (Suryawanshi et al., 2021)	Kolkata, India	Ward-level demographics, homes, markets, workplaces, schools modeled	Detailed urban representation, counterfactual policy assessment	Calibration dependency, data-intensive
Supermarket ABM (Ying & O'Clery, 2021)	Supermarkets	Customer movement networks, proximity-based infection, layout, masks, one-way aisles tested	Public-facing, retail policy insights, open-source code	Simplified transmission synthetic data
Public-Facing ABM (Wang et al., 2021)	General public simulation	Unity-based interactive ABM for visual learning of transmission & interventions	Accessible interface, education-focused	Limited epidemiological complexity, small-scale
NetLogo Multi-Country ABM (Staffini et al., 2021)	Italy, Germany, Sweden, Brazil	Dynamic random networks, real data policy/time-stamp responsive ABM	Multi-country comparison, real-time policy reflections	Simplified network, no vaccination or variants
AnyLogic Campus ABM (Malaysia) (Gan & Amerudin, 2022)	University campus settings	AnyLogic model simulating classroom/lab/office risks, social distance, ventilation, exposure modeled	Institutional planning, practical recommendations	Campus-specific, not scalable to city/national level

Among the most widely used, Covasim (Kerr et al., 2021) provided a flexible SEIR-based ABM framework capable of simulating testing, contact tracing, vaccination, and diverse NPIs, and has been adapted to national and local contexts. Similarly, OpenABM-Covid19 (Hinch et al., 2021) focused on explicit contact networks, rapid scenario testing, and app-based tracing, primarily in the UK. Both models are open-source and widely adopted, though they face limitations in long-term behavioral representation or scalability to very large populations.

Other models addressed more context-specific dynamics. COVID-ABS (Silva et al., 2020) integrated epidemiological and economic dimensions in Brazil, allowing policymakers to explore health–economy trade-offs, though at the cost of coarse-grained individual representation. At the urban scale, CityCOVID (Ozik et al., 2021) offered a high-resolution model of Chicago, incorporating realistic mobility and social networks, while COMOKIT (Gaudou et al., 2020) provided a modular framework applied to Vietnam but generalizable to other regions, enabling "what-if" experiments on policy interventions.

In addition to these, more recent models expanded the ABM landscape. The Telangana ABM (Narassima et al., 2020) simulated COVID19 spread across several districts of India, focusing on healthcare capacity and intervention scenarios. The Kolkata ABM (Suryawanshi et al., 2021) emphasized high-density urban environments and their role in transmission heterogeneity. Specialized applications also emerged, such as a supermarket transmission ABM (Ying & O'Clery, 2021) exploring infection risks in public spaces, a university campus ABM (Gan & Amerudin, 2022) assessing outbreak management strategies, and the Unity-based interactive ABM (Wang et al., 2021), which served as an educational tool for understanding epidemic dynamics. Lastly, the NetLogo Multi-Country ABM (Staffini et al., 2021) simulated COVID19 dynamics across Italy, Germany, Sweden, and Brazil, using dynamic random networks responsive to real-world policy timelines, thereby enabling cross-country comparisons, albeit without incorporating vaccination or viral variants.

A growing body of reviews has synthesized the lessons learned from COVID19 ABMs. Lorig et al. (2021) systematically examined agent-based simulations of COVID19, emphasizing their methodological diversity and the critical role of transparent documentation. Kong et al. (2022) further reviewed the compartmental structures and dynamics embedded in these models, highlighting both the innovations and the recurring limitations. A key theme across these studies is the importance of model calibration and validation. For instance, Ajbar et al. (2021) employed real-time epidemiological data from Saudi Arabia to estimate model parameters, addressing the inverse modeling problem and demonstrating how parameter uncertainty directly affects prediction reliability. Without rigorous calibration, ABMs risk generating misleading conclusions, particularly in high-stakes policy contexts. In their scoping review, Bonnet et al. (2024) examined 80 studies that integrated epidemiological and macroeconomic modeling of COVID19, categorizing them into four main types: compartmental–utility-maximization models, stylized epidemiological–macroeconomic models, epidemiological models linked to Computable General Equilibrium (CGE) or Input–Output frameworks, and epi-econ ABMs. The review highlighted that most models focused on high-income countries, with limited attention to long-term recovery trajectories and scarce consideration of inequality and poverty, as only 14% assessed disparities and just one study explicitly incorporated poverty impacts. While epidemiological components were often calibrated and validated, economic dimensions typically received less rigorous treatment, and sensitivity analyses covering both health and economic outcomes were infrequent, particularly in ABM studies. The authors conclude that although integrated epi-econ modeling provides valuable insights, significant gaps remain in scope, equity considerations, and methodological rigor, calling for expanded application in low- and middle-income contexts, inclusion of inequality and poverty measures, and enhanced long-term forecasting capacity to better inform future pandemic preparedness.

COVID19 ABMs have proven especially valuable in exploring the consequences of NPIs. While NPIs such as lockdowns, school closures, and mobility restrictions successfully reduced transmission rates (Buhat et al., 2020), they also imposed severe social and economic costs (Novakovic & Marshall, 2022). ABMs allowed researchers to investigate not only the epidemiological effectiveness of these interventions but also their broader systemic implications, offering a holistic perspective that traditional models could not provide. This has reinforced the value of ABMs as tools for policy analysis, bridging the gap between epidemiological insight and real-world decision-making.

The Cypriot context provides a striking example of why such models are necessary. With a population of less than one million, Cyprus reported over 600,000 infections, more than half of its residents, and more than 1,500 deaths by 2023 (World Health Organization, 2023). The high rate of asymptomatic transmission, combined with the vulnerability of specific population groups, placed immense pressure on healthcare systems and demanded timely, data-driven policy responses. The intermittent use of NPIs managed to slow down transmission but also raised questions regarding their long-term sustainability. ABMs, by integrating individual-level data with mobility patterns and social structures, present a way forward in designing more targeted, efficient, and sustainable intervention strategies for small but highly interconnected populations such as Cyprus.

In summary, COVID19 catalyzed an extraordinary expansion in the application of ABMs to infectious disease modeling. By explicitly capturing heterogeneity, mobility, and human behavior, these models have enriched both theoretical understanding and practical decision-making. They have also highlighted the importance of transparent reporting, rigorous calibration, and balanced model complexity. Ultimately, COVID19–related ABMs demonstrate not only the power but also the challenges of using agent-based approaches to inform public health in real time.

Building upon these advances, the present PhD research applies the principles of agent-based modeling to the Cypriot context through the development of the EPIMO-LCA model. This model is specifically designed to capture human mobility behaviors and evaluate the impact of governmental countermeasures on the spread of COVID19 in Cyprus. Unlike large-scale global models, EPIMO-LCA is designed to integrate localized human mobility data, governmental countermeasures, and epidemiological dynamics within a unified framework.

Chapter 5 first presents the questionnaire-based survey that captures the mobility behaviors of Cypriot residents (Section 5.1). It then details the architecture, data inputs, and methodological design of EPIMO-LCA (Section 5.2), while also discussing its limitations and potential future improvements. By integrating epidemiological modeling with localized mobility patterns, the EPIMO-LCA model aims to provide not only a retrospective analysis of the pandemic's progression but also a decision-support framework for managing future outbreaks.

4 Monitoring COVID19 in Cyprus

In comparison to the SARS-CoV outbreak of 2002 and the MERS-CoV outbreak of 2012, the spread of SARS-CoV-2 was remarkably rapid. To reach 1,000 infections, MERS required nearly two and a half years, SARS achieved this milestone in approximately four months, while the novel SARS-CoV-2 reached the same threshold in just 48 days. Consequently, on January 30, 2020, the WHO declared COVID19 a Public Health Emergency of International Concern (World Health Organization, 2020). The emergency phase officially concluded on May 5, 2023.

Understanding the spatiotemporal dynamics of COVID19 proved essential for mitigating its impact, clarifying the pandemic's scope and consequences, and guiding policymaking, planning, and community responses. Health geography, as an interdisciplinary field, played a central role in exploring the interplay between public health policies, disease spread, and human mobility. Such perspectives highlight how interventions, healthcare infrastructure, and human behaviors are linked with spatial and temporal trends.

The COVID19 crisis underscored the importance of an interdisciplinary approach, in which geography provides a unique holistic framework that captures both biophysical and social dimensions. Because many uncertainties of the pandemic carried a spatial component, geospatial analyses became indispensable. Research efforts increasingly employed GIS, spatial statistics, predictive modeling, and big geospatial data to capture transmission dynamics, evaluate intervention strategies, and forecast outbreak trajectories.

At the same time, data-driven approaches, leveraging sources such as mobile phone mobility records, airline travel networks, and national health datasets, enhanced the capacity to model disease diffusion and inform timely policy responses. Equally important were interactive, web-based mapping platforms, such as the widely recognized Johns Hopkins University COVID19 dashboard, which played a pivotal role in visualizing global pandemic dynamics and improving data transparency for both the scientific community and the general public.

This chapter focuses on the application of geoinformatics in monitoring and understanding the spread of COVID19 in Cyprus. It situates the Cypriot experience within the broader global context of the pandemic, emphasizing how spatial data, mapping technologies, and epidemiological analysis supported public health decision-making. The chapter begins by outlining the national response framework, describing the containment and mitigation measures, the vaccination strategy, and the epidemiological surveillance mechanisms implemented by the Cypriot authorities throughout the different phases of the pandemic.

In addition to contextual analysis, this chapter also presents the results of the thesis, highlighting the cartographic and analytical outputs produced through the integration of spatial technologies. Chapter 4.2 showcases a range of visual products, including static and dynamic digital maps and an integrated Web-GIS platform, designed to visualize the spatial distribution and temporal evolution of COVID19 cases. These tools enable high-resolution monitoring of epidemiological data and support effective information management, providing valuable insights for both scientific analysis and public health response in Cyprus.

4.1 The Case of Cyprus

The COVID19 pandemic has had profound global socioeconomic repercussions. By October 2023, it accounted for approximately 770 million confirmed cases of SARS-CoV-2 infection and nearly 7 million deaths worldwide. In Cyprus, the focus of this study, more than 661,000 confirmed cases and 1,360 deaths had been recorded by that same date (*WHO COVID19 Dashboard*, 2021). The virus exhibited a strong capacity for continuous mutation, which affected both transmissibility and immune evasion. As a result, Cyprus experienced six distinct waves of infections between March 2020 and October 2022.

In early March 2020, the Ministry of Health of Cyprus established a specialized unit dedicated to contact tracing of positive COVID19 cases. According to national legislation, the Department of Medical and Public Health Services holds primary responsibility for infectious disease prevention and management. In January 2020, a task force was activated within the Surveillance and Control of Communicable Diseases Unit to oversee surveillance activities, maintain communication with international organizations (ECDC, WHO, EU), and coordinate COVID19 testing protocols. Response actions were directed by the Medical Services Directorate and the General Secretary of the Ministry of Health, in close collaboration with the Scientific Advisory Committee, the Council of Ministers, and the President of the Republic. The Scientific Advisory

Committee was composed of academic experts from universities and members of the Surveillance and Control Unit. Data analysis was conducted by the Health Monitoring Unit. To address the surge in emergency calls, a volunteer support team was also established.

Parallel to these initiatives, the Ministry of Research, Innovation, and Digital Policy partnered with the University of Cyprus and the KIOS Center of Excellence to develop a digital platform for monitoring the spread of COVID19. This platform not only provided daily updates on case numbers but also delivered information on vaccination progress (*KIOS CoE COVID19 Cyprus Cases Dashboard*, 2021). Additionally, the Ministry introduced a series of digital tools to enhance healthcare crisis management, including citizen support services, facilitation of electronic transactions with public services, processing of exceptional movement requests during lockdowns, and the dissemination of reliable pandemic-related information.

In terms of healthcare infrastructure, Ammochostos General Hospital (AGH) was designated as the primary reference center for COVID19 patients in December 2019, with its Intensive Care Unit (ICU) equipped with ventilators. A second ICU was later established at Nicosia General Hospital (NGH) to accommodate the growing patient load. During the first wave, ICU availability in Cyprus was not critically threatened; however, in anticipation of subsequent waves, capacity was significantly increased. In May 2020, a new ICU with 28 beds was built at NGH, and by the second wave, Cyprus had 54 ICU beds dedicated to COVID19 patients, of which 39 were occupied by mid-January 2021. Preparations for a potential third wave expanded hospital capacity with 100 additional beds, supplementing the existing 200 in standard wards, along with approximately 65 active ICU beds dedicated to the treatment of COVID19 patients. The COVID19 surveillance system in Cyprus is described in detail in the work of Agapiou et al. (2021).

Initially, all PCR testing was centralized at the Cyprus Institute of Neurology and Genetics in Nicosia. To scale capacity, testing was extended to one public and eleven private hospital laboratories. By mid-April 2020, Cyprus achieved one of the highest per capita testing rates in the EU. During the second wave, laboratory-based testing was supplemented with rapid antigen tests and random community sampling. In August 2020, mobile laboratory units were deployed to support localized outbreak detection. Cyprus also collaborated with the European Centre for Disease Prevention and Control (ECDC) to monitor circulating variants. By October 2020, as the number of cases increased dramatically, it became increasingly challenging to maintain contact tracing for every new case. In response, individuals who tested positive were tasked with notifying their close contacts themselves and instructing them to go into isolation. If a close contact developed symptoms before the Unit could trace them, they were advised to contact their personal doctor.

Preventive guidance on hand hygiene, respiratory etiquette, and social distancing was disseminated as early as January 2020, prior to the first reported case in Cyprus on March 9, 2020. Containment measures included international travel restrictions, school closures, and bans on mass gatherings. The first national lockdown was imposed on March 23, 2020 (restrictions on non-essential travel and shutdown of most retail establishments), with strict curfew measures added on March 30 due to widespread non-compliance.

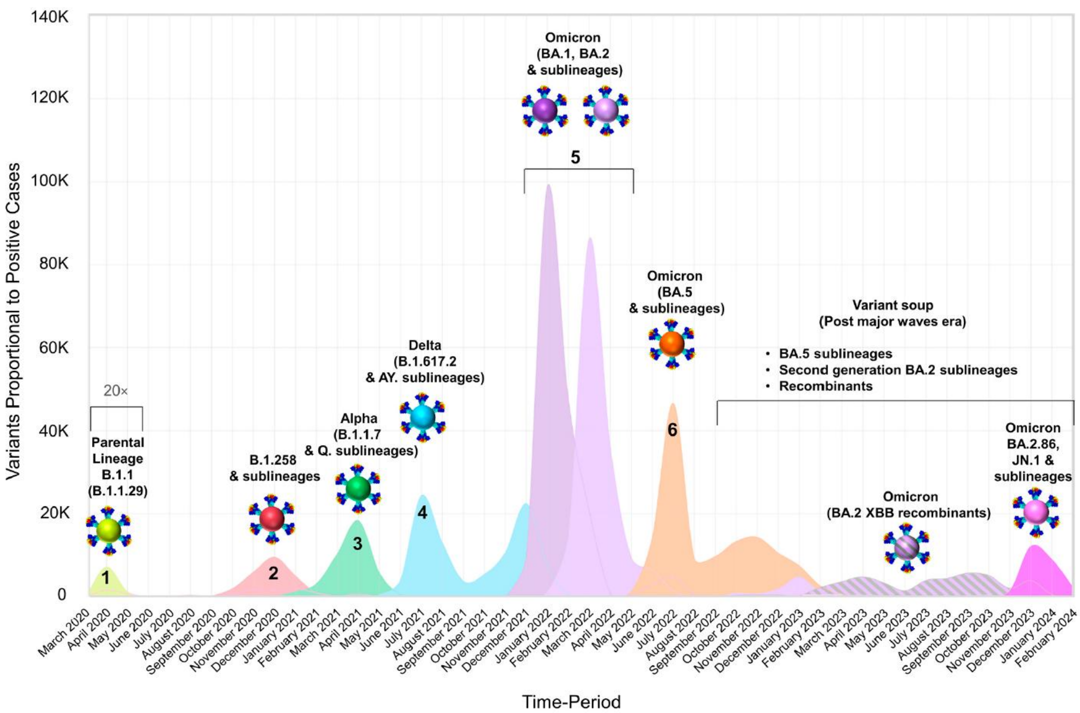

Figure 22. Overview of the progression (monthly positive SARS-CoV-2 cases) of the virus within the Republic of Cyprus, highlighting the predominant SARS-CoV-2 variants in each wave of cases from March 2020 to February 2024. By color: bright green (B.1.1), red (B.1.258), green (Alpha), light blue (Delta), purple (Omicron 1), lilac (Omicron 2) and orange (Omicron 5). For better visibility, values under the black bracket (March-May 2020) have been multiplied by 20. Figure from (Chrysostomou et al., 2024).

Following the first wave peak in April 2020, a phased easing began in May 2020, and borders reopened in June to tourists from low-risk countries. Nevertheless, a resurgence of cases led to renewed restrictions in November 2020 and a second full lockdown in January 2021.

Like many countries, Cyprus experienced successive epidemic waves driven by new variants. By October 2021, the WHO had identified five SARS-CoV-2 Variants of Concern (VOCs): Alpha, Beta, Gamma, Delta, and Omicron (WHO. Tracking SARS-CoV-2 Variants, n.d.). These variants, along with their sublineages led to the emergence of consecutive waves in the SARS-CoV-2 epidemic and include Alpha (B.1.1.7), Beta (B.1.351), Gamma (P.1), Delta (B.1.617.2) and Omicron (B.1.1.529). These waves were characterized by significant surges in new infections, reaching a peak before gradually receding (Wagner, 2020).

Between March 2020 and February 2024, Cyprus experienced a total of six consecutive waves of SARS-CoV-2 infections, each associated with specific virus lineages and variants (fig.22).

The initial wave of the pandemic in Cyprus (April–June 2020) was associated with the B.1.1 lineage, while the second wave (September 2020–January 2021) was driven primarily by the B.1.258 variant. Subsequent waves were dominated by Variants of Concern (VOCs). Specifically, the third wave (February–May 2021) was linked to the Alpha variant, and the fourth wave (June–September 2021) to the Delta variant. The fifth wave (November 2021–May 2022) was marked by the emergence of Omicron, which resulted in the highest number of new infections during the pandemic. This wave included two distinct peaks: the first, in January 2022, dominated by Omicron BA.1, and the second, in March 2022, driven by Omicron BA.2. The sixth and final major epidemic wave occurred between late May and August 2022, when Omicron BA.5 became the prevailing variant. From November 2022 to February 2023, BA.5 continued to dominate, before being gradually replaced by XBB subvariants through November 2023. A short-lived "wavelet" caused by JN.1 emerged in late 2023, but subsided by early 2024. Importantly, this later phase was not characterized by major epidemic waves, suggesting a transition from pandemic surges to more endemic transmission dynamics in Cyprus (Chrysostomou et al., 2021, 2022, 2024). Figure 23 display COVID19 cases, testing and percentage positivity from March 2020 to February 2024.

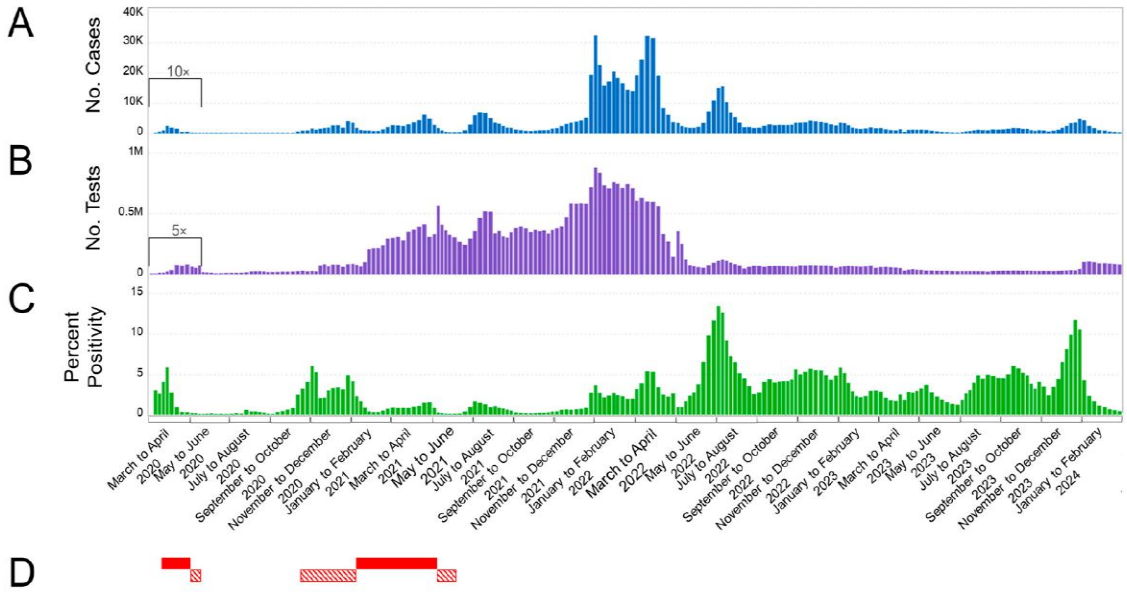

Figure 23. COVID19 cases, testing and percentage positivity from March 2020 to February 2024. (A) illustrates the weekly count of positive SARS-CoV-2 cases. For better visibility, values under the black bracket (1 March 2020 - 17 May 2020) have been multiplied by a factor of 10. (B) showcases the weekly count of SARS-CoV-2 tests (PCR and rapid). For better visibility, values under the black bracket (1 March 2020 - 17 May 2020) have been multiplied by a factor of 5. (C) display the weekly SARS-CoV-2 testing percent positivity. Calculated by dividing the weekly count of positive SARS-CoV-2 cases by the total number of SARS-CoV-2 tests conducted during that specific week. (D) Identifies periods of full lockdown (marked by red polygons) and partial lockdown (marked by polygons with diagonal red lines) in Cyprus. Figure from (Chrysostomou et al., 2024).

According to the decrees by the Ministry of Health, the Republic of Cyprus implemented a total of three partial and two full lockdowns until the official end of COVID19 pandemic in 2023. The initial lockdown was enforced from 24 March to 3 May in 2020, followed by the second lockdown spanning from 10 January to 9 May in 2021. In early April 2020, Cyprus faced a shortage of medical supplies, notably surgical masks, which resulted in a high infection rate among healthcare professionals in the country. The first partial lockdown occurred in 4 May 2020, the second from 23 October 2020 to 9 January 2021 and the third from 10 May to 10 June 2021.

Meanwhile, all-cause "excess mortality" in Cyprus remained notably high through 2021 and 2022. Analysis from Eurostat via local research revealed that total deaths exceeded expected baselines by approximately 23% in 2021 and 25% in 2022, despite excluding confirmed COVID19 fatalities. The third quarter of 2021 alone saw a 34% excess—raising concerns about indirect impacts of the pandemic, such as delayed care or health service disruptions (C. Economidou et al., 2024; OECD & European Observatory on Health Systems and Policies, 2023). These insights reflect a crucial transition: COVID19's acute phase has abated, but its influence persists through variant evolution and residual mortality impacts. Finally, on May 5, 2023, the WHO officially declared the emergency phase of the pandemic concluded, marking the watershed moment from crisis to managed endemicity.

4.1.1 Containment and Mitigation Measures

The first case of COVID19 in the Republic of Cyprus was reported on March 9, 2020, followed shortly after by the country's first COVID19-related death on March 21.

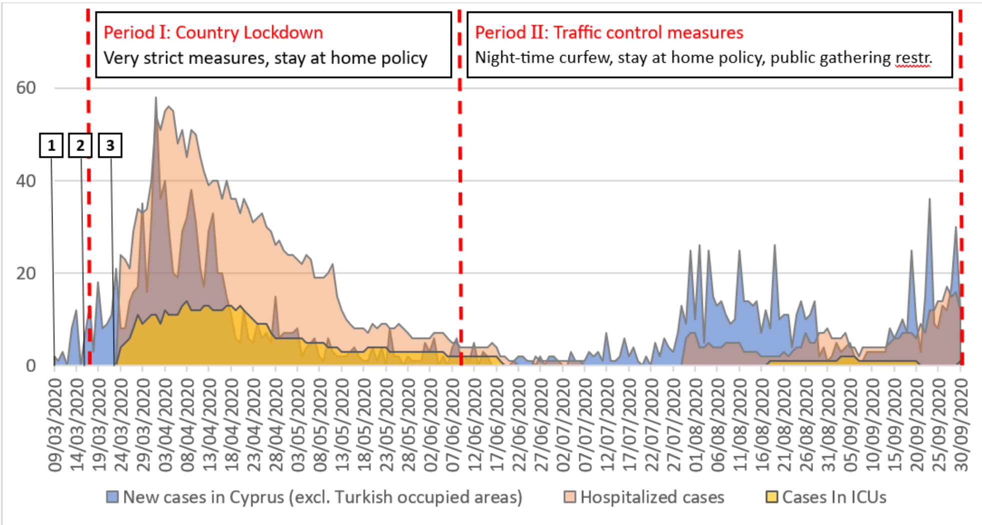

Figure 24. Government response measures to COVID19 in Cyprus along with the number of daily new cases, hospitalized cases and cases in ICUs in the areas controlled by the Republic of Cyprus, from the onset of the pandemic until September 2020. Key events: 1) first COVID case in Cyprus is confirmed (09/03), closure of the 4 check points forbiting any movement from/to the northern occupied part of the island (10/03) and cancellation of all public events and restrictions on public gatherings (10/03), 2) International flight travel controls - entry ban on all foreign travelers, except for Cyprus nationals and individuals (15/03 and total border closure on 21/03) and suspension of operations of all non-essential businesses in the private sector (15/03), 3) outside movements are limited from 3 per day (23/03) to 1 per day (30/03) to again 3 per day (30/04), all requiring authorization until the curfew is lifted (21/05).

Thoughout 2020, the government reacted swiftly, adopting a broad range of NPIs to limit virus transmission (Fig. 24 and 25). In the absence of effective treatments or vaccines, the country relied primarily on NPIs during the initial stages of the pandemic. With the rollout of vaccines in late December 2020, emphasis gradually shifted toward testing, contact tracing, and mass vaccination, with the ultimate goal of reopening the economy and restoring international travel.

Evidence from international and national studies confirms the effectiveness of NPIs in controlling early COVID19 waves (Flaxman et al., 2020; Han et al., 2020). In Cyprus, enhanced testing, rigorous contact tracing, lockdowns, and mobility restrictions were key in reducing virus spread and preventing the healthcare system from being overwhelmed (Agapiou et al., 2021; Alexandrou et al., 2021; Gountas et al., 2021). Travel restrictions and border controls also proved crucial in delaying viral importation and limiting community transmission (*Cyprus Ministry of Health. Important Announcements Regarding COVID19*, 2020).

Despite their effectiveness, these measures came with indirect societal costs. Economic decline, disruption of education, reduced access to healthcare for chronic patients, and significant mental health impacts were among the adverse consequences (Lytras & Tsiodras, 2021). A particularly challenging issue was the «pandemic fatigue», a term used by the WHO to describe the gradual decline in public motivation to comply with protective behaviors and vaccination uptake (WHO, 2020). It manifests in various ways, including neglecting public health recommendations regarding vaccinations and booster shots, disregarding safety measures like mask-wearing and handwashing, losing interest in staying informed about the pandemic, underestimating the risks associated with COVID19, feeling a sense of hopelessness about the future, and increasing consumption of alcohol and food. This fatigue became increasingly evident in Cyprus as the pandemic evolved and strict measures persisted across multiple waves.

Strict measures and policies including mandatory 14-day quarantine for incoming travelers, the closure of schools, hotels, and local businesses, compulsory mask-wearing indoors and outdoors, and specific hours for movement restrictions were enforced throughout 2020 and 2021. Simultaneously, health authorities increased diagnostic testing across the population and intensified efforts to quickly identify and isolate contacts of confirmed cases. Digital tools were also integrated into the enforcement and monitoring of these measures. For instance, the SMS-based movement approval system allowed residents to leave their homes only for specific purposes, combining spatial control with digital verification.

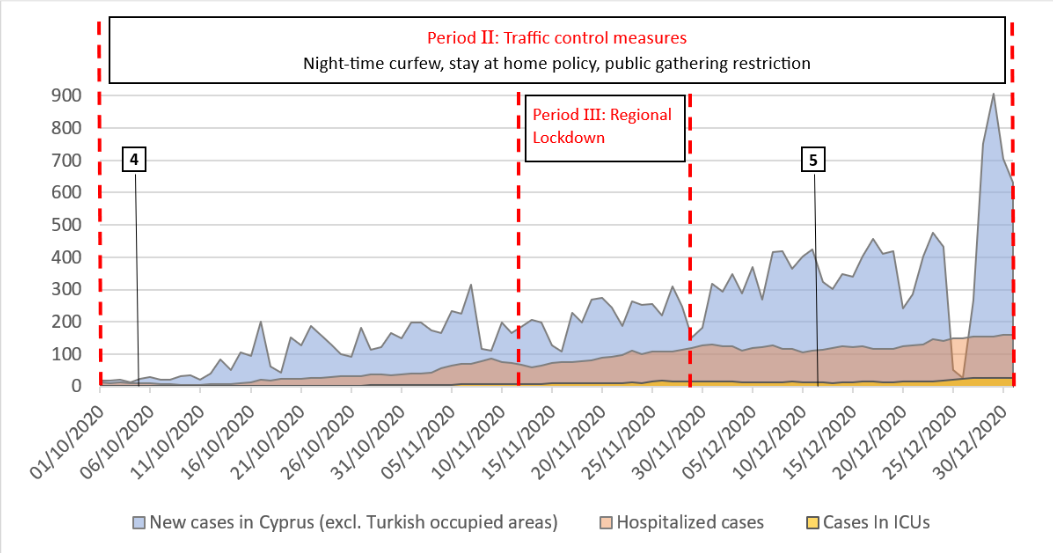

Figure 25. Government response measures to COVID19 in Cyprus along with the number of daily new cases, hospitalized cases and cases in ICUs in the areas controlled by the Republic of Cyprus, from the 1st of October until end of December 2020. Key events: 4) The use of face mask is mandatory in closed and open public spaces (05/10) and 5) closure of all public spaces and non-essential shops, restaurants and cafes (11/12).

This strategy, although restrictive, proved effective in reducing unnecessary mobility and curbing community transmission during critical phases of the outbreak. All of these measures, coupled with the public's adherence to personal hygiene practices, mask use, limitations on travel and the maintenance of social distancing, resulted in a significant and rapid decline in COVID19 cases during the early months of the pandemic on the island. Cyprus experienced two infection waves in 2020, one in March and another in December. Public health responses unfolded in four phases:

- Period 1 (10–14 March): Closure of schools and cancellation of mass gatherings (75+ participants).
- Period 2 (15–23 March): Closure of entertainment venues, restrictions in public service areas, and international travel controls.
- Period 3 (24–30 March): Closure of most retail services.
- Period 4 (31 March–3 May): Full border closure, suspension of flights (except repatriations), stay-at-home order, and night curfew. In addition, the checkpoints with the northern-part of Cyprus (Turkish-occupied areas) were also closed (Reuters, 2020).

The first national lockdown began on March 24 and lasted for two months, until May 21, 2020. A robust test–trace–isolate strategy was simultaneously deployed. International travel to and from Cyprus was suspended from March 21 to June 1, 2020, with strict travel restrictions remaining in place until the end of 2020, categorizing countries based on their epidemiological status (green for low risk, orange for low risk with high uncertainty, red for high risk, and gray for countries with special permits). By May 2020, and during the first wave of the epidemic, Cyprus had one of the highest testing rates in Europe (8,932 per 100,000 population), significantly surpassing many countries. For reference, the testing rates for the United Kingdom, the Netherlands, and Greece during the same period were 3,018, 1,217, and 926 tests per 100,000 population, respectively (Cyprus Ministry of Health, 2020b). Testing approaches included targeted testing of suspect cases and their contacts, repatriates at the airport and during their 14-day quarantine, teachers and students when schools reopened in mid-May, employees in essential services that continued their operation (e.g., customer services, public domain, etc.), and healthcare workers in public hospitals. Additionally, population screenings were conducted through random sampling in the general population.

The effectiveness of these interventions is reflected in the relatively low Infection Fatality Rate (IFR) during the first wave, estimated at 0.71% Gountas et al. (2021). The Infection Fatality Rate (IFR) is a crucial metric for assessing the impact of the COVID19 pandemic. A recent modeling study across various settings estimated the IFR to range from 0.5% to 1.4% (Hauser et al., 2020). Several factors contributed to the relatively low IFR, including the early implementation of measures, the island's geographic isolation, and its relatively late exposure to the virus compared to mainland Europe. However, the Infection Attack Rate (IAR) during the first wave was only 0.31%, leaving the population far from herd immunity (Flaxman et al., 2020). Consequently, by the conclusion of the first wave, Cyprus remained far from reaching herd immunity. The estimated collective immunity threshold for Cyprus was calculated at 62.4%, based on the formula 1-(1/R0) = 1-(1/2.66).

From May to July 2020, restrictions were gradually lifted in four reopening phases, allowing economic and social activities to resume. Airports reopened in June under strict testing protocols, initially offering free PCR testing to tourists before shifting to mandatory pre-arrival negative tests. Importantly, the reopening of airports in Cyprus did not result in a significant surge in positive cases but prompted the government to enforce mandatory COVID19 testing for all arrivals during the summer of 2020. A rise in cases followed the reopening of schools in September, leading to new restrictions in October and November.

The first phase commenced on May 4, 2020, with the reopening of construction sites, retail stores, and the public sector, all while adhering to mandatory health measures and guidelines. The second phase began on May 21, allowing the reopening of public schools, outdoor restaurants, and permitting unrestricted movement within the country. The third phase, which started on June 9, saw the reopening of airports, seaports, shopping centers, as well as indoor dining areas and hotels, theaters, and outdoor cinemas. Finally, on June 24, the fourth stage introduced further relaxation of restrictions regarding the maximum number of people allowed at public gatherings.

The second wave of infections began in late September 2020, fueled by school reopening, outbreaks in nursing homes, and increased social mixing. Regional lockdowns in Limassol and Paphos (November 12–29, 2020) proved insufficient, and stricter national measures were implemented in December. By the Christmas holidays, Cyprus was facing its most severe wave yet (FinancialMirror, 2020), necessitating further restrictions and eventually leading to the introduction of the "Safe Pass" system in 2021. Figure 26 illustrates the Government response measures chronologically until mid-2021.

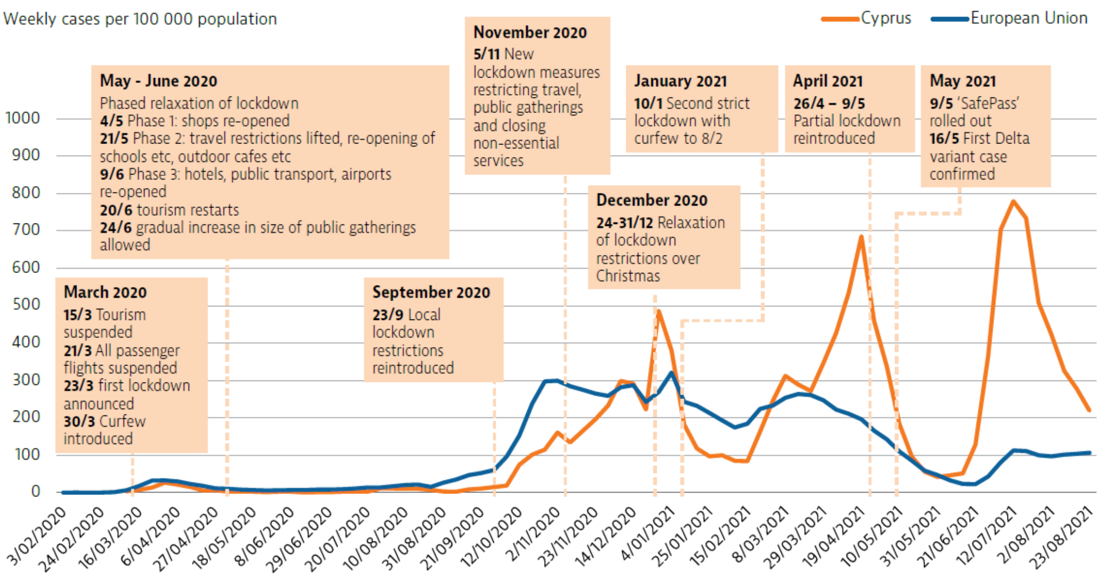

Figure 26. Government response measures to COVID19 in Cyprus along with the number of confirmed cases per 100k, from the onset of the pandemic until August 2021. source: (European Commission, 2021).

This system required proof of vaccination, recent recovery, or a negative test for access to public spaces and was later expanded to include public transport. Eventually it became a longer-term measure, extending its requirements beyond just hospitality venues, including its use for public transport. The strategy for the gradual relaxation of restrictive measures starting from February 1, 2021, was grounded in the three key pillars of testing, tracing, and vaccination. At the start of February 2021, schools and shops resumed their operations. However, despite the persistence of various other restrictions, there was a sustained high number of new cases, and the growing influx of hospitalized patients brought the healthcare system to the max of its capacity, particularly in terms of available intensive care beds. In response, a partial lockdown was implemented. Through this combination of strict containment measures, extensive testing, and eventually vaccination, Cyprus managed to delay large-scale transmission and limit mortality during the critical first year of the pandemic. Nevertheless, the country faced recurring challenges due to pandemic fatigue, social resistance to restrictions, and the economic pressures of prolonged lockdowns.

Following the early 2021 partial lockdown and the introduction of the Safe Pass, Cyprus continued to adapt its containment strategy in response to emerging challenges. By late November 2021, in reaction to rising case numbers driven by the Omicron variant, the government mandated Safe Pass requirements for individuals aged 6 and above and reduced the interval for booster eligibility from six to five-and-a-half months. Entry testing and tightened social distancing emerged rapidly: mandatory PCR tests on arrival were implemented from December 6, 2021 to January 10, 2022, alongside limits on gathering sizes, proof-of-status entry into hospitality venues, and revised protocols for healthcare workers and close contacts to limit onward transmission.

By spring 2022, the epidemiological situation improved, prompting the government to phase out many long-standing emergency measures. On April 11, Cyprus lifted its outdoor mask mandate, and by April 18, recovery or vaccination certificates were no longer required for shopping, work, or access to government offices, cultural sites, and festivals. Isolation periods for positive cases and close contacts were shortened, cinemas and theaters resumed normal capacities, and work-from-home expectations were significantly relaxed. Though mask mandates were briefly reinstated in July due to rising hospitalizations, they were lifted permanently by June 1—except in hospitals, eldercare settings, and public transport. Testing requirements for entering these venues persisted for unvaccinated individuals only.

On June 1, 2022, Cyprus fully lifted the indoor mask mandate (excluding healthcare settings) and ended travel-related documentation requirements, marking a return to pre-pandemic mobility and social functionality. As noted by the government, flight volumes and passenger traffic had nearly returned to pre-pandemic levels by this point. Since then, measures have remained minimal, reflecting a deliberate shift toward endemic management. While sporadic advisories were issued during summer surges, no major lockdowns or restrictions were implemented post-2022, signaling the island's transition into a phase of normalized control.

Summarizing the measures and policies implemented in Cyprus, the pandemic response can be characterized chronologically as follows:

- **2020 – Containment and Initial Response**

  The first year of the pandemic in Cyprus was defined by strict nationwide lockdowns, phased reopening strategies, and intensive border controls. Extensive testing and early containment helped delay large-scale community transmission, although localized outbreaks emerged following school and business reopenings.

- **2021 – Vaccination and Restrictive Measures**

  With the healthcare system under pressure, Cyprus introduced the “Safe Pass” system, combining vaccination, recovery, or testing requirements for access to public spaces. Mass testing and the vaccination campaign formed the backbone of policy, though recurring waves and social fatigue posed ongoing challenges.

- **2022 – Gradual Relaxation**

  As vaccination coverage increased and the Omicron variant became dominant, restrictions were progressively lifted. Mask mandates and Safe Pass requirements were gradually phased out, and policies shifted toward a more flexible, risk-based management approach.

- **2023 – Transition to Endemic Management**

  By 2023, Cyprus officially entered a phase of endemic management. Most restrictive measures were abandoned, with interventions limited to targeted recommendations in healthcare and high-risk settings. This marked the conclusion of the emergency response and the normalization of public life.

4.1.2 Vaccination Strategy

On December 15, 2020, the Ministry of Health of the Republic of Cyprus announced the National COVID19 Vaccination Plan, setting an ambitious target of vaccinating over 40% of the population within the first six months of 2021 (Cyprus Ministry of Health, 2020a). Vaccinations officially began on December 27, 2020, initially prioritizing residents and staff in long-term care facilities, as well as frontline healthcare workers. The vaccination rollout progressively expanded by age group, with access extended to all individuals aged 12 and above by early August 2021.

Eligible population groups were systematically announced by the Press and Information Office (PIO), beginning with high-risk individuals and gradually extending to younger cohorts. Appointments were booked via the COVID19 Vaccinations Portal on the General Health System (GeSY) platform. Vaccinations were administered across 38 Declared Vaccination Centers (DVCs) and other authorized facilities. To further enhance accessibility, the government introduced walk-in vaccination centers on July 15, 2021, operating on a first-come, first-served basis, while mobile units were deployed to reach remote areas.

By April 17, 2021, over 200,000 individuals, approximately 24% of the population, had received at least one vaccine dose. By the end of August 2021, 59% of the population was fully vaccinated, a rate surpassing the EU average (fig.27).

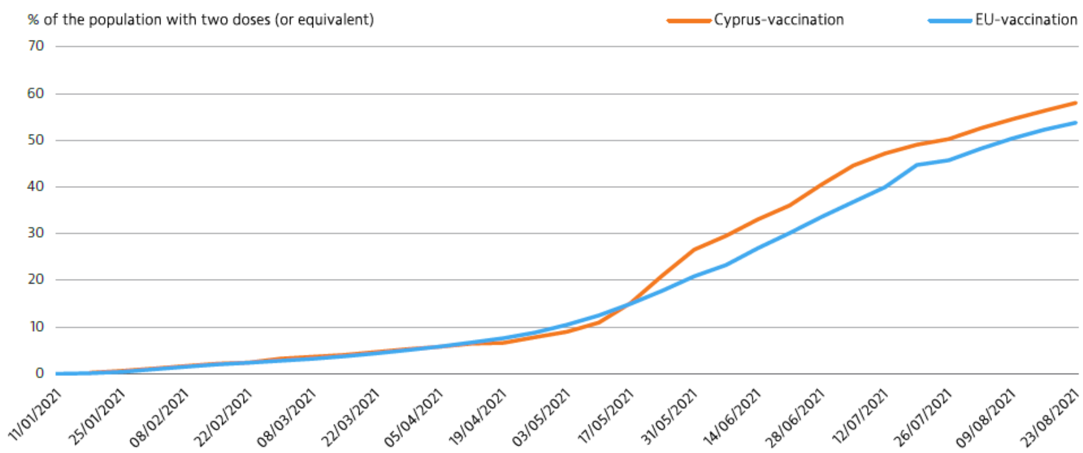

Figure 27. Percentage of population with two doses. source: European Commission, 2021.

According to the initial national strategy plan, the population was divided into six priority groups (Cyprus Ministry of Health, 2020a), with vaccinations distributed in the following sequence:

1. Residents and staff of senior care facilities, and high-risk healthcare professionals (e.g., ICU and emergency department staff).
2. Individuals aged 80 years and above, followed by those over 75.
3. Vulnerable groups with elevated risk of severe illness.
4. Healthcare professionals and residents of closed communities (e.g., prisons, refugee camps).
5. The general population, aged 12–74, prioritized by descending age groups.

Vaccination rollout was completed in eight months, beginning with the most vulnerable groups in late December 2020 and gradually extending access to the general population by August 2021 (Harris, 2021). Table 4 summarizes the implementation of the vaccination plan in the areas controlled by the Republic of Cyprus (excluding Turkish-occupied areas).

Table 4. Implementation of Cyprus national COVID19 vaccination plan. Source: Cyprus Ministry of Health and Cyprus Statistical Service (CyStat).

Target group	First access to vaccination	Target population (CyStat)
Residents and staff of senior people's homes and institutions for chronic adult illnesses.	27/12/2020	6,176
Healthcare professionals of high risk	27/12/2020	1,000
80+	January 2021	33,530
70+	February 2021	99,959
65+	March 2021	144,800
Vulnerable groups of people with increased risk of serious illness	April 2021	26,173
40-64	April 2021	268,700
30+ (via Personal Doctors)	April 2021	557,268
20+ (via Personal Doctors)	May 2021	695,590
20-39	May 2021	281,973
18+	June 2021	716,952
16+	June 2021	735,854
operation of "walk-in" vaccination centers	July 2021	735,854
12+	August 2021	772,087

Figure 28 illustrates Cyprus' vaccination progress across districts and age groups, comparing cumulative coverage at the early stages of the rollout (January 2021) with the situation six months later (July 2021).

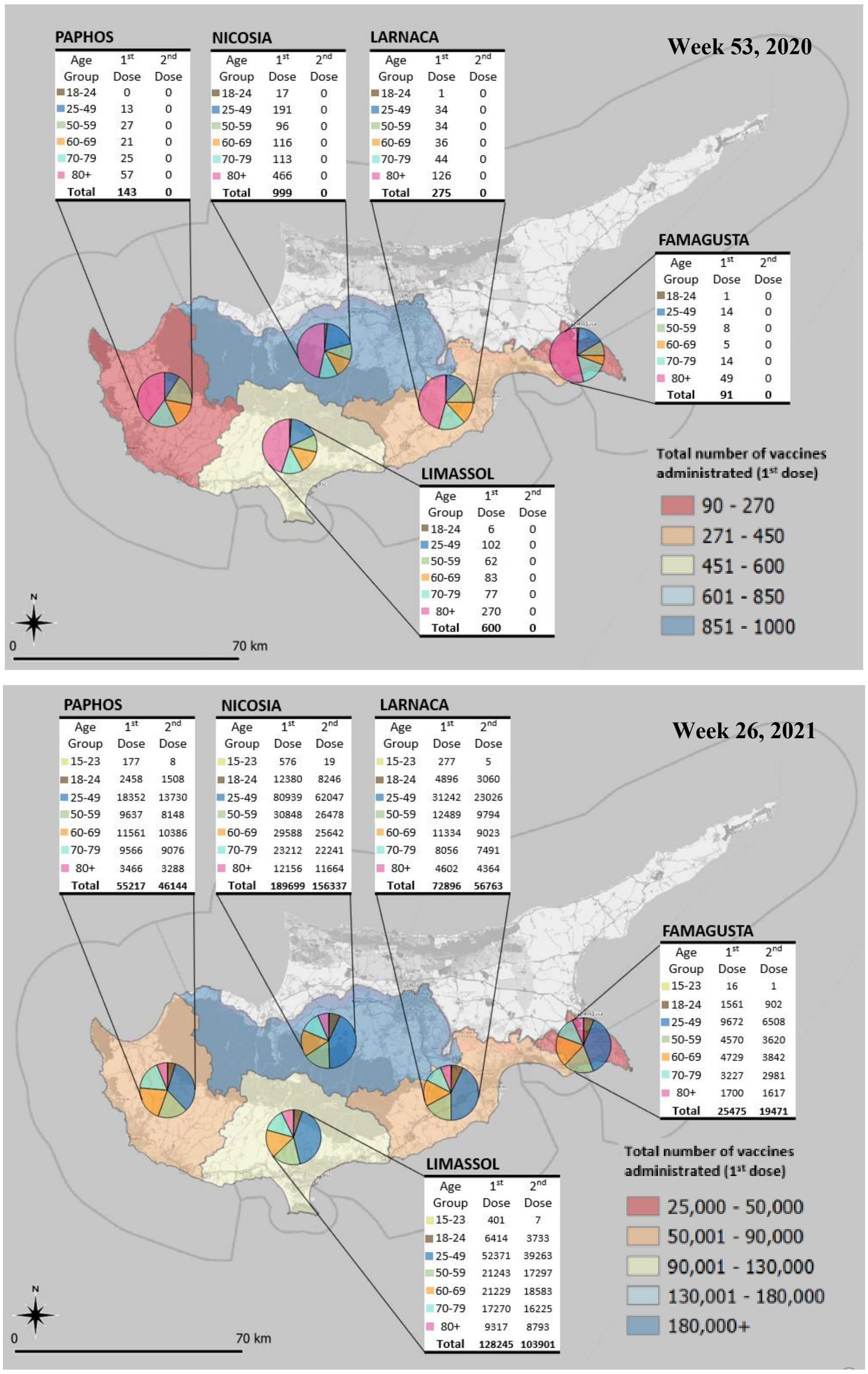

Figure 28. Cyprus' COVID19 vaccination progress, displaying the total number of first vaccine doses administered by age group in each district. Up: cumulative vaccinations up to 03/01/2021 (week 53 of 2020). Down: the status six months later, with total vaccinations up to 04/07/2021 (week 26 of 2021).

The implementation followed a clearly phased strategy, prioritizing the most vulnerable groups before progressively expanding access to the wider population. Vaccinations began on 27 December 2020 with residents and staff of senior people's homes and institutions for chronic illnesses (6,176 individuals), as well as high-risk healthcare professionals (around 1,000 staff). In January 2021, the program moved to the elderly aged 80+ (33,530 people), followed in February by those aged 70+ (99,959) and in March by the 65+ age group (144,800). In April 2021, vaccinations extended to vulnerable groups such as individuals with diabetes, severe obesity, or other chronic conditions (26,173), along with the 40–64 age group (268,700). Access was gradually widened through the GeSY platform, with 30+ citizens eligible from April (557,268), followed by the 20+ population in May (695,590), including a subgroup of 20–39 years (281,973). By June 2021, eligibility had opened to all adults aged 18+ (716,952), further extended to those 16+ (735,854). From July 2021, "walk-in" vaccination centres operated in all districts to facilitate faster access, and by August 2021, the campaign covered all individuals aged 12 and above (772,087).

4.1.3 Epidemiological Surveillance

Alongside policy measures and medical interventions, Cyprus invested in technological solutions to enhance epidemiological surveillance and public communication. A series of local, geoinformatics-driven initiatives were developed, providing essential insights into the pandemic's spatial and temporal evolution.

In response to the multifaceted challenges of the COVID19 crisis, both the public sector and the research community in Cyprus launched innovative projects aimed at improving monitoring and decision-making. These included dashboards and mapping applications that visualized confirmed cases, deaths, testing activity, and vaccination coverage across districts. The National COVID19 Portal and other official platforms offered daily updates, while academic institutions, such as the University of Cyprus, developed independent monitoring tools (e.g., https://covid19.ucy.ac.cy/). Furthermore, the integration of data into GIS environments (ArcGIS, QGIS) enabled more advanced spatial analysis, supporting authorities in evaluating intervention effectiveness and identifying local transmission hotspots.

Digital contact tracing applications and web-based communication tools were also introduced to strengthen responsiveness and awareness. While their adoption levels varied, these initiatives highlighted the growing importance of digital geoinformatics within Cyprus' public health infrastructure.

The most significant system established during this period was the Emergency Management System for Handling COVID19 Cases. Developed collaboratively by the KIOS Center of Excellence and the University of Cyprus in partnership with the Ministry of Health and the Deputy Ministry of Research, Innovation, and Digital Policy, this platform replaced the initial manual case reporting process. It functions as an integrated, automated system for managing both suspected and confirmed cases, offering real-time data analysis and immediate situational awareness of the pandemic's spread. Access to the system is restricted to authorized professionals, including staff of the Ministry of Health's Epidemiological Surveillance Unit, first responders of the national hotline (1420), authorized physicians, and clinical laboratories.

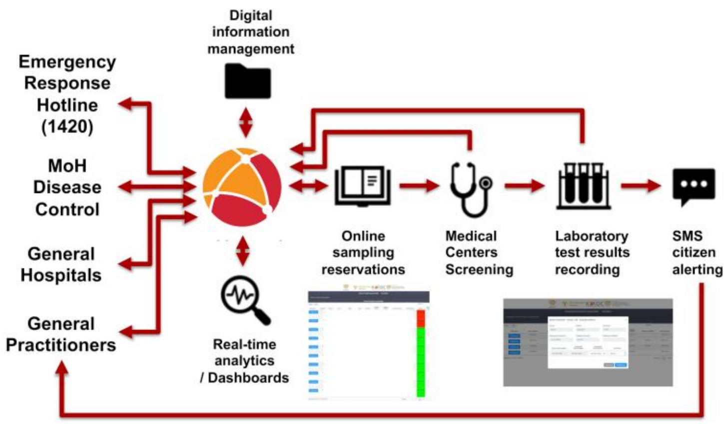

Figure 29. The emergency management system offers a decentralized data management service with various interfaces catering to different user roles. Additionally, it streamlines procedures related to scheduling patient test sampling at healthcare centers, reporting test results, and notifying patients of their test results. Source: (KIOS CoE, 2020).

This infrastructure provides decentralized data management with user-specific interfaces, streamlining procedures for test scheduling, reporting, and patient notification. Its algorithms enable real-time visualization through dashboards, helping health experts and policymakers to track the spread of COVID19 and respond more effectively. The platform thus became the backbone of Cyprus' digital epidemiological surveillance strategy. The system's algorithms facilitated real-time data analysis and information visualization via dashboards, serving as a valuable resource for health experts and decision-makers to access current data on the virus's spread in Cyprus. Moreover, it expedited the identification of suspected and confirmed COVID19 cases in Cyprus, aiding healthcare professionals in effectively managing and mitigating the virus's transmission.

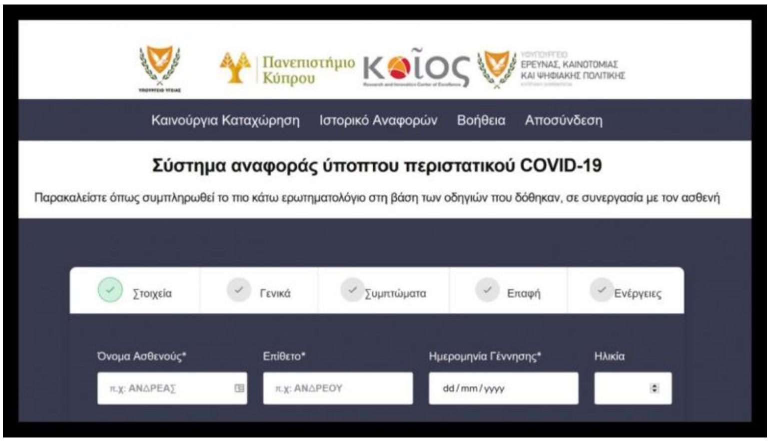

Figure 30. The “Emergency Management System for Handling COVID19 Cases” entry form. Source: (Webb, 2020).

In addition to government-led initiatives, Cyprus’ academic and research community contributed significantly to the development of geoinformatics tools. The KIOS COVID19 Dashboard (fig.31) presents interactive maps and statistics on confirmed cases, categorized by district, postal area, age, and gender. Data is sourced directly from the Emergency Management System and updated every four hours, offering near real-time monitoring.

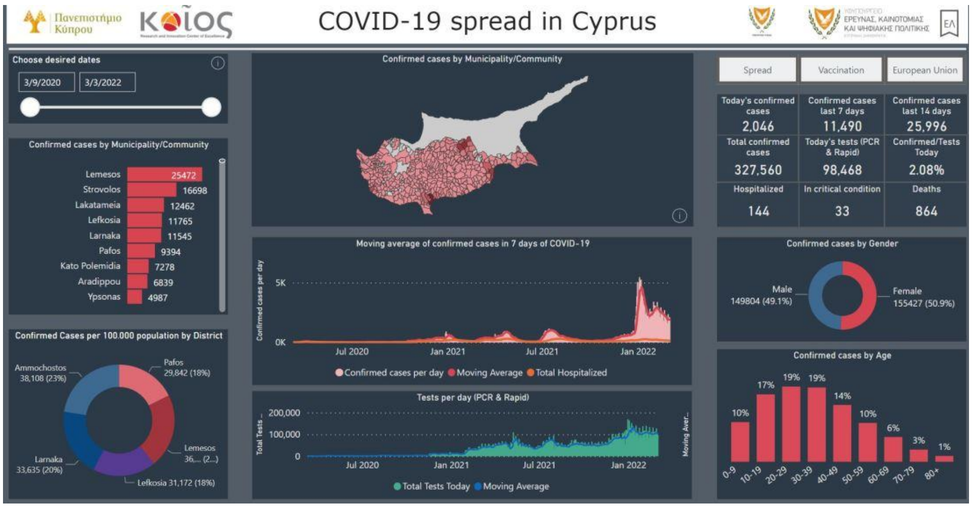

Figure 31. The interface of the platform. Source: (KIOS CoE COVID19 Cyprus Cases Dashboard, 2021)

The COVID19 Web-GIS Platform (fig. 32), developed by the Eratosthenes Center of Excellence at the Cyprus University of Technology, , is a Web-GIS system that serves as an online geoinformation tool for mapping, visualizing, and monitoring COVID19 cases and associated statistics. Additionally, it includes two supplementary applications, one for tracking the global progression of cases and another for mapping the origins of COVID19. The primary objective of this platform is to illustrate the spread of the COVID19 pandemic, disseminate valuable statistical information to government departments and authorities, and provide informative resources to the public.

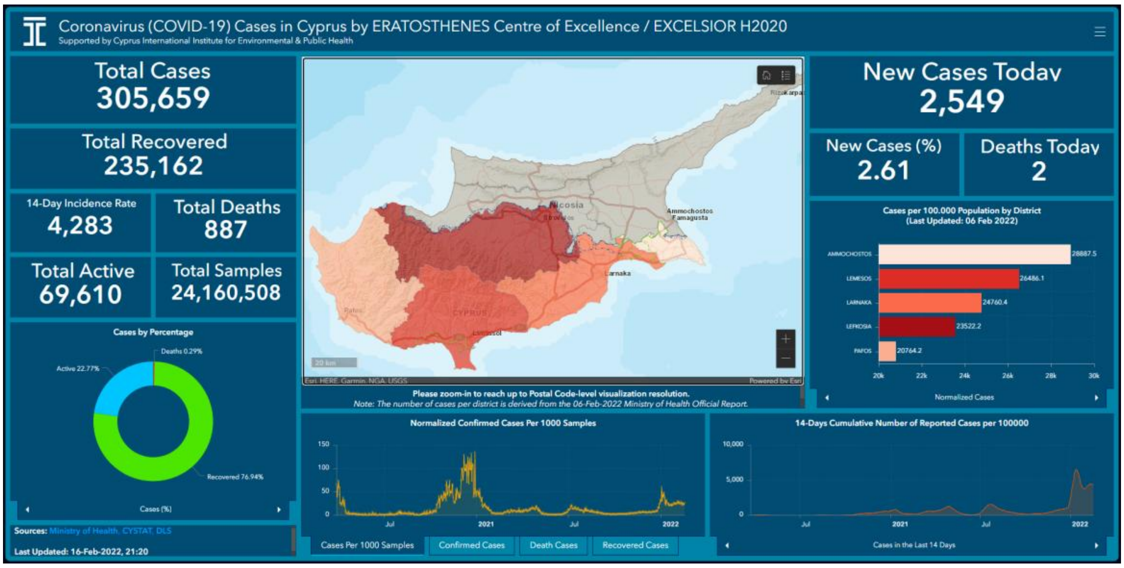

Figure 32. The interface of the Web-GIS platform. Source: (Eratosthenes CoE COVID19 Cyprus Cases Dashboard, 2021)

The CovTracer mobile application (fig.33), developed by the CYENS Center of Excellence, was designed to limit community spread by enabling voluntary digital contact tracing (Isaia et al., 2021). Users could record their movements over a 14-day period, with data stored locally on their devices. If a user tested positive, the application—using GPS, Bluetooth, and the Google-Apple Exposure Notification protocols—could notify individuals whose routes had intersected with the infected person. Importantly, ownership and access to the recorded data remained with the user, who could choose whether to share it with authorities or epidemiologists.

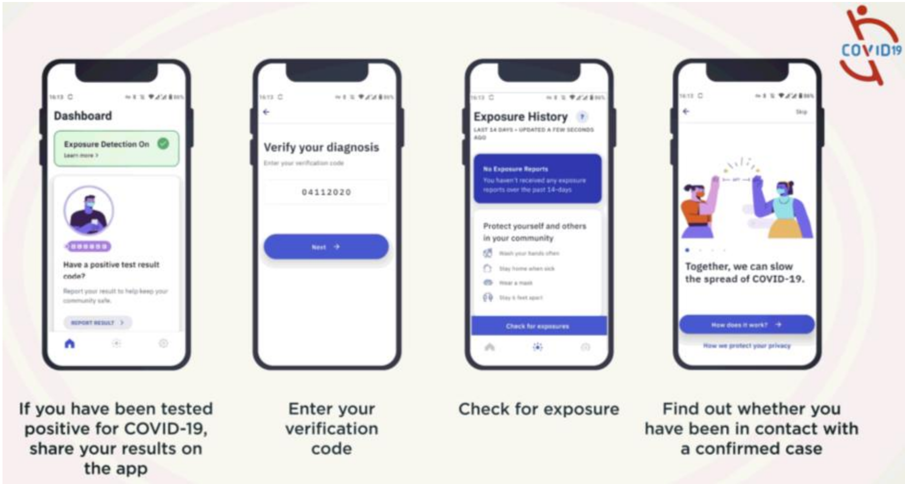

Figure 33. The interface of the contact tracing app. Source: (The CovTracer - Exposure Notification App, 2021).

These initiatives collectively demonstrate how Cyprus leveraged geoinformatics and digital innovation to strengthen epidemiological surveillance, facilitate informed decision-making, and enhance public communication during the COVID19 pandemic. The collective deployment of these platforms marked a turning point in Cyprus' public health infrastructure. The integration of geoinformatics offered several advantages like: (a) Spatial precision, allowing authorities to identify regional differences in transmission and vaccination uptake, (b) Timely communication, providing the public with daily updates and promoting compliance with health measures and (d) Decision support, enabling scenario modelling and evaluation of policy effectiveness. However, challenges also emerged. These included ensuring data privacy and security, maintaining user trust, addressing gaps in digital literacy, and ensuring interoperability between different systems. Moreover, while some tools achieved high visibility, others faced limited public adoption, illustrating the importance of both technical design and community engagement.

The Cypriot experience aligns with global evidence showing that smaller countries, due to their size and agility, were able to implement and adapt digital surveillance systems more rapidly (Harris, 2021). Nevertheless, the Cyprus case highlights the importance of academic-government collaboration in building resilient digital infrastructures. The combination of centralized government platforms with independent academic initiatives created a diversified ecosystem of tools, which collectively enhanced resilience and adaptability.

In conclusion, epidemiological surveillance in Cyprus during the COVID19 pandemic was shaped by a dynamic interplay between policy, research, and technology. The digital platforms and geoinformatics tools developed not only provided critical insights for managing the pandemic but also laid the foundation for future applications in public health crises, demonstrating the enduring value of investing in digital innovation.

4.2 Thesis Results

During the initial phase of data analysis, a range of cartographic outputs, including digital maps and a Web-GIS platform, was developed to visualize the spatial distribution of COVID19 and present key epidemiological statistics. The digital maps are categorized as either static or dynamic (animated). Static maps provide a single temporal snapshot of the epidemiological situation, whereas dynamic maps offer a time series of moving images, illustrating the progression of the pandemic over time.

As a natural next step, a user-friendly Web-GIS platform was developed to enable interactive exploration. This platform allows users to adjust parameters, visualize maps and statistics, and examine the spatiotemporal progression of the disease in Cyprus. Users can navigate through both space (zooming and panning) and time (via a time slider), enhancing the accessibility and interpretability of the data.

Although the technologies employed are not novel per se, these cartographic products represent unique research outputs in the Cypriot context. Their distinctiveness lies in the absence of locally developed tools offering such detailed spatial and temporal resolution. To the best of the author's knowledge, no comparable integrated Web-GIS platform or comprehensive thematic maps depicting the epidemiological evolution of COVID19 in Cyprus have been produced to date. All maps presented below are also accessible on the PhD project website (https://epimo-geo.ct.ws). All maps are produced using QGIS, OpenStreetMap, and ArcGIS Pro/Online platforms.

Being a crucial part of data analytics, the collection of COVID19 related data in Cyprus involved the systematic identification, retrieval, cleaning, processing, and integration of both spatial and non-spatial datasets. The datasets compiled contain comprehensive information on confirmed cases, daily tests, hospitalizations, intensive care admissions, and vaccination statistics, as well as governmental decrees and public health response measures.

Data forming the spatial database were obtained from authoritative national and international sources, including the Cyprus Ministry of Health (https://www.pio.gov.cy/coronavirus), the Cyprus National Open Data Portal (https://data.gov.cy), the Cyprus National COVID19 Portal (https://covid19.ucy.ac.cy), the ECDC (https://www.ecdc.europa.eu/en/publications-data), and the WHO (https://covid19.who.int/data).

All collected datasets underwent extensive preprocessing, including data cleaning, normalization, and geospatial referencing, before being integrated into a spatial database using ArcGIS and QGIS. This enabled the harmonization of heterogeneous data sources, ensuring consistency and compatibility for the production of static, dynamic, and interactive maps, as well as the Web-GIS dashboard. The structured spatial database forms the backbone of all the cartographic work done.

4.2.1 Static Maps

Two thematic digital maps were created using open-source software (QGIS and OpenStreetMap) to depict the spatial distribution of: (a) COVID19 cases and deaths, and (b) COVID19 vaccinations recorded during 2020 in the areas controlled by the Republic of Cyprus. The first map composition (fig.34) is designed as a dashboard illustrating the monthly spatial distribution of confirmed COVID19 cases and deaths. To facilitate comparison across time, the dashboard includes ten inset maps, each representing the monthly distribution of positive cases and deaths by district from the beginning of the pandemic through the end of the year. Due to limitations in the available data, cumulative COVID19 cases are presented from March (the start of the pandemic) to September, whereas from October onwards, case numbers are reported as totals over a 14-day period. Mortality statistics represent cumulative deaths from the onset of the pandemic. In the inset maps, positive cases are visualized using a color gradient across polygons (yellow for fewer cases to lilac for higher counts), while deaths are represented as a heatmap with red intensity. The dashboard-style map also includes key statistics and explanatory text: on the left, weekly confirmed cases and deaths across the island are presented according to the ECDC, on the right, demographic information (age distribution, gender, and district of residence) of deceased individuals is shown, along with a historical overview of the disease in Cyprus.

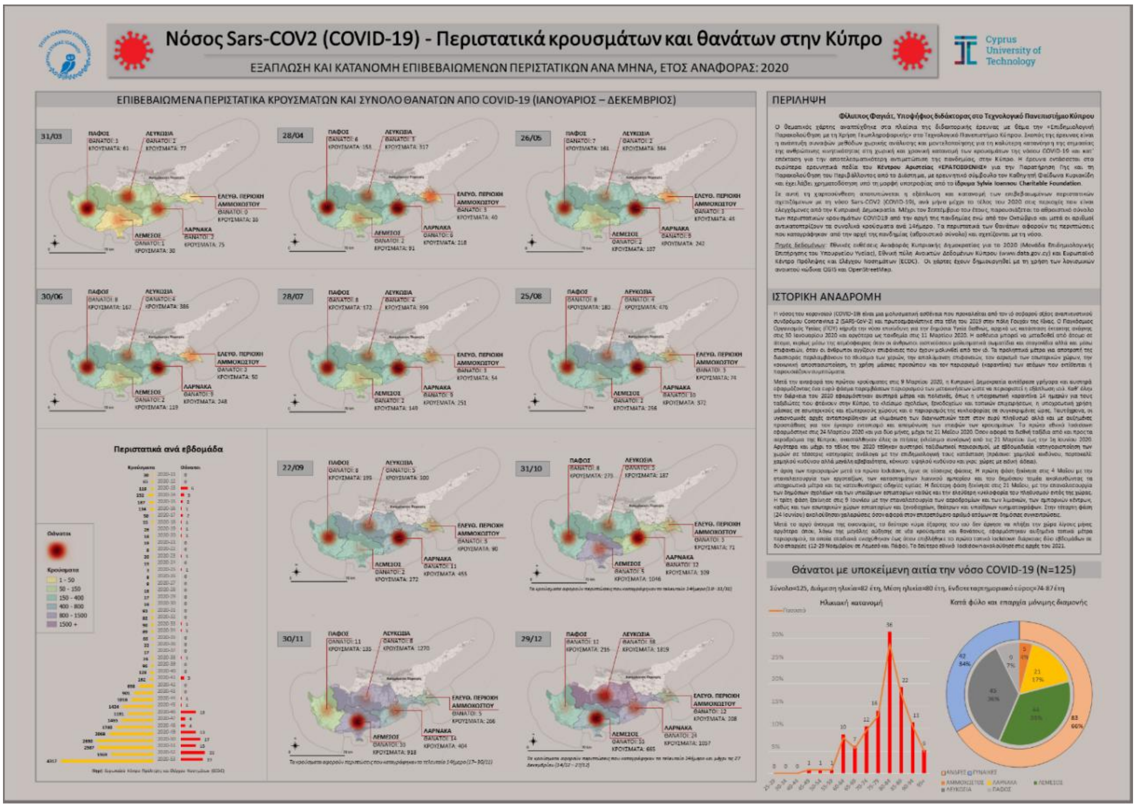

Figure 34. Dashboard-style digital map showcasing important COVID19 statistics, per month for each district of Cyprus (excluding Turkish-occupied areas).

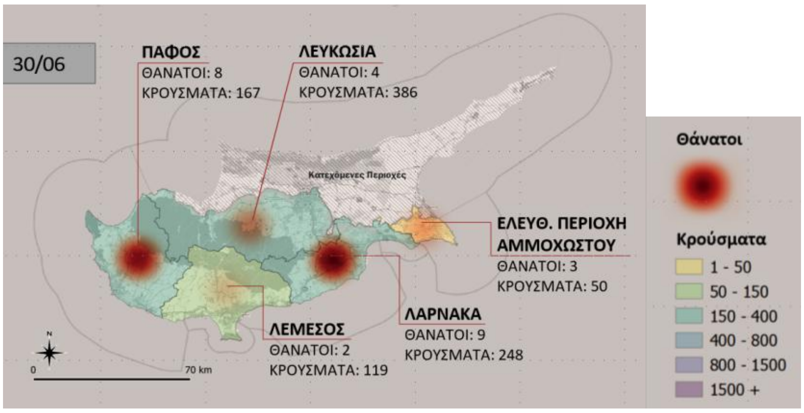

Figure 35. An example of Inset map within the first map, showing the spatial distribution of confirmed COVID19 cases and deaths per district (data for June 30, 2020).

The second map composition (fig.36) focuses on the spatial distribution of COVID19 vaccination coverage in 2020. Unlike the first, this composition is not a dashboard but consists of a single inset map on the left, depicting the number of vaccines administered per district, broken down by age group. The map is complemented by key statistics and explanatory text. At the bottom, statistics summarize the total number of vaccinations by age group and district, including the type of vaccines administered. On the right, historical context regarding vaccination campaigns in Cyprus is provided.

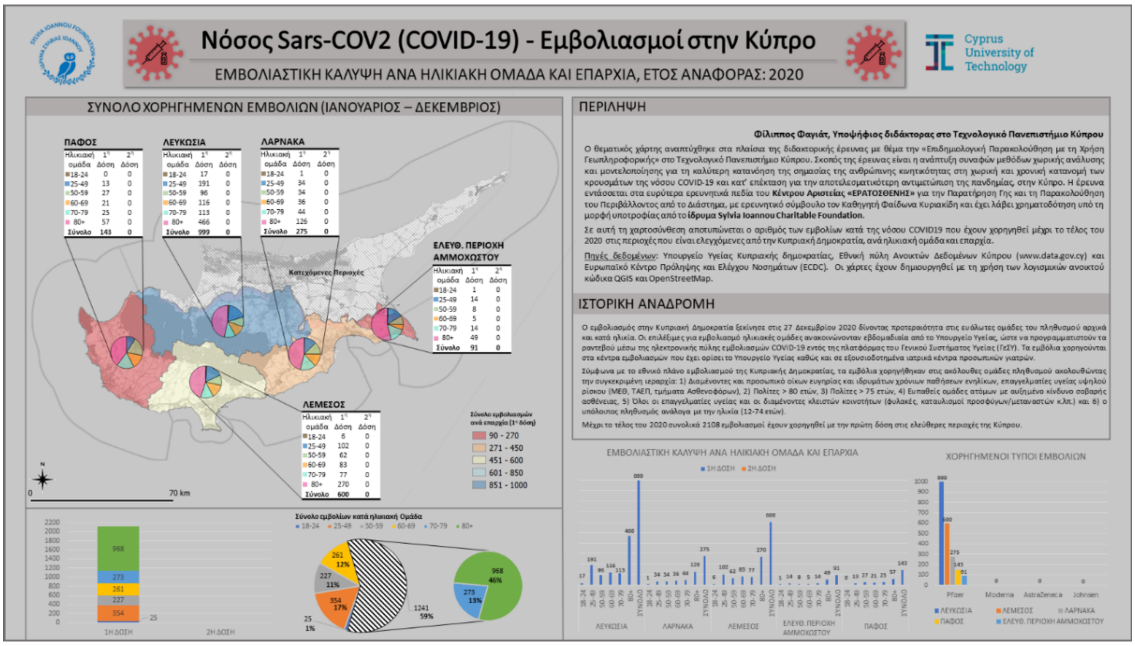

Figure 36. Digital map showing the spatial distribution of vaccinated individuals, for each district of Cyprus (excluding Turkish-occupied areas)

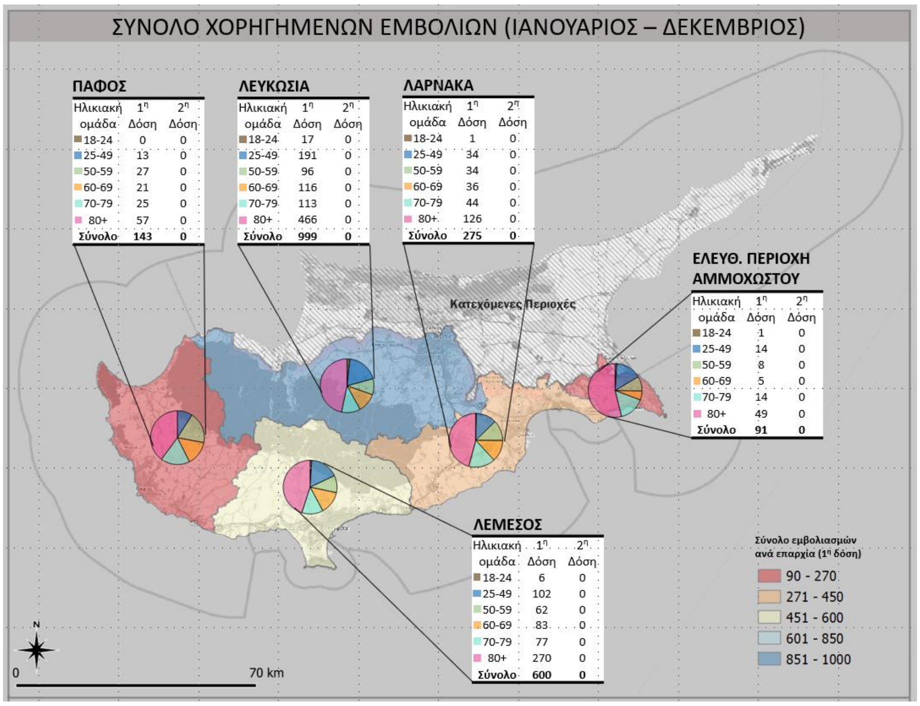

Figure 37. The inset map of the second map composition, showing the spatial distribution of administered vaccines (1st and 2nd dose) and total vaccination coverage by age group for each district (data until December 2020).

The inset map (fig.37) uses a color gradient to represent cumulative first-dose vaccinations (red for fewer to blue for higher numbers) and includes pie charts illustrating the proportion of vaccines administered to different age groups within each district.

The static maps presented here demonstrate the substantial potential of digital cartography in visualizing and analyzing the spatiotemporal dynamics of COVID19 in Cyprus. They provide a comprehensive and representative example of what can be achieved by integrating detailed epidemiological and vaccination data into user-friendly visual formats.

4.2.2 Dynamic Maps

Building on more advanced cartographic technologies, the following animated maps are digital .gif files that illustrate the temporal evolution of epidemiological statistics across administrative units, automatically cycling through sequential snapshots.

Specifically, the animated maps (fig 38 and 39) display the weekly spatial distribution of confirmed COVID19 cases (statistics per 100k population) by district, using a color gradient from green (fewer cases) to red (more cases). Additionally, the size of the circles represents the weekly cumulative total of cases.

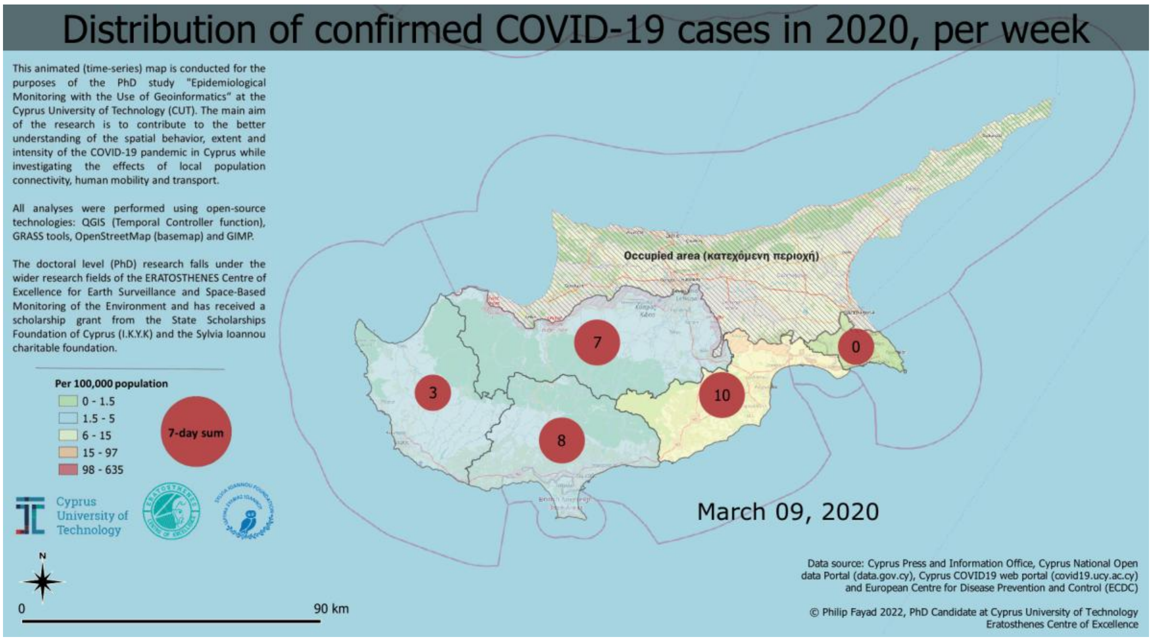

Figure 38. Snapshot of the animated .gif map. Spatial distribution of confirmed COVID19 cases in 2020, per week for each district.

Using a similar design approach, another animated map (fig.40 and 41) depicts the weekly spatial distribution of COVID19 deaths (mortality rate) by district, with a color gradient from yellow (fewer deaths) to dark red (more deaths). The symbol size corresponds to the cumulative number of deaths from the beginning of the pandemic.

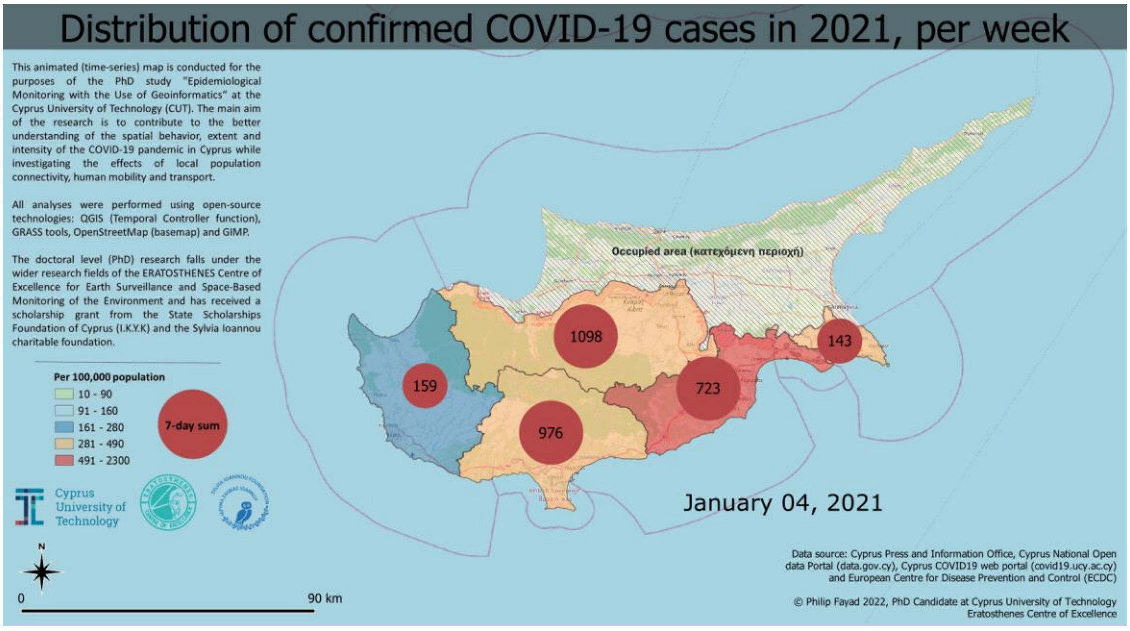

Figure 39. Snapshot of the animated .gif map. Spatial distribution of confirmed COVID19 cases in 2021, per week for each district.

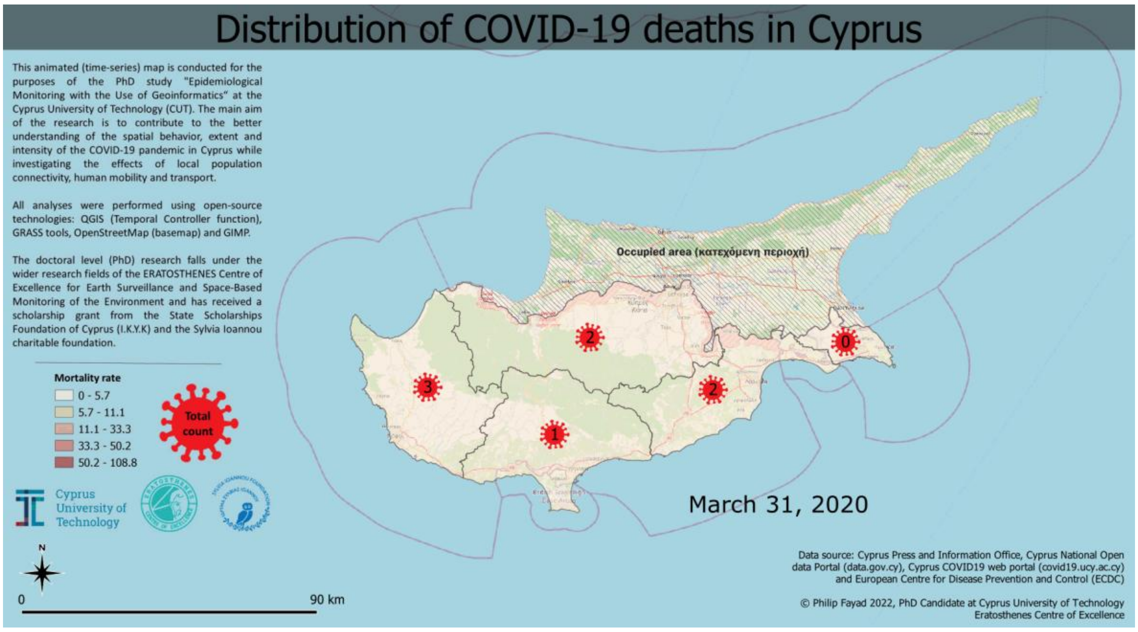

Figure 40. Snapshot of the animated .gif map. Spatial distribution of confirmed COVID19 deaths and mortality rate in 2020, per week for each district.

The mortality rate, expressed as a percentage, is a measure of the number of deaths in a particular population over a specific period of time. It is commonly calculated by dividing the number of deaths that occurred during a given time period by the total population at risk during that same time period, and then multiplying by 100 to express the result as a percentage.

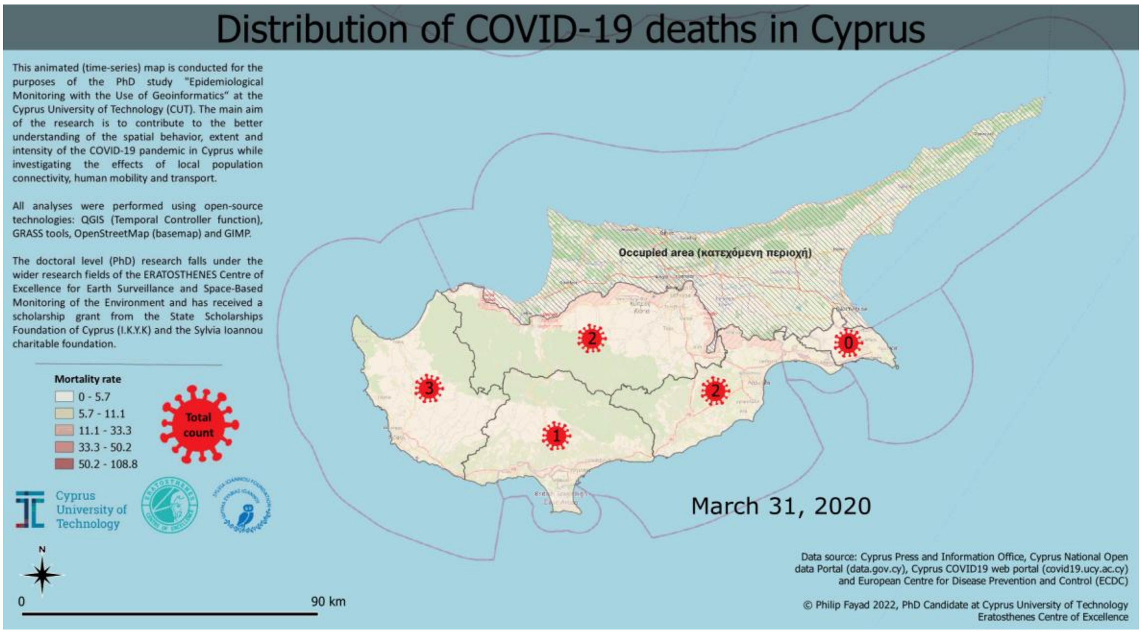

Figure 41. Snapshot of the animated .gif map. Spatial distribution of confirmed COVID19 deaths and mortality rate in 2021, per week for each district.

The last category of animated maps (fig.42 and 43) represents the weekly vaccination coverage of the population, by age group and district. A color gradient from yellow (fewer vaccinations) to intense green (more vaccinations) reflects the cumulative weekly total of administered vaccines within each administrative unit. The overall vaccination percentage in each district is dynamically updated in accompanying text, while pie charts display the distribution of vaccinated individuals by age group.

In summary, the dynamic maps presented here exemplify the power of temporal visualization in capturing the evolving landscape of the COVID19 pandemic. They allow for a clear and intuitive understanding of trends in case incidence, mortality, and vaccination coverage over time and across space. These animated products not only provide valuable insights for public health monitoring and decision-making but also highlight the potential for continuous development: as new data become available, additional animations can be produced, refined, and expanded. Collectively, they represent a flexible and scalable framework for visualizing epidemiological phenomena in Cyprus and beyond.

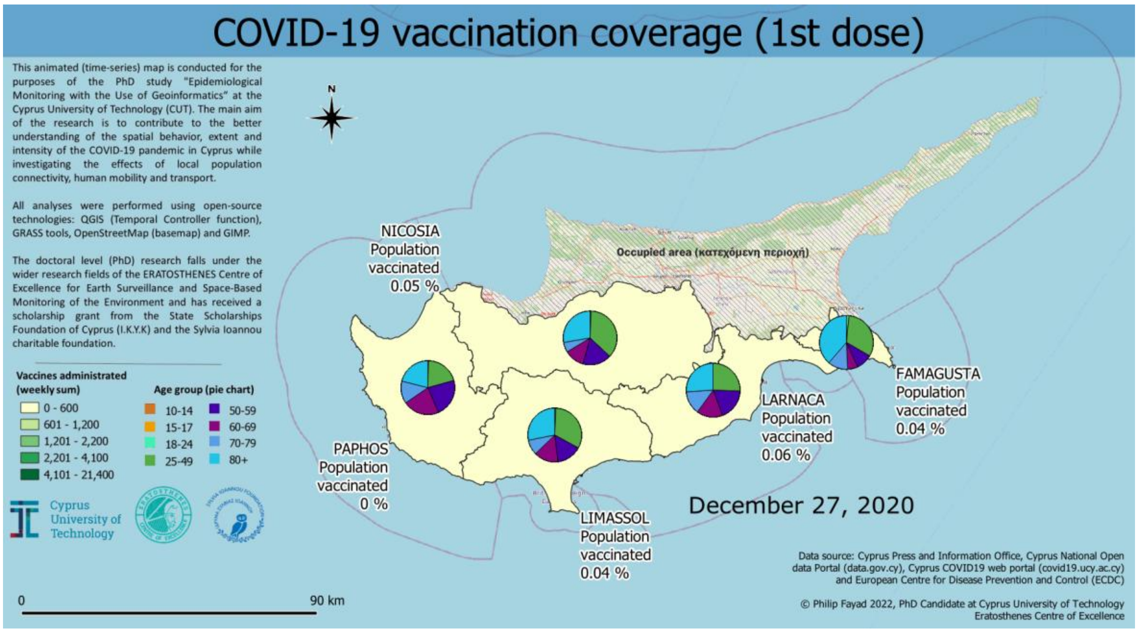

Figure 42. Snapshot of the animated .gif map. Vaccination coverage (first dose), per week for each district.

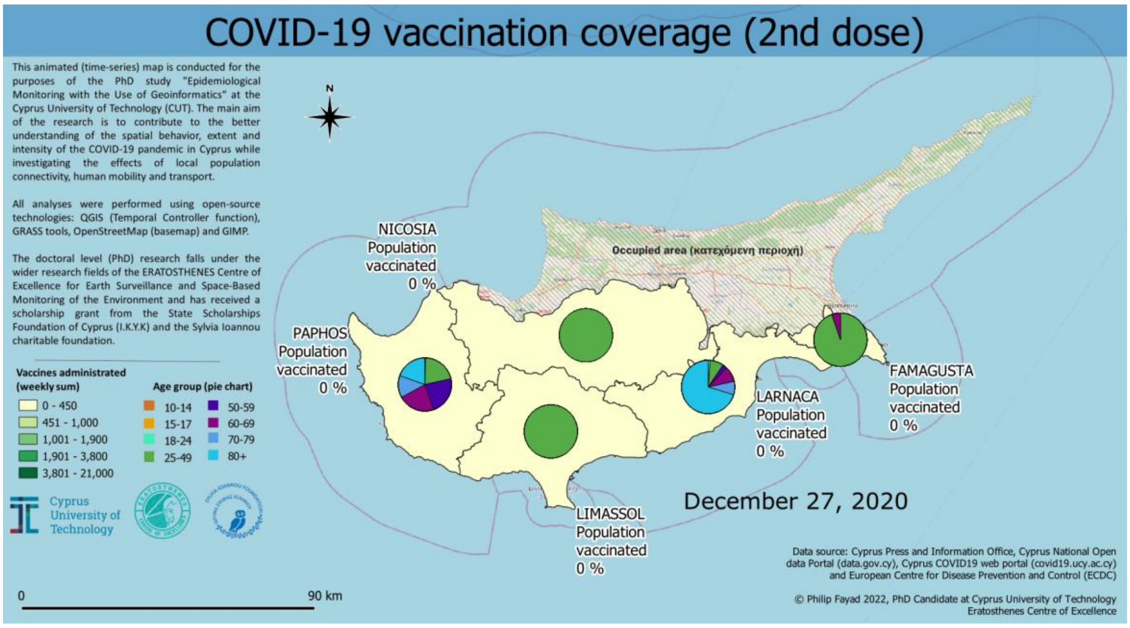

Figure 43. Snapshot of the animated .gif map. Vaccination coverage (second dose), per week for each district.

4.2.3 Web-GIS Dashboard

The developed Web-GIS platform is a unique tool in Cyprus, representing a comprehensive historical record of the spatiotemporal spread of COVID19 within the territory of the Republic of Cyprus (non-occupied areas). It provides an interactive dashboard that captures the progression of the virus from March 2020, when the first cases appeared in Cyprus, until the end of 2022, when the WHO officially declared the end of the pandemic.

At the center of the dashboard (fig.44), the main map dynamically displays the distribution of confirmed COVID19 cases (per 100k population) by district. The map's data are categorized into five groups based on frequency and value range, visualized using a gradient of red shades. Users can freely navigate the map spatially or utilize predefined "bookmarks" to quickly access key areas. The integrated TimeSlider tool allows temporal navigation, enabling users to explore changes in case distribution over weeks and months. Selecting any district polygon on the map provides detailed, district-specific information, enhancing user engagement and understanding.

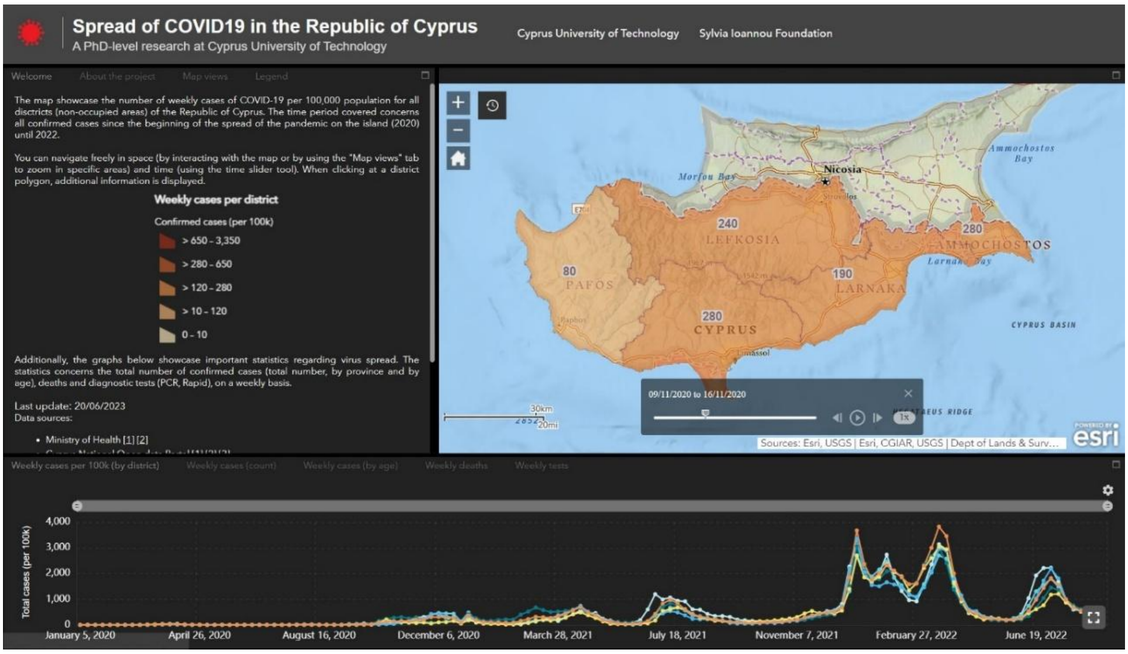

Figure 44. The Web-GIS Dashboard developed, showcasing COVID19 data.

In addition to the interactive map, the dashboard includes five critical epidemiological indicators (fig.45), reflecting weekly recordings of:

a) confirmed cases by district (per 100k population),
b) total confirmed cases,
c) confirmed cases by age group,
d) total deaths, and
e) total diagnostic tests (PCR and Rapid) conducted across Cyprus.

This multi-layered information allows users to gain a comprehensive overview of both spatial and demographic trends, integrating case data, mortality, and testing statistics in a single interactive environment.

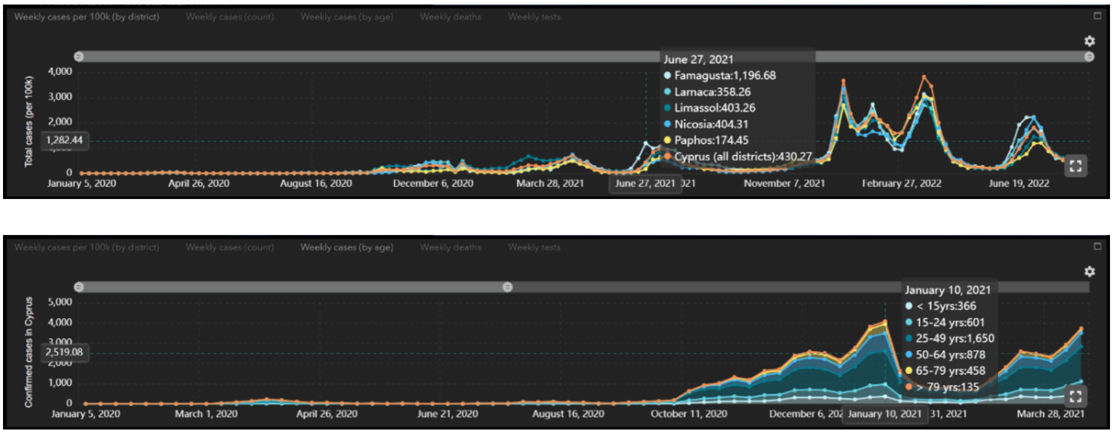

Figure 45. The bottom part of the dashboard, showcasing key epidemiological indicators.

By combining advanced spatial visualization, temporal tracking, and user interactivity, this Web-GIS dashboard demonstrates the potential of digital tools for public health monitoring and decision-making. Its design ensures accessibility for a wide audience, from researchers and policymakers to the general public, allowing for an intuitive exploration of complex epidemiological data. As new data become available, the dashboard can be continuously updated and expanded, creating opportunities for ongoing analysis and visualization. Overall, it serves as a representative example of what can be achieved when modern GIS technologies are applied to real-world public health challenges.

4.2.4 Conclusions

The development of cartographic products enabled a comprehensive visualization of COVID19 epidemiological trends in Cyprus. Both static and dynamic maps, complemented by an interactive Web-GIS platform, provided multi-dimensional perspectives of the disease's spatiotemporal progression. The combined use of static maps, dynamic maps, and the Web-GIS dashboard demonstrates the potential of geospatial analysis for monitoring and understanding the COVID19 pandemic. Static maps offer clear temporal snapshots, dynamic maps reveal evolving trends, and the Web-GIS platform provides an interactive, multi-layered perspective of epidemiological data. Together, these tools constitute a representative example of advanced digital cartography applied to public health. Importantly, they are adaptable; as new data emerge, additional maps and analyses can be generated, ensuring continuous monitoring and informed decision-making. This suite of cartographic products highlights the capacity of GIS-based methods to support research, policy, and public communication in epidemic management, establishing a model for future epidemiological mapping initiatives.

5 Capturing Human Mobility Behavior in Cyprus

Spatial relationships, primarily involving proximity and relative location, are at the heart of spatial analysis. Spatial statistical models are built upon the notion of spatial dependence. An effective statistical model should be capable of explaining the underlying "mechanism" that gives rise to the observed data. The concept of probability plays a fundamental role in our comprehension and interpretation of occasional events. In today's highly mobile world, people of all age groups move frequently. Children commute between their homes, daycares, and schools, while the working population travels between their residences and workplaces regularly. Many individuals also relocate from one region to another within the same municipality, country, or even between countries. Consequently, people encounter various risk factors in different locations, making it challenging to establish a clear link between disease contraction and specific environmental risk factors. This complexity results in potential inaccuracies in mapping associations between prior exposures and risks, which can lead to erroneous conclusions and hypotheses about disease causation. This challenge highlights the need for individual-level follow-up studies to accurately measure real exposure. However, these studies are often labor-intensive and costly. An intriguing alternative is to develop spatio-epidemiological models that rely more on individual-level data rather than coarse spatial information. These individual-level data can be collected through methods such as questionnaires or by leveraging modern GPS and GIS technologies. Building a database that captures an individual's spatial exposure history can significantly enhance spatial analyses aimed at uncovering the causes of diseases.

Cyprus, like many other countries, experiences diverse mobility patterns among its residents. Commuting to work or school, running errands, and leisure activities all contribute to the overall mobility landscape. The choice of transportation modes, such as private vehicles, public transit, walking, or cycling, varies depending on factors like distance, convenience, cost, and infrastructure availability. Urban areas in Cyprus often witness higher levels of congestion during peak commuting hours, leading to increased travel times and environmental impacts. Efforts to promote sustainable transportation alternatives, such as improved public transit systems, cycling infrastructure, and pedestrian-friendly urban designs, aim to mitigate these challenges and promote healthier and more environmentally friendly mobility behaviors.

This chapter examines the human mobility behavior of Cypriot residents through the design, implementation, and analysis of a dedicated mobility questionnaire. Serving as the empirical foundation for constructing the Human Mobility Schedule (HMS), the survey was developed to capture the spatiotemporal dynamics of daily movement patterns across Cyprus. It provides valuable insights into travel frequency, purpose, duration, distance, and modes of transportation, offering a comprehensive picture of how residents move within the island.

Section 5.1 presents the development of the questionnaire, which aimed to improve the understanding of population mobility behavior and its potential implications for epidemiological modeling. Based on the collected responses, a detailed mobility schedule was constructed, representing typical resident activities and locations in two-hour intervals throughout the week. In addition to mobility characteristics, the survey gathered information on participants' attitudes and behavioral responses to public health measures, such as mask use, vaccination willingness, and compliance with lockdown restrictions, thereby offering insights into behavioral adaptation during pandemic conditions.

Section 5.2 discusses the findings of the questionnaire, analyzing the responses across different age groups and districts of Cyprus. The analysis reveals patterns of travel distances, commuting habits, frequency and duration of trips, and preferred modes of transport. It further distinguishes between mobility behaviors on workdays and weekends, highlighting temporal variations and contextual factors influencing residents' daily routines. Collectively, these findings provide essential behavioral input parameters for the EPIMO-LCA model developed in the following chapter, ensuring that the simulation of disease spread is grounded in empirically observed human mobility patterns.

5.1 A Questionnaire for the Cypriot Residents

To incorporate human mobility into the ABM software, which models the spread and progression of COVID19 while accounting for population movement, it is essential to rely on data specific to Cyprus. To accurately capture the mobility patterns of Cypriot residents, a dedicated digital questionnaire (via Google Forms) was designed and broadly disseminated for completion. This initiative is motivated by the notable lack of detailed mobility data regarding individuals' movement and transportation behaviors in Cyprus.

The design of the questionnaire was informed by established approaches in human mobility research, travel behavior analysis, and time-use studies. Previous work has demonstrated that questionnaire-based data collection remains a fundamental method for capturing individual-level mobility patterns, including travel frequency, purpose, distance, and transport mode (Axhausen et al., 2002; Stopher & Greaves, 2007). Such surveys enable the construction of detailed mobility profiles that reflect daily routines and spatial interactions, which are essential for modelling human movement and activity systems.

In addition to trip-based information, the inclusion of time-use components has been widely recognized as critical for understanding spatiotemporal behavior. Time-use surveys allow the reconstruction of daily activity schedules and provide insights into when and where individuals interact within different environments (González et al., 2008). In this context, the development of a structured Human Mobility Schedule (HMS), based on two-hour intervals across weekdays and weekends, aligns with established methodologies for capturing temporal regularities and variability in human activity patterns. Such approaches are particularly relevant in epidemiological modelling, where the timing and location of interactions directly influence disease transmission dynamics.

Furthermore, recent studies in spatial epidemiology emphasize the importance of incorporating behavioral and perception-based variables, especially in the context of infectious disease spread and public health interventions. Individual compliance with measures such as mask usage, social distancing, and vaccination has been shown to significantly affect transmission outcomes (Ferguson et al., 2020). Therefore, the questionnaire developed in this research integrates both quantitative mobility characteristics and behavioral responses to COVID-19 policies, ensuring a comprehensive representation of human mobility and its interaction with epidemiological processes. Importantly, the survey was adapted to the Cypriot context, addressing the lack of localized mobility datasets and enabling the development of a data-driven, context-specific modelling framework.

The developed survey aims to improve our understanding of the spatiotemporal mobility patterns of residents, providing insights into travel frequency, purpose, duration, distance, and modes of transportation across the island. Based on the survey responses, a detailed mobility schedule is constructed, representing typical resident activities and locations in two-hour intervals throughout the week. Additionally, the survey collects participants' attitudes and responses regarding key measures and policies for potential future pandemics, including mask usage, vaccination, and lockdown compliance.

Targeting the adult general population of Cyprus (students, unemployed, employed and retirees), the questionnaire was distributed in various community organizations, patient associations, institutions, universities, educational bodies, and research centers across the areas controlled by the Republic of Cyprus (excluding Turkish-occupied areas). Moreover, to ensure maximum outreach, it was extensively promoted to the general public through digital platforms such as Facebook, X and LinkedIn. To verify the accuracy of the demographic coverage of the participants, a statistical comparison was made with the national census data of the Republic of Cyprus from 2019. Specifically, the latest official census data on the population distribution across five districts of Cyprus were used for comparison (Statistical service of the Republic of Cyprus, 2019)

The questionnaire, consisting of three parts (APPENDIX), is targeted at individuals over 18 years old and residents of Cyprus. The first part seeks demographic information (gender, age, permanent residence area, and employment). Subsequently, key mobility characteristics are gathered (frequency, purpose, duration, distance, and mode of transportation). The second part involves completing a mobility timeline, indicating the approximate location every two hours within a typical day. In the third part, participants are asked for their opinions on some significant measures to limit the spread of COVID19. The digital form is created on the Google Forms platform, and participation is anonymous. To take part, participants must confirm that they are 18 years and above and consent to the provision of their information (fig.46 below).

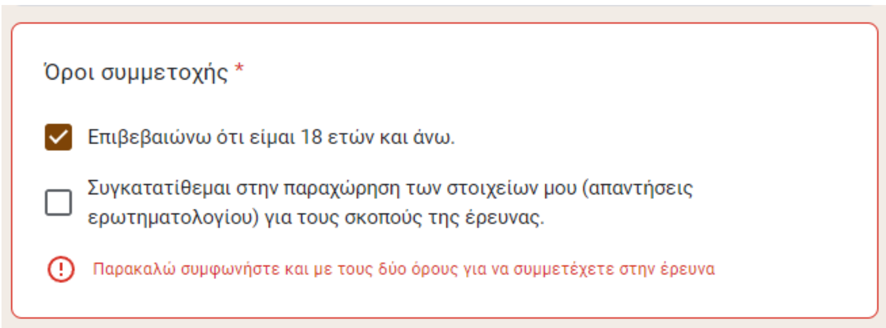

Figure 46. Participants must consent to take part in the survey.

To achieve maximum reach (target group: students, employees, and retirees residing in the Republic of Cyprus), the questionnaire has been disseminated to various organizations, associations, institutions, universities, educational bodies, and research centers. Additionally, it has been promoted through digital channels like Facebook and LinkedIn.

Participation was voluntary and not binding. At any point during completion, participants could discontinue, and their responses would be immediately withdrawn. The estimated time for completing the questionnaire is 10 minutes. The purpose of the mobility questionnaire is to capture the daily typical movements of Cypriot citizens. Through statistical analysis of the collected data, the main mobility profiles of Cypriot citizens will be generated, which will then be integrated into the ABM epidemiological model. The full questionnaire is attached at the last pages of the dissertation (APPENDIX). Ethical approval for the project was obtained from the Cyprus National Bioethics Committee [ref: ΕΕΒΚ ΕΠ2023.01.273]. This ensured that the study was conducted in full compliance with ethical standards and data protection measures. Survey demographics are compared with the 2019 Cyprus census across districts to evaluate sample representativeness, while statistical tests (t-tests) on age and gender distributions confirm the reliability of the dataset for most regions and demographic groups.

5.1.1 Demographics

Across all regions, the majority of participants fall within the 25-44 age group, followed by the 45-49 age group. Regarding gender distribution, according to the national census data of the Republic of Cyprus (2019), there is a relatively equal gender split, with women (51%) slightly outnumbering men (49%). However, in this study, gender distribution is relatively balanced across all districts overall except in Nicosia, which exhibits a skew towards males. Consequently, there is a higher proportion of male participants (60%) compared to female participants (40%). Furthermore, the majority of participants (85%) work with physical presence, while a very small percentage (3%) work remotely. Eight percent of the participants are unemployed, and 4% are currently retired. Regarding educational status, most participants (77%) are not currently attending an educational institution, while the remaining participants are currently enrolled as students at the bachelor's level (11%), master's level (7%), and doctoral level (5%).

Table 5. Demographics

Demographics			Gender (%)		Occupation (%)				Currently student (%)			
Residency / Age	N	%	Female	Male	On-site	Remote	Retired	Not employed	Bachelor	Doctoral	Master	Non
Famagusta	44	6	2	3	5	0	0	1	1	0	0	4
< 25	7	1	1	0	0	0	0	1	1	0	0	0
25 - 44	21	3	0	2	3	0	0	0	0	0	0	2
45 - 59	10	1	1	1	1	0	0	0	0	0	0	1
60 +	6	1	0	0	1	0	0	0	0	0	0	1
Larnaca	91	12	5	6	11	1	0	1	1	1	1	9
< 25	5	1	0	0	0	1	0	1	1	0	0	0
25 - 44	63	8	3	5	8	0	0	0	0	1	1	6
45 - 59	16	2	1	1	2	0	0	0	0	0	0	2
60 +	7	1	1	0	1	0	0	0	0	0	0	1
Limassol	274	36	16	19	30	0	2	2	3	1	2	27
< 25	20	3	1	1	1	0	0	1	2	0	0	1
25 - 44	148	19	10	9	18	0	0	1	1	1	2	14
45 - 59	76	10	4	6	9	0	0	0	0	0	0	9
60 +	30	4	1	3	2	0	2	0	0	0	0	3
Nicosia	334	42	16	26	34	2	2	3	5	3	4	33
< 25	26	3	1	2	1	0	0	2	3	0	0	1
25 - 44	177	22	8	14	21	1	0	1	2	2	3	17
45 - 59	92	12	5	7	10	1	0	0	0	1	1	10
60 +	39	5	2	3	2	0	2	0	0	0	0	5
Paphos	44	6	1	4	5	0	0	1	1	0	0	4
< 25	7	1	0	1	1	0	0	1	1	0	0	0
25 - 44	21	3	0	2	2	0	0	0	0	0	0	2
45 - 59	14	2	1	1	2	0	0	0	0	0	0	2
60 +	2	0	0	0	0	0	0	0	0	0	0	0
Grand Total	**787**	**100**	**40**	**60**	**85**	**3**	**4**	**8**	**11**	**5**	**7**	**77**

In Nicosia, the highest response rate stands at 42%, closely mirroring its population percentage of 39% based on the national census data of 2019. The region exhibits a dynamic workforce, with a majority engaged in on-site employment (34%) or remote work arrangements (2%). Furthermore, a significant portion of respondents are currently pursuing bachelor-level (5%), master-level (4%), and doctoral-level (3%) studies. Limassol follows with the second-highest response rate of 36%, surpassing its population percentage of 28% as per the national census data of 2019. Larnaca's responses contribute to 12% of the total, which falls below its population percentage of 17% according to the national census data of 2019. This suggests a relatively low but still reasonable representation from Larnaca residents compared to their population size. Similarly, Paphos accounts for 6% of the responses, which is lower but still reasonable representation than its population percentage of 11% according to the national census data of 2019. Responses from Famagusta represent 6% of the total, which aligns with its population percentage of 5.5% according to the national census data of 2019. Figure 47 illustrate the spatial distribution of the participants across Cyprus (excluding Turkish-occupied areas).

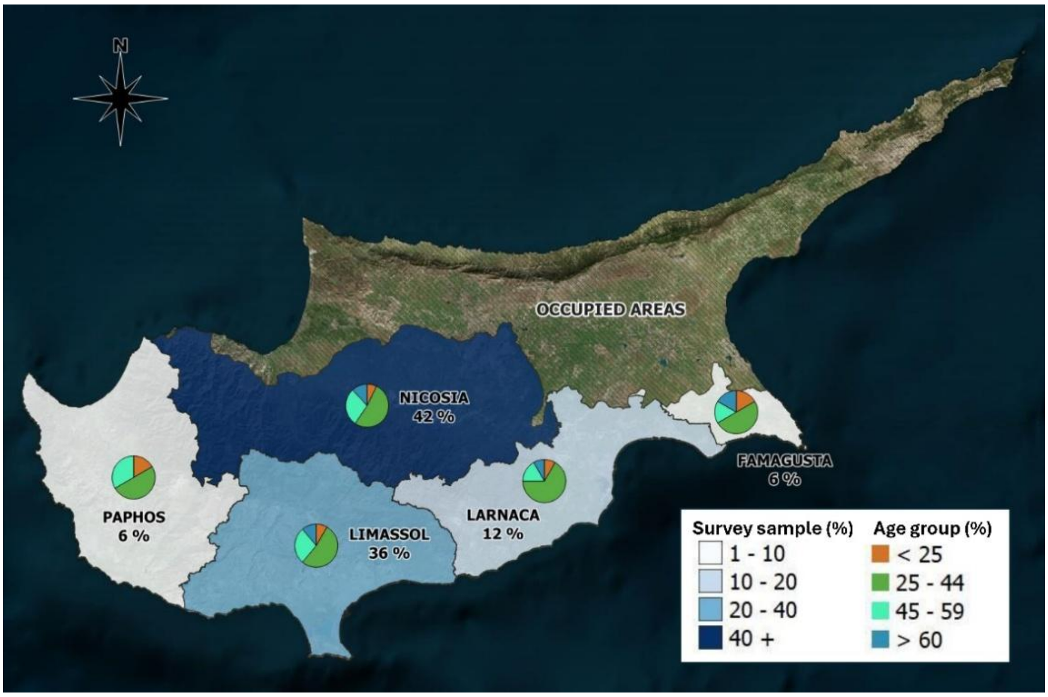

Figure 47. The spatial distribution of the participants closely approximates the population distribution (2019 country census) across the five districts of Cyprus (excluding Turkish-occupied areas). Pie charts illustrate the participation rates by age group.

When comparing the age groups of participants in the survey with the national census data of 2019, several observations can be made:

- Age < 20: The response rate of 1% is significantly lower than the population percentage of 22%, indicating a substantial underrepresentation of individuals in this age group in the survey.
- Age 20 - 24: The response rate of 7% aligns with the population percentage of 7%, indicating an accurate representation in this age group.
- Age 25 - 29: Similarly, the response rate of 9% matches the population percentage of 9%, indicating an accurate representation.

- Age 30 - 34: The response rate of 14% slightly exceeds the population percentage of 9%, suggesting a slight overrepresentation of individuals (5% more) in this age group.
- Age 35 - 39: With a response rate of 16%, higher than the population percentage of 8%, there's a slight overrepresentation (8% more) in this age group.
- Age 40 - 44: The response rate of 15% is slightly higher than the population percentage of 7%, indicating a slight overrepresentation (8% more) in this age group.
- Age 45 - 49: Similarly, the response rate of 11% exceeds the population percentage of 6%, suggesting a slight overrepresentation (5% more) in this age group.
- Age 50 - 54: With a response rate of 10%, slightly higher than the population percentage of 6%, there's a slight overrepresentation (4% more) in this age group.
- Age 55 - 59: The response rate of 5% aligns with the population percentage of 6%, indicating an accurate representation.
- Age 60 - 64: Similarly, the response rate of 6% matches the population percentage of 6%, suggesting an accurate representation.
- Age 65+: The response rate of 5% falls below the population percentage of 16%, indicating a significant underrepresentation in this age group within the survey.

In conclusion, the survey reveals varying levels of representation across different age groups. While age brackets between 20 and 64 demonstrate relatively accurate representation, some deviations are noted. Notably, there is a substantial underrepresentation of individuals under the age of 20 and those aged 65 and above. Specifically, the response rate of 1% for individuals under 20 contrasts starkly with their population percentage of 22%, indicating a significant disparity. Conversely, the response rates for age groups between 20 and 64 generally align well with their respective population percentages, with slight overrepresentations noted in some brackets, particularly in the 35-39 and 40-44 age groups. However, the response rate for individuals aged 65 and above falls short, at 5%, compared to their population percentage of 16%, highlighting a notable gap in representation of this age group.

5.1.2 Sample Representativeness

The comparison between the survey sample and the Cyprus Census data across different districts (tables 6 to 9) reveals important insights regarding the representativeness and potential statistical significance of the survey.

Table 6. Percentage of participants by age group. Survey sample vs Cyprus census 2019 (in parenthesis).

	20-24	25-29	30-34	35-39	40-44	45-49	50-54	55-59	60-64	total
Famagusta	0.70 (0.67)	0.14 (0.71)	0.70 (0.70)	0.97 (0.65)	1.12 (0.64)	0.56 (0.62)	0.70 (0.59)	0.14 (0.52)	0.56 (0.45)	5.59 (5.55)
Larnaca	0.66 (2.17)	1.33 (2.35)	2.65 (2.15)	2.26 (1.93)	2.13 (1.90)	1.06 (1.88)	0.8 (1.78)	0.27 (1.48)	0.40 (1.37)	11.56 (17.01)
Limassol	2.67 (3.45)	3.60 (3.80)	4.67 (3.58)	5.87 (3.19)	5.60 (3.13)	4.27 (3.06)	3.74 (3.01)	2.13 (2.47)	2.27 (2.31)	34.82 (28.00)
Nicosia	3.36 (4.81)	4.16 (5.56)	5.37 (5.27)	7.66 (4.57)	6.58 (4.27)	5.11 (3.93)	5.1 (3.94)	2.15 (3.38)	2.95 (3.18)	42.44 (38.91)
Paphos	0.56 (1.18)	0.42 (1.35)	1.39 (1.28)	0.42 (1.16)	0.70 (1.17)	1.12 (1.15)	0.56 (1.11)	0.28 (1.03)	0.14 (1.07)	5.59 (10.50)

In Famagusta, most age groups are well represented, with only minor differences. For example, the 25-29 age group shows a small discrepancy (0.1% in the survey vs. 0.7% in the census), and the 35-39 and 40-44 age groups are slightly over-represented, though the variation is minimal. In Larnaka, the survey captures a reasonable reflection of the population. While younger age groups, such as 20-24 (0.6% vs. 1.6%) and 25-29 (1.3% vs. 1.8%), are slightly under-represented, middle-aged groups like 30-34 and 35-39 are well represented. In Limassol, the survey shows strong representation for age groups like 30-34, 35-39, and 40-44, particularly the 35-39 group, which accounts for 5.6% of the survey compared to 2.5% in the census. This indicates a good but slightly over-representation of younger and middle-aged demographics. For Nicosia, the survey provides balanced age representation, with only slight under-representation in younger groups like 20-24 (3.2% in the survey vs. 4.8% in the census) and 25-29 (3.9% vs. 5.6%). Meanwhile, middle-aged groups, such as 35-39 (7.2% vs. 4.6%) and 40-44 (6.2% vs. 4.3%), are well covered. In Paphos, while there is some under-representation across most age groups, particularly among younger individuals (e.g., 20-24 at 0.5% vs. 1.2% in the census and 25-29 at 0.4% vs. 1.3%), the survey still offers valuable insights into the region's population.

In conclusion, the survey shows strong representation across middle-aged groups (35-44) in nearly all districts, with some minor under-representation in younger age cohorts (20-29). Overall, the sample provides a solid demographic overview, reflecting the general population well.

Table 7 compares the survey sample distribution by district and gender with the corresponding Cyprus Census data, allowing us to assess the representativeness of the sample in terms of geographic and gender distribution. Starting with Famagusta, the survey captures a balanced gender distribution, with 4% males and 2% females, closely matching the census, which reports 3% for both genders. In Larnaca, the male sample (7%) is nearly in line with the census figure (8%), while the female sample (5%) shows only a slight under-representation compared to the census (9%). In Limassol, both males (19% in the survey vs. 14% in the census) and females (16% in the survey vs. 14% in the census) are well represented, with a particularly strong showing among males. For Nicosia, the survey provides a solid representation of males, comprising 26% of the sample compared to 19% in the census, while females are slightly under-represented (16% vs. 20%), but still reasonably reflected. In Paphos, although both males (4% in the survey vs. 5% in the census) and females (1% vs. 5%) are under-represented, the survey still offers valuable insights into gender distribution in the region, with females being more notably under-represented.

Table 7. Percentage of participants by gender. Survey sample vs Cyprus census 2019 (in parenthesis).

	male	**female**	**total**
Famagusta	3.68 (2.76)	1.91 (2.79)	5.59 (5.55)
Larnaka	6.99 (8.34)	4.57 (8.70)	11.56 (17.01)
Limassol	19.06 (13.52)	15.76 (14.48)	34.82 (28.00)
Nicosia	26.43 (18.83)	16.01 (20.08)	42.44 (38.91)
Paphos	4.19 (5.19)	1.40 (5.32)	5.59 (10.50)

In conclusion, the survey sample generally aligns well with the census data, showing only minor variations in gender representation. Famagusta reflects a balanced gender distribution, while Larnaca demonstrates a good match for males, with a slight under-representation of females. Limassol shows strong representation for both genders, and Nicosia has a solid representation of males, with only a slight under-representation of females. Paphos, while showing some under-representation, particularly among females, still provides useful data on the population.

To evaluate the representativeness of the survey sample in comparison to census data, t-tests were conducted on the gender and age distributions across all districts (table 8-9).

Table 8. T-test for age groups and gender (survey sample vs Cyprus census 2019)

	age group									gender	
	20-24	**25-29**	**30-34**	**35-39**	**40-44**	**45-49**	**50-54**	**55-59**	**60-64**	**male**	**female**
p-value	0.394	0.512	0.774	0.494	0.485	0.799	0.935	0.293	0.594	0.675	0.620

Table 9. T-test for age groups and gender by district (survey sample vs Cyprus census 2019)

	Famagusta	**Larnaka**	**Limassol**	**Nicosia**	**Paphos**
p-value (gender)	0.983	0.155	0.186	0.768	0.221
p-value (age)	0.967	0.068	0.137	0.551	0.001

The t-test results for gender in each district indicated no statistically significant differences, with p-values comfortably above the 0.05 threshold. The lowest values of Larnaka ($p = 0.155$) and Limassol ($p = 0.186$), still approach acceptability. This suggests that the gender composition within each district's survey sample closely aligns with the actual population proportions, supporting the sample's representativeness in terms of gender. The analysis of age group representativeness yielded mostly positive results. Famagusta ($p = 0.967$), Larnaka ($p = 0.068$), Limassol ($p = 0.137$) and Nicosia ($p = 0.551$) show no statistically significant differences, indicating that the age distributions in these survey samples reliably reflect their respective populations. Paphos ($p = 0.001$) show some statistical difference, though still close to conventional thresholds in representativeness, particularly given the broad age range included. Island-wide, gender and age distribution of the survey sample closely aligns with Cyprus census data, as indicated by high p-values for both genders (male: $p = 0.675$; female: $p = 0.620$) and across all age groups (p-values ranging from 0.293 to 0.935). These results confirm the sample's representativeness for gender and most age groups, supporting the reliability of generalizing demographic-related findings from the survey to the broader population in Cyprus, with some caution advised for certain districts and age group inferences.

5.2 Questionnaire Results

The questionnaire, administered via Google Form, consisted of 23 questions is divided into three main sections. It remained open for a duration of 3 months (from November 20, 2023, to February 20, 2024), during which information was gathered anonymously and voluntarily from residents in Cyprus who were >= 18 years old. In the first part, information regarding demographic (gender, age, district of residence and employment) and key mobility characteristics (frequency, purpose, duration, distance, and means of transportation) is collected. The second section accumulates critical information regarding the mobility timeline of the individuals, indicating location and activity every two hours during a typical day. By analyzing the collected data (responses) from the questionnaire, the mobility profiles of Cypriot residents are created for each age group.

The findings obtained from the analysis of the questionnaire have been published in the peer-reviewed European Journal of Geography (Fayad et al., 2024).

Following the systematic analysis of the questionnaire responses, the subsequent sections present the empirical findings regarding the spatial variability of mobility behavior and the degree of acceptance of COVID19 measures across Cyprus. The results are structured both at an aggregate national level and at a more granular district level, thereby allowing the identification of regional differences and commonalities in mobility patterns and attitudes. Particular emphasis is placed on key dimensions of human mobility, including travel distances, trip frequency, duration, and modes of transportation, as well as the temporal distribution of mobility activities during typical weekdays and weekends. This information contributes to a more comprehensive understanding of the spatiotemporal dynamics of everyday life under pandemic conditions. In parallel, the chapter examines participants' perceptions and levels of acceptance concerning the principal interventions and health policies adopted during the pandemic, such as mask usage, social distancing, lockdown restrictions, and vaccination.

5.2.1 Traveling distance

Table 10 illustrates data on traveling distances for various activities such as entertainment and dining, grocery shopping, and general shopping. According to survey findings, the majority (60%) of respondents prefer engaging in entertainment and dining activities within a short 10 km distance, with an additional 23% willing to travel between 10 and 20 km for this purpose. For grocery shopping, most participants (64%) opt for locations within a 5 km range, while 26% are comfortable traveling between 5 and 10 km. The remaining distances for grocery shopping show a relatively even distribution. Similarly, general shopping activities exhibit a preference for shorter distances, with 76% of participants traveling within a 10 km radius and an additional 14% within a 10 – 20 km range. Overall, the data indicates a tendency for people to stick to relatively close distances for everyday activities like grocery shopping, while being more open to traveling longer distances for entertainment, dining, and general shopping purposes.

Table 10. Participants' responses regarding traveling distances for various activities

Traveling Distance	**Entertainment and dining** (N)	**Entertainment and dining** (%)	**Grocery shopping** (N)	**Grocery shopping** (%)	**Shopping** (N)	**Shopping** (%)
< 5 km	160	20	501	64	301	38
5 - 10 km	312	40	201	26	299	38
10 - 20 km	184	23	58	7	110	14
20 - 30 km	69	9	14	2	36	5
> 30 km	62	8	13	2	41	5
Grand Total	**787**	**100%**	**787**	**100%**	**787**	**100%**

The overall trend of higher engagement within shorter traveling distances (< 10 km) is consistent across all age groups (table 11). Despite some fluctuations, the pattern of preferring nearby locations for daily activities like grocery shopping and entertainment remains prevalent across all demographics. Additionally, the majority of participants across all age groups show reluctance to travel distances exceeding 20 km for any activity, particularly for grocery shopping. Participants under the age of 25 (constituting 8% of the sample) predominantly travel distances below 5 km, mainly for grocery shopping (55%), while opting for longer distances primarily for entertainment and dining purposes. The remaining age groups follow a similar pattern with participants aged 25 to 44 (comprising 55% of the sample), 45 to 59 (26% of the sample) and over 60 years old (11% of the sample) predominantly travel distances below 5 km mainly for grocery shopping (63%, 68% and 64% respectively). In general, longer distances are primarily traveled for entertainment and dining purposes. It is noteworthy that movements within distances less than 5 km are mostly carried out by individuals in older age groups (45-59 and 60+ years), accounting for the majority within their respective age group (46%). Additionally, travels exceeding 20 km are primarily undertaken by individuals under the age of 25, for the purposes of entertainment, dining and general shopping, constituting the majority (18%) within the age group.

Table 11. Participants' responses regarding traveling distances for various activities, per age group

Traveling distance	Entertainment and dining	Grocery shopping	Shopping	Total	% of all participants
Age < 25					**8%**
< 5 km	17%	55%	37%	36%	3%
5 - 10 km	31%	23%	25%	26%	2%
10 - 20 km	29%	12%	18%	20%	2%
20 - 30 km	12%	5%	12%	10%	0.5%
> 30 km	11%	5%	8%	8%	0.5%
Age 25 - 44					**55%**
< 5 km	18%	63%	34%	38%	21%
5 - 10 km	42%	27%	43%	37%	20%
10 - 20 km	24%	8%	15%	16%	9%
20 - 30 km	9%	1%	5%	5%	3%
> 30 km	8%	1%	3%	4%	2%
Age 45 - 59					**26%**
< 5 km	24%	68%	46%	46%	12%
5 - 10 km	38%	22%	33%	31%	8%
10 - 20 km	24%	6%	12%	14%	4%
20 - 30 km	8%	2%	2%	4%	1%
> 30 km	6%	2%	7%	5%	1%
Age 60 +					**11%**
< 5 km	29%	64%	44%	46%	5%
5 - 10 km	39%	27%	36%	34%	4%
10 - 20 km	15%	6%	10%	10%	1%
20 - 30 km	5%	1%	4%	3%	0.5%
> 30 km	12%	1%	7%	7%	0.5%

Table 12 showcase traveling distance behaviors across the Cypriot districts. In Famagusta, a significant portion of participants (50–56.8%) reported traveling less than 5 km for grocery shopping and general shopping, while entertainment and dining trips were somewhat more distributed, with 38.6% traveling 5–10 km. Travel beyond 20 km is rare, indicating localized mobility in this region.

Table 12. Participants' responses regarding traveling distances for various activities, by district of residence

	Entertainment and dining (%)	Grocery shopping (%)	Shopping (%)
Famagusta	**100**	**100**	**100**
< 5 km	34.1	56.8	50.0
5 - 10 km	38.6	25.0	25.0
10 - 20 km	15.9	11.4	13.6
20 - 30 km	6.8	4.5	6.8
> 30 km	4.5	2.3	4.5
Larnaca	**100**	**100**	**100**
< 5 km	11.0	50.5	33.0
5 - 10 km	31.9	31.9	28.6
10 - 20 km	31.9	11.0	25.3
20 - 30 km	14.3	4.4	6.6
> 30 km	11.0	2.2	6.6
Limassol	**100**	**100**	**100**
< 5 km	20.4	62.0	36.1
5 - 10 km	40.1	27.7	39.4
10 - 20 km	23.7	6.2	13.1
20 - 30 km	7.7	1.1	4.0
> 30 km	8.0	2.9	7.3
Nicosia	**100**	**100**	**100**
< 5 km	19.5	71.9	39.8
5 - 10 km	41.9	20.7	41.0
10 - 20 km	23.7	6.6	12.3
20 - 30 km	9.0	0.9	4.2
> 30 km	6.0	0.0	2.7
Paphos	**100**	**100**	**100**
< 5 km	31.8	45.5	38.6
5 - 10 km	36.4	36.4	38.6
10 - 20 km	9.1	9.1	9.1
20 - 30 km	4.5	4.5	4.5
> 30 km	18.2	4.5	9.1

In Larnaka, participants also tend to travel shorter distances for groceries, with 50.5% staying within 5 km. However, entertainment and dining activities are spread out more evenly between different distances, with 31.9% traveling 5-10 km and another 31.9% traveling 10-20 km. Shopping behavior is more evenly distributed, with a notable portion of 33% traveling less than 5 km, 28.6% traveling 5-10 km and 25.3% traveling 10-20 km. Limassol shows a strong tendency for short-distance grocery shopping, with 62% of participants traveling less than 5 km. Shopping patterns are slightly more distributed, with 39.4% traveling 5-10 km and 36.1% traveling less than 5 km. For entertainment, there is significant movement within 5-10 km (40.1%). In Nicosia, short-distance grocery shopping is dominant, with 71.9% of participants traveling less than 5 km. However, for entertainment and dining, there is a larger spread across distances, with 41.9% traveling 5-10 km. Shopping behaviors mirror entertainment, with 41% of participants traveling similar distances. Paphos show a more distributed travel pattern. For grocery shopping, 45.5% travel less than 5 km, but 36.4% travel between 5-10 km. Shopping and entertainment follow similar patterns, with a large proportion traveling within 5-10 km (38.6% for both activities).

5.2.2 Mobility Frequency

Tables 13 to 15 record the frequency of participants' movements (per week) concerning their purpose of travel (Workplace, visiting other houses, Entertainment, Dining, physical exercise and sports, Grocery shopping and general shopping). Regarding the purpose for which they do not travel at all, a high number of participants do not include in their weekly schedule visits to sports facilities (51%) and general shopping (24%). Additionally, many individuals do not visit dining establishments (16%) and entertainment venues (14%) and others rarely visit other households on a weekly basis (8%). Eleven percent of the participants do not need to commute to their workplace.

By category and in descending order, most people commute more than 5 times per week for Workplace (65%), once for shopping (49%), once for dining (42%), once for Entertainment (36%), once for visiting other houses (32%), twice for Grocery shopping (32%), and once for physical exercise and sports (15%). Lastly, at least three times per week, participants commute for Workplace (75%), visiting other houses (36%), Grocery shopping (32%), Entertainment (25%), physical exercise and sports (22%), dining (19%), and shopping (13%).

Table 13. Participants' responses regarding weekly travelling frequencies for various activities

Mobility freq. (times/week)	Workplace	visiting other houses	Entertainment	Dining	physical exercise and sports	Grocery shopping	Shopping
0	11%	8%	14%	16%	51%	6%	24%
1	3%	32%	36%	42%	15%	30%	49%
2	11%	24%	25%	23%	12%	32%	14%
3	7%	17%	14%	11%	10%	15%	6%
4	3%	5%	4%	3%	5%	7%	2%
5 +	65%	14%	7%	5%	7%	10%	5%

The table 14 below displays the frequency and the preferred mode of transportation of the participants for five primary purposes of travel (to/from University, to/from workplace, to/from school (children), within district of residence, outside district of residence). For each of these categories, the two most popular means of transportation are presented.

Table 14. Participants' responses regarding weekly travel frequencies and preferable mode for various purposes

Mobility freq. (times/week)	to/from University		to/from workplace		to/from school (children)		within district of residence		outside district of residence	
	Car	**Walk**	**Car**	**Walk**	**Car**	**Bus**	**Car**	**Walk**	**Car**	**Bus**
1-2	4%	4%	7%	5%	4%	2%	6%	35%	52%	4%
3-5	12%	3%	28%	4%	16%	4%	19%	14%	13%	1%
5-10	6%	2%	34%	1%	16%	2%	28%	4%	8%	1%
10+	9%	2%	20%	1%	7%	1%	45%	3%	10%	1%
Grand total	**31%**	**11%**	**88%**	**11%**	**43%**	**9%**	**98%**	**56%**	**83%**	**7%**

According to the participants, commuting to/from the university is predominantly done by car (31%) and by foot (11%), mostly 3-5 times per week (15%). Similarly, commuting to/from the workplace follows a similar pattern, with cars prevailing (89%) over walking (11%). For participants' children commuting to/from school, most do so 3-5 times weekly

(20%), with a notable preference for cars (43%) and buses as the immediate alternative (9%). Regarding movements within the district of residence, these are mostly done with a car (98%) and walking (56%), more than 10 times per week by most people (48%). Significant car usage is also observed for commuting outside the district of residence, at 83%, followed by buses at only 7%. Notably, these commutes occur mostly 1-2 times per week (56%).

Overall, car usage appears to dominate significantly across all categories compared to other modes of transportation (Motorbike, Bus, Taxi, Bicycle, Walk). Walking takes second place in preference (to/from university, to/from workplace, within district of residence), followed by buses in third place (to/from school - children, outside district of residence).

Table 15 showcase mobility frequency behaviors across the Cypriot districts. In Famagusta, workplace mobility is notably high, with 63.6% of participants traveling to work five or more times a week, indicating regular commuting patterns. However, for social visits, entertainment, and dining, mobility is generally lower, with most participants engaging in these activities only one or two times per week. Physical exercise is infrequent in the district, as 59.1% report no participation in sports or exercise. Grocery shopping is primarily done twice a week (34.1%), while non-essential shopping occurs less often, with 38.6% of participants shopping only once per week.

In Larnaca, workplace mobility remains significant, with 61.5% of participants commuting five or more times weekly. Social visits and entertainment are more frequent compared to Famagusta, with 35.2% and 39.6% of participants, respectively, visiting other houses and engaging in entertainment activities once per week. Dining out is also common, with 45.1% reporting they dine once per week. Physical exercise in Larnaca is also low, with 59.3% of participants not engaging in any form of exercise. Grocery shopping habits are similar to Famagusta, with most people shopping two times a week (35.2%).

In Limassol, workplace mobility is also high, with 64.6% of participants commuting five or more times per week. Social visits (30.7%) and entertainment (39.1%) occur mostly once a week, and dining is frequent, with 44.2% dining out weekly. Physical exercise follows the same trend as other districts, with 51.1% reporting no regular activity.

Grocery shopping is frequent, with 30.3% shopping once per week and 34.3% shopping twice weekly, while shopping for non-essentials is less common, with 50.4% of participants engaging in it just once a week.

In Nicosia, workplace mobility reaches its peak, with 67.1% commuting five or more times per week, the highest rate among all districts. Social visits (31.7%) and dining (41.6%) are most commonly done once a week. Physical exercise shows slightly lower inactivity (47%) compared to other districts, though still a large proportion of people remain inactive. Grocery shopping in Nicosia is frequent, with 34.1% shopping once a week, and similarly, non-essential shopping follows a similar pattern, with 48.2% shopping once weekly.

Table 15. Participants' responses regarding weekly travelling frequencies for various activities, by district of residence

Mobility freq. (times/week)	**workplace**	**visiting other houses**	**entertainment**	**Dining**	**physical exercise and sports**	**Grocery shopping**	**Shopping**
Famagusta	100	100	100	100	100	100	100
0	11.4	4.5	11.4	15.9	59.1	9.1	27.3
1	2.3	40.9	31.8	40.9	13.6	15.9	38.6
2	18.2	15.9	25.0	25.0	9.1	34.1	15.9
3	4.5	20.5	13.6	9.1	6.8	25.0	4.5
4	0.0	2.3	2.3	2.3	0.0	6.8	4.5
5 +	63.6	15.9	15.9	6.8	11.4	9.1	9.1
Larnaca	100	100	100	100	100	100	100
0	9.9	5.5	17.6	11.0	59.3	7.7	26.4
1	1.1	35.2	39.6	45.1	7.7	29.7	51.6
2	16.5	25.3	18.7	22.0	12.1	35.2	15.4
3	7.7	18.7	17.6	15.4	13.2	15.4	4.4
4	3.3	3.3	2.2	3.3	4.4	5.5	0.0
5 +	61.5	12.1	4.4	3.3	3.3	6.6	2.2
Limassol	100	100	100	100	100	100	100
0	11.7	9.5	12.4	16.1	51.1	4.7	23.4
1	2.9	30.7	39.1	44.2	14.2	30.3	50.4
2	10.2	24.5	25.5	20.8	12.4	34.3	13.5

3	8.8	16.8	13.5	10.6	7.3	15.0	6.9
4	1.8	5.8	4.0	3.6	5.5	5.8	1.5
5 +	64.6	12.8	5.5	4.7	9.5	9.9	4.4
Nicosia	100	100	100	100	100	100	100
0	9.9	7.8	15.0	16.2	47.0	5.4	25.1
1	4.2	31.7	32.9	41.6	17.7	34.1	48.2
2	8.7	25.7	27.8	24.3	13.5	28.7	14.7
3	6.9	16.8	12.9	9.9	10.8	14.7	6.3
4	3.3	5.1	5.4	3.3	5.7	8.1	1.8
5 +	67.1	12.9	6.0	4.8	5.4	9.0	3.9
Paphos	100	100	100	100	100	100	100
0	11.4	11.4	6.8	15.9	52.3	6.8	18.2
1	4.5	27.3	40.9	27.3	15.9	13.6	43.2
2	11.4	13.6	13.6	31.8	6.8	27.3	6.8
3	2.3	15.9	18.2	9.1	9.1	15.9	11.4
4	4.5	9.1	6.8	4.5	6.8	9.1	9.1
5 +	65.9	22.7	13.6	11.4	9.1	27.3	11.4

Finally, in Paphos, workplace mobility remains high, with 65.9% of participants commuting five or more times per week. Social visits (27.3%) and dining (27.3%) occur mostly once per week. Entertainment activities are more frequent in Paphos compared to other districts, with 40.9% of participants engaging in entertainment once a week. Physical exercise remains low, with 52.3% reporting no activity. Grocery shopping is slightly less frequent compared to other districts, with a notable proportion (27.3%) shopping twice a week.

In summary, workplace mobility is consistently high across all districts, particularly in Nicosia and Paphos. Entertainment and dining tend to be more frequent in Limassol and Nicosia, where participants engage in these activities more often. Physical exercise shows a general trend of inactivity across all districts, while grocery shopping is commonly done once or twice per week, with higher frequencies in urban districts like Limassol and Nicosia. These mobility patterns reflect how regional differences, urbanization, and infrastructure influence behavior.

5.2.3 Human Mobility Schedule (HMS)

In this section, the results regarding the mobility patterns of Cypriot residents, as derived from the questionnaire, are presented. Initially, the spatiotemporal mobility of the general sample (graphs xx-xx) is discussed, followed by an analysis of these behaviors by age group (graphs xx-xx). In the xx-xx graphs, the indicative locations of participants are recorded every two hours for a typical working day, in the xx-xx graphs for a typical Saturday, and in the xx-xx graphs for a typical Sunday. This approach allows for critical conclusions to be drawn regarding the common mobility behaviors of citizens in Cyprus, on a weekly basis for various age groups.

A typical working day (fig.48) for the participants follows the following schedule. The majority of people (> 84%) are at home from the beginning of the day until 6 am, where a gradual transition to other locations and activities begins, such as for work purposes (11%) and physical exercise (3%). From 8 am until 4 pm, most of the people are at their workplace (> 54%), at home (> 23%), and at their academic institution (> 6%). At 6 pm, the majority are at home (30%), at their workplace (25%), at grocery shopping locations (13%) and engaging in physical exercise (12%). From 8 pm until the end of the day, most people gradually return to their homes (> 57%), while a significant number, that gradually decrease until midnight, are engaged in sports (8%), are at workplace (7%) and at entertainment (7%) and dining venues (6%).

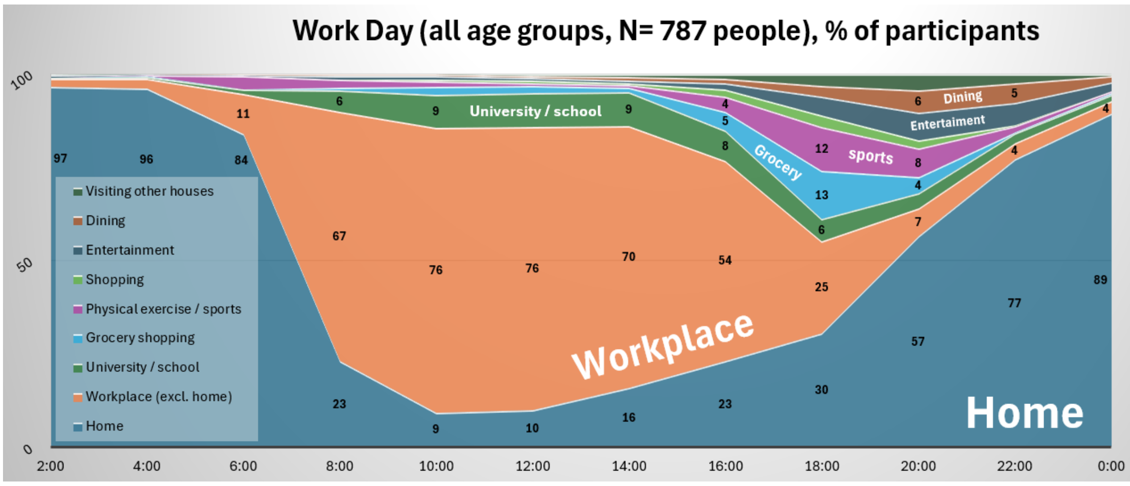

Figure 48. Participants' responses (all ages) regarding their mobility timeline, portraying location and activity every two hours, during a typical workday.

On a typical Saturday (fig. 49), the majority of people are at home (from 36% to 94%) throughout the day. Meanwhile, the following activities are also depicted. From the beginning of the day until 6 am, a small number of individuals are at their workplace (2%), at entertainment (2%) and dining venues (1%). From 8 am until 6 pm, there is an increase in the number of people at their workplace (from 6% to 12%) and at sports facilities (from 2% to 7%). Most visits (up to 12%) to other houses are recorded between 2 pm and 10 pm. Transitions for grocery shopping (up to 14%) and shopping (up to 6%) occur between 10 am and 4 pm. Meanwhile, from 10 am until midnight, there is a considerable interest in transitioning to entertainment (8% - 21%) and dining (6% - 17%) venues.

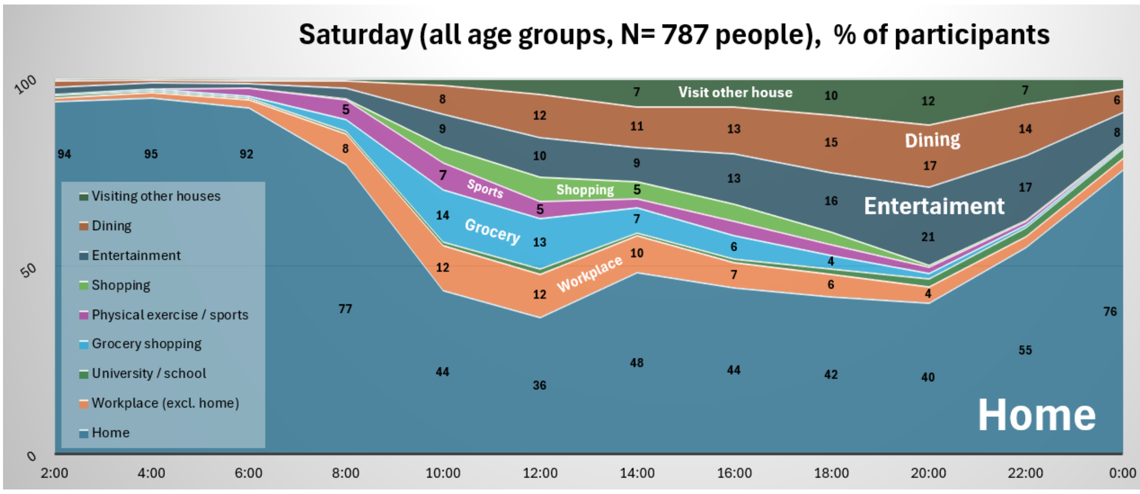

Figure 49. Participants' responses (all ages) regarding their mobility timeline, portraying location and activity every two hours, during a typical Saturday.

Likewise, on a typical Sunday (fig.50), there is a fairly similar profile to that of a typical Saturday. Once again, the majority (39% to 94%) of people are at home throughout the day. However, there is increased interest in other activities. Transition for physical exercise is made by most individuals (up to 5%) between 8 am and 12 noon. A significant percentage of people (10% to 15%) visit other houses from noon until 6 pm while from 8 am until 10 pm, there is a steady percentage of people at their workplace (up to 6%) and a rapid increase in activities related to entertainment (from 4% to 16%) and dining (from 4% to 19%). From 8 pm until the end of the day, the majority of participants (> 64%) are back at their homes.

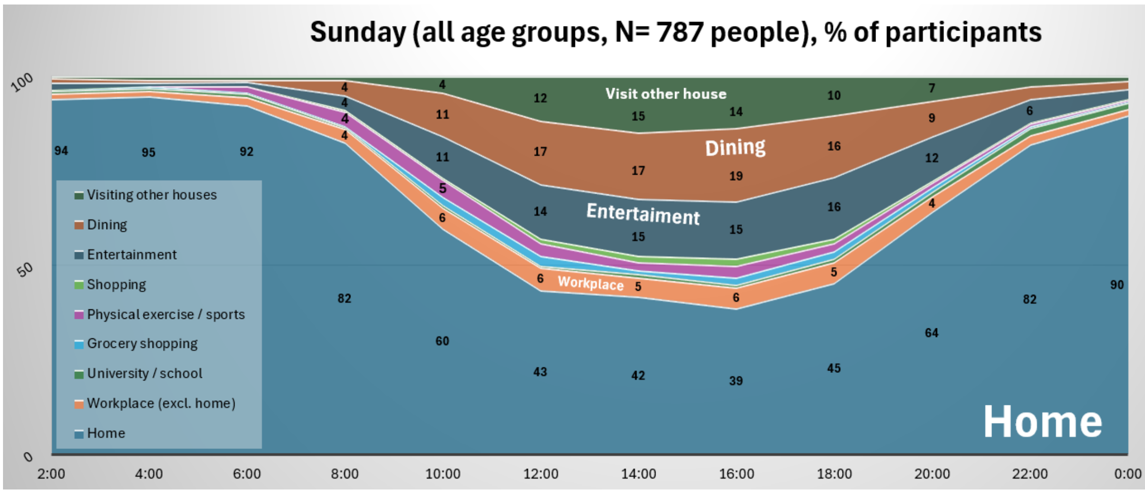

Figure 50. Participants' responses (all ages) regarding their mobility timeline, portraying location and activity every two hours, during a typical Sunday.

Focusing on individuals under 25 years old (fig.51), which represent a sample of 65 individuals or 8% of the total, differences in preferences among participants compared to other age groups are observed. More specifically, on a typical workday, from the beginning of the day until 6 am, the majority of individuals (> 86%) are at home, while a significant number are in workplaces (2% - 6%), entertainment venues (2% - 5%), and dining locations (< 2%). From 8 am until 6 pm, a significant number of people are at academic institutions (31% - 57%), workplaces (20% - 28%) and at home (9% - 38%).

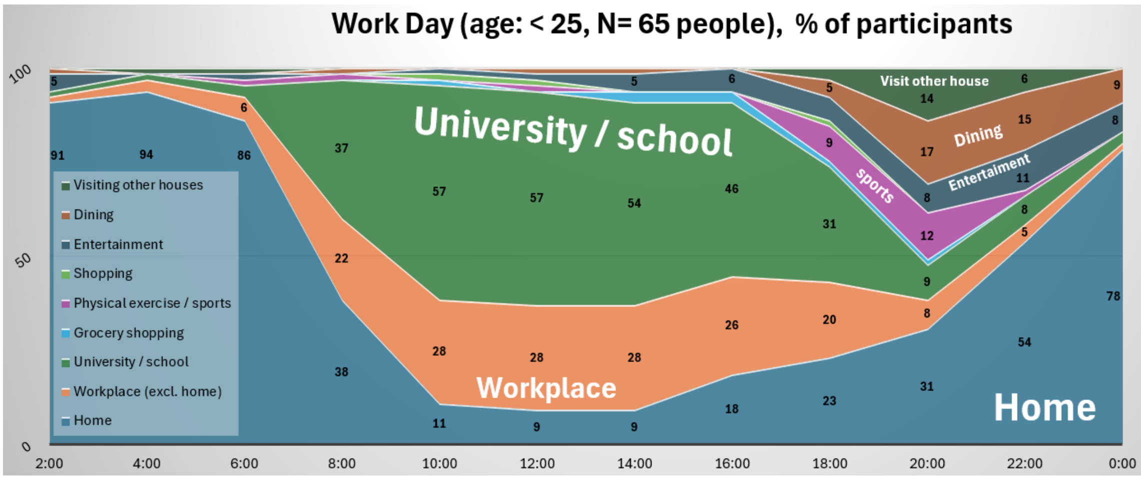

Figure 51. Participants' responses (age < 25) regarding their mobility timeline, portraying location and activity every two hours, during a typical workday.

During these hours, there is increased interest in visiting entertainment venues (up to 6%), peaking (up to 11%) in preference from 8 pm and until the end of the day, along with dining venues (9% - 17%). Transition to physical exercise venues is made by the majority (9% - 12%) from 6 pm to 8 pm, while visits to other homes mainly occur between 6 pm to 10 pm (3% - 14%). From 8 pm until the end of the day, with a rapid gradual increase, the majority of participants are at home (up to 78%).

Following the general trend, on a typical Saturday (fig.52) the majority of individuals under 25 years old are at home throughout the day (35% up to 88%). From the beginning of the day until 6 am, a small number of individuals indicate being in entertainment (up to 12%) and dining venues (up to 3%). From 8 am until 6 pm, there is a significant increase in the number of people in workplaces (6% - 15%). From 10 am until 6 pm, transitions mainly occur to physical exercise venues (3% - 5%) and shopping venues (2% - 8%). The highest percentage for grocery shopping purposes is recorded at noon (12%) and at 2 pm (9%). Most visits to other homes are recorded from 2 pm until the end of the day (2% to 20%), with the peak (20%) happening at 8 pm. Meanwhile, from 10 am until midnight, there is a significantly increased interest in visiting entertainment (8% - 26%) and Dining venues (3% - 18%).

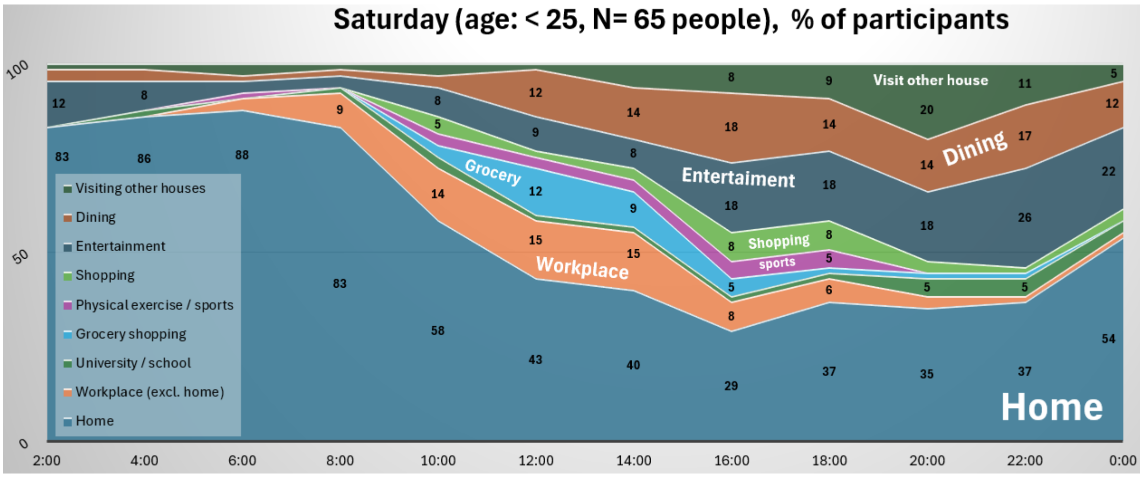

Figure 52. Participants' responses (age < 25) regarding their mobility timeline, portraying location and activity every two hours, during a typical Saturday.

On a typical Sunday for participants under 25 years old (fig.53) , the majority (ranging from 35% to 91%) of people are at home throughout the day. The second most preferred choice (15% to 23%) at all hours is entertainment venues, with the highest number of individuals opting for this type of leisure from 10 am until midnight. During the same hours, a significant number of people (5% to 12%) are in dining venues, while from noon to 8 pm, many individuals (8% - 14%) visit other households. The highest percentage for shopping purposes (5%) occurs from 2 to 6 pm, and for grocery shopping (5%) at noon and 4 pm. Transition to physical exercise venues occurs at a consistently low rate (3%) from 6 am until 6 pm. Similarly low but consistent number of people are at workplace locations from 6 am and until the end of the day.

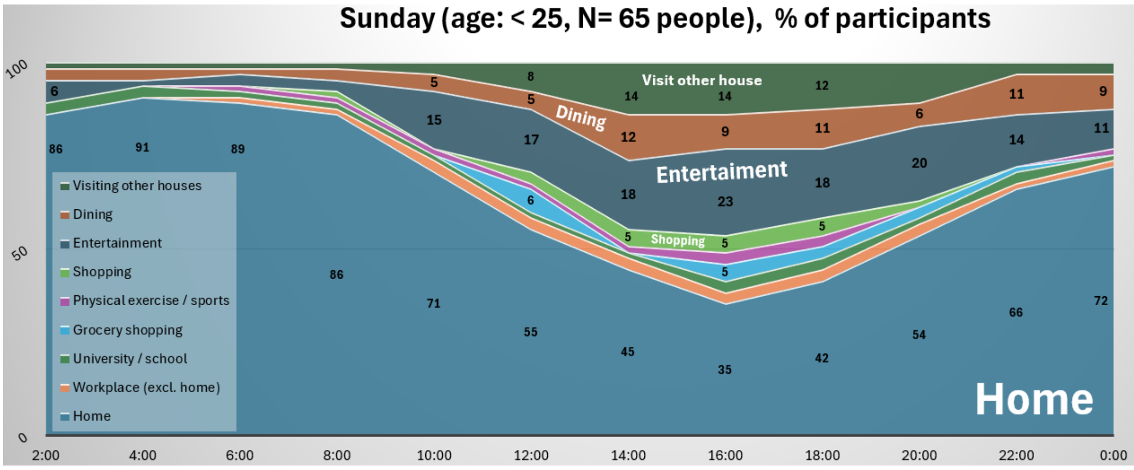

Figure 53. Participants' responses (age < 25) regarding their mobility timeline, portraying location and activity every two hours, during a typical Sunday.

During a typical workday, individuals aged 25-44 (fig.54), representing a sample of 430 individuals or 55% of the total, adhere to the following schedule. From the beginning of the day until 4 am, the majority of individuals (97%) are at home, while at 6 am some people are at their workplaces (12%) and others at physical exercise venues (3%). From 8 am until 4 pm, there is a significant rise of people at workplace (ranging from 61% to 85%), while a large number are at home (6% to 20%) and at academic institutions (3% to 6%). At 6 pm, there is a dramatic decrease in individuals at workplaces (29%) and a gradual decline (down to 5%) is reported until midnight. Additionally, during the same time period, there is a gradual increase in the percentage of individuals that are home (ranging from 54% to 89%) and an increased interest for visiting other households (3%) and entertainment (2% - 6%) and dining venues (2% - 5%). Preference in physical exercise by the majority of individuals is recorded between 6 to 8 am (3%) and from 4 to 8 pm (ranging from 4% to 13%). Activities such as grocery shopping (6% - 14%) and general shopping (2% - 4%) are at their peak from 4 to 8 pm.

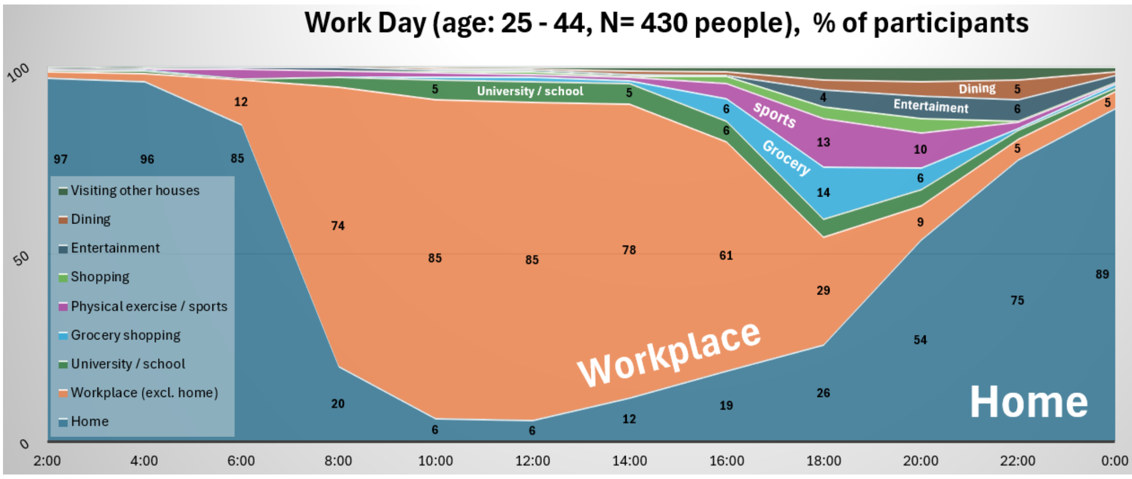

Figure 54. Participants' responses (age 25 - 44) regarding their mobility timeline, portraying location and activity every two hours, during a typical workday.

On their typical Saturday (fig.55), the majority (30% to 96%) of participants in this age group are at home throughout the day. From 8 am until 4 pm, a significant number is at their workplaces (6% to 13%) and at locations related to physical exercise (4% to 6%). Between 10 am and 6 pm, there is a peak in activities such as grocery shopping (ranging from 4% to 14%) and general shopping (ranging from 4% to 7%). Visits to other households at Saturdays are implemented by the majority between 12 noon and 10 pm (ranging from 5% to 14%). Meanwhile, from 10 am until midnight, there is a very high interest in activities regarding entertainment (8% to 20%) and dining (8% to 19%).

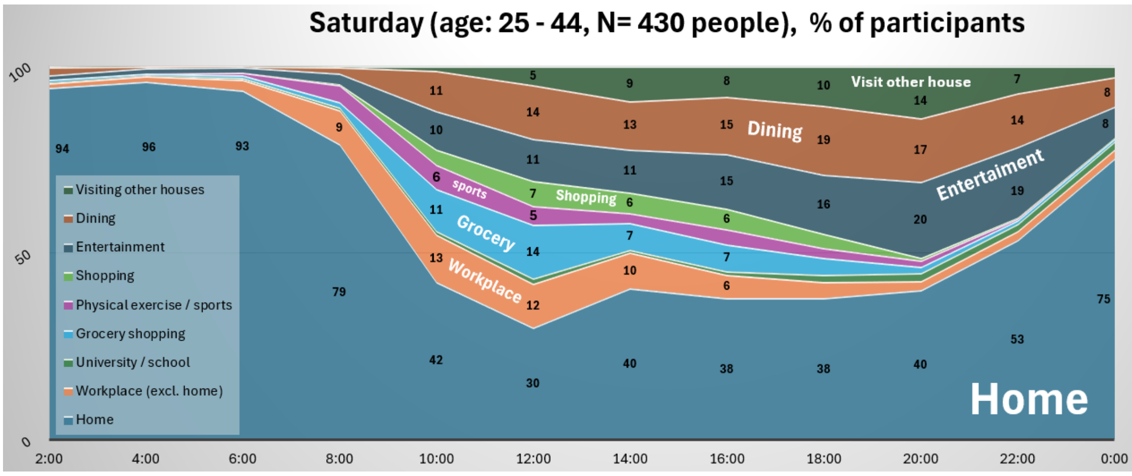

Figure 55. Participants' responses (age 25 - 44) regarding their mobility timeline, portraying location and activity every two hours, during a typical Saturday.

On Sundays (fig.56), even more people prefer to be at home (31% to 96%) throughout the day, while from 10 am until 6 pm, there is a steady number (around 5%) of people at workplaces. Physical exercise activities are preferred by the majority (3%) between 8 am and 4 pm on this day. From 10 am until 8 pm, a significant number of individuals are visiting other households (up to 20%), entertainment (up to 21%), and dining venues (up to 21%). Grocery shopping (up to 3%) and general shopping (up to 3%) occur between 10 am and 6 pm.

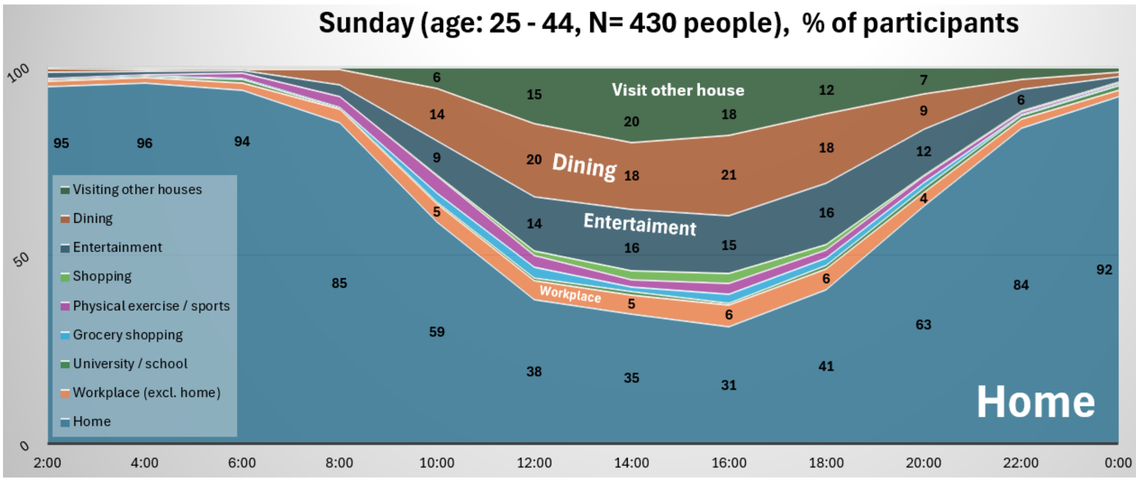

Figure 56. Participants' responses (age 25 - 44) regarding their mobility timeline, portraying location and activity every two hours, during a typical Sunday.

In the age group of 45-59 (fig.57), comprising a sample of 209 individuals or 26% of the total, a typical workday mobility pattern unfolds as follows. Throughout the early hours until 6 am, a vast majority (> 81%) of people remain at home, while a portion head to their workplaces (up to 13%) or engage in physical exercise (up to 4%). From 8 am until 4 pm, there's a notable presence (ranging from 53% to 83%) in workplace locations, with a substantial contingent being at home (8% to 26%) and some at academic institutions (up to 5%). At 6 pm, there's a sharp decline in workplace attendance (down to 19%), steadily diminishing until midnight (3%). The proportion of individuals at home gradually rises (up to 91%) and there is an increased interest in entertainment venues (up to 8%) and dining out (up to 7%) in the same time period. Physical exercise activities mostly occur at 6 am (4%) and between 4 to 8 pm (up to 13%), while activities like grocery shopping (up to 18%), general shopping (up to 3%), and visiting other households (2%) peak from 4 to 8 in the evening.

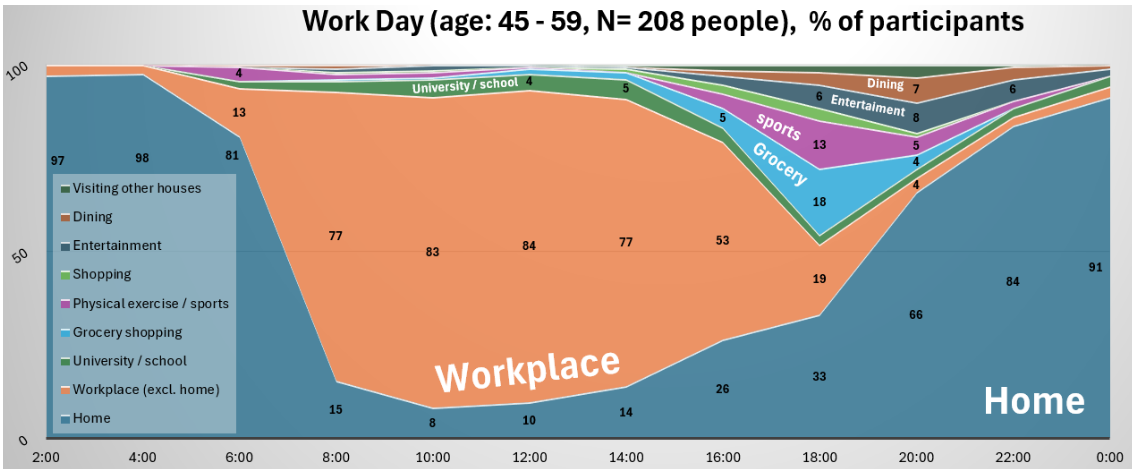

Figure 57. Participants' responses (age 45 - 59) regarding their mobility timeline, portraying location and activity every two hours, during a typical workday.

On their typical Saturday (fig.58), the majority (ranging from 42% to 97%) of individuals in this age group, are at home throughout the day. From 8 am until 6 pm, a significant number of people are either at work (5% - 9%) or engaged in grocery shopping (up to 20%). An increased interest in physical exercise (up to 11%) is observed from 6 am until 4 pm and visits to shopping locations (up to 8%) occur from 10 am to 6 pm. Between noon and 10 pm, there is an increased preference in visiting other households (up to 10%). Moreover, from 10 am and until the end of the day, there is a notable interest of people going to entertainment (up to 23%) and dining (up to 14%) venues.

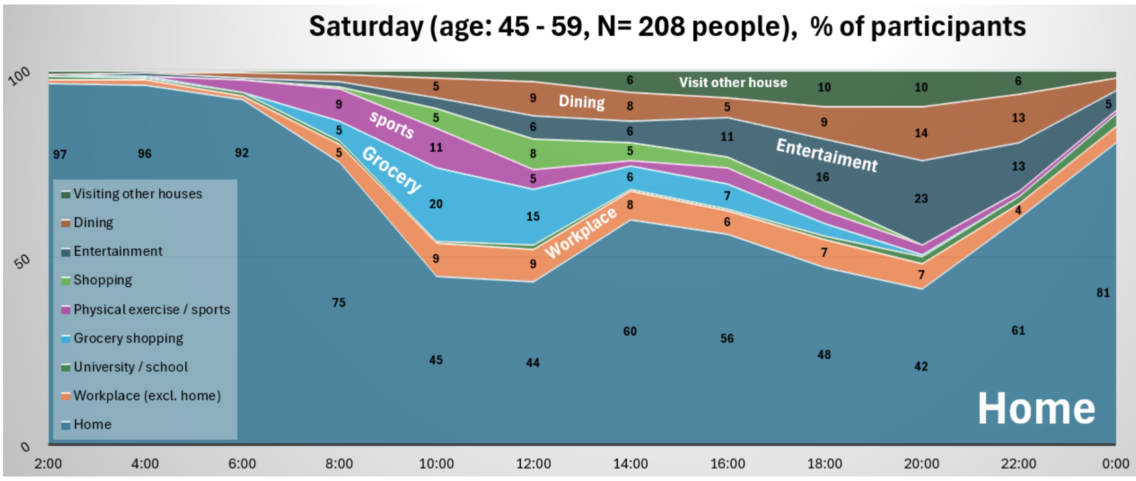

Figure 58. Participants' responses (age 45 - 59) regarding their mobility timeline, portraying location and activity every two hours, during a typical Saturday.

On Sundays (fig.59), even more people (ranging from 58% to 95%) are located at home throughout the day, while a consistent percentage remains at work from 10 am until 8 pm. The majority (up to 6%) of people are at physical exercise locations between 8 am and 4 pm. From 10 am until 8 pm, an increased number of people are recorded being at dining (up to 22%) and entertainment (up to 15%) venues and visiting other households (up to 10%). Limited preference is stated for grocery shopping (up to 2%) and general shopping (up to 1%) activities between 10 am and 6 pm.

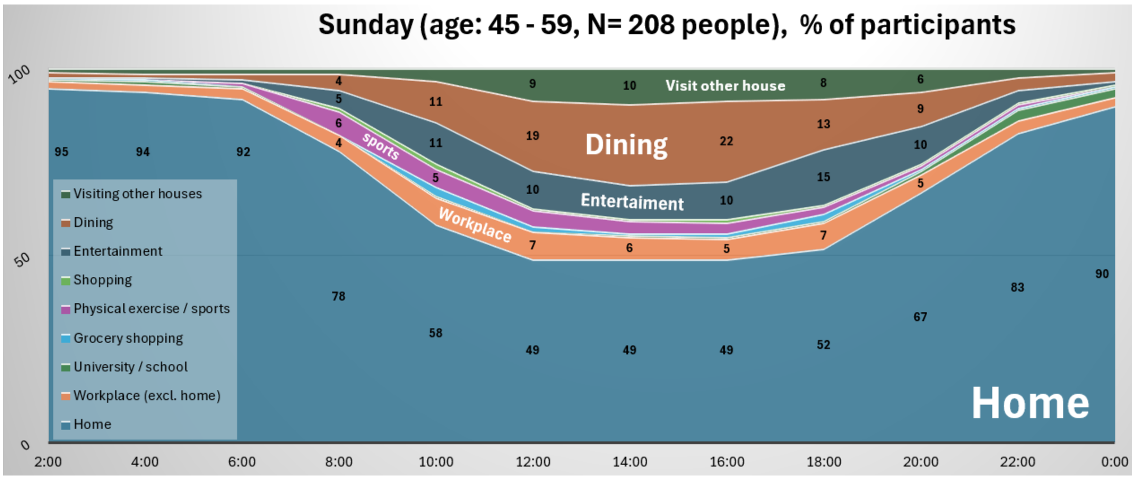

Figure 59. Participants' responses (age 45 - 59) regarding their mobility timeline, portraying location and activity every two hours, during a typical Sunday.

In the age group of individuals over 60 (fig.60) with a sample of 84 people or 11% of the total, a typical working day follows the following mobility pattern. From the beginning of the day until 6 am, the majority of individuals (> 86%) are at home, while at 6 am, some people are engaged in physical exercise (7%) and work (5%) locations. From 10 am until 4 pm, most individuals are in their workplace (up to 51%) and at home (up to 45%). At 6 pm, there is a dramatic decrease of individuals in workplaces (23%) with a gradual decline (down to 4%) until 10 pm, while simultaneously there is a gradual increase in the percentage of individuals staying at home (up to 95%). Increased interest in entertainment venues (up to 11%) is observed from 4 pm to 10 pm while dining venues are preferred by the most (7%) at 8 pm. Physical exercise activities are implemented by the majority (up to 8%) between 6 am to 8 am and 4 pm to 8 pm, while grocery shopping records its highest preference (up to 14%) during the 8 am to 12 noon and at 6 pm. Visiting other households is done by the majority (5%) at 6 pm.

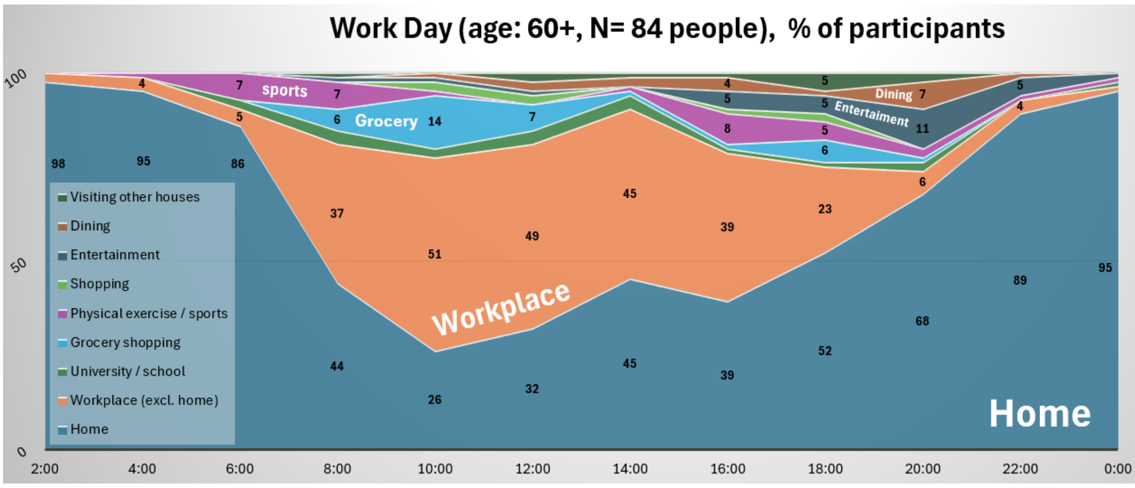

Figure 60. Participants' responses (age > 60) regarding their mobility timeline, portraying location and activity every two hours, during a typical workday.

On a typical Saturday (fig.61), the majority (36% to 95%) of participants in this age group are located at home throughout the day. From 8 am until 8 pm, a large number (10% to 15%) of people are at their workplaces, while others (up to 7%) engage in physical exercise activities from 6 am to 10 am. Most participants go for grocery shopping (up to 20%) between 8 am and 12 noon, for shopping (5%) at 12 noon and visit other households (5%) at 6 pm. There is an increased interest for entertainment (up to 20%) between 10 am until 10 pm and for dining (up to 21%) between 2 pm to 10 pm.

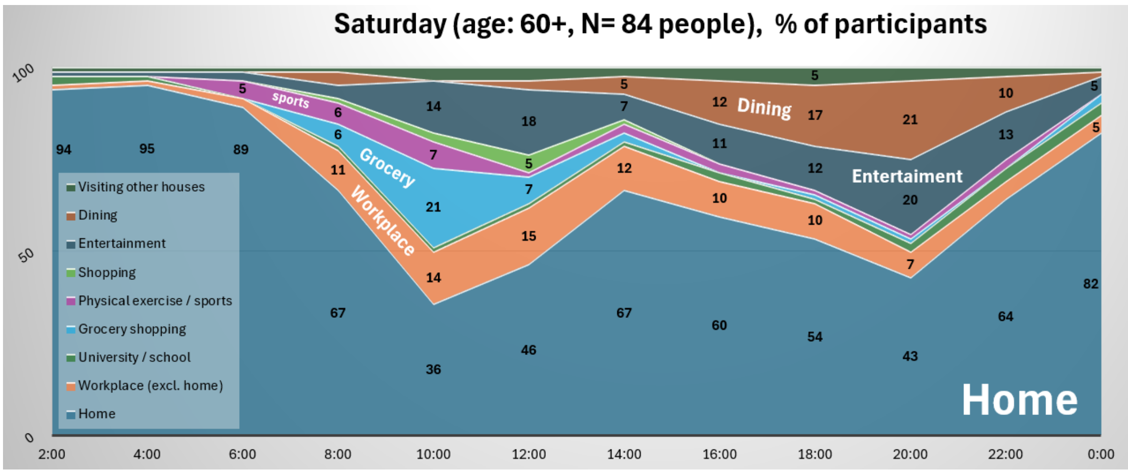

Figure 61. Participants' responses (age > 60) regarding their mobility timeline, portraying location and activity every two hours, during a typical Saturday.

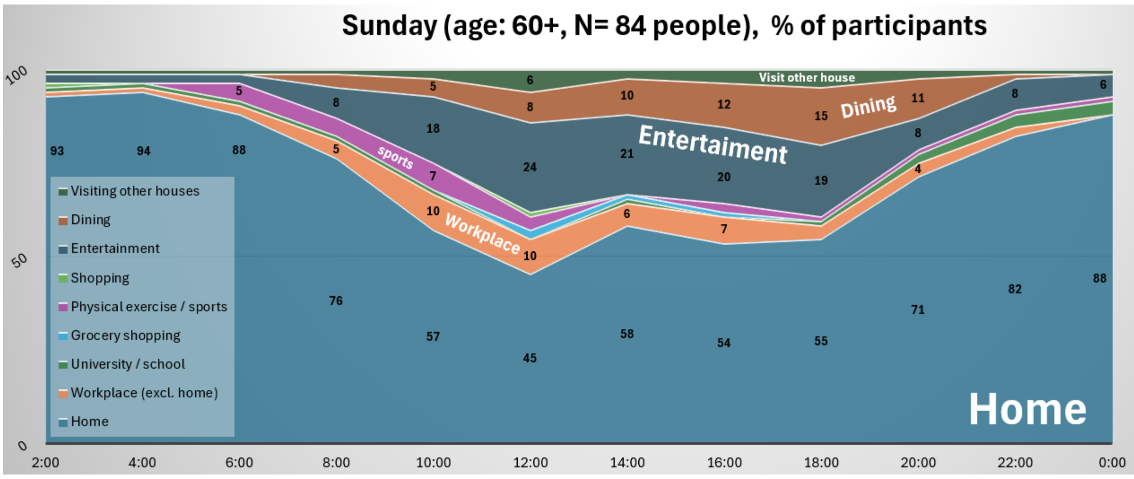

Figure 62. Participants' responses (age > 60) regarding their mobility timeline, portraying location and activity every two hours, during a typical Sunday.

Following the same pattern as the other age groups, on Sundays (fig.62), the majority of individuals (ranging from 45% to 94%) in this age group are at home at all hours, while a significant (up to 10%) portion of people are at their workplace from 8 am until 4 pm. Physical exercise is executed by the most (up to 7%) between 6 am and 12 noon. Additionally, on this day there a very low preference is noted for activities such as grocery shopping (2%) and shopping (1%), preferred by the most at 12 noon. Additionally, the majority (6%) of people visit other households during this time. An increased number of individuals are observed to be in entertainment venues (up to 15%) from 8 am until midnight and in dining places (up to 15%) from 10 am until 8 pm.

5.2.4 Adoption to COVID19 measures

The tables 16 to 20 present the opinion and acceptance of the participants regarding significant measures to address the coronavirus pandemic. Table 16 presents the percentage of participants who either agree or disagree with various measures related to COVID19, including mask use, social distancing, lockdown measures, and vaccination. The majority of participants, constituting 84%, agree with the implementation of mask use, indicating widespread acceptance of this preventive measure. Similarly, a significant proportion, 77%, agree with practicing social distancing. However, opinions on lockdown measures and vaccination appear to be more divided, with 59% agreeing with lockdown measures and 71% agreeing with vaccination. Conversely, 16% of participants disagree with mask use, while 23% disagree with social distancing measures. Notably, a higher percentage, 41%, disagree with lockdown measures, while 29% disagree with vaccination efforts. Overall, the data suggests varying levels of agreement and disagreement among participants regarding these crucial COVID19 containment measures.

Table 16. Participants' responses regarding acceptance of important preventive measures adopted during COVID19 pandemic.

% of participants	mask use	social distancing	lockdown	vaccination
Agree	84%	77%	59%	71%
Disagree	16%	23%	41%	29%

Table 17. Participants' responses regarding acceptance of important preventive measures adopted during COVID19 pandemic, by district.

	mask use	social distancing	lockdown	vaccination
Famagusta	100	100	100	100
Agree	68.2	59.1	50.0	65.9
Disagree	31.8	40.9	50.0	34.1
Larnaca	100	100	100	100
Agree	91.2	86.8	58.2	78.0
Disagree	8.8	13.2	41.8	22.0
Limassol	100	100	100	100
Agree	79.6	74.1	55.5	67.2
Disagree	20.4	25.9	44.5	32.8
Nicosia	100	100	100	100
Agree	87.7	79.3	64.7	74.6
Disagree	12.3	20.7	35.3	25.4
Paphos	100	100	100	100
Agree	81.8	77.3	47.7	63.6
Disagree	18.2	22.7	52.3	36.4

Opinions on COVID19 measures vary by district (table 17). In Famagusta, opinions on mask use and social distancing are somewhat divided. While 68.2% of participants agree with mask use, only 59.1% support social distancing measures, indicating a notable level of hesitancy. The opinions on lockdowns are split evenly, with 50% agreeing and 50% disagreeing. Vaccination has stronger support, with 65.9% agreeing, but still, a significant portion (34.1%) is opposed. In Larnaka, there is a clear majority in favor of most measures. Mask use (91.2%) and social distancing (86.8%) enjoy very high levels of support. Agreement with lockdown measures is lower but still supported by 58.2% of the population, while 78% favor vaccination. Overall, Larnaka shows stronger alignment with public health measures than other regions.

Limassol also shows relatively high support for mask use (79.6%) and social distancing (74.1%). Opinions on lockdowns are more divided, with 55.5% agreeing and 44.5% disagreeing. Vaccination support is slightly lower here (67.2%), with 32.8% opposed. This shows that while most people in Limassol agree with preventive measures, there is still significant resistance. In Nicosia, there is widespread agreement with most COVID19 measures. Mask use is supported by 87.7% of the population, and social distancing has similarly high approval (79.3%). Support for lockdowns is the highest among all districts (64.7%), and vaccination is also widely supported (74.6%). Nicosia stands out as the district with the most robust overall backing for these measures. In Paphos, there is strong support for mask use (81.8%) and social distancing (77.3%). However, opinions on lockdowns are more divided, with only 47.7% agreeing and a majority (52.3%) disagreeing. Vaccination support is moderate, with 63.6% in favor and 36.4% against, indicating a higher level of skepticism compared to some other districts. The public opinion on COVID19 measures varies across districts, with mask use and social distancing receiving strong support in most areas, especially in Larnaka and Nicosia, while lockdowns are more divisive, particularly in Famagusta and Paphos, where a significant portion of the population disagrees with them. Vaccination enjoys broad approval, though skepticism remains higher in Famagusta and Paphos compared to the stronger support seen in Nicosia and Larnaka. Overall, urban districts tend to show more consistent backing for public health measures, while more rural or coastal areas are slightly more resistant.

Table 18 outlines the percentage of participants' behaviors concerning mask use and social distancing in different scenarios. Only 5% of participants consistently adhere to wearing masks always and everywhere, while a larger proportion, 28%, opts for mask usage in enclosed or crowded spaces exclusively. Conversely, 14% admit to never wearing masks, indicating a significant portion of non-compliance. Regarding social distancing, a similar pattern emerges, with 7% consistently practicing it always and everywhere, and 26% adhering to it solely in enclosed or crowded settings. A notable proportion, 32% and 30%, report sometimes apply mask use and social distancing only when overcrowding occurs, underscoring a reactive approach to these measures. The data suggests a diverse range of adherence levels to mask use and social distancing protocols, highlighting the need for targeted interventions to promote consistent compliance across different scenarios.

Table 18. Participants' responses regarding the level of adoption of important preventive measures during the COVID19 pandemic.

% of participants	mask use	social distancing
Always and everywhere	5%	7%
Always in enclosed and/or crowded spaces	28%	26%
Never	14%	14%
Sometimes	21%	23%
Sometimes on overcrowding	32%	30%

Measures' level of adoption varies by district (table 19). In Famagusta, about a third of the population (34.1% for masks, 31.8% for distancing) adheres to these measures in enclosed or crowded spaces, while only 6.8% report following them "always and everywhere." A notable portion either uses these measures sometimes (27.3% for masks, 20.5% for distancing) or only during overcrowding (20.5% for masks, 25% for distancing), and a significant minority never follows these guidelines (11.4% for masks, 15.9% for distancing). In Larnaka, compliance is slightly higher, with around 35% adhering to mask use and distancing in enclosed spaces, and more people (29.7% for masks, 31.9% for distancing) following them in overcrowding situations. Only 5.5% and 9.9% follow the measures everywhere. Similarly, Limassol sees a lower percentage of people consistently following the rules, with a larger portion (33.2% for masks, 30.3% for distancing) only complying during overcrowding and a similar minority not using masks (13.5%) or practicing distancing (12%). In Nicosia, mask use and social distancing in enclosed spaces are common for about 27% of the population, while a larger portion applies these measures during overcrowding (31.7% for masks, 29.3% for distancing), and around 15% never adhere to them. Paphos shows the highest rate of non-compliance, with 20.5% and 22.7% never using masks or practicing distancing, respectively, and a significant portion (40.9% for masks, 27.3% for distancing) following these measures only during overcrowding.

Table 19. Participants' responses regarding the level of adoption of important preventive measures during the COVID19 pandemic, by district.

	mask use	social distancing
Famagusta	100.0	100.0
Always and everywhere	6.8	6.8
Always in enclosed and/or crowded spaces	34.1	31.8
Never	11.4	15.9
Sometimes	27.3	20.5
Sometimes on overcrowding	20.5	25.0
Larnaca	100.0	100.0
Always and everywhere	5.5	9.9
Always in enclosed and/or crowded spaces	35.2	31.9
Never	13.2	9.9
Sometimes	16.5	16.5
Sometimes on overcrowding	29.7	31.9
Limassol	100.0	100.0
Always and everywhere	4.4	8.0
Always in enclosed and/or crowded spaces	27.0	25.2
Never	13.5	12.0
Sometimes	21.9	24.5
Sometimes on overcrowding	33.2	30.3
Nicosia	100.0	100.0
Always and everywhere	5.1	6.0
Always in enclosed and/or crowded spaces	27.2	25.7
Never	13.8	15.0
Sometimes	22.2	24.0
Sometimes on overcrowding	31.7	29.3
Paphos	100.0	100.0
Always and everywhere	4.5	9.1
Always in enclosed and/or crowded spaces	15.9	22.7
Never	20.5	22.7
Sometimes	18.2	18.2
Sometimes on overcrowding	40.9	27.3

Across all districts, the highest adherence levels tend to be in enclosed or crowded spaces, while a notable portion of the population only practices these measures in specific situations, such as overcrowding, or not at all.

Table 20 presents the number of times participants have been infected with COVID19 to date, along with the percentage of participants falling into each category. The majority of participants, comprising 45%, report experiencing one infection, while 28% indicate having been infected twice. A smaller proportion, 14%, report no infections to date. Additionally, 10% of participants report three infections, with 2% reporting four infections. Notably, only 1% of participants report experiencing five or more infections, suggesting a relatively low occurrence of multiple infections within the surveyed population. Overall, the data provides insights into the prevalence and frequency of COVID19 infections among participants, highlighting the varying degrees of exposure within the population.

Table 20. Participants' responses regarding the number of times they have been infected with COVID19 to date.

Times infected with COVID19 to date	% of participants
0	14%
1	45%
2	28%
3	10%
4	2%
5 +	1%

Out of the total of 787 individuals who participated in the survey, 217 individuals (27.5%) reported having a chronic health condition for which they receive long-term treatment or are monitored by a specialist (e.g., respiratory, cardiological, nephrological, hematological, autoimmune, oncological, psychiatric, hypertension, high cholesterol, diabetes, etc.). Regarding their physical exercise habits, participants were asked about the type of environment where they exercise. Notably, the majority (44%) reported not exercising at all, while 30% exercise indoors (e.g., gym) and the remaining 26% exercise outdoors.

5.2.5 Conclusions

Questionnaire findings better capture the mobility behaviors of individuals aged 20-64, the most active demographic segment in Cyprus, offering key insights into their travel patterns, commuting habits and preferences regarding transportation modes and destinations. The results offer several unique advantages and added value, particularly when compared to the larger-scale reports typically produced by the European Commission. While European Commission data provides a broad overview and macro-level trends, the localized, district-specific insights offered by this study make this survey data set particularly valuable for more targeted, regional-level analysis and decision-making. Furthermore, survey datasets differ from other datasets like Map Box Movement, Strava, social media data, and Google's Community Mobility Report in several key ways. While these alternative datasets are often based on passive data collection from mobile devices, apps, or social media activity, the current survey dataset is based on direct responses from participants, offering qualitative insights alongside quantitative data. This means that it captures not only mobility patterns but also the underlying motivations, perceptions, and opinions of individuals regarding their behavior. In contrast, datasets like Google's Community Mobility Reports or MapBox provide high-frequency, real-time movement data, but lack the context of why people are moving or adhering to certain behaviors. Strava and similar platforms are also more focused on specific activities like exercise, and their user bases are typically self-selected and not always representative of the general population. The questionnaire results presented, with its demographic matching to the census, provide a more representative and comprehensive view of mobility and behavior making it a valuable complement to more granular, real-time movement data from other sources.

Populations from all districts of Cyprus are well represented, capturing regional variations in mobility behaviors. A clear timeline of daily mobility was established, highlighting activity and location changes at two-hour intervals during typical workdays, Saturdays, and Sundays. The survey sample demonstrates a generally good alignment with the census data, with minor variations in gender and age group representation across districts. In Famagusta, gender distribution is well-balanced, closely matching census data. Larnaka shows a reasonable match for males but a more noticeable under-representation of females. Limassol demonstrates strong representation for both genders, with a noticeable over-representation of males, while Nicosia exhibits robust male representation and a slight under-representation of females. Age-wise, the survey shows strong representation among middle-aged cohorts (30-44) in most districts, with under-representation among younger age groups (particularly 20-29) in districts like Larnaka and Paphos. While Paphos shows some under-representation for both genders and younger age groups, the district still contributes valuable demographic insights. Overall, the survey sample provides a reliable demo-graphic overview and reflects the general population trends across Cyprus. Island-wide results suggest that the sample is statistically representative of the population in terms of both gender and age distributions, enabling credible generalizations of age- and gender-related in-sights to the broader population in Cyprus.

The findings reveal that residents generally tend to travel shorter distances, particularly for routine activities like grocery shopping, while they are more inclined to venture further for entertainment, dining, and general shopping. This pattern of shorter travel distances, particularly within 10 kilometers, holds true across all age groups. The latest National Travel Survey (Statistical service of the Republic of Cyprus, 2010) supports this, showing a high car usage rate (84% of participants) with an average trip duration of 15 minutes and an average trip distance of 10 kilometers per person. Additionally, our study finds that longer distances are predominantly traveled for entertainment and dining purposes. Interestingly, individuals aged 45 and above are more likely to make movements within distances less than 5 kilometers, while those under 25 are more prone to travel distances exceeding 20 kilometers, mainly for entertainment, dining, and general shopping purposes. Shorter travel distances (<5 km) are more common for grocery shopping across all districts, especially in Nicosia and Limassol, likely due to urban density and proximity to services. In contrast, entertainment and dining often involve slightly longer trips, particularly in districts like Larnaka and Paphos.

Regarding mobility frequency and transportation preferences, on a weekly basis most individuals commute more than five times per week for work, once for shopping, once for dining, once for entertainment, once for visiting other houses, twice for grocery shopping and once for physical exercise and sports. Workplace mobility is consistently high across all districts, particularly in Nicosia and Paphos. Entertainment and dining tend to be more frequent in Limassol and Nicosia, where participants engage in these activities more often. Physical exercise shows a general trend of inactivity across all districts, while grocery shopping is commonly done once or twice per week, with higher frequen-cies in urban districts like Limassol and Nicosia. These patterns reflect how urban planning, population density, and available services shape mobility behavior.

Car usage is the predominant mode of transportation across all categories. Walking emerges as the second most preferred mode for commuting to and from university, work, and within the district of residence. Buses rank third for traveling to and from children's school and outside the district of residence. Most of the above findings align with the recent European Commission report on mobility patterns (CEU. MOVE. et al., 2022). According to that study, Cyprus stands out with the highest percentage (26%) of car trips for distances under 3 km, yet it has the lowest percentage (29%) for trips over 10 km among the 27 EU countries. Driving is particularly dominant, accounting for about 70% of travel time on working days (the highest proportion in the EU) with an average car trip of 23 minutes at an average speed of 33 km/h. Regarding short distance travelling (trips under 300 km) per person, Cyprus reports a daily average of 38 km (40% higher than the EU average) and daily average duration of 70 minutes (slightly below the EU average). Urban mobility (trips under 100 km within the same Functional Urban Area) sees an average travel distance of 10 km per person per day and an average duration of 21 minutes. The study also indicate that Cyprus also leads in car ownership, with 32% of individuals living in households with three or more cars, vastly exceeding the EU average of 6%. Two Eurobarometer reports find similar results. The reports from the European Commission (2014, 2015) highlight a high dependence on cars, with over 80% of respondents using a car daily, and note that Cyprus has the lowest usage of public transport services in the EU.

The mobility timeline of Cyprus residents on a typical workday exhibit distinct patterns throughout the day. In the early morning hours, the majority of individuals (> 84%) remain at home, with a gradual transition to other activities such as commuting for work and physical exercise starting at 6 am. During typical working hours (8 am to 4 pm), most people are at their workplace, while others are at home or academic institutions. By 6 pm, there is a notable shift, with a significant portion of individuals returning home, while others are still engaged in activities like grocery shopping, physical exercise, or remaining at work. Towards the end of the day, the trend leans heavily towards returning home (>

57%), with fewer individuals engaged in sports, work, entertainment, or dining out. On a typical Saturday, the mobility timeline of Cyprus residents reflects a pattern where the majority of individuals (ranging from 36% to 94%) remain at home throughout the day. Early in the morning until 6 am, a small percentage are already at their workplace or entertainment and dining venues. From 8 am to 6 pm, there is a notable increase in individuals at their workplace and sports facilities. Visits to other houses peak between 2 pm and 10 pm, while transitions for grocery shopping and general shopping occur between 10 am and 4 pm. Moreover, from 10 am until midnight, there is a significant interest in transitioning to entertainment and dining venues, suggesting a preference for leisure activities and dining out during weekends. On a typical Sunday, the mobility timeline of Cyprus residents closely mirrors that of a typical Saturday, with the majority (ranging from 39% to 94%) remaining at home throughout the day. Notable patterns include a transition for physical exercise by most individuals in the morning hours, followed by a significant number visiting other houses during the afternoon. From morning until early evening, there is a consistent percentage of individuals at their workplace, while activities related to entertainment and dining see a rapid increase, peaking in the late afternoon and evening hours. By the end of the day, the majority of participants have returned to their homes, indicating a trend towards winding down and relaxation as the weekend draws to a close. Despite the recent COVID19 pandemic, the vast majority of participants are currently working with physical presence, suggesting minimal impact on employment statuses or remote work adoption. Exercise habits vary, with a significant portion not exercising at all, while others prefer indoor or outdoor activities. The high percentage of 44% reporting no exercise at all, indicates an increased tendency towards sedentary lifestyles in the population. The lack of physical activity may be associated with various factors such as professional obligations to work in physical presence and preference for other activities besides exercise. As sedentary lifestyles can have negative impacts on health, it is important for people to incorporate physical activity into their daily routines for their overall well-being.

In the context of this survey study, several limitations are acknowledged. Firstly, the lack of detailed information on the exact locations of transitions limits the ability to analyze mobility patterns in higher spatial resolution. Secondly, the survey records human movement with a two-hour interval. This temporal resolution may overlook short-term mobility events, potentially leading to an incomplete understanding of short-duration trips and rapid movement changes. Lastly, the use of an electronic questionnaire presents a barrier for individuals who are not well-versed in technology, particularly older adults, resulting in potential underrepresentation of certain demographic groups and a bias towards more tech-savvy participants.

6 Simulating Human Mobility Behavior in Cyprus

This chapter presents the development and application of the EPIMO-LCA, an ABM designed to simulate the spatial and temporal dynamics of COVID19 transmission in the city of Larnaka, Cyprus. Implemented in NetLogo, the model adopts a spatially explicit SEIR framework that integrates behavioral, demographic, and mobility characteristics of the local population. These elements are derived directly from the findings of the mobility questionnaire discussed in Chapter 5, ensuring that the simulation is grounded in empirically observed human behavior. By combining epidemiological structure with realistic mobility routines, the EPIMO-LCA model enables the exploration of how individual movement patterns influence the course of an epidemic within an urban environment.

Section 6.1 details the design and implementation of the EPIMO-LCA model, including its data inputs, methodological framework and computational interface.

Section 6.2 focuses on the validation of the model, aiming to assess its ability to reproduce observed epidemiological patterns under real-world conditions. This is achieved through a systematic comparison between simulated outputs and officially reported COVID19 case data for two distinct periods corresponding to the dominance of the Delta and Omicron variants in Cyprus. The section further examines the influence of key behavioral and policy-related parameters on model performance, while also discussing the limitations of the modelling approach and the methodological adaptations adopted to address them. Through this validation process, the reliability and applicability of the EPIMO-LCA model as a tool for epidemiological analysis and decision support are critically evaluated.

6.1 The EPIMO-LCA Model

The ABM developed in this study simulates the transmission of COVID19 using the SEIR epidemiological framework, specifically tailored to the Republic of Cyprus. One of its core strengths lies in the integration of GIS. The EPIMO-LCA model incorporates several innovative elements that distinguish it from other models in the literature. It integrates realistic spatial data via GIS, enabling precise visualization and analysis of geographic distribution. It features a highly detailed classification of agents based on both age and behavior, allowing for the assessment of public health policies at the individual level. The temporal and spatial dynamics of movement add a high degree of realism to interactions and disease spread. Moreover, the model is flexible and adaptable to a range of scenarios, making it a powerful tool for evaluating policy interventions at the national scale as well as in other countries with similar demographic and geographic characteristics.

The EPIO-LCA model employs detailed spatial datasets,such as shapefiles for residential areas, workplaces, businesses, road networks, and population distribution from WorldPop 2020 database (https://www.worldpop.org) to position and distribute agents across the simulated space. This allows for an accurate representation of real-world population density and differentiation between various types of buildings. Another key feature is the dynamic assignment of characteristics to the population.

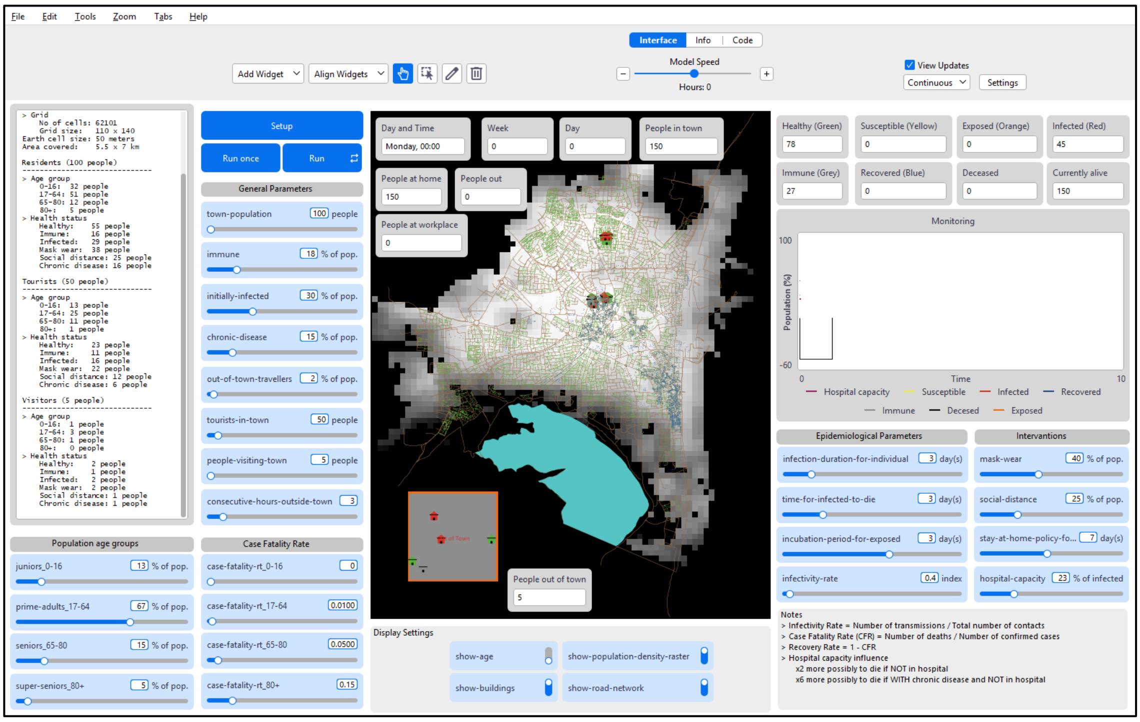

Figure 63. The proposed "EPIMO-LCA" model, developed within Netlogo (v7.0)

The model distinguishes between residents, visitors from other districts and tourists, with detailed configurations for age groups and personal attributes, such as chronic health conditions, mask usage, social distancing practices, and immunity status. It also assigns each agent to predefined “default” buildings, including homes and workplaces, creating a realistic baseline for daily activity patterns. Mobility is managed through a detailed schedule that varies by age group and specifies the time of day for different types of activities, such as staying at home, going to work, or engaging in outdoor activities. This scheduling allows the simulation to capture behavioral changes throughout a typical seven-day week, reflecting realistic daily and weekly rhythms of movement and interaction. At the epidemiological level, the SEIR model is applied to each individual agent, tracking transitions between states, Healthy, Susceptible, Exposed, Infected, Recovered, and Deceased. These transitions incorporate delays, such as incubation periods, and individual recovery or mortality rates, taking into account factors like case fatality rates and the demographic characteristics of each age group.

In terms of temporal and spatial dynamics, EPIMO-LCA offers a more fine-grained perspective than is typical in similar studies. Activities are scheduled on an hourly basis, and the timing of epidemiological transitions—such as moving from susceptible to exposed, or from infected to deceased—is tracked with high temporal resolution. This level of detail captures fluctuations in risk and transmission potential that models using aggregated time steps may overlook. The inclusion of a dedicated visitor management component is another uncommon feature. By modelling both resident and visitor/tourist populations, as well as movements beyond the core geographic area, the model is able to account for the role of external agents in sustaining or amplifying outbreaks. This capability extends its applicability beyond static local scenarios to situations involving cross-regional mobility and transient populations.

6.1.1 Data input

The datasets of the EPIMO-LCA model are divided into three main categories:

- Spatial and demographic data – defining the physical and population structure of the simulation environment.
- Mobility data – determining the movement patterns of agents within and outside the city.
- Epidemiological data – governing disease transmission, progression, and health outcomes.

The spatial configuration of the simulation environment is based on GIS datasets (fig.64, table 21). These datasets determine the geolocation and allocation of agents, the classification of buildings, and the visual rendering of the simulation environment. The spatial and demographic datasets used in the EPIMO-LCA model were derived from multiple authoritative sources.

Table 21. Spatial and demographic datasets used in the model

#	Data Type	Dataset	Description
1	raster-pop-distr	Cy-worldpop2020_100m	Raster file – Population distribution/density
2	shp-buildings-home	"data/shp/Buildings-home.shp"	Shapefile – Residential buildings
3	shp-buildings-out	"data/shp/Buildings-out.shp"	Shapefile – Buildings for outdoor activities (e.g., shopping, leisure)
4	shp-buildings-workplace	"data/shp/Buildings-workplace.shp"	Shapefile – Buildings containing workplaces
5	shp-walkway	"data/shp/LCA-Roads-AOI.shp"	Shapefile – Road network.
6	shp-AOI	"data/shp/LCA-AOI.shp"	Shapefile – Area of interest polygon (Larnaka)
7	shp-salt_lake	"data/shp/aliki-LCA.shp"	Shapefile – Salt Lake within the city.

The geographic extent of the study area corresponds to the administrative boundaries of Larnaka, Cyprus, including the urban perimeter and the nearby Salt Lake. These boundaries, along with the local road network and building footprints, were obtained from the Department of Lands and Surveys (DLS) of Cyprus.

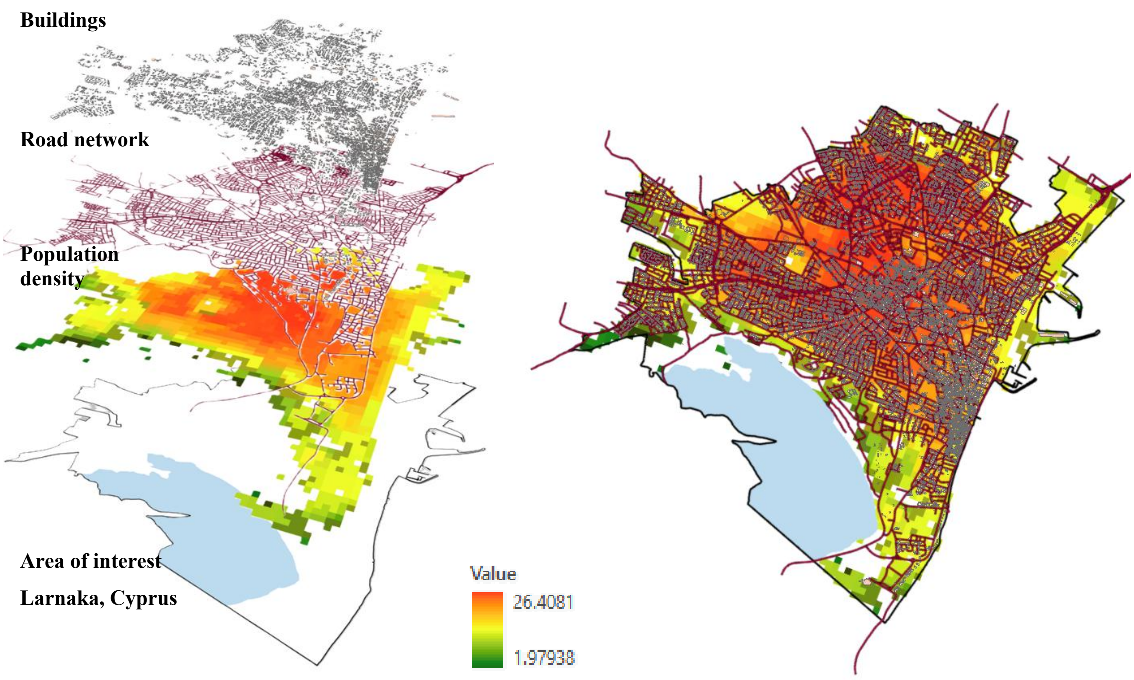

Figure 64. Data used in the model

The area of interest spans approximately 5,500 meters in width and 7,000 meters in height, ensuring coverage of both the central urban fabric and its immediate surroundings. The road network was provided in vector line format, while building footprints were supplied as vector polygons, totaling 17,198 individual structures.

The raw building data underwent additional processing to classify each structure into one of three primary categories, leveraging the official urban zoning map of Larnaka. This classification produced three subsets: residential buildings (11,796 polygons), workplaces (5,753 polygons), and buildings dedicated to outdoor activities, leisure, and shopping (5,424 polygons). This categorization allows the model to assign agents to default home and work locations, as well as to destinations for recreational or commercial activities, thereby introducing a spatially explicit structure to mobility patterns.

Population distribution data was sourced from the WorldPop 2020 dataset (https://hub.worldpop.org/geodata/summary?id=49960), which provides estimates of the total number of people per 100m grid cell in GeoTIFF format. The dataset is aligned with official United Nations population estimates (2019 Revision of World Population Prospects) and employs a Random Forest-based dasymetric redistribution method (Stevens et al., 2015). This approach integrates geospatial covariates related to population distribution and outputs from the Built-Settlement Growth Model (BSGM) developed by Nieves et al. (2020).

Before integration into the model, all datasets were reprojected to a common spatial reference system and aligned spatially to ensure consistency across layers. Building polygons and road networks were clipped to the area of interest, and population raster data was overlaid to determine agent allocation per residential structure based on density values. This combination of locally sourced cadastral data and globally validated population datasets provides a robust, high-fidelity spatial foundation for the model, ensuring both geographical accuracy and demographic realism in the simulation process.

The mobility parameters described below (table 22) define how agents (residents, visitors from other districts and tourists) move within and outside the city. They also regulate building capacities and the time agents spend in specific locations.

Table 22. The mobility parameters of the model

#	Parameter Name	Default Value	Description
1	town-population	INPUT, number (e.g. 50,000)	Total number of **city residents**. Each is assigned a default home and workplace within the city.
2	people-visiting-town	INPUT, number (e.g. 1,000)	Number of **visitors** entering the city for work or leisure activities. Each is assigned a default workplace in the city.
3	tourists-in-town	INPUT, number (e.g. 1,000)	Number of **tourists** in the city for leisure activities. Each is assigned a default homeplace in the city.
4	juniors_0-16, prime-adults_17-64, seniors_65-80, super-seniors_80+	INPUT, % of town-population (e.g. 30%)	Percentage distribution across age groups for both residents and visitors. Sum must not exceed 100% (error check).
5	capacity	5	Maximum number of people allowed in each residential building
		area_m² × 0.40	Maximum number of people allowed in each outdoor, leisure and shopping building H (0.40 people per m2)
		area_m² × 0.30	Maximum number of people allowed in each workplace building (0.30 people per m2)
6	out-of-town-travellers	INPUT, % of town-population (e.g. 30%)	Proportion of city residents travelling outside the city each hour for work, shopping or leisure. One fixed value.
7	consecutive-hours-outside-town	INPUT, number (e.g. 3)	Number of consecutive hours city residents remain outside the city. One fixed value
8	home-mobility-schedule_0-16 home-mobility-schedule _17-64 home-mobility-schedule _65-80 home-mobility-schedule _80+	Mobility Schedule List [e.g. 0.3, .., 0.3]	Proportion of people (city residents and visitors) at home for each hour over a week (24×7=168 values per age group)
9	workplace-mobility-schedule_0-16 workplace-mobility-schedule_17-64	Mobility Schedule List [e.g. 0.3, .., 0.3]	Proportion of people (city residents and visitors) at workplace for each hour over a week (24×7=168 values per age group)

	workplace-mobility-schedule_65-80 workplace-mobility-schedule_80+		
10	out-mobility-schedule_0-16 out-mobility-schedule_17-64 out-mobility-schedule_65-80 out-mobility-schedule_80+	Mobility Schedule List [e.g. 0.4, .., 0.4]	Proportion of people (city residents and visitors) at outdoor, leisure and shopping for each hour over a week (24×7=168 values per age group)

Lastly, the epidemiological parameters (table 23) regulate the infection process, recovery, mortality, and the effects of mitigation measures such as mask-wearing, social distancing, and hospital capacity.

Table 23. The epidemiological parameters of the model

#	Parameter Name	Default Value	Description
1	infectivity-rate	INPUT, number (e.g. 1)	Probability of disease transmission per contact **infectivity-rate = Number of transmissions / Total number of contacts**
2	incubation-period-for-exposed	INPUT, number (e.g. 7)	Length of incubation period (number of days) before symptoms. Used in process: exposed-to-infected.
3	immune	INPUT, % of population (e.g. 10%)	Initial proportion of immune individuals who cannot be infected or transmit the disease during the simulation
4	initially-infected	INPUT, % of population (π.χ. 5%)	Initial proportion of infected individuals. Combined with immune must not exceed 100%.
5	infection-duration-for-individual	INPUT, number (e.g. 7)	Duration (number of days) of infection for an individual
6	time-for-infected-to-die	INPUT, number (e.g. 10)	Time (number of days) from infection to death if not recovered.
7	stay-at-home-policy-for-infected	INPUT, number (e.g. 7)	Number of days infected individuals remain in self-isolation (at home)

8	case-fatality-rt_0-16 case-fatality-rt _17-64 case-fatality-rt _65-80 case-fatality-rt _80+	INPUT, number (e.g. 0.35)	Mortality rate per age group. Estimation of death risk Used in process: infected-to-deceased.
9	recovery-rt_0-16, recovery-rt _17-64, recovery-rt _65-80, recovery-rt _80+	INPUT, number (e.g. 0.80)	Recovery rate per age group. Used in process: infected-to-recovered.
10	chronic-disease	INPUT, % of population (e.g. 10%)	Proportion of population with chronic diseases, increasing mortality risk. Used in process: infected-to-deceased
11	mask-wear	INPUT, % of population (e.g. 20%)	Proportion of population wearing masks, reducing transmission probability. Used in process: susceptible-to-exposed
12	social-distance	INPUT, % of population (e.g. 30%)	Proportion of population practicing social distancing, reducing transmission probability. Cannot be infected or transmit the disease during the simulation
13	hospital-capacity	INPUT, % of infected (e.g. 30%)	Hospital beds available (as a proportion of infected people), reducing mortality. Used in process: infected-to-deceased

6.1.2 Methodology

To simulate the spread of COVID19 using an agent-based approach, the NetLogo software is employed as an open-source platform capable of representing and analyzing a model of this complexity. The EPIMO-LCA model implements a spatially explicit SEIR framework, incorporating behavioral, demographic, and mobility characteristics of the population in Larnaka, Cyprus. Having one of the highest car ownership rates in the world (629+ cars per 1000 inhabitants), Cyprus' residents rely heavily on private car commuting (Obrien, 2022). Based on this fact, in our simulation we don't include any public transportation parameters assuming all agents use private cars with an average speed of 50km/h (speed limit in urban areas).

A core component of the model is the HMS, which contains detailed information on mobility patterns for different age groups on an hourly basis. The HMS represents the primary daily mobility activities of individuals according to their age category, based on empirical data from the results of the specialized questionnaire survey (chapter 5.1) conducted for the purposes of this research. The current version of EPIMO-LCA utilizes separate weekly mobility schedules for the four main age categories, juniors (0–16 years), prime adults (17–64 years), seniors (65–80 years) and super seniors (80+ years), each containing three activity types each hour:

- Home mobility – proportion of individuals at home
- Workplace mobility – proportion at work or school (including students)
- Out mobility – proportion engaged in shopping, leisure, or other activities outside home/work

At the start of each simulation run, user-defined input parameters are loaded, including total population size, epidemiological parameters (incubation period, recovery period, case fatality rates), behavioral factors (mask usage, social distancing, immunity rates), and mobility schedules for each age group. The model first imports spatial datasets, including the Larnaka road network, building polygons with associated capacity values, and a raster layer representing population distribution. Using this raster, agents are allocated to default residential buildings proportionally to local population density, ensuring that no building exceeds its capacity. Default Workplace or school destinations are then assigned based on the agent's age and mobility profile.

Each agent is characterized by twenty distinct properties encompassing demographic, mobility, and epidemiological attributes (Table 24). Properties 1–12 are assigned during model initialization based on the input parameters, whereas properties 13–20 are dynamic and evolve during the simulation as agents interact with one another, reflecting changes in their epidemiological state and current location.

Once initialization is complete, the simulation advances in hourly time-steps (ticks). At each tick, agents determine their current target location according to the HMS and travel to their destination. Upon arrival, building occupancy is updated and crowd capacity constraints are enforced.

State transitions then proceed according to the SEIR logic (table 25) and are visually represented through agent color changes: green for Healthy, yellow for Susceptible, orange for Exposed, red for Infectious, and blue for Recovered.

Table 24. Agent properties

No.	Property	Type	Function
1	age	numeric	Specifies the agent's exact age.
2	age-group	categorical	Classifies the agent into mobility schedule category (0–16, 17–64, or other if extended).
3	chronic-disease?	boolean	Indicates presence of chronic illness, increasing mortality risk.
4	mask-wear?	boolean	Determines if the agent adheres to mask-use measures.
5	social-distance?	boolean	Determines if the agent respects social-distancing measures.
6	immune?	boolean	Identifies agents immune through vaccination, prior infection, or medication.
7	tourist?	boolean	Identifies agent as tourist
8	visitor?	boolean	Identifies agent as visitor (visiting from outside town)
9	home-building	coordinates	Assigned the default homeplace building.
10	workplace-building	coordinates	Assigned the default workplace or educational institution building.
11	case-fatality-rate	numeric	Individual probability of death once infected, based on age and health condition.
12	recovery-rate	numeric	Individual probability of recovery after infection.
13	SEIR-status?	categorical	Tracks epidemiological state (Healthy, Healthy and Immune, Susceptible, Infected, Exposed, Recovered).
14	out-of-town?	boolean	Tracks If currently in or out of town
15	destination-building	coordinates	Current assigned destination building.
16	previous-dest-type	categorical	Type of last visited location (home, work, out).
17	quarantine-hours-left?	numeric	Remaining time in quarantine for infected, if applicable. countdown
18	incubation-hours-left?		Remaining time in incubation period for exposed. countdown
19	infection-hours-left?	numeric	Time until recovery for infected. countdown
20	time-for-infected-to-die?	numeric	Time until death for infected. countdown

Table 25. Model processes and calculations (epidemiological states)

#	Process	Default Value	Description
1	healthy-to-susceptible	Random value random-float	Probability of becoming susceptible after contact with infectious individual. Valid for healthy, non-immune people that are not practicing social distancing. **if random-float 20 <= infectivity-rate**
2	susceptible-to-exposed	Random value random-float	Probability of becoming exposed: higher without masks, lower with masks: **No mask = 1 in 2 people (random-float 1 <= 0.50)** **using mask = 1 in 3 people (random-float 1 <= 0.66)**
3	exposed-to-infected	Number of all exposed people	All exposed become infected after the incubation period. incubation-period-for-exposed
4	infected-to-recovered	Random value random-float	Recovery probability different per age group, after infection duration (infection-duration-for-individual) **if random-float 1 <= recovery-rt_<age_group>**
5	infected-to-deceased	Random value random-float	Mortality probability different per age group, adjusted for hospitalisation and chronic disease: **x2 more possible to die if not in hospital** **if random-float 10 <= (2 * case-fatality-rt_<age_group>)** **x3 more possible to die if with chronic disease AND in hospital** **if random-float 10 <= (3 * case-fatality-rt_< age_group >)** **x6 more possible to die if with chronic disease AND not in hospital** **if random-float 10 <= (6 * case-fatality-rt_< age_group >)**

If a healthy, non-immune agent not practicing social distancing comes into contact with an infectious agent, a healthy-to-susceptible probability check (eq. 12) is performed:

$$\text{healthy-to-susceptible} = \text{if random-float } 20 \leq \text{infectivity-rate} \qquad \text{(eq. 12)}$$

Susceptible agents then undergo an infection-risk calculation based on mask use (eq. 13 - 14). Without a mask, the probability of becoming exposed is 1 in 2, while with a mask it is reduced to 1 in 3:

$$\text{susceptible-to-exposed (no mask use)} = \text{if random-float } 1 \leq 0.50 \qquad \text{(eq. 13)}$$

susceptible-to-exposed (with mask use) = if random-float 1 ≤ 0.66 (eq. 14)

All exposed agents progress to the infectious state once the incubation period (incubation-period-for-exposed) has elapsed. Infectious agents then either recover or die depending on age-specific probabilities and additional health conditions. Recovery probability is determined using age-specific recovery rate (eq. 15), after the infection duration (infection-duration-for-individual parameter):

infected-to-recovered = if random-float 1 <= recovery-rt_<age_group> (eq. 15)

Mortality risk is calculated using age-specific case fatality rates, adjusted for hospitalisation status and chronic disease (eq. 16 to 18).

if not hospitalized (×2 likelihood of death):

infected-to-deceased = if random-float 10 <= (2 * case-fatality-rt_<age_group>) (eq.16)

if hospitalised with a chronic disease (×3 likelihood of death):

infected-to-deceased = if random-float 10 <= (3 * case-fatality-rt_< age_group >) (eq.17)

if not hospitalised and with a chronic disease (×6 likelihood of death):

infected-to-deceased = if random-float 10 <= (6 * case-fatality-rt_< age_group >) (eq.18)

Recovered and immune agents remain permanently protected from reinfection and cannot infect others until the end of the simulation. If quarantine is enabled, infectious agents are restricted to their home location for the specified duration. The simulation proceeds in hourly steps until all agents reach a terminal state (Healthy, Immune, Infectious, Recovered, Deceased), after which epidemiological, spatial, and behavioural statistics are recorded.

The following graph (fig.65) summarizes the SEIR state-transition phases followed by the EPIMO-LCA model.

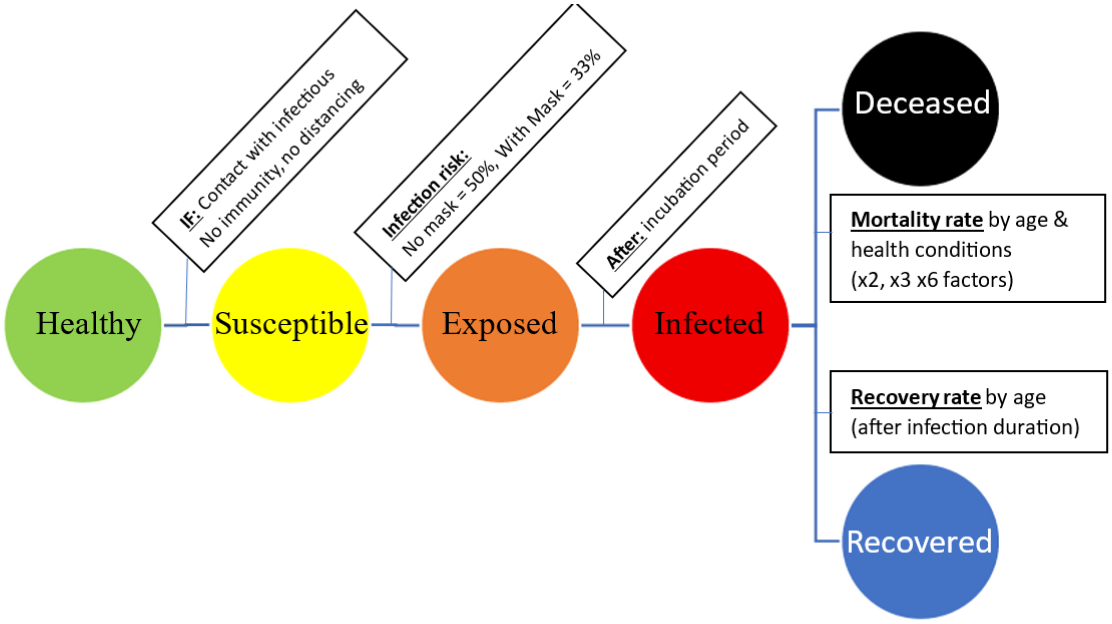

Figure 65. The SEIR state-transition phases of the model

The EPIMO-LCA model generates a set of key output values during each simulation run, which are essential for evaluating and comparing the impact of different intervention scenarios. These outputs provide both quantitative indicators and temporal dynamics that help in understanding the spread of the disease, the burden on healthcare systems, and the long-term immunity of the population.

One of the primary outputs is the number of active cases, recorded on an hourly basis, which enables direct comparison between scenarios and highlights the progression of the epidemic over time. Closely related to this is the maximum number of simultaneous infections (peak active cases), a crucial measure for estimating the peak demand on healthcare systems. The time to peak (expressed in hours from the start of the simulation) serves as a key planning metric, indicating when healthcare resources will be most needed.

Mortality-related indicators are also recorded. The model logs cumulative deaths, capturing the total number of agents transitioning from "Infected" to "Deceased" at each timestep. This metric reflects the human cost of the epidemic and is directly influenced by parameters such as case fatality rates and hospital capacity. Additionally, the model monitors peak hospital demand, showing the highest number of infected individuals requiring hospital care, and days over hospital capacity, which quantify the duration of system overload—both essential for understanding healthcare system resilience.

From a long-term epidemiological perspective, the final immunity level, the combined proportion of agents in the "Recovered" and "Immune" states at the end of the simulation, serves as an indicator of herd immunity and future vulnerability. Dynamic outputs, such as the curve of new cases, plotted as the hourly number of agents transitioning from "Exposed" to "Infected," allow for visual inspection of epidemic phases, including acceleration, plateau, and decline. Finally, the end time, the day when active infections drop to zero or remain below 1% of the peak, provides a measure of epidemic duration and potential for resurgence.

All output data can be exported directly from NetLogo using `export-monitor` or `export-world` commands, producing CSV files for further analysis. By systematically comparing these metrics across scenarios, the model enables precise quantification of the impact of varying parameters, offering a robust basis for evidence-based decision-making in epidemic management.

6.1.3 Interface

The User Interface (UI) of the EPIMO-LCA model has been designed to offer a comprehensive and interactive environment where users can define simulation parameters, visualize spatial outputs, and monitor epidemiological trends in real time.

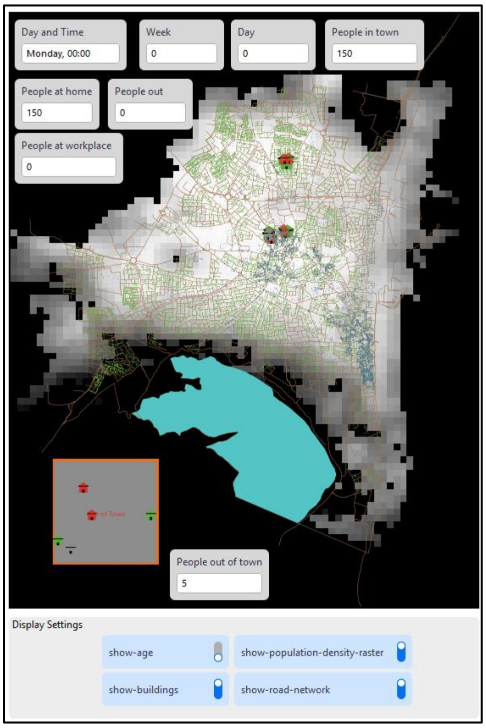

Figure 66. User Interface (The central map area)

In the central section (fig.66), the simulation map displays the geographic environment of Larnaka, including population density (raster), building footprints, and road networks (vector data). Agents are placed within this map and move according to their mobility schedules and activity patterns. Their epidemiological states are color-coded, allowing the spread of infection to be visually tracked over time. Important real-time statistics are shown at the upper part of the map

Below the map, the user can toggle display settings, such as buildings, road networks, and population density for focused view.

The layout is divided into three main sections: the left panel for parameter inputs and textual monitoring, the central panel for spatial visualization, and the right panel for graphical and statistical monitoring.

An inset map in the bottom-center shows the “Out of Town” area, representing locations outside the main area of interest where agents can temporarily travel.

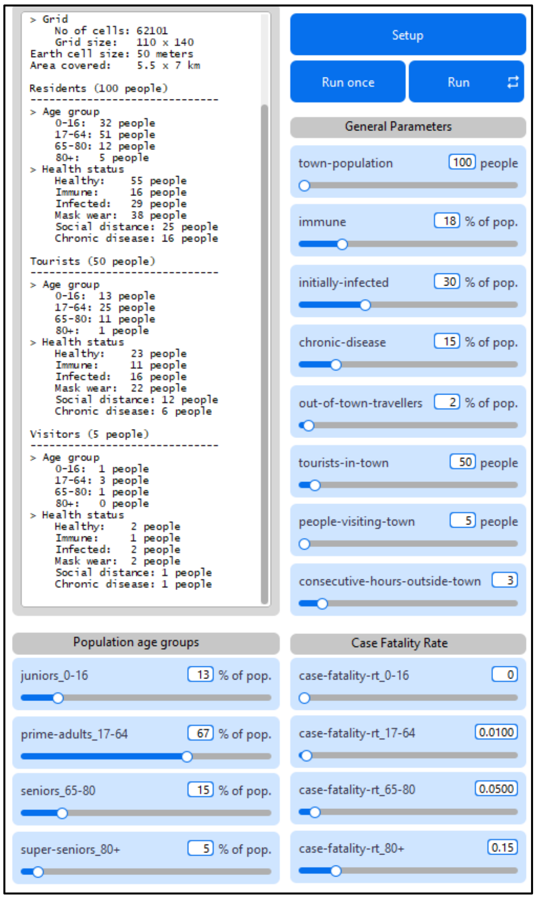

Figure 67. User Interface
(The left side of the model)

On the left-hand side (fig.67), the user can configure populations (city residents and tourists as well as visitors from other districts) and demographic parameters.

Mobility-related settings, such as the proportion of residents traveling outside the city, the duration of time spent outside, and the number of visiting individuals, can also be defined.

Demographic parameters include the proportion of immune, initially infected individuals and the share of the population with chronic diseases and the age group distribution, expressed as a percentage of the total population. Age groups are divided into four categories: juniors (0–16 years), representing children and adolescents, prime adults (17–64 years), representing the working-age population, seniors (65–80 years), representing older adults and super seniors (80+ years), representing the oldest population group. For each age group, users can also set the Case Fatality Rate (CFR), which determines the percentage of infected individuals that will die. These rates can be independently adjusted for each age category, allowing the model to reflect different age-specific vulnerabilities.

Also in the left panel, there is a summary monitor that presents an overview of the initial simulation setup. This includes the total number of people in each epidemiological state (Healthy, Immune, Infected, Mask Wearers, Social Distance Compliant, Chronic

Disease), separated for both residents and visitors. This monitor provides a quick snapshot of the starting conditions before running the simulation, ensuring that the input settings match the intended experimental design.

At the right side (fig.68), the user can adjust epidemiological and intervention parameters.

Epidemiological parameters include the infection duration, the time of the infected to die, the incubation period and the infectivity rate of the disease. Additionally, intervention parameters such as mask usage, social distancing compliance, hospital capacity, and stay-at-home policy duration, are fully customizable. Each parameter is entered as a percentage, numerical value, or fixed time unit, giving the user flexibility to replicate a wide variety of scenarios.

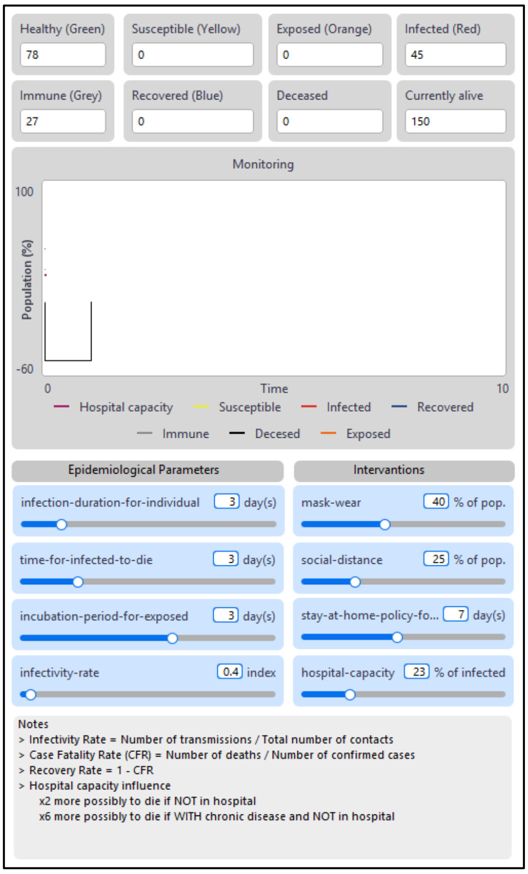

Figure 68. User Interface (The right side of the model)

Real-time epidemic monitoring is achieved through both a time-series chart and numerical counters. The chart shows the progression of each epidemiological category—Healthy, Susceptible, Exposed, Infected, Immune, Recovered, and Deceased—over the course of the simulation, alongside a hospital capacity line to indicate when healthcare limits are exceeded. Below the chart, numeric monitors provide the exact count of individuals in each category at any given moment, enabling precise quantitative tracking in addition to visual trend analysis.

The proposed model differs from many existing models in the literature through its integrated, individual-level approach and its use of detailed spatial and demographic data. While many traditional SEIR-based studies rely on compartmental models, treating the population as a homogeneous whole and analyzing disease spread at a macroscopic scale, EPIMO-LCA adopts an agent-based methodology. Here, each agent possesses unique attributes and interacts according to realistic behavioral rules, resulting in a richer and more nuanced representation of epidemic dynamics. This approach is further enhanced by the direct integration of spatial data, including vector shapefiles and raster imagery, enabling a precise representation of the geographical layout. This spatial realism makes the model well suited for assessing local pandemic management strategies and evaluating targeted protective measures. Another notable distinction lies in the level of demographic detail. EPIMO-LCA divides the population into four distinct age groups (0–16, 17–64, 65–80, and 80+), allowing for differentiated mortality, recovery, and behavioral parameters in each category. Many comparable models use fewer categories or apply generalized assumptions about age distribution. This granularity enables the inclusion of critical behaviors—such as mask use, social distancing, and the prevalence of chronic health conditions—at the individual level. In contrast, such factors are often averaged or omitted entirely in other modelling approaches, which can obscure important subgroup-specific effects.

6.2 Model Validation

Model validation constitutes a critical step in assessing the reliability and robustness of the proposed EPIMO-LCA agent-based model. It ensures that the model is capable of adequately reproducing real-world epidemiological patterns and provides confidence in its use as a decision-support and research tool. In this study, the validation process focuses on evaluating the model's ability to approximate observed COVID19 case trends under realistic assumptions and data constraints.

To achieve this, the model was validated across two distinct time periods, each characterized by different epidemiological dynamics. For each period, simulation parameters were calibrated to reflect real-world conditions, and the model outputs were systematically compared against officially reported COVID19 cases. This comparison between simulated results and observed data forms the basis for assessing the model's performance.

The selection of the validation periods was guided by both data reliability and epidemiological relevance. During these phases, Cyprus experienced exceptionally high testing volumes, ranging from approximately 500,000 to 880,000 diagnostic tests per week nationwide. This intensive testing effort resulted in increased detection of cases and, consequently, a more reliable representation of the actual epidemiological situation. The high sampling intensity is assumed to reduce uncertainty in reported cases, allowing for a closer approximation to true infection levels. In addition, the selected periods were characterized by the availability and consistency of data in a stable format, ensuring completeness and comparability throughout the analysis.

In order to enable a meaningful comparison between simulation outputs and real-world data, a series of transformations were applied to the official epidemiological data obtained from the Ministry of Health. Initially, the reported number of cases was downscaled from the district level (Larnaka District, approximately 150,000 inhabitants) to the city level (Larnaka Municipality, approximately 50,000 inhabitants). This was achieved through proportional adjustment, by dividing the reported values by three, under the assumption of a relatively uniform spatial distribution of cases within the district.

Subsequently, an adjustment based on the infection–detection rate (IDR) was applied to estimate the true number of infections from reported cases. The IDR reflects the proportion of actual infections that are detected and recorded in official statistics. For both validation periods, a value of IDR = 0.15 was adopted, in line with estimates provided by the Institute for Health Metrics and Evaluation (IHME) for the European region during periods dominated by the Delta and Omicron variants. This implies that reported cases were divided by 0.15 to approximate the total number of infections (for example, 2 reported cases correspond to approximately 13 actual infections). Given the absence of reliable subnational or time-specific IDR estimates, this value was selected as a reasonable empirical approximation within a broader range (0.10–0.20), acknowledging the inherent uncertainty associated with such assumptions.

The simulation component of the validation process was conducted using a reduced synthetic population of 10,000 agents, primarily to optimize computational efficiency and reduce execution time. To ensure comparability with real-world data, the simulation outputs were subsequently scaled to match the actual population of Larnaka (approximately 50,000 inhabitants) by applying a multiplication factor of five. This approach assumes that the simulated population adequately represents the structure and dynamics of the real population, allowing epidemiological patterns to scale proportionally.

The parameterization of the model was informed by the dominant epidemiological conditions during each validation period. In particular, the adoption of an IDR value corresponding to the Omicron-dominant phase was considered necessary, as this variant prevailed in Cyprus and across the European region during the study period. Due to the lack of detailed estimates accounting for variant co-circulation or short-term temporal variability, the use of a single representative value was deemed appropriate, providing a consistent and transparent basis for model calibration.

During the validation process, it was observed that rapid peaks in infection curves were not fully reproduced by the simulations. This limitation is primarily attributed to the static nature of the model parameters within each simulation run, where behavioral patterns and transmission dynamics remain fixed throughout the simulation period. In reality, however, epidemic trajectories are influenced by rapidly changing factors, including policy interventions, behavioral adaptations, and shifts in variant transmissibility.

To address this limitation, each validation period was divided into multiple consecutive simulation intervals, allowing parameters to be adjusted between runs. Specifically, for the first validation period (delta phase), three simulations sequential were performed (27/06/2021–11/07/2021, 12/07/2021–30/07/2021, and 31/07/2021–29/08/2021), while for the second validation period (omicron phase), two simulations were conducted (28/11/2021–26/12/2021 and 27/12/2021–07/01/2022). This segmentation approach enables the model to indirectly capture temporal variations in transmission dynamics, approximating changes in population behavior and intervention measures over time. At the same time, it highlights a structural limitation of the current modelling approach, namely the absence of dynamic parameter adaptation within a single simulation run.

Addressing this limitation, potentially through the incorporation of adaptive mechanisms or artificial intelligence techniques, represents an important direction for future research and model enhancement.

6.2.1 Period 1: Delta Dominance Phase

The first validation period corresponds to the dominance of the Delta variant in Cyprus, covering the summer months from June to September 2021. In contrast to the Omicron phase, this period is characterized by lower transmissibility, lower levels of population immunity, and a more structured implementation of public health measures. At the same time, increased seasonal mobility, including tourism and social activities, contributed to the spread of the virus.

To reflect temporal variations in epidemiological conditions and policy measures, the period was divided into three consecutive simulation intervals. The parameters applied in each sub-period are summarized in tables 26, 27, and 28.

Table 26. Model parameters for Delta sub-period 1 (15 days, 27/06/2021 – 11/07/2021)

Parameter	Value
Time for infected to die	4 days
Infection duration	9 days
Stay-at-home policy (infected)	5 days
Town population	10,000
Town Visitors	500
Town Tourists	100
Age distribution (0–16 / 17–64 / 65–80 / 80+) (% of population)	13% / 67% / 15% / 5%
Out-of-town travellers (% of population)	2%
Consecutive time outside town	3 hours
Infectivity rate	0.40
Incubation period (for exposed)	3 days
Immune (% of population)	35%
Initially infected (% of population)	0.1%
Case fatality rate (0–16 / 17–64 / 65–80 / 80+)	0 / 0.1 / 0.2 / 0.3
Chronic disease (% of population)	15%
Mask usage (% of population)	20%
Social distancing (% of population)	20%
Hospital capacity (% of infected)	23%

Table 27. Model parameters for Delta sub-period 2 (19 days, 12/07/2021 – 30/07/2021)

Parameter	Value
Time for infected to die	4 days
Infection duration	8 days
Stay-at-home policy (infected)	7 days
Town population	10,000
Town Visitors	500
Town Tourists	100
Age distribution (0–16 / 17–64 / 65–80 / 80+) (% of population)	13% / 67% / 15% / 5%
Out-of-town travellers (% of population)	2%

Consecutive time outside town	3 hours
Infectivity rate	0.40
Incubation period (for exposed)	3 days
Immune (% of population)	35%
Initially infected (% of population)	0.3%
Case fatality rate (0–16 / 17–64 / 65–80 / 80+)	0 / 0.1 / 0.2 / 0.3
Chronic disease (% of population)	15%
Mask usage (% of population)	20%
Social distancing (% of population)	50%
Hospital capacity (% of infected)	23%

Table 28. Model parameters for Delta sub-period 3 (37 days, 31/07/2021 – 29/08/2021)

Parameter	**Value**
Time for infected to die	4 days
Infection duration	9 days
Stay-at-home policy (infected)	7 days
Town population	10,000
Town Visitors	500
Town Tourists	100
Age distribution (0–16 / 17–64 / 65–80 / 80+) (% of population)	13% / 67% / 15% / 5%
Out-of-town travellers (% of population)	2%
Consecutive time outside town	3 hours
Infectivity rate	0.40
Incubation period (for exposed)	3 days
Immune (% of population)	35%
Initially infected (% of population)	0.1%
Case fatality rate (0–16 / 17–64 / 65–80 / 80+)	0 / 0.1 / 0.2 / 0.3
Chronic disease (% of population)	15%
Mask usage (% of population)	20%
Social distancing (% of population)	50%
Hospital capacity (% of infected)	23%

The detailed simulation results, including all six runs, observed case data, and mean simulation values, are presented in table 29 and figures 69 - 70. The results indicate a satisfactory agreement between the simulated and observed epidemic curves, successfully capturing both the rise and decline of the Delta wave.

Table 29. Simulation results (COVID19 cases during the Delta variance).

sim_date	Day	sim_1	sim_2	sim_3	sim_4	sim_5	sim_6	MoH_cases	simulation_mean_value
27/06/2021	8	50	50	50	50	50	50	73	50
28/06/2021	9	88	67	58	64	75	55	73	68
29/06/2021	10	105	108	76	84	111	67	93	92
30/06/2021	11	118	129	91	98	135	84	107	109
01/07/2021	12	136	139	115	110	138	93	113	122
02/07/2021	13	144	147	121	132	146	96	147	131
03/07/2021	14	161	149	139	146	165	105	113	144
04/07/2021	15	133	102	124	111	133	80	120	114
05/07/2021	16	136	108	126	115	146	82	180	119
06/07/2021	17	152	124	128	127	170	95	180	133
07/07/2021	18	135	116	130	123	164	93	207	127
08/07/2021	19	130	109	132	112	136	93	193	119
09/07/2021	20	151	127	133	115	133	101	87	127
10/07/2021	21	148	155	113	129	149	123	67	136
11/07/2021	22	173	162	118	139	162	145	60	150
12/07/2021	23	150	150	150	150	150	150	120	150
13/07/2021	24	175	184	172	174	176	179	93	177
14/07/2021	25	231	230	201	195	213	208	240	213
15/07/2021	26	274	244	231	246	229	224	247	241
16/07/2021	27	290	263	273	283	242	240	287	265
17/07/2021	28	317	285	290	297	263	270	233	287
18/07/2021	29	333	300	313	314	283	290	233	305
19/07/2021	30	210	221	205	202	199	220	320	209
20/07/2021	31	210	226	223	204	198	238	167	216
21/07/2021	32	221	240	228	223	214	262	240	231
22/07/2021	33	209	223	218	207	205	249	260	219
23/07/2021	34	170	206	211	190	181	241	153	200
24/07/2021	35	140	211	205	156	176	239	147	188
25/07/2021	36	145	204	173	123	180	240	173	177
26/07/2021	37	153	203	164	115	166	235	253	173
27/07/2021	38	155	196	161	114	164	250	200	173
28/07/2021	39	152	199	169	122	158	268	220	178
29/07/2021	40	177	200	164	115	166	270	200	182
30/07/2021	41	187	204	169	122	171	251	153	184
31/07/2021	42	50	50	50	50	50	50	147	50
01/08/2021	43	55	59	57	63	60	67	60	60
02/08/2021	44	61	76	70	75	64	79	107	71

03/08/2021	45	67	86	71	84	97	83	113	81
04/08/2021	46	80	94	80	99	100	95	113	91
05/08/2021	47	95	96	80	111	100	105	127	98
06/08/2021	48	96	98	82	117	106	108	120	101
07/08/2021	49	61	55	56	82	61	71	107	65
08/08/2021	50	66	55	58	80	60	71	80	65
09/08/2021	51	73	61	60	79	63	74	173	68
10/08/2021	52	70	58	53	79	59	58	100	63
11/08/2021	53	64	44	48	73	60	47	120	56
12/08/2021	54	61	39	49	74	53	56	100	55
13/08/2021	55	50	39	45	64	59	52	113	51
14/08/2021	56	45	39	48	54	61	46	93	49
15/08/2021	57	46	40	61	52	63	50	47	52
16/08/2021	58	50	44	60	66	74	50	113	57
17/08/2021	59	46	46	65	65	87	48	60	60
18/08/2021	60	48	41	70	65	96	44	80	61
19/08/2021	61	54	43	76	68	101	49	87	65
20/08/2021	62	56	44	80	74	108	47	80	68
21/08/2021	63	58	48	85	79	114	36	47	70
22/08/2021	64	61	49	94	80	109	39	60	72
23/08/2021	65	60	50	95	83	109	40	80	73
24/08/2021	66	58	53	90	85	105	34	80	71
25/08/2021	67	57	49	100	80	106	30	60	70
26/08/2021	68	65	50	100	77	104	29	87	71
27/08/2021	69	64	50	98	81	108	29	87	72
28/08/2021	70	55	49	105	86	106	30	73	72
29/08/2021	71	61	53	104	79	100	30	53	71

In particular, the model reproduces the gradual increase in cases during early July, the peak observed in mid-July, and the subsequent stabilization and decline during August. Compared to the Omicron phase, the epidemic dynamics are smoother, reflecting both the lower infectivity rate and the more consistent adherence to public health measures. Although minor discrepancies are observed in daily fluctuations, these differences are expected due to stochastic variability and unobserved local factors. Overall, the model demonstrates strong capability in simulating moderate transmission dynamics under varying intervention intensities.

According to the announcements of the Press and Information Office (https://www.gov.cy/pio), during the study period corresponding to the dominance of the

Delta variant, a different policy approach was observed, combining targeted restrictions with gradual reopening measures and strong emphasis on vaccination uptake. In particular, the introduction and progressive enforcement of the SafePass system (from 9 July 2021) constituted a central intervention, requiring proof of vaccination, recovery, or a negative test for access to high-risk settings and gatherings exceeding 20 individuals. At the same time, capacity limits were applied in mass events such as sports matches, cinemas, and theatres (initially 50% and later increased to 75% for vaccinated or recovered individuals), reflecting a partial relaxation under controlled conditions. In parallel, significant efforts were made to accelerate vaccination coverage through targeted incentives, including financial and social benefits for vaccinated individuals, as well as expansion of eligibility to younger age groups (e.g., vaccination availability for ages 16–17). Additional measures included stricter entry requirements to workplaces and public services via SafePass, limitations in physical presence, and encouragement of remote interactions where possible.

Regarding mobility, international travel was facilitated through the adoption of the EU Digital COVID Certificate (from 1 July 2021), allowing easier entry for vaccinated, recovered, or tested individuals, indicating a clear relaxation compared to earlier phases of the pandemic. However, testing requirements and categorization of countries (green, orange, red) remained in place, maintaining a level of control over imported cases.

Despite the implementation of these measures, the epidemiological trend during this period showed a sustained increase in cases, consistent with the onset of the fourth wave. This suggests that although interventions such as SafePass and vaccination incentives likely contributed to partial mitigation, they were insufficient to fully contain transmission under the higher transmissibility of the Delta variant and increased social mobility during the summer period. This observation is further supported by the model results, where the simulated curve aligns more closely with scenarios of moderate intervention effectiveness, indicating that real-world compliance and impact of measures were limited in practice.

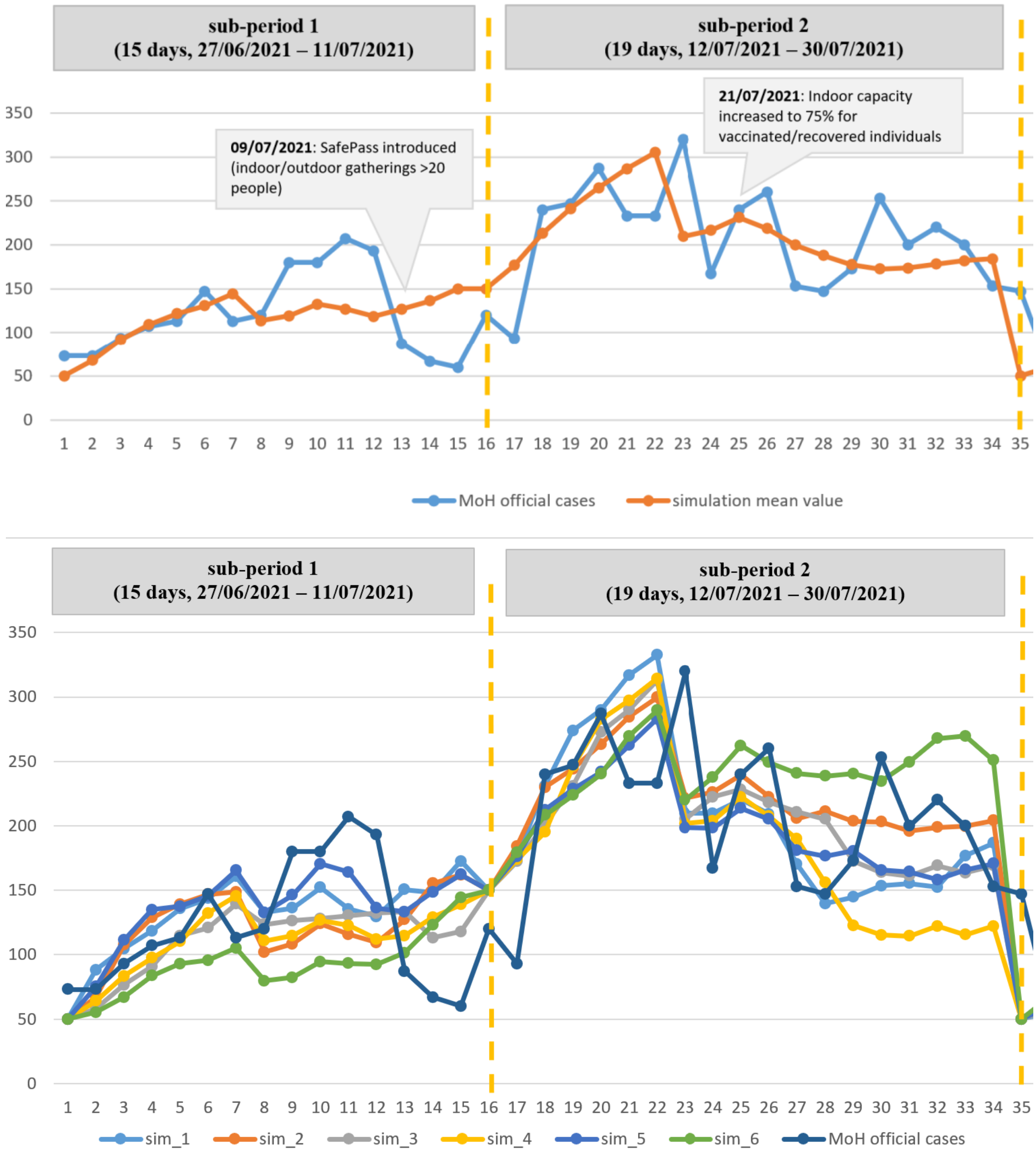

Figure 69. Simulation results for sub-period 1 and 2 (Delta phase).

The observed peaks are primarily associated with increased mobility and social mixing during the summer period, combined with the high transmissibility of the Delta variant. The delayed and partial effectiveness of interventions, such as the SafePass system, is reflected in the persistence of secondary peaks rather than immediate suppression. Conversely, the observed declines correspond to the gradual impact of control measures, behavioral adaptation, and increasing population immunity. However, the continued fluctuation in case numbers highlights the inability of the measures to fully stabilize transmission, a finding that is consistent with the model outputs, which capture the general trend but fail to reproduce short-term variability.

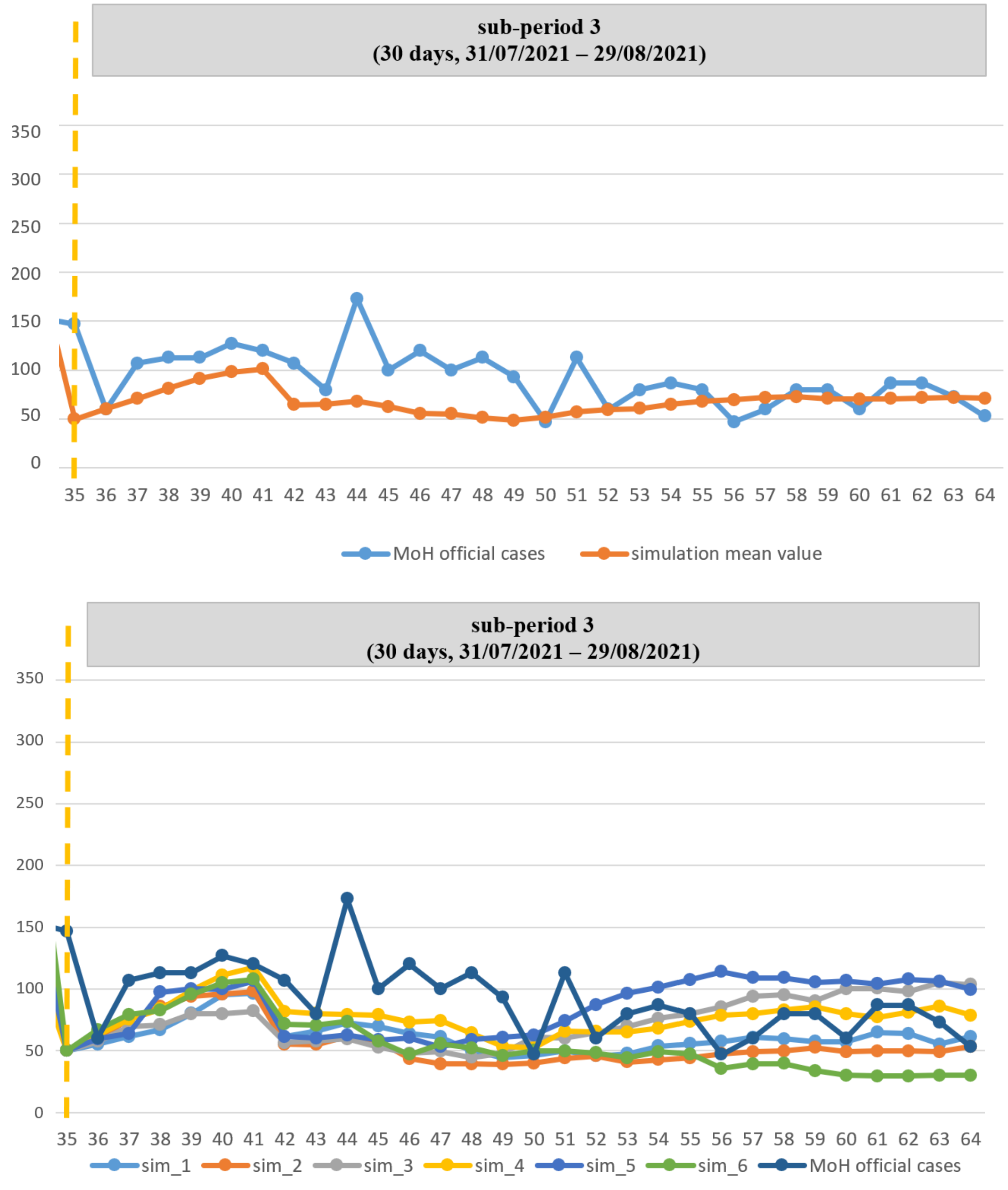

Figure 70. Simulation results for sub-period 3 (Delta phase).

6.2.2 Period 2: Omicron Dominance Phase

The second validation period corresponds to the rapid escalation and peak of the Omicron variant in Cyprus, spanning from 28 November 2021 to 7 January 2022. This period is characterized by the widespread dominance of the Omicron variant, coinciding with the Christmas and New Year holiday season, during which mobility patterns and social interactions deviated significantly from typical conditions. At the same time, Cyprus recorded the highest volume of diagnostic testing throughout the pandemic, ranging from approximately 500,000 to 880,000 tests per week. This intensive testing effort is assumed to enhance the reliability of reported case data and reduce uncertainty in estimating actual infection levels.

Despite the presence of public health measures, this phase was also marked by evident pandemic fatigue, leading to reduced compliance with protective measures. In parallel, changes in governmental policies, such as reduced isolation periods for confirmed cases, further influenced transmission dynamics. As a result, the effectiveness of interventions during this period remains uncertain, a characteristic that is reflected both in real-world observations and in the model outputs.

To capture these rapidly evolving conditions, the validation period was divided into two consecutive simulation intervals, allowing for parameter adjustments between runs. The parameters used for each sub-period are presented in Tables 30 and 31.

Table 30. Model parameters for Omicron sub-period 1 (29 days, 28/11/2021 – 26/12/2021)

Parameter	Value
Time for infected to die	4 days
Infection duration	8 days
Stay-at-home policy (infected)	5 days
Town population	10,000
Town Visitors	500
Town Tourists	100
Age distribution (0–16 / 17–64 / 65–80 / 80+) (% of population)	13% / 67% / 15% / 5%
Out-of-town travellers (% of population)	2%
Consecutive time outside town	3 hours
Infectivity rate	0.80

Incubation period (for exposed)	3 days
Immune (% of population)	55%
Initially infected (% of population)	0.2%
Case fatality rate (0–16 / 17–64 / 65–80 / 80+)	0 / 0.1 / 0.2 / 0.3
Chronic disease (% of population)	15%
Mask usage (% of population)	40%
Social distancing (% of population)	25%
Hospital capacity (% of infected)	23%

Table 31. Model parameters for Omicron sub-period 2 (13 days, 27/12/2021 – 07/01/2022)

Parameter	Value
Time for infected to die	4 days
Infection duration	8 days
Stay-at-home policy (infected)	0 days
Town population	10,000
Town Visitors	500
Town Tourists	100
Age distribution (0–16 / 17–64 / 65–80 / 80+) (% of population)	13% / 67% / 15% / 5%
Out-of-town travellers (% of population)	2%
Consecutive time outside town	3 hours
Infectivity rate	0.80
Incubation period (for exposed)	3 days
Immune (% of population)	55%
Initially infected (% of population)	0.5%
Case fatality rate (0–16 / 17–64 / 65–80 / 80+)	0 / 0.1 / 0.2 / 0.3
Chronic disease (% of population)	15%
Mask usage (% of population)	0%
Social distancing (% of population)	0%
Hospital capacity (% of infected)	23%

The simulation results for the six model runs, alongside the reported cases from the Ministry of Health and the corresponding mean simulation values, are presented in table 32 and figure 71. The results demonstrate a strong agreement between simulated and observed trends, particularly in capturing the sharp increase in cases during the transition from late December to early January.

Table 32. Simulation results (COVID19 cases during the Omicron variance).

sim_date	Day	sim_1	sim_2	sim_3	sim_4	sim_5	sim_6	MoH_cases	simulation_mean_value
28/11/2021	0	106	112	100	121	115	112	67	111
29/11/2021	1	125	122	107	132	119	140	167	124
30/11/2021	2	139	151	118	149	125	141	160	137
01/12/2021	3	159	176	131	161	134	159	160	153
02/12/2021	4	182	188	149	178	147	181	153	171
03/12/2021	5	105	120	102	128	73	130	133	110
04/12/2021	6	116	130	123	141	79	144	140	122
05/12/2021	7	129	148	139	154	94	168	87	139
06/12/2021	8	132	150	143	158	103	161	200	141
07/12/2021	9	125	148	155	155	103	155	160	140
08/12/2021	10	123	132	154	148	106	162	147	137
09/12/2021	11	110	121	154	149	118	164	147	136
10/12/2021	12	112	122	151	141	114	161	147	133
11/12/2021	13	123	123	151	131	127	156	140	135
12/12/2021	14	116	129	138	134	134	157	133	134
13/12/2021	15	104	138	131	136	139	168	180	136
14/12/2021	16	111	131	141	123	135	170	200	135
15/12/2021	17	117	138	132	134	145	154	167	137
16/12/2021	18	119	140	128	135	149	162	187	139
17/12/2021	19	132	148	131	137	155	166	173	145
18/12/2021	20	131	159	132	143	155	164	167	147
19/12/2021	21	126	176	127	156	162	171	100	153
20/12/2021	22	137	191	135	164	171	171	227	162
21/12/2021	23	140	198	131	179	175	153	233	163
22/12/2021	24	135	218	132	174	178	145	173	164
23/12/2021	25	125	246	132	166	180	153	220	167
24/12/2021	26	115	257	131	161	188	145	193	166
25/12/2021	27	119	245	137	159	202	149	87	168
26/12/2021	28	137	244	144	166	217	152	253	177
26/12/2021	29	315	322	326	330	350	326	407	328
27/12/2021	30	434	417	408	447	440	427	420	429
28/12/2021	31	519	489	488	556	496	499	613	508
29/12/2021	32	602	554	563	615	552	578	707	577
30/12/2021	33	671	648	669	682	636	675	693	663
31/12/2021	34	547	599	560	580	536	557	467	563
01/01/2022	35	635	695	633	677	619	645	693	651
02/01/2022	36	701	788	728	759	691	723	987	732

03/01/2022	37	739	817	755	786	695	746	913	756
04/01/2022	38	730	828	776	771	694	748	913	758
05/01/2022	39	733	874	809	771	723	781	627	782
06/01/2022	40	744	911	870	801	765	783	1067	812
07/01/2022	41	771	934	879	839	776	768	627	828

According to the announcements of the Press and Information Office (https://www.gov.cy/pio), during the study period a progressively intensified set of non-pharmaceutical interventions was implemented in Cyprus, reflecting the rapid deterioration of the epidemiological situation during the emergence of the Omicron variant.

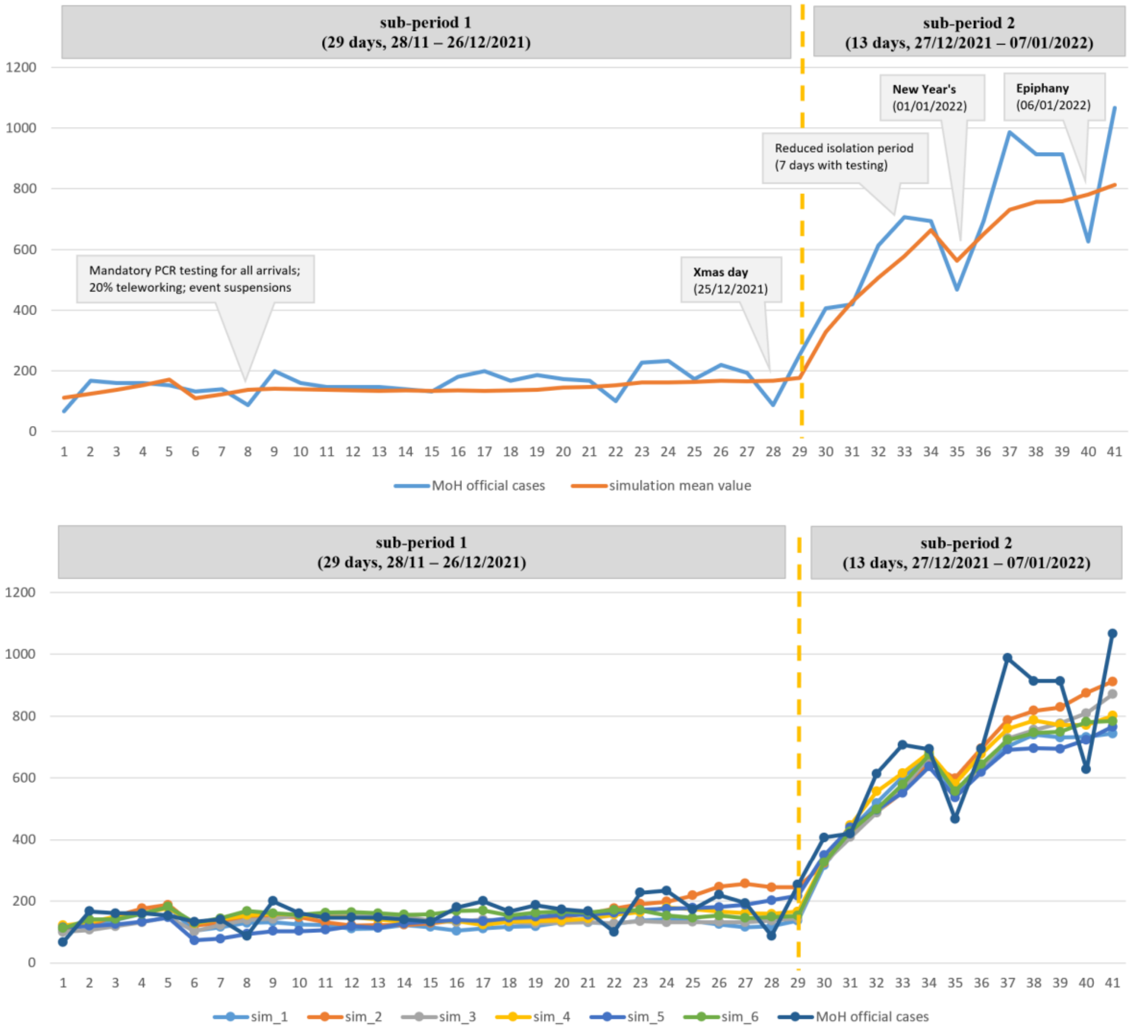

Figure 71. Simulation results for sub-period 1 and 2 (Omicron phase).

These measures included the expansion of the booster vaccination campaign to the adult population, the tightening of SafePass requirements, and the introduction of extensive testing protocols across multiple domains, such as mandatory PCR testing for all arrivals, frequent rapid testing in workplaces, and systematic testing in schools. At the same time, mobility and social interaction were increasingly restricted through teleworking (gradually increased from 20% to 50%), reduced gathering limits (from 20 to 10 individuals), capacity constraints in public venues (from 300 to 200 persons), and additional measures targeting high-risk settings such as entertainment venues, where entry required recent testing and activities such as dancing were prohibited. Furthermore, adjustments to epidemiological protocols were introduced, including the reduction of the isolation period for confirmed cases, allowing release on day 8 following negative rapid tests on days 6 and 7, which effectively increased the rate at which individuals could return to daily activities.

Despite this comprehensive and progressively stricter policy framework, the observed epidemiological curve continued to rise sharply, indicating limited effectiveness of the implemented measures during this phase. This trend is further supported by the model validation results for sub-period 2, where the simulated infection curve aligns closely with the scenario assuming zero compliance (i.e., 0% use of masks and social distancing). This convergence suggests that, in practice, the impact of the measures was substantially reduced, potentially due to behavioral fatigue, reduced adherence due to holiday session (Christmas period), or the inherently high transmissibility of the Omicron variant, ultimately leading to sustained and increasing transmission dynamics.

The observed peaks during period 2 are strongly associated with increased social interactions during the Christmas and New Year holidays, where family gatherings and indoor activities significantly intensified transmission. The main peak reflects both the high contact rates during festive days and the delayed manifestation of infections due to incubation and reporting lags. Notably, case numbers remain elevated even after New Year, indicating sustained transmission and continued social mixing until the Epiphany period. Short-term fluctuations within the peak are likely attributed to reporting effects rather than actual epidemiological changes. The subsequent decline is delayed and occurs only after the normalization of social behavior, highlighting the dominant role of human behavior over formal interventions during holiday periods.

6.2.3 Conclusions

The validation results demonstrate that the EPIMO-LCA ABM is capable of reliably reproducing the main epidemiological trends observed during both the Delta and Omicron phases in Cyprus. Across different transmission regimes, the model successfully captures the overall trajectory, magnitude, and temporal evolution of reported cases, confirming its robustness as a spatially explicit epidemiological modelling framework.

The comparison between simulated and observed data highlights the model's sensitivity to behavioral parameters, particularly mobility patterns, compliance with protective measures, and policy interventions.

Despite its overall strong performance, the validation process also reveals an important limitation of the modelling framework, namely the static nature of model parameters within each simulation run. In the current implementation, key parameters—such as mobility behavior, compliance levels, and intervention intensity—remain fixed throughout each simulation period. As a result, the model is not able to fully capture abrupt temporal changes, such as those driven by sudden behavioral shifts (e.g., holiday gatherings) or rapid policy adjustments. This limitation is particularly evident in the Omicron phase, where sharp peaks and short-term fluctuations in observed data are only partially reproduced by the model.

To address this constraint, a segmented simulation approach was adopted, whereby each validation period was divided into multiple consecutive simulation runs with updated parameter values. This approach allows the model to approximate temporal variability by indirectly incorporating changes in behavior and policy between sub-periods. While this strategy improves the alignment between simulated and observed data, it remains a workaround rather than a fully integrated solution, as it does not allow for continuous, real-time adaptation of parameters within a single simulation.

Overall, the validation confirms that the EPIMO-LCA model provides a credible and empirically grounded representation of COVID19 transmission dynamics in a small, interconnected population. However, it also highlights the need for future methodological enhancements, particularly the incorporation of dynamic parameterization mechanisms that can capture evolving behavioral and policy-driven changes over time. Potential improvements may include the integration of adaptive rules, feedback loops, or artificial intelligence techniques, enabling the model to respond more realistically to rapidly changing epidemiological conditions.

In conclusion, the EPIMO-LCA model constitutes a valuable tool for supporting epidemiological analysis, scenario exploration, and evidence-based public health decision-making in Cyprus and similar contexts, while also providing a solid foundation for further methodological advancements in agent-based epidemiological modelling.

7 Discussion

This section synthesizes the findings of this dissertation and reflects on the broader implications of integrating geoinformatics, human mobility analysis, and agent-based modelling in the study of epidemiological crises. Building upon the theoretical foundations, empirical analysis, and simulation results presented in the previous chapters, this chapter critically evaluates the contribution of the research in addressing key gaps identified in the Cypriot context.

In particular, the chapter revisits the central objective of the thesis, namely, to demonstrate how geoinformatics can enhance the understanding and management of epidemic dynamics, by examining the role of spatial analysis, mobility behavior, and localized modelling in explaining the spread of COVID19. It further situates the EPIMO-LCA model within the broader scientific landscape, highlighting its contribution as a data-driven, context-aware framework tailored to small, interconnected populations.

The discussion that follows is structured into four main parts: a summary of the thesis, a synthesis of the main findings, an assessment of model limitations, and a set of future research directions. Together, these sections provide a comprehensive reflection on the scientific contribution, practical relevance, and future potential of the proposed approach.

7.1 Thesis Summary

This dissertation explored the role of geoinformatics and human mobility modelling in understanding and managing epidemiological crises, with a particular focus on the COVID19 pandemic in Cyprus. The research was structured around the integration of spatial data, human mobility behavior, and agent-based modelling, aiming to bridge existing gaps in localized epidemiological analysis for small, interconnected populations.

The theoretical foundation of the study (Chapters 2 and 3) established the importance of human mobility as a key driver of disease transmission, highlighting the role of spatial-temporal dynamics, behavioral patterns, and population flows. In parallel, the contribution of geoinformatics in epidemiology was examined, emphasizing disease mapping, spatial analysis, and simulation approaches, particularly through ABMs.

Chapter 4 contextualized the research within the Cypriot case study, presenting how geoinformatics tools were applied to monitor the spread of COVID19. The development of static and dynamic maps, as well as a Web-GIS dashboard, demonstrated the value of spatial data infrastructures in supporting real-time epidemiological surveillance and decision-making.

Chapter 5 introduced the empirical component of the study, focusing on the collection and analysis of primary mobility data through a structured questionnaire. The findings provided detailed insights into travel behavior, daily activity patterns, and responses to COVID19 measures, forming the basis for the construction of a realistic HMS.

Building upon these components, Chapter 6 presented the EPIMO-LCA agent-based model, which integrates epidemiological dynamics with empirically derived mobility behavior. The model was validated against real-world data for both the Delta and Omicron phases, demonstrating its ability to reproduce observed trends and highlighting the critical influence of human behavior on transmission dynamics.

Overall, the dissertation delivers a holistic framework that combines geoinformatics, mobility data, and agent-based modelling, contributing to the understanding of how localized behavioral patterns shape epidemic evolution.

7.2 Main Findings

The results of this research highlight several key findings regarding the relationship between human mobility, policy interventions, and epidemic dynamics.

First, the study confirms that human mobility behavior is a dominant driver of disease transmission, often outweighing the theoretical effectiveness of policy measures. This is particularly evident in the Omicron phase (Period 1), where a sharp increase in cases was observed despite the implementation of progressively stricter measures. The alignment between observed data and simulation scenarios with minimal compliance (0% mask usage and social distancing) suggests that behavioral fatigue and social pressures, especially during holiday periods, can significantly reduce the effectiveness of interventions.

Second, the comparison between the Delta and Omicron phases reveals two distinct transmission regimes. The Delta phase is characterized by moderate but sustained transmission, influenced by increased mobility during the summer and partially mitigated by structured interventions such as SafePass and vaccination campaigns. In contrast, the

Omicron phase exhibits rapid, behavior-driven spikes, demonstrating how sudden changes in social behavior can lead to abrupt epidemic surges that are difficult to control through static policy measures.

A key contribution of this research is the incorporation of empirical mobility data, which provides valuable insights into the mobility behavior of Cypriot residents. The questionnaire results reveal a strong dependence on private vehicles, with mobility patterns dominated by short-distance travel for daily activities. At the same time, mobility behavior varies across districts and activity types, reflecting localized socio-spatial dynamics. The findings also highlight structured daily mobility routines, with clear temporal patterns in movement and activity distribution throughout the day.

Importantly, the results indicate that Cyprus exhibits distinctive mobility characteristics compared to larger countries, due to its small size and island geography. These include a high frequency of short-distance trips, strong connectivity between urban and rural areas, and dense infrastructure networks that facilitate movement. In addition, the centralization of key services—such as healthcare, education, and public administration—within a limited number of urban centers significantly influences travel behavior, requiring frequent movement from surrounding areas.

These findings provide added value at a local and district level, offering insights that go beyond national-scale analyses and enabling more targeted policy interventions. From a planning perspective, the results suggest the need to reduce car dependency, enhance alternative transportation options, and promote more sustainable and active mobility patterns, particularly given the observed low engagement in physical activity.

Furthermore, the integration of primary mobility data into the modelling process proved to be critical. The use of questionnaire-derived data allowed for the development of realistic mobility schedules, enhancing the model's ability to simulate daily routines and interaction patterns. This highlights the value of combining bottom-up (data-driven) and top-down (model-based) approaches in epidemiological research. The study demonstrates the importance of localized modelling approaches. The EPIMO-LCA model, calibrated using Cyprus-specific data, provides more realistic insights compared to generalized models. This reinforces the need for context-aware epidemiological tools, particularly in small and highly interconnected regions where population behavior can vary significantly over short spatial and temporal scales.

Additionally, the geoinformatics outputs (maps and Web-GIS dashboard) demonstrate that visualization and spatial analysis are essential components of epidemic monitoring, enabling the identification of patterns, hotspots, and temporal trends that are not easily captured through numerical data alone.

Concluding, the findings of this study are further supported by recent efforts in the broader European context. A study by Thomopoulos & Tsichlas (2024), focusing on Greece, demonstrates the growing importance of agent-based modelling for capturing country-specific epidemiological dynamics. Their work highlights how synthetic populations, social interaction patterns, and behavioral assumptions can be integrated into SEIR-based frameworks to evaluate intervention strategies. However, compared to the present research, their approach remains at an early developmental stage, relying primarily on aggregated data and simplified behavioral assumptions. In contrast, this dissertation advances the state of the art by incorporating empirically derived mobility patterns from a dedicated questionnaire survey, enabling a more realistic and context-sensitive representation of human behavior in Cyprus.

This comparison further reinforces one of the key findings of this study: that accurate representation of human mobility and behavior is critical for reproducing real-world epidemiological trends and for improving the reliability of simulation-based policy evaluation.

7.3 Model Limitations

The EPIMO-LCA model, while incorporating several innovative elements for simulating infectious disease transmission in an urban context, inevitably entails certain methodological limitations and simplifying assumptions that should be acknowledged.

Limitations include fixed and predefined mobility schedules, simplified representation of social interactions, static epidemiological parameters and limited consideration of non-biological parameters. A primary limitation is the static parameterization within each simulation run. In the current implementation, key parameters, such as mobility behavior, compliance levels, and intervention intensity, remain fixed throughout the simulation period. This restricts the model's ability to capture dynamic and abrupt changes, such as those observed during holiday periods or following rapid policy shifts. To partially address this limitation, a segmented simulation approach was adopted, whereby each validation period was divided into multiple consecutive runs with updated parameters. While this approach improves the alignment between simulated and observed data, it represents a methodological workaround rather than a fully integrated solution, as it does not allow for continuous adaptation within a single simulation environment.

Additionally, the model implements activity schedules for home, work, and outdoor activities as fixed lists of hourly probabilities, customized for each age group. While this allows for precise control over movement patterns, it does not fully capture the dynamic and adaptive nature of human mobility under unpredictable circumstances—such as sudden behavioral shifts in response to policy changes like lockdowns or travel restrictions. In contrast, some models in the literature adopt adaptive mobility strategies, where schedules are updated in real time based on incoming data or scenario triggers. Although the current approach is static, it could be modified to incorporate adaptive logic with relative ease. Although the model allocates agents to specific residential, workplace, and leisure locations, it does not implement an explicit social network structure. In many advanced epidemiological simulations, social networks are used to define repeated contacts, interaction frequencies, and relational clustering, providing a more realistic depiction of disease spread within communities. In EPIMO-LCA, interactions are instead determined solely by co-location in shared spaces, without modelling persistent social ties such as family, friendship, or workplace connections. Regarding the epidemiological aspect, mortality and recovery rates in the model are defined as fixed values per age group. While this stratification increases realism compared to uniform rates, the parameters do not adapt dynamically to factors such as the emergence of new viral variants or changes in treatment effectiveness. Models that incorporate time-varying parameters may better capture epidemiological shifts over the course of an outbreak. Additionally, although EPIMO-LCA accounts for interventions such as mask-wearing and social distancing, it does not extend to simulating psychosocial factors or population responses to public information campaigns. Some integrated modelling frameworks incorporate behavioral science elements, allowing them to simulate how attitudes, trust, and risk perception influence compliance with health measures.

In order to ensure computational efficiency and maintain focus on the study's primary objectives, the EPIMO-LCA model adopts a set of simplifying assumptions regarding population characteristics, spatial allocation, and epidemiological processes. The spatial population distribution is based on WorldPop 2020 data and is treated as static, meaning that demographic shifts occurring after 2020 are not reflected in the simulation. Each agent is assigned a home location according to population density patterns and a workplace allocated randomly within the designated urban zones. This approach provides a practical starting point for large-scale modelling, although it does not incorporate actual commuting data that could offer greater accuracy. Mobility patterns are fixed for each age group according to a predefined weekly schedule. These schedules remain constant throughout the simulation and do not adapt to public health interventions such as remote work mandates, school closures, or restrictions on movement. Visitors to the city follow the same mobility patterns as residents, an assumption that does not reflect potential differences in behavior linked to tourism, short-term events, or seasonal gatherings. Such simplifications are necessary for computational tractability but inevitably reduce the variability and context-specific realism of agent movements.

From an epidemiological perspective, the model employs the SEIR framework without additional compartments for asymptomatic, pre-symptomatic, or partially immune vaccinated individuals. Parameters such as mask usage, social distancing compliance, and the presence of chronic illnesses are assigned randomly across the population, without stratification by age group or calibration to empirical survey data. Immunity, once assigned, is considered both permanent and complete for the duration of the simulation, whereas in reality immunity may wane over time or vary according to viral variants. Furthermore, the mechanics of disease transmission and health outcomes are represented in a simplified form. Transmission is assumed to occur instantly among all agents co-located within the same building or location, without modelling airborne particle dispersion, physical distancing, or contact duration. Infectiousness-related parameters, including infection duration, incubation period, and time to death, are fixed across all age groups, and mortality and recovery outcomes are determined solely by age-specific rates, chronic disease status, and hospital capacity. The model does not simulate persistent social relationships such as family or workplace networks, instead relying on random co-location events to generate interactions. Similarly, building capacities are estimated using general density coefficients rather than detailed, venue-specific occupancy data.

The above limitations and assumptions should be considered when interpreting simulation results. While they do not undermine the model's ability to explore relative scenario differences and evaluate intervention strategies, they may constrain the precision of absolute predictions in real-world contexts. Nonetheless, EPIMO-LCA offers a robust and flexible framework that could be expanded in future work to include dynamic behavioral responses, network-based social interactions, and evolving epidemiological parameters in response to emerging variants or changing public health measures.

7.4 Future Directions

The EPIMO-LCA model provides significant added value through its strong foundation in real-world spatial, demographic, and behavioral data. By integrating the WorldPop 2020 population dataset alongside detailed spatial representations of buildings and road networks, the model ensures that agent distribution and interactions are grounded in realistic geographic contexts. This spatial explicitness enhances both the credibility of simulation outcomes and their interpretability within the specific socio-spatial structure of the study area.

In addition, the model demonstrates a high degree of flexibility and configurability, allowing for the adjustment of key epidemiological and behavioral parameters, including mask usage, social distancing compliance, immunity levels, and age-group distributions. This enables the exploration of a wide range of public health strategies through "what-if" analyses, without requiring structural modifications to the model. A further strength lies in the incorporation of time-sensitive mobility patterns, where daily and weekly schedules differentiated by age group and activity type allow for a more realistic representation of human interactions. Compared to more computationally intensive approaches, the model achieves a balance between realism and efficiency, ensuring usability and accessibility without compromising analytical depth.

Moreover, the model's localized design, tailored to the demographic and spatial characteristics of Larnaka, provides context-aware insights that are directly relevant for Cyprus and other regions of similar scale. At the same time, its generalized SEIR framework ensures adaptability, allowing the model to be applied to other infectious diseases or emerging variants by adjusting a limited set of core parameters. This combination of localization and generalization enhances the long-term relevance and reusability of the EPIMO-LCA framework.

Building on this foundation, several directions for future research emerge that could further enhance the model's realism, applicability, and scientific contribution.

A primary priority is the transition from static to dynamic parameterization, allowing model parameters to evolve continuously in response to changing behavioral patterns, policy interventions, and epidemiological conditions. This would address one of the key limitations identified in this study and could be achieved through the integration of adaptive rules, feedback mechanisms, or machine learning techniques.

Another important direction involves the incorporation of behavioral and social heterogeneity. Extending the model to include social network structures, persistent relationships (e.g., households, workplaces), and adaptive behavior would enable a more realistic representation of human interactions. In this context, integrating socioeconomic characteristics—such as income, occupation, household size, and access to healthcare—would allow the model to capture inequalities in exposure and health outcomes, supporting the design of targeted and equitable public health interventions.

The refinement of transmission mechanisms also represents a key area for improvement. Introducing proximity- and duration-based contact calculations, as well as differentiating environments based on transmission risk (e.g., indoor vs. outdoor, ventilation conditions), would enhance the accuracy of infection dynamics. Similarly, incorporating more advanced representations of vaccination and immunity, including waning immunity, booster strategies, and heterogeneous vaccine response, would improve the model's relevance for long-term epidemiological planning.

From a policy analysis perspective, the model could be extended to support cost–benefit evaluation of NPIs. By integrating economic indicators—such as productivity loss, reduced mobility, and implementation costs—alongside epidemiological outcomes, the model could provide valuable insights into the trade-offs between public health protection and economic impact. In parallel, the simulation of public health system processes, including testing, contact tracing, and targeted quarantine strategies, would enable a more comprehensive evaluation of intervention effectiveness.

Another promising research direction is the investigation of population resilience and epidemic rebound scenarios. By simulating the reintroduction of the virus under varying conditions of immunity and mobility, the model could identify high-risk scenarios and inform decisions on the safe relaxation of measures. In addition, incorporating super-spreader dynamics and contact heterogeneity would allow the model to assess the disproportionate role of highly connected individuals in transmission and evaluate the effectiveness of targeted containment strategies.

The integration of real-time and large-scale data sources, such as mobility data from mobile devices or digital platforms, represents another significant opportunity. Coupled with the development of advanced geoinformatics visualization tools, including interactive dashboards and dynamic mapping environments, this would enhance both the analytical and operational value of the model.

Furthermore, the incorporation of Artificial Intelligence (AI) has the potential to significantly advance the EPIMO-LCA framework. Machine learning techniques could support automated parameter calibration, detection of hidden patterns in large datasets, and the generation of adaptive behavioral rules. AI-driven predictive analytics could also improve the model's ability to forecast epidemic trajectories and evaluate intervention scenarios under uncertainty, transforming the model into a more responsive and self-adjusting system.

Finally, technical and usability enhancements could further strengthen the model's research and operational capabilities. These include performance optimization for large-scale simulations, automated data export for integration with external analytical tools (e.g., R or Python), and enhanced visualization features such as heatmaps and real-time monitoring of key indicators.

BIBLIOGRAPHY

A. Rvachev, L., & Longini, I. M. (1985). A mathematical model for the global spread of influenza. *Mathematical Biosciences*, *75*(1), 3–22. https://doi.org/10.1016/0025-5564(85)90064-1

Adams, J. S. (2001). THE QUANTITATIVE REVOLUTION IN URBAN GEOGRAPHY. *Urban Geography*, *22*(6), 530–539. https://doi.org/10.2747/0272-3638.22.6.530

Agapiou, S., Anastasiou, A., Baxevani, A., Nicolaides, C., Hadjigeorgiou, G., Christofides, T., Constantinou, E., Nikolopoulos, G., & Fokianos, K. (2021). Modeling the first wave of Covid-19 pandemic in the Republic of Cyprus. *Scientific Reports*, *11*(1), 7342. https://doi.org/10.1038/s41598-021-86606-3

Ajbar, A., Alqahtani, R. T., & Boumaza, M. (2021). Dynamics of an SIR-Based COVID-19 Model With Linear Incidence Rate, Nonlinear Removal Rate, and Public Awareness. *Frontiers in Physics*, *9*, 634251. https://doi.org/10.3389/fphy.2021.634251

Ajelli, M., Gonçalves, B., Balcan, D., Colizza, V., Hu, H., Ramasco, J. J., Merler, S., & Vespignani, A. (2010). Comparing large-scale computational approaches to epidemic modeling: Agent-based versus structured metapopulation models. *BMC Infectious Diseases*, *10*(1), 190. https://doi.org/10.1186/1471-2334-10-190

Aleman, D. M., Wibisono, T. G., & Schwartz, B. (2011). A Nonhomogeneous Agent-Based Simulation Approach to Modeling the Spread of Disease in a Pandemic Outbreak. *Interfaces*, *41*(3), 301–315. https://doi.org/10.1287/inte.1100.0550

Alexandrou, C., Harmandaris, V., Irakleous, A., Koutsou, G., & Savva, N. (2021). Modeling the evolution of COVID-19 via compartmental and particle-based approaches: Application to the Cyprus case. *PLOS ONE*, *16*(5), e0250709. https://doi.org/10.1371/journal.pone.0250709

Altun, K., Altuntaş, S., & Dereli, T. (2021). An interaction-oriented multi-agent SIR model to assess the spread of SARS-CoV-2. *Hacettepe Journal of Mathematics and Statistics*, *50*(5), 1548–1559. https://doi.org/10.15672/hujms.751734

AnyLogic simulation software. (2025). https://www.anylogic.com

Arino, J., McCluskey, C. C., & Van Den Driessche, P. (2003). Global Results for an Epidemic Model with Vaccination that Exhibits Backward Bifurcation. *SIAM Journal on Applied Mathematics*, *64*(1), 260–276. https://doi.org/10.1137/S0036139902413829

Arnold-Forster, A. (2020). Mapmaking and Mapthinking: Cancer as a Problem of Place in Nineteenth-century England. *Social History of Medicine: The Journal of the Society for the Social History of Medicine*, *33*(2), 463–488. https://doi.org/10.1093/shm/hky059

Asgari, F., Gauthier, V., & Becker, M. (2013). *A survey on Human Mobility and its applications*. https://doi.org/10.48550/ARXIV.1307.0814

Astorri, F., Beaubien, S. E., Ciotoli, G., & Lombardi, S. (2002). An assessment of gas emanation hazard using a geographic information system and geostatistics. *Health Physics*, *82*(3), 358–366. https://doi.org/10.1097/00004032-200203000-00008

Axhausen, K. W., Zimmermann, A., Schönfelder, S., Rindsfüser, G., & Haupt, T. (2002). Observing the rhythms of daily life: A six-week travel diary. *Transportation*, *29*(2), 95–124. https://doi.org/10.1023/A:1014247822322

Axtell, R. (2000). Why Agents? On the Varied Motivations for Agent Computing in the Social Sciences. *The Brookings Institution*, (17), 1–23.

Bachar, M., Khamsi, M. A., & Bounkhel, M. (2021). A mathematical model for the spread of COVID-19 and control mechanisms in Saudi Arabia. *Advances in Difference Equations*, *2021*(1), 253. https://doi.org/10.1186/s13662-021-03410-z

Bae, J. W., Shin, K., Lee, H.-R., Lee, H. J., Lee, T., Kim, C. H., Cha, W.-C., Kim, G. W., & Moon, I.-C. (2018). Evaluation of Disaster Response System Using Agent-Based Model With

Geospatial and Medical Details. *IEEE Transactions on Systems, Man, and Cybernetics: Systems*, *48*(9), 1454–1469. https://doi.org/10.1109/TSMC.2017.2671340

Bailey, N. T. J. (1975). The mathematical theory of infectious diseases and its applications. 2nd edition. *The Mathematical Theory of Infectious Diseases and Its Applications. 2nd Edition.*

Balcan, D., Hu, H., Goncalves, B., Bajardi, P., Poletto, C., Ramasco, J. J., Paolotti, D., Perra, N., Tizzoni, M., Van Den Broeck, W., Colizza, V., & Vespignani, A. (2009). Seasonal transmission potential and activity peaks of the new influenza A(H1N1): A Monte Carlo likelihood analysis based on human mobility. *BMC Medicine*, *7*(1), 45. https://doi.org/10.1186/1741-7015-7-45

Barrett, C. L., Bisset, K. R., Eubank, S. G., Xizhou Feng, & Marathe, M. V. (2008). EpiSimdemics: An efficient algorithm for simulating the spread of infectious disease over large realistic social networks. *2008 SC - International Conference for High Performance Computing, Networking, Storage and Analysis*, 1–12. https://doi.org/10.1109/SC.2008.5214892

Barrett, M. S., Chua, W.-J., Crits-Christoph, P., Gibbons, M. B., & Thompson, D. (2008). Early withdrawal from mental health treatment: Implications for psychotherapy practice. *Psychotherapy: Theory, Research, Practice, Training*, *45*(2), 247–267. https://doi.org/10.1037/0033-3204.45.2.247

Bauch, C. T., Lloyd-Smith, J. O., Coffee, M. P., & Galvani, A. P. (2005). Dynamically Modeling SARS and Other Newly Emerging Respiratory Illnesses: Past, Present, and Future. *Epidemiology*, *16*(6), 791–801. https://doi.org/10.1097/01.ede.0000181633.80269.4c

Berry, B. J. L. (1993). GEOGRAPHY'S QUANTITATIVE REVOLUTION: INITIAL CONDITIONS, 1954-1960. A PERSONAL MEMOIR. *Urban Geography*, *14*(5), 434–441. https://doi.org/10.2747/0272-3638.14.5.434

Bhat, C. R., & Koppelman, F. S. (1999). Activity-Based Modeling of Travel Demand. In R. W. Hall (Ed.), *Handbook of Transportation Science* (Vol. 23, pp. 35–61). Springer US. https://doi.org/10.1007/978-1-4615-5203-1_3

Bivand, R. S. (2021). Progress in the R ecosystem for representing and handling spatial data. *Journal of Geographical Systems*, *23*(4), 515–546. https://doi.org/10.1007/s10109-020-00336-0

Bobashev, G. V., Goedecke, D. M., Yu, F., & Epstein, J. M. (2007). A Hybrid Epidemic Model: Combining The Advantages Of Agent-Based And Equation-Based Approaches. *2007 Winter Simulation Conference*, 1532–1537. https://doi.org/10.1109/WSC.2007.4419767

Boccaletti, S., Bianconi, G., Criado, R., Del Genio, C. I., Gómez-Gardeñes, J., Romance, M., Sendiña-Nadal, I., Wang, Z., & Zanin, M. (2014). The structure and dynamics of multilayer networks. *Physics Reports*, *544*(1), 1–122. https://doi.org/10.1016/j.physrep.2014.07.001

Boelaert, M., Arbyn, M., & Van der Stuyft, P. (1998). Geographical information systems (GIS), gimmick or tool for health district management? *Tropical Medicine & International Health: TM & IH*, *3*(3), 163–165. https://doi.org/10.1046/j.1365-3156.1998.00221.x

Bonabeau, E. (2002). Agent-based modeling: Methods and techniques for simulating human systems. *Proceedings of the National Academy of Sciences*, *99*(suppl_3), 7280–7287. https://doi.org/10.1073/pnas.082080899

Bonnet, G., Pearson, C. A. B., Torres-Rueda, S., Ruiz, F., Lines, J., Jit, M., Vassall, A., & Sweeney, S. (2024). A Scoping Review and Taxonomy of Epidemiological-Macroeconomic Models of COVID-19. *Value in Health*, *27*(1), 104–116. https://doi.org/10.1016/j.jval.2023.10.008

Bookstaber, R. (2012). Using Agent-Based Models for Analyzing Threats to Financial Stability. *SSRN Electronic Journal*. https://doi.org/10.2139/ssrn.2642420

Briggs, D. J. (2002). *GIS for emergency preparedness and health risk reduction*. Kluwer Academic Publishers.

Brown, B. (2015, October 29). *5 Benefits of Geographic Information Systems in Healthcare*. https://hitconsultant.net/2015/10/29/5-benefits-of-geographic-information-systems-in-healthcare/#.Xe0UX-jXJPY

Buhat, C. A. H., Lutero, D. SM., Olave, Y. H., Torres, M. C., & Rabajante, J. F. (2020). *Transmission of Respiratory Infectious Diseases between Neighboring Cities using Agent-based Model and Compartmental Model* [Preprint]. Infectious Diseases (except HIV/AIDS). https://doi.org/10.1101/2020.06.24.20138818

Burrough, P. A., McDonnellmRachael A, & Lloyd, C. D. (2015). *Principles of geographical information systems* (3. ed). Oxford university press.

C. Economidou, E., Markou, N., Prokopi, K., Avraam, D., & S. Soteriades, E. (2024). Excess Mortality in Cyprus during the COVID-19 Epidemic. *Journal of Community Medicine & Public Health*, *8*(1). https://doi.org/10.29011/2577-2228.100407

Cegielski, W. H., & Rogers, J. D. (2016). Rethinking the role of Agent-Based Modeling in archaeology. *Journal of Anthropological Archaeology*, *41*, 283–298. https://doi.org/10.1016/j.jaa.2016.01.009

CEU. MOVE., Univ. Eiffel., TRT., Panteia., GDCC., & STRATEC. (2022). *Study on new mobility patterns in European cities: Final report. Task A, EU wide passenger mobility survey.* Publications Office. https://data.europa.eu/doi/10.2832/728583

Chan, H. F., Skali, A., & Torgler, B. (2020). *A global dataset of human mobility* (CREMA Working Paper 2020–04). Center for Research in Economics, Management and the Arts (CREMA). http://hdl.handle.net/10419/225546

Chardonnel, S. (2007). Time-Geography: Individuals in Time and Space. In L. Sanders (Ed.), *Models in Spatial Analysis* (1st ed., pp. 97–126). Wiley. https://doi.org/10.1002/9780470612255.ch4

Chatzimilioudis, G., Konstantinidis, A., Laoudias, C., & Zeinalipour-Yazti, D. (2012). Crowdsourcing with Smartphones. *IEEE Internet Computing*, *16*(5), 36–44. https://doi.org/10.1109/MIC.2012.70

Chen, J., Taylor, J. E., & Wei, H.-H. (2012). Modeling building occupant network energy consumption decision-making: The interplay between network structure and conservation. *Energy and Buildings*, *47*, 515–524. https://doi.org/10.1016/j.enbuild.2011.12.026

Chen, X., Ong, Y.-S., Tan, P.-S., Zhang, N., & Li, Z. (2013). Agent-Based Modeling and Simulation for Supply Chain Risk Management—A Survey of the State-of-the-Art. *2013 IEEE International Conference on Systems, Man, and Cybernetics*, 1294–1299. https://doi.org/10.1109/SMC.2013.224

Choi, M., Afzal, B., & Sattler, B. (2006). Geographic information systems: A new tool for environmental health assessments. *Public Health Nursing (Boston, Mass.)*, *23*(5), 381–391. https://doi.org/10.1111/j.1525-1446.2006.00577.x

Chrysostomou, A. C., The COMESSAR Network, & Kostrikis, L. G. (2024). Into the Cauldron of the Variant Soup: Insights into the Molecular Epidemiology and Transition to Endemicity of SARS-CoV-2 in Cyprus (November 2022–February 2024). *Viruses*, *16*(11), 1686. https://doi.org/10.3390/v16111686

Chrysostomou, A. C., Vrancken, B., Haralambous, C., Alexandrou, M., Aristokleous, A., Christodoulou, C., Gregoriou, I., Ioannides, M., Kalakouta, O., Karagiannis, C., Koumbaris, G., Loizides, C., Mendris, M., Papastergiou, P., Patsalis, P. C., Pieridou, D., Richter, J., Schmitt, M., Shammas, C., … Kostrikis, L. G. (2022). Genomic Epidemiology of the SARS-CoV-2 Epidemic in Cyprus from November 2020 to October 2021: The

Passage of Waves of Alpha and Delta Variants of Concern. *Viruses*, *15*(1), 108. https://doi.org/10.3390/v15010108
Chrysostomou, A. C., Vrancken, B., Koumbaris, G., Themistokleous, G., Aristokleous, A., Masia, C., Eleftheriou, C., Ioannou, C., Stylianou, D. C., Ioannides, M., Petrou, P., Georgiou, V., Hatziyianni, A., Lemey, P., Vandamme, A.-M., Patsalis, P. P., & Kostrikis, L. G. (2021). A Comprehensive Molecular Epidemiological Analysis of SARS-CoV-2 Infection in Cyprus from April 2020 to January 2021: Evidence of a Highly Polyphyletic and Evolving Epidemic. *Viruses*, *13*(6), 1098. https://doi.org/10.3390/v13061098
Clarke, K. (1996). On Epidemiology and Geographic Information Systems: A Review and Discussion of Future Directions. *Emerging Infectious Diseases*, *2*(2), 85–92. https://doi.org/10.3201/eid0202.960202
Coccia, M. (2020). Factors determining the diffusion of COVID-19 and suggested strategy to prevent future accelerated viral infectivity similar to COVID. *Science of The Total Environment*, *729*, 138474. https://doi.org/10.1016/j.scitotenv.2020.138474
Colizza, V., Barrat, A., Barthélemy, M., & Vespignani, A. (2006). The role of the airline transportation network in the prediction and predictability of global epidemics. *Proceedings of the National Academy of Sciences*, *103*(7), 2015–2020. https://doi.org/10.1073/pnas.0510525103
Conway, S. R. (2006). An agent-based model for analyzing control policies and the dynamic service-time performance of a capacity-constrained air traffic management facility. *ICAS 2006-25th Congress of the International Council of the Aeronautical Sciences*.
Cromley, E. K. (2012). *GIS and public health* (2nd ed). The Guilford Press.
Croner, C. M. (1998). *Public health geographic information systems (GIS) news and information; 1994-1997. Working Paper Series (National Center for Health Statistics (U.S.) Cognitive Methods Staff) ; No. 23*. (cdc:13298). https://stacks.cdc.gov/view/cdc/13298
Crooks, A. T., & Hailegiorgis, A. B. (2014). An agent-based modeling approach applied to the spread of cholera. *Environmental Modelling & Software*, *62*, 164–177. https://doi.org/10.1016/j.envsoft.2014.08.027
Csáji, B. Cs., Browet, A., Traag, V. A., Delvenne, J.-C., Huens, E., Van Dooren, P., Smoreda, Z., & Blondel, V. D. (2013). Exploring the mobility of mobile phone users. *Physica A: Statistical Mechanics and Its Applications*, *392*(6), 1459–1473. https://doi.org/10.1016/j.physa.2012.11.040
Cui, J., Takeuchi, Y., & Saito, Y. (2006). Spreading disease with transport-related infection. *Journal of Theoretical Biology*, *239*(3), 376–390. https://doi.org/10.1016/j.jtbi.2005.08.005
Cuschieri, S., Pallari, E., Hatziyianni, A., Sigurvinsdottir, R., Sigfusdottir, I. D., & Sigurðardóttir, Á. K. (2022). A year of Covid-19: Experiences and lessons learnt by small European island states—Cyprus, Iceland and Malta. *European Journal of Public Health*, *32*(2), 316–321. https://doi.org/10.1093/eurpub/ckab217
Cyprus Ministry of Health. (2020a). *Cyprus national vaccination plan for COVID19*. https://www.pio.gov.cy/coronavirus/uploads/NationalVaccinationPlan.pdf
Cyprus Ministry of Health. (2020b). *National Surveillance Report for the Coronavirus Disease 2019 (COVID-19)*. Epidemiological Surveillance Unit, Ministry of Health of the Republic of Cyprus. https://www.pio.gov.cy/corona virus/pdf/ep1205ien.pdf
Cyprus Ministry of Health. Important Announcements regarding COVID-19. (2020). https://www.pio.gov.cy/coronavirus/eng/categories/important-announcements
Daszak, P., Cunningham, A. A., & Hyatt, A. D. (2000). Emerging Infectious Diseases of Wildlife—Threats to Biodiversity and Human Health. *Science*, *287*(5452), 443–449. https://doi.org/10.1126/science.287.5452.443

De Montjoye, Y.-A., Hidalgo, C. A., Verleysen, M., & Blondel, V. D. (2013). Unique in the Crowd: The privacy bounds of human mobility. *Scientific Reports*, *3*(1), 1376. https://doi.org/10.1038/srep01376

Demissie, M. G., Phithakkitnukoon, S., Sukhvibul, T., Antunes, F., Gomes, R., & Bento, C. (2016). Inferring Passenger Travel Demand to Improve Urban Mobility in Developing Countries Using Cell Phone Data: A Case Study of Senegal. *IEEE Transactions on Intelligent Transportation Systems*, *17*(9), 2466–2478. https://doi.org/10.1109/TITS.2016.2521830

Dent, D. M. (2006). Cartographies of Disease. Maps, Mapping, and Medicine. Tom Koch, ESRI Press, Redlands, CA, 2005, 388 pp, $ 28.32. *World Journal of Surgery*, *30*(8), 1626–1626. https://doi.org/10.1007/s00268-006-0176-4

Desjardins, M. R., Hohl, A., & Delmelle, E. M. (2020). Rapid surveillance of COVID-19 in the United States using a prospective space-time scan statistic: Detecting and evaluating emerging clusters. *Applied Geography*, *118*, 102202. https://doi.org/10.1016/j.apgeog.2020.102202

Dibble, C., Wendel, S., & Carle, K. (2007). Simulating Pandemic Influenza Risks Of Us Cities. *2007 Winter Simulation Conference*, 1548–1550. https://doi.org/10.1109/WSC.2007.4419770

Doi, S., Inoue, T., Ide, H., Nakamura, T., Fujita, S., & Takabayashi, K. (2013). Using GIS to Simulate Inpatient's Behavior and Visualize Healthcare Demand. *Procedia Computer Science*, *22*, 1361–1368. https://doi.org/10.1016/j.procs.2013.09.225

Duan, W., Qiu, X., Cao, Z., Zheng, X., & Cui, K. (2013). Heterogeneous and Stochastic Agent-Based Models for Analyzing Infectious Diseases' Super Spreaders. *IEEE Intelligent Systems*, *28*(4), 18–25. https://doi.org/10.1109/MIS.2013.29

Dung, P., ICJ, O., Akintola, A., Y, D., AO, K., Babagana, M., Muhammad, S., IM, O., & Kamoru, A. (2017). The Role of GIS And Remote Sensing in the Control of Malaria. *Online Journal of Health and Allied Sciences*, *16*, 7.

Dunham, J. B. (2005). An Agent-Based Spatially Explicit Epidemiological Model in MASON. *Journal of Artificial Societies and Social Simulation*, *9*(1), 3.

Elliott, P., Cuzick, J., English, D., & Stern, R. (1996). *Geographical and Environmental Epidemiology*. Oxford University Press. https://doi.org/10.1093/acprof:oso/9780192622358.001.0001

Epstein, J. M., Parker, J., Cummings, D., & Hammond, R. A. (2008). Coupled Contagion Dynamics of Fear and Disease: Mathematical and Computational Explorations. *PLoS ONE*, *3*(12), e3955. https://doi.org/10.1371/journal.pone.0003955

Eratosthenes CoE COVID-19 Cyprus Cases Dashboard. (2021). https://excelsior2020.eu/covid-19-web-services/

Esri China. (2021, January 3). *List of Novel Coronavirus Dashboards*. https://storymaps.arcgis.com/stories/a1746ada9bff48c09ef76e5a788b5910

Eubank, S., Guclu, H., Anil Kumar, V. S., Marathe, M. V., Srinivasan, A., Toroczkai, Z., & Wang, N. (2004). Modelling disease outbreaks in realistic urban social networks. *Nature*, *429*(6988), 180–184. https://doi.org/10.1038/nature02541

European Commission. (2014). *Special Eurobarometer 406: Attitudes of Europeans towards urban mobility* (Version v1.00) [Dataset]. http://data.europa.eu/88u/dataset/S1110_79_4_406

European Commission. (2015). *Special Eurobarometer 420: Passenger Rights* (Version v1.00) [Dataset]. http://data.europa.eu/88u/dataset/S2011_82_1_420

European Commission. (2021). *Cyprus: Country Health Profile 2021*. OECD Publishing.

Fabbri, G., Federico, S., Fiaschi, D., & Gozzi, F. (2024). Mobility decisions, economic dynamics and epidemic. *Economic Theory*, *77*(1–2), 495–531. https://doi.org/10.1007/s00199-023-01485-1

Fayad, P., Hadjipetrou, S., Leventis, G., Kavroudakis, D., & Kyriakidis, P. (2023). Designing an Agent-Based Model for a City-Level Simulation of COVID-19 Spread in Cyprus: *Proceedings of the 13th International Conference on Simulation and Modeling Methodologies, Technologies and Applications*, 218–224. https://doi.org/10.5220/0012054000003546

Fayad, P., Kyriakidis, P., Tsioutis, C., & Kavroudakis, D. (2024). A Survey to Capture the Mobility Behavior of Residents in the Republic of Cyprus. *European Journal of Geography*, *15*(4), 305–318. https://doi.org/10.48088/ejg.p.fay.15.4.305.318

Ferguson, N., Laydon, daniel, Nedjati Gilani, gemma, Imai, N., Ainslie, kylie, Baguelin, marc, Bhatia, sangeeta, Boonyasiri, adhiratha, Cucunuba Perez, zulma, Cuomo-Dannenburg, gina, Dighe, amy, Dorigatti, ilaria, Fu, han, Gaythorpe, katy, Green, will, Hamlet, arran, Hinsley, wes, Okell, lucy, van Elsland, S., … Ghani, azra. (2020). *Report 9: Impact of non-pharmaceutical interventions (NPIs) to reduce COVID19 mortality and healthcare demand*. https://doi.org/10.25561/77482

FinancialMirror. (2020, September 12). *COVID19: Cyprus closes for Christmas*. https://www.financialmirror.com/2020/12/09/covid19-cyprus-closes-for-christmas/

Flahault, A., & Valleron, A. (1992). A method for assessing the global spread of HIV-1 infection based on air travel. *Mathematical Population Studies*, *3*(3), 161–171. https://doi.org/10.1080/08898489209525336

Flaxman, S., Mishra, S., Gandy, A., Unwin, H. J. T., Mellan, T. A., Coupland, H., Whittaker, C., Zhu, H., Berah, T., Eaton, J. W., Monod, M., Imperial College COVID-19 Response Team, Perez-Guzman, P. N., Schmit, N., Cilloni, L., Ainslie, K. E. C., Baguelin, M., Boonyasiri, A., Boyd, O., … Bhatt, S. (2020). Estimating the effects of non-pharmaceutical interventions on COVID-19 in Europe. *Nature*, *584*(7820), 257–261. https://doi.org/10.1038/s41586-020-2405-7

Folcik, V. A., An, G. C., & Orosz, C. G. (2007). The Basic Immune Simulator: An agent-based model to study the interactions between innate and adaptive immunity. *Theoretical Biology and Medical Modelling*, *4*(1), 39. https://doi.org/10.1186/1742-4682-4-39

Fremont, A. (2007). Global maritime networks. *Journal of Transport Geography*, *15*(6), 431–442. https://doi.org/10.1016/j.jtrangeo.2007.01.005

Frias-Martinez, E., Williamson, G., & Frias-Martinez, V. (2011). An Agent-Based Model of Epidemic Spread Using Human Mobility and Social Network Information. *2011 IEEE Third International Conference on Privacy, Security, Risk and Trust and 2011 IEEE Third International Conference on Social Computing*, 57–64. https://doi.org/10.1109/PASSAT/SocialCom.2011.142

Gallotti, R., & Barthelemy, M. (2014). Anatomy and efficiency of urban multimodal mobility. *Scientific Reports*, *4*(1), 6911. https://doi.org/10.1038/srep06911

Gallotti, R., & Barthelemy, M. (2015). The multilayer temporal network of public transport in Great Britain. *Scientific Data*, *2*(1), 140056. https://doi.org/10.1038/sdata.2014.56

GAMA Platform. (2025). gama-platform.github.io

Gan, W. X., & Amerudin, S. (2022). Agent-Based Model for Analyzing COVID-19 Infection in the Campus Using AnyLogic Software. In M. Ben Ahmed, A. A. Boudhir, İ. R. Karaș, V. Jain, & S. Mellouli (Eds.), *Innovations in Smart Cities Applications Volume 5* (Vol. 393, pp. 519–530). Springer International Publishing. https://doi.org/10.1007/978-3-030-94191-8_42

Garske, T., Yu, H., Peng, Z., Ye, M., Zhou, H., Cheng, X., Wu, J., & Ferguson, N. (2011). Travel patterns in China. *PloS One*, *6*(2), e16364. https://doi.org/10.1371/journal.pone.0016364

Gatrell, A. C., & Elliott, S. J. (2015). *Geographies of health: An introduction* (Third edition). John Wiley & Sons Inc.

Gattrell, A., & Loytonen, M. (Eds.). (1998). *GIS And Health: GISDATA 6* (0 ed.). CRC Press. https://doi.org/10.1201/9781482273090

Gaudou, B., Huynh, N. Q., Philippon, D., Brugière, A., Chapuis, K., Taillandier, P., Larmande, P., & Drogoul, A. (2020). COMOKIT: A Modeling Kit to Understand, Analyze, and Compare the Impacts of Mitigation Policies Against the COVID-19 Epidemic at the Scale of a City. *Frontiers in Public Health*, *8*, 563247. https://doi.org/10.3389/fpubh.2020.563247

Ghorpade, A., Pereira, F., Zhao, F., Zegras, C., & Ben-Akiva, M. (2015). *An integrated stop-mode detection algorithm for real world smartphone-based travel survey*.

Giannotti, F., Nanni, M., Pedreschi, D., Pinelli, F., Renso, C., Rinzivillo, S., & Trasarti, R. (2011). Unveiling the complexity of human mobility by querying and mining massive trajectory data. *The VLDB Journal*, *20*(5), 695–719. https://doi.org/10.1007/s00778-011-0244-8

Giuliani, D., Dickson, M. M., Espa, G., & Santi, F. (2020). Modelling and Predicting the Spatio-Temporal Spread of Coronavirus Disease 2019 (COVID-19) in Italy. *SSRN Electronic Journal*. https://doi.org/10.2139/ssrn.3559569

Glass, G. E., Schwartz, B. S., Morgan, J. M., Johnson, D. T., Noy, P. M., & Israel, E. (1995). Environmental risk factors for Lyme disease identified with geographic information systems. *American Journal of Public Health*, *85*(7), 944–948. https://doi.org/10.2105/AJPH.85.7.944

Gomez, J., Prieto, J., Leon, E., & Rodríguez, A. (2021). INFEKTA—An agent-based model for transmission of infectious diseases: The COVID-19 case in Bogotá, Colombia. *PLOS ONE*, *16*(2), e0245787. https://doi.org/10.1371/journal.pone.0245787

González, M. C., Hidalgo, C. A., & Barabási, A.-L. (2008). Understanding individual human mobility patterns. *Nature*, *453*(7196), 779–782. https://doi.org/10.1038/nature06958

Gountas, I., Quattrocchi, A., Mamais, I., Tsioutis, C., Christaki, E., Fokianos, K., & Nikolopoulos, G. (2021). Effect of public health interventions during the first epidemic wave of COVID-19 in Cyprus: A modelling study. *BMC Public Health*, *21*(1), 1898. https://doi.org/10.1186/s12889-021-11945-9

Grimm, V., Berger, U., DeAngelis, D. L., Polhill, J. G., Giske, J., & Railsback, S. F. (2010). The ODD protocol: A review and first update. *Ecological Modelling*, *221*(23), 2760–2768. https://doi.org/10.1016/j.ecolmodel.2010.08.019

Grimm, V., Railsback, S. F., Vincenot, C. E., Berger, U., Gallagher, C., DeAngelis, D. L., Edmonds, B., Ge, J., Giske, J., Groeneveld, J., Johnston, A. S. A., Milles, A., Nabe-Nielsen, J., Polhill, J. G., Radchuk, V., Rohwäder, M.-S., Stillman, R. A., Thiele, J. C., & Ayllón, D. (2020). The ODD Protocol for Describing Agent-Based and Other Simulation Models: A Second Update to Improve Clarity, Replication, and Structural Realism. *Journal of Artificial Societies and Social Simulation*, *23*(2), 7. https://doi.org/10.18564/jasss.4259

Hägerstraand, T. (1970). WHAT ABOUT PEOPLE IN REGIONAL SCIENCE? *Papers in Regional Science*, *24*(1), 7–21. https://doi.org/10.1111/j.1435-5597.1970.tb01464.x

Haklay, M., & Weber, P. (2008). OpenStreetMap: User-Generated Street Maps. *IEEE Pervasive Computing*, *7*(4), 12–18. https://doi.org/10.1109/MPRV.2008.80

Han, E., Tan, M. M. J., Turk, E., Sridhar, D., Leung, G. M., Shibuya, K., Asgari, N., Oh, J., García-Basteiro, A. L., Hanefeld, J., Cook, A. R., Hsu, L. Y., Teo, Y. Y., Heymann, D., Clark, H., McKee, M., & Legido-Quigley, H. (2020). Lessons learnt from easing COVID-19 restrictions: An analysis of countries and regions in Asia Pacific and Europe. *The Lancet*, *396*(10261), 1525–1534. https://doi.org/10.1016/S0140-6736(20)32007-9

Hanski, I. (1998). Metapopulation dynamics. *Nature*, *396*(6706), 41–49. https://doi.org/10.1038/23876

Hanson, S. (2005). Perspectives on the geographic stability and mobility of people in cities. *Proceedings of the National Academy of Sciences*, *102*(43), 15301–15306. https://doi.org/10.1073/pnas.0507309102

Hanson, S., & Huff, O. J. (1988). Systematic variability in repetitious travel. *Transportation*, *15*(1–2). https://doi.org/10.1007/BF00167983

Harris, C. (2021, November 17). COVID vaccine: Who in Europe is leading the race to herd immunity? *Euronews*. https://www.euronews.com/2021/11/17/covid-19-vaccinations-in-europe-which-countries-are-leading-the-way

Hasan, S., Zhan, X., & Ukkusuri, S. V. (2013). Understanding urban human activity and mobility patterns using large-scale location-based data from online social media. *Proceedings of the 2nd ACM SIGKDD International Workshop on Urban Computing*, 1–8. https://doi.org/10.1145/2505821.2505823

Hauser, A., Counotte, M. J., Margossian, C. C., Konstantinoudis, G., Low, N., Althaus, C. L., & Riou, J. (2020). Estimation of SARS-CoV-2 mortality during the early stages of an epidemic: A modeling study in Hubei, China, and six regions in Europe. *PLOS Medicine*, *17*(7), e1003189. https://doi.org/10.1371/journal.pmed.1003189

Hawelka, B., Sitko, I., Beinat, E., Sobolevsky, S., Kazakopoulos, P., & Ratti, C. (2014). Geo-located Twitter as proxy for global mobility patterns. *Cartography and Geographic Information Science*, *41*(3), 260–271. https://doi.org/10.1080/15230406.2014.890072

Heckbert, S., Baynes, T., & Reeson, A. (2010). Agent-based modeling in ecological economics: Agent-based modeling in ecological economics. *Annals of the New York Academy of Sciences*, *1185*(1), 39–53. https://doi.org/10.1111/j.1749-6632.2009.05286.x

Helbing, D., Farkas, I. J., Molnar, P., & Vicsek, T. (2002). Simulation of Pedestrian Crowds in Normal and Evacuation Situations. In M. Schreckenberg & S. D. Sharma (Eds.), *Pedestrian and Evacuation Dynamics* (pp. 21–58). Springer.

Helbing, D., & Johansson, A. (2009). Pedestrian, Crowd and Evacuation Dynamics. In R. A. Meyers (Ed.), *Encyclopedia of Complexity and Systems Science* (Vol. 7, pp. 6476–6495). Springer. https://doi.org/10.1007/978-0-387-30440-3_382

Helbing, D., Johansson, A., Mathiesen, J., Jensen, M. H., & Hansen, A. (2006). Analytical Approach to Continuous and Intermittent Bottleneck Flows. *Physical Review Letters*, *97*(16), 168001. https://doi.org/10.1103/PhysRevLett.97.168001

Helbing, D., & Molnár, P. (1995). Social force model for pedestrian dynamics. *Physical Review E*, *51*(5), 4282–4286. https://doi.org/10.1103/PhysRevE.51.4282

Hethcote, H. W. (1989). Three Basic Epidemiological Models. In S. A. Levin, T. G. Hallam, & L. J. Gross (Eds.), *Applied Mathematical Ecology* (Vol. 18, pp. 119–144). Springer Berlin Heidelberg. https://doi.org/10.1007/978-3-642-61317-3_5

Hethcote, H. W. (2000). The Mathematics of Infectious Diseases. *SIAM Review*, *42*(4), 599–653. https://doi.org/10.1137/S0036144500371907

Hinch, R., Probert, W. J. M., Nurtay, A., Kendall, M., Wymant, C., Hall, M., Lythgoe, K., Bulas Cruz, A., Zhao, L., Stewart, A., Ferretti, L., Montero, D., Warren, J., Mather, N., Abueg, M., Wu, N., Legat, O., Bentley, K., Mead, T., … Fraser, C. (2021). OpenABM-Covid19—An agent-based model for non-pharmaceutical interventions against COVID-19 including contact tracing. *PLOS Computational Biology*, *17*(7), e1009146. https://doi.org/10.1371/journal.pcbi.1009146

Holme, P. (2003). CONGESTION AND CENTRALITY IN TRAFFIC FLOW ON COMPLEX NETWORKS. *Advances in Complex Systems*, *06*(02), 163–176. https://doi.org/10.1142/S0219525903000803

Hossmann, T., Spyropoulos, T., & Legendre, F. (2011). A complex network analysis of human mobility. *2011 IEEE Conference on Computer Communications Workshops (INFOCOM WKSHPS)*, 876–881. https://doi.org/10.1109/INFCOMW.2011.5928936
Huang, Z., & Tatem, A. J. (2013). Global malaria connectivity through air travel. *Malaria Journal*, *12*(1), 269. https://doi.org/10.1186/1475-2875-12-269
Hufnagel, L., Brockmann, D., & Geisel, T. (2004). Forecast and control of epidemics in a globalized world. *Proceedings of the National Academy of Sciences*, *101*(42), 15124–15129. https://doi.org/10.1073/pnas.0308344101
Hunecke, M. (2009). *ADD HOME. Mobility Management for housing areas—From car-dependency to free choice*. https://trimis.ec.europa.eu/project/mobility-management-housing-areas-car-dependency-free-choice
Hunt, C. A., Kennedy, R. C., Kim, S. H. J., & Ropella, G. E. P. (2013). Agent-based modeling: A systematic assessment of use cases and requirements for enhancing pharmaceutical research and development productivity. *WIREs Systems Biology and Medicine*, *5*(4), 461–480. https://doi.org/10.1002/wsbm.1222
Hunter, E., Mac Namee, B., & Kelleher, J. D. (2017). A Taxonomy for Agent-Based Models in Human Infectious Disease Epidemiology. *Journal of Artificial Societies and Social Simulation*, *20*(3), 2. https://doi.org/10.18564/jasss.3414
Hunter, T., Moldovan, T., Zaharia, M., Merzgui, S., Ma, J., Franklin, M. J., Abbeel, P., & Bayen, A. M. (2011). Scaling the mobile millennium system in the cloud. *Proceedings of the 2nd ACM Symposium on Cloud Computing*, 1–8. https://doi.org/10.1145/2038916.2038944
Isaia, P., Laoudias, C., Kamilaris, A., & Panayiotou, C. G. (2021). CovTracer-EN: The Journey of Covid-19 Digital Contact Tracing in Cyprus. *2021 International Conference on Indoor Positioning and Indoor Navigation (IPIN)*, 1–8. https://doi.org/10.1109/IPIN51156.2021.9662621
Jack, K., & Holt, M. (2008). Community profiling as part of a health needs assessment. *Nursing Standard*, *22*(18), 51–56. https://doi.org/10.7748/ns2008.01.22.18.51.c6311
Jalayer, M., Orsenigo, C., & Vercellis, C. (2020). *CoV-ABM: A stochastic discrete-event agent-based framework to simulate spatiotemporal dynamics of COVID-19*. https://arxiv.org/abs/2007.13231
Jennings, N. R. (2000). On agent-based software engineering. *Artificial Intelligence*, *117*(2), 277–296. https://doi.org/10.1016/S0004-3702(99)00107-1
Jia, T., Jiang, B., Carling, K., Bolin, M., & Ban, Y. (2012). An empirical study on human mobility and its agent-based modeling. *Journal of Statistical Mechanics: Theory and Experiment*, *2012*(11), P11024. https://doi.org/10.1088/1742-5468/2012/11/P11024
Johansson, A., Batty, M., Hayashi, K., Al Bar, O., Marcozzi, D., & Memish, Z. A. (2012). Crowd and environmental management during mass gatherings. *The Lancet Infectious Diseases*, *12*(2), 150–156. https://doi.org/10.1016/S1473-3099(11)70287-0
Johns Hopkins. (n.d.). *Coronavirus COVID-19 Global Cases dashboard*. Retrieved 15 March 2024, from https://gisanddata.maps.arcgis.com/apps/dashboards/bda7594740fd40299423467b48e9ecf6
Jones, K. E., Patel, N. G., Levy, M. A., Storeygard, A., Balk, D., Gittleman, J. L., & Daszak, P. (2008). Global trends in emerging infectious diseases. *Nature*, *451*(7181), 990–993. https://doi.org/10.1038/nature06536
Jovanović, A., Klimek, P., Renn, O., Schneider, R., Øien, K., Brown, J., DiGennaro, M., Liu, Y., Pfau, V., Jelić, M., Rosen, T., Caillard, B., Chakravarty, S., & Chhantyal, P. (2020). Assessing resilience of healthcare infrastructure exposed to COVID-19: Emerging risks, resilience indicators, interdependencies and international standards. *Environment Systems and Decisions*, *40*(2), 252–286. https://doi.org/10.1007/s10669-020-09779-8

Karamshuk, D., Boldrini, C., Conti, M., & Passarella, A. (2011). Human mobility models for opportunistic networks. *IEEE Communications Magazine*, *49*(12), 157–165. https://doi.org/10.1109/MCOM.2011.6094021

Kazmi, S. J. H., & Usery, E. L. (2001). Application of remote sensing and gis for the monitoring of diseases: A unique research agenda for geographers. *Remote Sensing Reviews*, *20*(1), 45–70. https://doi.org/10.1080/02757250109532427

Kermack, W., & McKendrick, A. G. (1927). A contribution to the mathematical theory of epidemics. *Proceedings of the Royal Society of London. Series A, Containing Papers of a Mathematical and Physical Character*, *115*(772), 700–721. https://doi.org/10.1098/rspa.1927.0118

Kerr, C. C., Stuart, R. M., Mistry, D., Abeysuriya, R. G., Rosenfeld, K., Hart, G. R., Núñez, R. C., Cohen, J. A., Selvaraj, P., Hagedorn, B., George, L., Jastrzębski, M., Izzo, A. S., Fowler, G., Palmer, A., Delport, D., Scott, N., Kelly, S. L., Bennette, C. S., … Klein, D. J. (2021). Covasim: An agent-based model of COVID-19 dynamics and interventions. *PLOS Computational Biology*, *17*(7), e1009149. https://doi.org/10.1371/journal.pcbi.1009149

Khashoggi, B. F., & Murad, A. (2020). Issues of Healthcare Planning and GIS: A Review. *ISPRS International Journal of Geo-Information*, *9*(6), 352. https://doi.org/10.3390/ijgi9060352

Kifle, Z. S., & Obsu, L. L. (2022). Mathematical modeling for COVID-19 transmission dynamics: A case study in Ethiopia. *Results in Physics*, *34*, 105191. https://doi.org/10.1016/j.rinp.2022.105191

Kim, Y., & Cho, N. (2022). A Simulation Study on Spread of Disease and Control Measures in Closed Population Using ABM. *Computation*, *10*(1), 2. https://doi.org/10.3390/computation10010002

KIOS CoE. (2020, July 5). *KIOS researchers step-up to support the fight against COVID-19*. https://www.kios.ucy.ac.cy/kios-researchers-step-up-to-support-the-fight-against-covid-19

KIOS CoE COVID-19 Cyprus Cases Dashboard. (2021). https://covid19.ucy.ac.cy

Kistemann, T., Dangendorf, F., & Schweikart, J. (2002). New perspectives on the use of Geographical Information Systems (GIS) in environmental health sciences. *International Journal of Hygiene and Environmental Health*, *205*(3), 169–181. https://doi.org/10.1078/1438-4639-00145

Kitamura, R., Chen, C., Pendyala, R. M., & Narayanan, R. (2000). Micro-simulation of daily activity-travel patterns for travel demand forecasting. *Transportation*, *27*(1), 25–51. https://doi.org/10.1023/A:1005259324588

Kivela, M., Arenas, A., Barthelemy, M., Gleeson, J. P., Moreno, Y., & Porter, M. A. (2014). Multilayer networks. *Journal of Complex Networks*, *2*(3), 203–271. https://doi.org/10.1093/comnet/cnu016

Kleinberg, J. (2007). The wireless epidemic. *Nature*, *449*(7160), 287–288. https://doi.org/10.1038/449287a

Koch, T. (2005). Mapping the Miasma: Air, Health, and Place in Early Medical Mapping. *Cartographic Perspectives*, (52), 4–27. https://doi.org/10.14714/CP52.376

Kölbl, R., & Helbing, D. (2003). Energy laws in human travel behaviour. *New Journal of Physics*, *5*, 48–48. https://doi.org/10.1088/1367-2630/5/1/348

Kong, L., Duan, M., Shi, J., Hong, J., Chang, Z., & Zhang, Z. (2022). Compartmental structures used in modeling COVID-19: A scoping review. *Infectious Diseases of Poverty*, *11*(1), 72. https://doi.org/10.1186/s40249-022-01001-y

Krieger, N. (2003). Place, Space, and Health: GIS and Epidemiology: *Epidemiology*, *14*(4), 384–385. https://doi.org/10.1097/01.ede.0000071473.69307.8a

Kuhn, J. R., Courtney, J. F., Morris, B., & Tatara, E. R. (2010). Agent-based analysis and simulation of the consumer airline market share for Frontier Airlines. *Knowledge-Based Systems*, *23*(8), 875–882. https://doi.org/10.1016/j.knosys.2010.06.002

Kuupiel, D., Adu, K. M., Bawontuo, V., Adogboba, D. A., Drain, P. K., Moshabela, M., & Mashamba-Thompson, T. P. (2020). Geographical Accessibility to Glucose-6-Phosphate Dioxygenase Deficiency Point-of-Care Testing for Antenatal Care in Ghana. *Diagnostics*, *10*(4), 229. https://doi.org/10.3390/diagnostics10040229

Kyriakidis, P., Kavroudakis, D., Fayad, P., Hadjipetrou, S., Leventis, G., & Papakonstantinou, A. (2021). Promoting the adoption of agent-based modelling for synergistic interventions and decision-making during pandemic outbreaks. *AGILE: GIScience Series*, *2*, 1–5. https://doi.org/10.5194/agile-giss-2-44-2021

Lawson, A. (Ed.). (1999). *Disease mapping and risk assessment for public health*. Wiley.

Lawson, A. B., Biggeri, A. B., Boehning, D., Lesaffre, E., Viel, J. F., Clark, A., Schlattmann, P., & Divino, F. (2000). Disease mapping models: An empirical evaluation. Disease Mapping Collaborative Group. *Statistics in Medicine*, *19*(17–18), 2217–2241. https://doi.org/10.1002/1097-0258(20000915/30)19:17/18<2217::aid-sim565>3.0.co;2-e

Lawyer, G. (2015). Measuring the potential of individual airports for pandemic spread over the world airline network. *BMC Infectious Diseases*, *16*(1), 70. https://doi.org/10.1186/s12879-016-1350-4

Lee, B. Y., Brown, S. T., Cooley, P., Potter, M. A., Wheaton, W. D., Voorhees, R. E., Stebbins, S., Grefenstette, J. J., Zimmer, S. M., Zimmerman, R. K., Assi, T.-M., Bailey, R. R., Wagener, D. K., & Burke, D. S. (2010). Simulating School Closure Strategies to Mitigate an Influenza Epidemic. *Journal of Public Health Management and Practice*, *16*(3), 252–261. https://doi.org/10.1097/PHH.0b013e3181ce594e

Lee, L. M., Teutsch, S. M., Thacker, S. B., & St Louis, M. E. (Eds.). (2010). *Principles & practice of public health surveillance* (Third edition). Oxford University Press.

Lessani, M. N., Li, Z., Jing, F., Qiao, S., Zhang, J., Olatosi, B., & Li, X. (2023). Human mobility and the infectious disease transmission: A systematic review. *Geo-Spatial Information Science*, 1–28. https://doi.org/10.1080/10095020.2023.2275619

Levinson, D., & Wu, Y. (2005). The rational locator reexamined: Are travel times still stable? *Transportation*, *32*(2), 187–202. https://doi.org/10.1007/s11116-004-5507-4

Leyk, S., Binder, C. R., & Nuckols, J. R. (2009). Spatial modeling of personalized exposure dynamics: The case of pesticide use in small-scale agricultural production landscapes of the developing world. *International Journal of Health Geographics*, *8*(1), 17. https://doi.org/10.1186/1476-072X-8-17

Liang, X., Zhao, J., Dong, L., & Xu, K. (2013). Unraveling the origin of exponential law in intra-urban human mobility. *Scientific Reports*, *3*(1), 2983. https://doi.org/10.1038/srep02983

Lin, K., Kansal, A., Lymberopoulos, D., & Zhao, F. (2010). Energy-accuracy trade-off for continuous mobile device location. *Proceedings of the 8th International Conference on Mobile Systems, Applications, and Services*, 285–298. https://doi.org/10.1145/1814433.1814462

Linard, C., Ponçon, N., Fontenille, D., & Lambin, E. F. (2009). A multi-agent simulation to assess the risk of malaria re-emergence in southern France. *Ecological Modelling*, *220*(2), 160–174. https://doi.org/10.1016/j.ecolmodel.2008.09.001

Liu, P., Beeler, P., & Chakrabarty, R. K. (2020). *COVID-19 Progression Timeline and Effectiveness of Response-to-Spread Interventions across the United States* [Preprint]. Infectious Diseases (except HIV/AIDS). https://doi.org/10.1101/2020.03.17.20037770

Loraamm, R. W. (2020). Incorporating behavior into animal movement modeling: A constrained agent-based model for estimating visit probabilities in space-time prisms. *International Journal of Geographical Information Science*, *34*(8), 1607–1627. https://doi.org/10.1080/13658816.2019.1658875

Lorig, F., Johansson, E., & Davidsson, P. (2021). Agent-Based Social Simulation of the Covid-19 Pandemic: A Systematic Review. *Journal of Artificial Societies and Social Simulation*, *24*(3), 5. https://doi.org/10.18564/jasss.4601

Lytras, T., & Tsiodras, S. (2021). Lockdowns and the COVID-19 pandemic: What is the endgame? *Scandinavian Journal of Public Health*, *49*(1), 37–40. https://doi.org/10.1177/1403494820961293

Macal, C., & North, M. (2014). Introductory tutorial: Agent-based modeling and simulation. *Proceedings of the Winter Simulation Conference 2014*, 6–20. https://doi.org/10.1109/WSC.2014.7019874

Malleson, N., Heppenstall, A., See, L., & Evans, A. (2013). Using an Agent-Based Crime Simulation to Predict the Effects of Urban Regeneration on Individual Household Burglary Risk. *Environment and Planning B: Planning and Design*, *40*(3), 405–426. https://doi.org/10.1068/b38057

Malone, J. B., Bergquist, N. R., Huh, O. K., Bavia, M. E., Bernardi, M., El Bahy, M. M., Fuentes, M. V., Kristensen, T. K., McCarroll, J. C., Yilma, J. M., & Zhou, X. N. (2001). A global network for the control of snail-borne disease using satellite surveillance and geographic information systems. *Acta Tropica*, *79*(1), 7–12. https://doi.org/10.1016/S0001-706X(01)00098-5

Mandyata, C. B., Olowski, L. K., & Mutale, W. (2017). Challenges of implementing the integrated disease surveillance and response strategy in Zambia: A health worker perspective. *BMC Public Health*, *17*(1), 746. https://doi.org/10.1186/s12889-017-4791-9

Mao, L. (2014). Modeling triple-diffusions of infectious diseases, information, and preventive behaviors through a metropolitan social network—An agent-based simulation. *Applied Geography*, *50*, 31–39. https://doi.org/10.1016/j.apgeog.2014.02.005

Marchetti, C. (1994). Anthropological invariants in travel behavior. *Technological Forecasting and Social Change*, *47*(1), 75–88. https://doi.org/10.1016/0040-1625(94)90041-8

Mehdizadeh, M., Nordfjaern, T., & Klöckner, C. A. (2022). A systematic review of the agent-based modelling/simulation paradigm in mobility transition. *Technological Forecasting and Social Change*, *184*, 122011. https://doi.org/10.1016/j.techfore.2022.122011

Merler, S., Ajelli, M., Fumanelli, L., Gomes, M. F. C., Piontti, A. P. y, Rossi, L., Chao, D. L., Longini, I. M., Halloran, M. E., & Vespignani, A. (2015). Spatiotemporal spread of the 2014 outbreak of Ebola virus disease in Liberia and the effectiveness of non-pharmaceutical interventions: A computational modelling analysis. *The Lancet Infectious Diseases*, *15*(2), 204–211. https://doi.org/10.1016/S1473-3099(14)71074-6

Merler, S., Ajelli, M., Fumanelli, L., & Vespignani, A. (2013). Containing the accidental laboratory escape of potential pandemic influenza viruses. *BMC Medicine*, *11*(1), 252. https://doi.org/10.1186/1741-7015-11-252

Mills, G. S., & Neuhauser, K. S. (1999). Statistical Evaluation of Population Data for Calculation of Radioactive Material Transport Accident Risks. *Risk Analysis*, *19*(4), 613–619. https://doi.org/10.1111/j.1539-6924.1999.tb00432.x

Moein, S., Nickaeen, N., Roointan, A., Borhani, N., Heidary, Z., Javanmard, S. H., Ghaisari, J., & Gheisari, Y. (2021). Inefficiency of SIR models in forecasting COVID-19 epidemic: A case study of Isfahan. *Scientific Reports*, *11*(1), 4725. https://doi.org/10.1038/s41598-021-84055-6

Mohamed K., E. M., Come, E., Oukhellou, L., & Verleysen, M. (2017). Clustering Smart Card Data for Urban Mobility Analysis. *IEEE Transactions on Intelligent Transportation Systems*, *18*(3), 712–728. https://doi.org/10.1109/TITS.2016.2600515

Mollalo, A., Vahedi, B., & Rivera, K. M. (2020). GIS-based spatial modeling of COVID-19 incidence rate in the continental United States. *Science of The Total Environment*, *728*, 138884. https://doi.org/10.1016/j.scitotenv.2020.138884

Narassima, M. S., Jammy, G. R., Pant, R., Choudhury, L., Aadharsh, R., Yeldandi, V., Anbuudayasankar, S. P., Rangasami, R., & John, D. (2020). *An Agent Based Model for assessing spread and health systems burden for COVID-19 using a synthetic population in Rangareddy district, Telangana state, India*. https://doi.org/10.1101/2020.06.04.20121848

NetLogo software. (2025). https://www.netlogo.org

Nicolaides, C., Cueto-Felgueroso, L., González, M. C., & Juanes, R. (2012). A Metric of Influential Spreading during Contagion Dynamics through the Air Transportation Network. *PLoS ONE*, *7*(7), e40961. https://doi.org/10.1371/journal.pone.0040961

Nieves, J. J., Bondarenko, M., Sorichetta, A., Steele, J. E., Kerr, D., Carioli, A., Stevens, F. R., Gaughan, A. E., & Tatem, A. J. (2020). Predicting Near-Future Built-Settlement Expansion Using Relative Changes in Small Area Populations. *Remote Sensing*, *12*(10), 1545. https://doi.org/10.3390/rs12101545

North, M. J., Macal, C. M., Aubin, J. St., Thimmapuram, P., Bragen, M., Hahn, J., Karr, J., Brigham, N., Lacy, M. E., & Hampton, D. (2010). Multiscale agent-based consumer market modeling. *Complexity*, *15*(5), 37–47. https://doi.org/10.1002/cplx.20304

Noulas, A., Scellato, S., Lathia, N., & Mascolo, C. (2012). Mining User Mobility Features for Next Place Prediction in Location-Based Services. *2012 IEEE 12th International Conference on Data Mining*, 1038–1043. https://doi.org/10.1109/ICDM.2012.113

Novakovic, A., & Marshall, A. H. (2022). The CP-ABM approach for modelling COVID-19 infection dynamics and quantifying the effects of non-pharmaceutical interventions. *Pattern Recognition*, *130*, 108790. https://doi.org/10.1016/j.patcog.2022.108790

Nykiforuk, C. I. J., & Flaman, L. M. (2011). Geographic Information Systems (GIS) for Health Promotion and Public Health: A Review. *Health Promotion Practice*, *12*(1), 63–73. https://doi.org/10.1177/1524839909334624

Obrien, A. (2022). *Infrastructure Solutions: How to make public transport attractive* (Infrastructure Solutions). European Investment bank.

O.D.D. description of the COMOKIT model. (2020, June 22). https://comokit.org/ressources/ODD-COMOKIT_v1.0.1.pdf

OECD & European Observatory on Health Systems and Policies (Eds.). (2023). *Cyprus: Country Health Profile 2023*. OECD Publishing. https://doi.org/10.1787/43898784-en

Olsen, J., & Jepsen, M. R. (2010). Human papillomavirus transmission and cost-effectiveness of introducing quadrivalent HPV vaccination in Denmark. *International Journal of Technology Assessment in Health Care*, *26*(2), 183–191. https://doi.org/10.1017/S0266462310000085

Ölvingson, C., Hallberg, J., Timpka, T., & Lindqvist, K. (2002). Ethical issues in public health informatics: Implications for system design when sharing geographic information. *Journal of Biomedical Informatics*, *35*(3), 178–185. https://doi.org/10.1016/S1532-0464(02)00527-0

Ozik, J., Wozniak, J. M., Collier, N., Macal, C. M., & Binois, M. (2021). A population data-driven workflow for COVID-19 modeling and learning. *The International Journal of High Performance Computing Applications*, *35*(5), 483–499. https://doi.org/10.1177/10943420211035164

Paez, A., Lopez, F. A., Menezes, T., Cavalcanti, R., & Pitta, M. G. D. R. (2021). A Spatio-Temporal Analysis of the Environmental Correlates of COVID-19 Incidence in Spain. *Geographical Analysis*, *53*(3), 397–421. https://doi.org/10.1111/gean.12241

Palmer, J. R. B., Espenshade, T. J., Bartumeus, F., Chung, C. Y., Ozgencil, N. E., & Li, K. (2013). New Approaches to Human Mobility: Using Mobile Phones for Demographic Research. *Demography*, *50*(3), 1105–1128. https://doi.org/10.1007/s13524-012-0175-z

Pappalardo, L., Simini, F., Rinzivillo, S., Pedreschi, D., Giannotti, F., & Barabási, A.-L. (2015). Returners and explorers dichotomy in human mobility. *Nature Communications*, *6*(1), 8166. https://doi.org/10.1038/ncomms9166

Perez, L., & Dragicevic, S. (2009). An agent-based approach for modeling dynamics of contagious disease spread. *International Journal of Health Geographics*, *8*(1), 50. https://doi.org/10.1186/1476-072X-8-50

Pergantas, P., Tsatsaris, A., Malesios, C., Kriparakou, G., Demiris, N., & Tselentis, Y. (2017). A spatial predictive model for malaria resurgence in central Greece integrating entomological, environmental and social data. *PLOS ONE*, *12*(6), e0178836. https://doi.org/10.1371/journal.pone.0178836

Pickle, L. W. (2002). Spatial Analysis of Disease. In C. Beam (Ed.), *Biostatistical Applications in Cancer Research* (Vol. 113, pp. 113–150). Springer US. https://doi.org/10.1007/978-1-4757-3571-0_7

Pillai, A. N., Toh, K. B., Perdomo, D., Bhargava, S., Stoltzfus, A., Longini, I. M., Pearson, C. A. B., & Hladish, T. J. (2024). Agent-based modeling of the COVID-19 pandemic in Florida. *Epidemics*, *47*, 100774. https://doi.org/10.1016/j.epidem.2024.100774

Plescia, M., Koontz, S., & Laurent, S. (2001). Community assessment in a vertically integrated health care system. *American Journal of Public Health*, *91*(5), 811–814. https://doi.org/10.2105/ajph.91.5.811

Rakowski, F., Gruziel, M., Bieniasz-Krzywiec, Ł., & Radomski, J. P. (2010). Influenza epidemic spread simulation for Poland—A large scale, individual based model study. *Physica A: Statistical Mechanics and Its Applications*, *389*(16), 3149–3165. https://doi.org/10.1016/j.physa.2010.04.029

Ravenstein, E. G. (1885). The Laws of Migration. *Journal of the Statistical Society of London*, *48*(2), 167. https://doi.org/10.2307/2979181

Ravenstein, E. G. (1889). The Laws of Migration. *Journal of the Royal Statistical Society*, *52*(2), 241. https://doi.org/10.2307/2979333

Reuters. (2020, February 28). *Cyprus to shut checkpoints for first time since 2003 over coronavirus*. https://www.reuters.com/article/us-china-health-cyprus-checkpoints-idUSKCN20M1T6/

Rhee, I., Shin, M., Hong, S., Lee, K., & Chong, S. (2008). On the Levy-Walk Nature of Human Mobility. *IEEE INFOCOM 2008 - The 27th Conference on Computer Communications*, 924–932. https://doi.org/10.1109/INFOCOM.2008.145

Rhee, I., Shin, M., Hong, S., Lee, K., Kim, S. J., & Chong, S. (2011). On the Levy-Walk Nature of Human Mobility. *IEEE/ACM Transactions on Networking*, *19*(3), 630–643. https://doi.org/10.1109/TNET.2011.2120618

Roberts, D. R., Washino, R. K., Dister, S. W., Beck, L. R., Ulloa, A., Hacker, C., Rodriguez, A. D., Rodriguez, M. H., Paris, J. F., Spanner, M. A., Meza, R. A., Legters, L. J., & Rejmankova, E. (1994). Remote Sensing as a Landscape Epidemiologic Tool to Identify Villages at High Risk for Malaria Transmission. *The American Journal of Tropical Medicine and Hygiene*, *51*(3), 271–280. https://doi.org/10.4269/ajtmh.1994.51.271

Rost, M., Barkhuus, L., Cramer, H., & Brown, B. (2013). Representation and communication: Challenges in interpreting large social media datasets. *Proceedings of the 2013*

Conference on Computer Supported Cooperative Work, 357–362. https://doi.org/10.1145/2441776.2441817
Rowland, T. W. (1998). The biological basis of physical activity. *Medicine &amp Science in Sports &amp Exercise*, *30*(3), 392–399. https://doi.org/10.1097/00005768-199803000-00009
Sadiq, F. I., Selamat, A., & Ibrahim, R. (2015). Human Activity Recognition Prediction for Crowd Disaster Mitigation. In N. T. Nguyen, B. Trawiński, & R. Kosala (Eds.), *Intelligent Information and Database Systems* (Vol. 9011, pp. 200–210). Springer International Publishing. https://doi.org/10.1007/978-3-319-15702-3_20
Schauer, L., Werner, M., & Marcus, P. (2014). Estimating Crowd Densities and Pedestrian Flows Using Wi-Fi and Bluetooth. *Proceedings of the 11th International Conference on Mobile and Ubiquitous Systems: Computing, Networking and Services*. 11th International Conference on Mobile and Ubiquitous Systems: Computing, Networking and Services, London, Great Britain. https://doi.org/10.4108/icst.mobiquitous.2014.257870
Schlich, R., & Axhausen, K. W. (2003). Habitual travel behaviour: Evidence from a six-week travel diary. *Transportation*, *30*(1), 13–36. https://doi.org/10.1023/A:1021230507071
Schneider, C. M., Belik, V., Couronné, T., Smoreda, Z., & González, M. C. (2013). Unravelling daily human mobility motifs. *Journal of The Royal Society Interface*, *10*(84), 20130246. https://doi.org/10.1098/rsif.2013.0246
Scholten, H. J., & de Lepper, M. J. (1991). The benefits of the application of geographical information systems in public and environmental health. *World Health Statistics Quarterly. Rapport Trimestriel De Statistiques Sanitaires Mondiales*, *44*(3), 160–170.
Shastry, V., Reeves, D. C., Willems, N., & Rai, V. (2022). Policy and behavioral response to shock events: An agent-based model of the effectiveness and equity of policy design features. *PLOS ONE*, *17*(1), e0262172. https://doi.org/10.1371/journal.pone.0262172
Silva, P. C. L., Batista, P. V. C., Lima, H. S., Alves, M. A., Guimarães, F. G., & Silva, R. C. P. (2020). COVID-ABS: An agent-based model of COVID-19 epidemic to simulate health and economic effects of social distancing interventions. *Chaos, Solitons & Fractals*, *139*, 110088. https://doi.org/10.1016/j.chaos.2020.110088
Simini, F., González, M. C., Maritan, A., & Barabási, A.-L. (2012). A universal model for mobility and migration patterns. *Nature*, *484*(7392), 96–100. https://doi.org/10.1038/nature10856
Simoes, J. (2006). *Modeling a Mumps Outbreak through Spatially Explicit Agents*. https://api.semanticscholar.org/CorpusID:21005890
Simon, P. M., Esser, J., & Nagel, K. (1999). SIMPLE QUEUEING MODEL APPLIED TO THE CITY OF PORTLAND. *International Journal of Modern Physics C*, *10*(05), 941–960. https://doi.org/10.1142/S0129183199000747
Skvortsov, A., Connell, R. B., Dawson, P., & Gailis, R. (2007). Epidemic modelling: Validation of agent-based simulation by using simple mathematical models. *Proceedings of Land Warfare Conference*, *2007*, 221–227.
Smith, E. R., & Conrey, F. R. (2007). Agent-Based Modeling: A New Approach for Theory Building in Social Psychology. *Personality and Social Psychology Review*, *11*(1), 87–104. https://doi.org/10.1177/1088868306294789
Snow, J. (1855). *On the mode of communication of cholera* [Map]. John Churchill. https://archive.org/details/b28985266/page/n57/mode/2up. https://archive.org/details/b28985266/page/n57/mode/2up
Solmaz, G., & Turgut, D. (2015). Pedestrian mobility in theme park disasters. *IEEE Communications Magazine*, *53*(7), 172–177. https://doi.org/10.1109/MCOM.2015.7158282
Solmaz, G., & Turgut, D. (2019). A Survey of Human Mobility Models. *IEEE Access*, *7*, 125711–125731. https://doi.org/10.1109/ACCESS.2019.2939203

Staffini, A., Svensson, A. K., Chung, U.-I., & Svensson, T. (2021). An Agent-Based Model of the Local Spread of SARS-CoV-2: Modeling Study. *JMIR Medical Informatics*, *9*(4), e24192. https://doi.org/10.2196/24192

Statistical service of the Republic of Cyprus. (2010). *Short distance passenger mobility survey* [Dataset]. https://library.cystat.gov.cy/Documents/Publication/PASSENGER_MOBILITY_SURVEY09-120810.pdf

Statistical service of the Republic of Cyprus. (2019). *Census of Population and Housing* [Dataset]. https://cystatdb.cystat.gov.cy/pxweb/en.

Stevens, F. R., Gaughan, A. E., Linard, C., & Tatem, A. J. (2015). Disaggregating Census Data for Population Mapping Using Random Forests with Remotely-Sensed and Ancillary Data. *PLOS ONE*, *10*(2), e0107042. https://doi.org/10.1371/journal.pone.0107042

Stopher, P. R., & Greaves, S. P. (2007). Household travel surveys: Where are we going? *Transportation Research Part A: Policy and Practice*, *41*(5), 367–381. https://doi.org/10.1016/j.tra.2006.09.005

Stouffer, S. A. (1940). Intervening Opportunities: A Theory Relating Mobility and Distance. *American Sociological Review*, *5*(6), 845. https://doi.org/10.2307/2084520

Sun, L., Axhausen, K. W., Lee, D.-H., & Huang, X. (2013). Understanding metropolitan patterns of daily encounters. *Proceedings of the National Academy of Sciences*, *110*(34), 13774–13779. https://doi.org/10.1073/pnas.1306440110

Suryawanshi, G., Madhavan, V., Mitra, A., & Chakrabarti, P. P. (2021). *City-scale Simulation of Covid-19 Pandemic and Intervention Policies using Agent-based Modelling*. https://arxiv.org/abs/2104.01650

Taghizadeh, E., & Mohammad-Djafari, A. (2022). SEIR Modeling, Simulation, Parameter Estimation, and Their Application for COVID-19 Epidemic Prediction. *MaxEnt 2022*, 18. https://doi.org/10.3390/psf2022005018

Testa, J., Mock, K., Taylor, C., Koyuk, H., Coyle, J., & Waggoner, R. (2012). Agent-based modeling of the dynamics of mammal-eating killer whales and their prey. *Marine Ecology Progress Series*, *466*, 275–291. https://doi.org/10.3354/meps09845

The CovTracer—Exposure Notification App. (2021). https://covtracer.dmrid.gov.cy

The Repast Suite. (2025). https://repast.github.io/

The WHO COVID19 dashboard. (2021). https://covid19.who.int

Thomopoulos, V., & Tsichlas, K. (2024). An Agent-Based Model for Disease Epidemics in Greece. *Information*, *15*(3), 150. https://doi.org/10.3390/info15030150

Tian, Y., Osgood, N. D., Al-Azem, A., & Hoeppner, V. H. (2013). Evaluating the Effectiveness of Contact Tracing on Tuberculosis Outcomes in Saskatchewan Using Individual-Based Modeling. *Health Education & Behavior*, *40*(1_suppl), 98S-110S. https://doi.org/10.1177/1090198113493910

Tizzoni, M., Bajardi, P., Decuyper, A., Kon Kam King, G., Schneider, C. M., Blondel, V., Smoreda, Z., González, M. C., & Colizza, V. (2014). On the use of human mobility proxies for modeling epidemics. *PLoS Computational Biology*, *10*(7), e1003716. https://doi.org/10.1371/journal.pcbi.1003716

Torous, J., Friedman, R., & Keshavan, M. (2014). Smartphone ownership and interest in mobile applications to monitor symptoms of mental health conditions. *JMIR mHealth and uHealth*, *2*(1), e2. https://doi.org/10.2196/mhealth.2994

Tracy, M., Cerdá, M., & Keyes, K. M. (2018). Agent-Based Modeling in Public Health: Current Applications and Future Directions. *Annual Review of Public Health*, *39*(1), 77–94. https://doi.org/10.1146/annurev-publhealth-040617-014317

Tsatsaris, A. (with Psaroulaki, A., Chochlakis, D., Kalogeropoulos, K., & Stathopoulos, N.). (2026). *Health Geography: Innovative Geospatial Epidemiology* (1st ed). Elsevier.

Tufte, E. R. (2013). *The visual display of quantitative information* (2nd ed., 8th print). Graphics Press.

Ukkusuri, S. V., Mathew, T. V., & Waller, S. T. (2007). Robust Transportation Network Design Under Demand Uncertainty. *Computer-Aided Civil and Infrastructure Engineering*, *22*(1), 6–18. https://doi.org/10.1111/j.1467-8667.2006.00465.x

Varga, L., Kovács, A., Tóth, G., Papp, I., & Néda, Z. (2016). Further We Travel the Faster We Go. *PLOS ONE*, *11*(2), e0148913. https://doi.org/10.1371/journal.pone.0148913

Vazquez-Prokopec, G. M., Bisanzio, D., Stoddard, S. T., Paz-Soldan, V., Morrison, A. C., Elder, J. P., Ramirez-Paredes, J., Halsey, E. S., Kochel, T. J., Scott, T. W., & Kitron, U. (2013). Using GPS Technology to Quantify Human Mobility, Dynamic Contacts and Infectious Disease Dynamics in a Resource-Poor Urban Environment. *PLoS ONE*, *8*(4), e58802. https://doi.org/10.1371/journal.pone.0058802

Viboud, C., Bjørnstad, O. N., Smith, D. L., Simonsen, L., Miller, M. A., & Grenfell, B. T. (2006). Synchrony, Waves, and Spatial Hierarchies in the Spread of Influenza. *Science*, *312*(5772), 447–451. https://doi.org/10.1126/science.1125237

Vytla, V., Ramakuri, S. K., Peddi, A., Kalyan Srinivas, K., & Nithish Ragav, N. (2021). Mathematical Models for Predicting Covid-19 Pandemic: A Review. *Journal of Physics: Conference Series*, *1797*(1), 012009. https://doi.org/10.1088/1742-6596/1797/1/012009

Wagner, A. (2020, June 7). *What makes a 'wave' of disease? An epidemiologist explains*. https://theconversation.com/what-makes-a-wave-of-disease-an-epidemiologist-explains-141573

Wall, P. A., & Devine, O. J. (2000). Interactive analysis of the spatial distribution of disease using a geographic information systems. *Journal of Geographical Systems*, *2*(3), 243–256. https://doi.org/10.1007/PL00011457

Wang, Y., Xiong, H., Liu, S., Jung, A., Stone, T., & Chukoskie, L. (2021). Simulation Agent-Based Model to Demonstrate the Transmission of COVID-19 and Effectiveness of Different Public Health Strategies. *Frontiers in Computer Science*, *3*, 642321. https://doi.org/10.3389/fcomp.2021.642321

Webb, H. (2020, April 14). University of Cyprus creates digital platform to track covid-19 cases. *European Office Of Cyprus (EOC)*. https://errin.eu/node/8274

WHO. (2020). *Pandemic Fatigue: Reinvigorating the Public to Prevent COVID-19*. https://iris.who.int/handle/10665/337574

WHO COVID-19 Dashboard. (2021). https://covid19.who.int

WHO COVID-19 Weekly Epidemiological Updates and Monthly Operational Update Reports. (n.d.). Retrieved 20 March 2024, from https://www.who.int/emergencies/diseases/novel-coronavirus-2019/situation-reports

WHO. Tracking SARS-CoV-2 Variants. (n.d.). Retrieved 15 March 2024, from https://www.who.int/activities/tracking-SARS-CoV-2-variants

Willem, L. (2015). *Agent-based models for infectious disease transmission exploration, estimation & computational efficiency*.

World Health Organization. (2004). *The atlas of heart disease and stroke / Judith Mackay and George Mensah ; with Shanthi Mendis and Kurt Greenland*. WHO IRIS. https://iris.who.int/handle/10665/43007

World Health Organization. (2020). *Statement on the second meeting of the International Health Regulations (2005) Emergency Committee regarding the outbreak of novel coronavirus (2019-nCoV)*. World Health Organization. https://www.who.int/news/item/30-01-2020-statement-on-the-second-meeting-of-the-international-health-regulations-(2005)-emergency-committee-regarding-the-outbreak-of-novel-coronavirus-(2019-ncov)

World Health Organization. (2023). *WHO Coronavirus (COVID-19) Dashboard*. https://covid19.who.int
World Health Organization. (2025). WHO. *Public Health Surveillance*. https://www.emro.who.int/health-topics/public-health-surveillance/index.html
WORLDOMETER. (2025). *WORLDOMETER. Cases and Deaths for COVID-19 Coronavirus Pandemic*. https://www.worldometers.info/coronavirus
Wu, F.-J., & Solmaz, G. (2018). CrowdEstimator: Approximating Crowd Sizes with Multi-modal Data for Internet-of-Things Services. *Proceedings of the 16th Annual International Conference on Mobile Systems, Applications, and Services*, 337–349. https://doi.org/10.1145/3210240.3210320
Yang, W., Zhang, D., Peng, L., Zhuge, C., & Hong, L. (2021). Rational evaluation of various epidemic models based on the COVID-19 data of China. *Epidemics*, *37*, 100501. https://doi.org/10.1016/j.epidem.2021.100501
Ying, F., & O'Clery, N. (2021). Modelling COVID-19 transmission in supermarkets using an agent-based model. *PLOS ONE*, *16*(4), e0249821. https://doi.org/10.1371/journal.pone.0249821
Zehavi, Y. (1977). *The" UMOT" Model*. Urban Projects Department [of] the World Bank.
Zellner, M. L. (2008). Embracing Complexity and Uncertainty: The Potential of Agent-Based Modeling for Environmental Planning and Policy. *Planning Theory & Practice*, *9*(4), 437–457. https://doi.org/10.1080/14649350802481470
Zhang, X.-B., Huo, H.-F., Xiang, H., & Meng, X.-Y. (2014). Dynamics of the deterministic and stochastic SIQS epidemic model with non-linear incidence. *Applied Mathematics and Computation*, *243*, 546–558. https://doi.org/10.1016/j.amc.2014.05.136
Zhao, M., Mason, L., & Wang, W. (2008). Empirical study on human mobility for mobile wireless networks. *MILCOM 2008 - 2008 IEEE Military Communications Conference*, 1–7. https://doi.org/10.1109/MILCOM.2008.4753151
Zhong, G., Wan, X., Zhang, J., Yin, T., & Ran, B. (2016). Characterizing Passenger Flow for a Transportation Hub Based on Mobile Phone Data. *IEEE Transactions on Intelligent Transportation Systems*, 1–12. https://doi.org/10.1109/TITS.2016.2607760
Zignani, M., Gaito, S., & Rossi, G. (2013). Extracting human mobility and social behavior from location-aware traces. *Wireless Communications and Mobile Computing*, *13*(3), 313–327. https://doi.org/10.1002/wcm.2209

APPENDIX

SURVEY TITLE: " Capturing the spatio-temporal mobility behaviors of the residents in the Republic of Cyprus"

PART 1 out of 4: Consent form to data confidentiality and data processing

1. I confirm that I am 18 years old and above
   (answers: AGREE, DO NOT AGREE)
2. I agree to the processing of personal data and to take part in the survey
   (answers: AGREE, DO NOT AGREE)

PART 2 out of 4: Demographics and key mobility characteristics

3. Gender
   (answers: Male, Female)
4. Age Group
   (answers: <20, 20-24, 25-29, 30-34, 35-39, 40-44, 45-49, 50-54, 55-59, 60-64, 65+)
4. Chronic Disease
   (answers: Yes, No)
5. District of residence
   (answers: Limassol, Nicosia, Larnaka, Paphos, Famagusta)
6. Region of residence
   (answers: choose one of 442 Communities and Municipalities)
7. Occupation
   (answers: Unemployed, On-site presence, Remote, Retired)
8. District of employment
   (answers: Unemployed / Retired / Remote work,
   Limassol, Nicosia, Larnaka, Paphos, Famagusta)
9. Region of employment
   (answers: Unemployed / Retired / Remote work, I do not know,
   choose one of 442 the Communities and Municipalities)
10. Currently attending an academic institution ?
    (answers: Not a student, BSc student, MSc student, PhD student)
11. District of studies
    (answers: Not a student, Remote studies, Limassol, Nicosia, Larnaka, Paphos, Famagusta)
12. How often (times per week) do you use the following means of transport for your transition to/from your school ?
    (answers: 0, 1-2, 3-5, 5-10, 10+)
    - Car
    - Motorbike
    - Bus
    - Taxi
    - Bicycle
    - Walk
13. How often (times per week) do you commute for the following purposes, on average ?
    (answers: 0, 1, 2, 3, 4, 5, 5+)
    - Workplace
    - Visiting another home (family and friends)
    - Entertainment (e.g. theatre, Cinema, Events, Festivals, etc)
    - Dining (e.g. Restaurants, Taverns, Cafes, Pizzerias, Bars, etc.)
    - Physical exercise and sports (training areas, gym, indoor and outdoor)
    - Grocery shopping (Supermarket, Mini Market, Kiosk, etc)
    - Shopping (Retail stores, Services and Goods other than food)
14. How often (times per week) do you use the following means of transport for your transition within your district of residence ?
    (answers: 0, 1-2, 3-5, 5-10, 10+)
    - Car

    - Motorbike
    - Bus
    - Taxi
    - Bicycle
    - Walk
15. How often (times per week) do you use the following means of transport for your transition outside your district of residence ?
    (answers: 0, 1-2, 3-5, 5-10, 10+)
    - Car
    - Motorbike
    - Bus
    - Taxi
16. How often (times per week) do you use the following means of transport for your transition to/from your workplace ?
    (answers: 0, 1-2, 3-5, 5-10, 10+)
    - Car
    - Motorbike
    - Bus
    - Taxi
    - Bicycle
    - Walk
17. How often (times per week) the following means of transport are being mostly used for the transition of your children to/from school ?
    (answers: 0, 1-2, 3-5, 5-10, 10+)
    - Car
    - Motorbike
    - Bus
    - Taxi
    - Bicycle
    - Walk
18. Starting from your location of residence, how far do you usually travel for your shopping (retail stores - Services and Goods other than food) ?
    (answers: <5 km, 5-10 km, 10-20 km, 20-30 km, >30 km)
19. Starting from your location of residence, how far do you usually travel for your entertainment (e.g. theatre, Cinema, Events, Festivals, etc) and dining (e.g. Restaurants, Taverns, Cafes, Pizzerias, Bars, etc.)
    (answers: <5 km, 5-10 km, 10-20 km, 20-30 km, >30 km)
20. Starting from your location of residence, how far do you usually travel for your grocery shopping (Supermarket, Mini Market, Kiosk, etc) ?
    (answers: <5 km, 5-10 km, 10-20 km, 20-30 km, >30 km)
21. State the type of venue you use mostly, for your physical exercise and sports
    (answers: Indoor space (e.g. gym), Outdoor space (e.g. park), I don't exercise)

<u>PART 3 out of 4: Human Mobility Schedule</u>

In this section, for each question the participant must choose one option from the following location/activity list for each timeslot.

Timeslots: 2 am, 4 am, 6 am, 8 am, 10 am, 12 am, 2 pm, 4 pm, 6 pm, 8 pm, 10 pm, 12 pm

Location/activity list:

- Home
- Workplace (not home)
- University / school
- Entertainment (e.g. theatre, Cinema, Events, Festivals, etc)
- Dining (e.g. Restaurants, Taverns, Cafes, Pizzerias, Bars, etc.)
- Physical exercise and sports (training areas, gym, indoor and outdoor)
- Grocery shopping (Supermarket, Mini Market, Kiosk, etc)
- Shopping (Retail stores, Services and Goods other than food)
- Visiting other houses (family and friends)

22. Determine your indicative location every two hours, for a typical workday
(answers: choose one option from the location/activity list for each timeslot)
23. Determine your indicative location every two hours, for a typical Saturday
(answers: choose one option from the location/activity list for each timeslot)
24. Determine your indicative location every two hours, for a typical Sunday
(answers: choose one option from the location/activity list for each timeslot)

PART 4 out of 4: Current opinions and acceptance to important COVID19 policies

25. Do you agree with the following statement: "Using a medical mask greatly reduces the spread of infectious diseases (such as COVID19)" ?
(answers: Agree, Disagree)
26. To what extent do you adopt the measure of wearing a medical mask, during periods with high numbers of COVID19 cases ?
(answers: Never, Sometimes, Sometimes in crowded spaces, Always in enclosed spaces and/or when crowded, Always and everywhere)
27. Do you agree with the following statement: "Applying the social distancing measure (keeping 2m distance at public and/or crowded spaces) greatly reduces the spread of infectious diseases (such as COVID19)" ?
(answers: Agree, Disagree)
28. To what extent do you adopt the social distancing measure (keeping 2m distance at public and/or crowded spaces), during periods with high numbers of COVID19 cases ?
(answers: Never, Sometimes, Sometimes in crowded spaces, Always in enclosed spaces and/or when crowded, Always and everywhere)
29. Do you agree with the following statement: "In cases of extremely dangerous epidemiological public health crises, the enforcement of a lockdown is an undesirable but necessary and beneficial measure to limit the spread of the virus" ?
(answers: Agree, Disagree)
30. Do you agree with the following statement: "Vaccination protects us and greatly reduces the spread of infectious diseases (such as COVID19)" ?
(answers: Agree, Disagree)
31. How many times you have been infected with COVID19 to date (either with a positive PCR or rapid test or due to symptoms even with a negative test) ?
(answers: 0, 1, 2, 3, 4, 5, 5+)
32. Have you been vaccinated against COVID19 (at least one dose) ?
(answers: Yes, No)

END OF SURVEY